

THE IMPACT OF AGE AND FRAILITY ON CARDIAC FUNCTION IN HEALTH AND
DISEASE CONDITIONS IN NATURALLY AGEING MICE

by

Hirad A. Feridooni

Submitted in partial fulfilment of the requirements
for the degree of Doctor of Philosophy

at

Dalhousie University
Halifax, Nova Scotia
September 2018

© Copyright by Hirad A. Feridooni, 2018

“Every failed experiment is one step closer to success.”

-Denzel Washington

TABLE OF CONTENTS

LIST OF TABLES	v
LIST OF FIGURES	vii
ABSTRACT	x
LIST OF ABBREVIATIONS AND SYMBOLS USED	xi
ACKNOWLEDGMENTS	xii
1 CHAPTER INTRODUCTION.....	1
1.1 OVERVIEW	1
1.2 AGE-DEPENDENT CHANGES IN THE FUNCTION AND STRUCTURE OF THE MALE HEART	4
1.3 AGE-DEPENDENT CHANGES IN CARDIAC FUNCTION AND STRUCTURE FOLLOWING IR	21
1.4 FRAILTY	36
1.5 HYPOTHESIS AND OBJECTIVES	45
2 CHAPTER MATERIALS AND METHODS	46
2.1 ANIMALS	46
2.2 FRAILTY INDEX.....	46
2.3 SCORING OF INDIVIDUAL HEALTH DEFICITS.....	48
2.4 CALCULATING A FRAILTY INDEX SCORE	59
2.5 RELIABILITY OF FRAILTY ASSESSMENT TOOL	59
2.6 FIBROSIS ASSAY	61
2.7 LANGENDORFF-PERFUSED ISOLATED HEARTS	62
2.8 CARDIAC TROPONIN-I ASSAY	66
2.9 INFARCT MEASUREMENT	68
2.10 VENTRICULAR MYOCYTE EXPERIMENTS	70
2.11 WESTERN BLOTS.....	73
2.12 STATISTICS.....	74
2.13 CHEMICALS	75

3	CHAPTER RESULTS.....	76
3.1	THE EFFECTS OF ADVANCED AGE ON CARDIAC CONTRACTILE FUNCTION AND STRUCTURE	76
3.2	INTER-RATER RELIABILITY OF THE MOUSE CLINICAL FI TOOL	90
3.3	THE RELATIONSHIP BETWEEN FRAILTY AND AGE-DEPENDENT CARDIAC CONTRACTILE DYSFUNCTION	109
3.4	THE IMPACT OF AGE AND FRAILTY ON CONTRACTILE FUNCTION FOLLOWING IR INJURY IN INTACT HEARTS	120
4	CHAPTER DISCUSSION	142
4.1	THE EFFECTS OF ADVANCED AGEING ON CARDIAC CONTRACTILE FUNCTION IN THE HEART	144
4.2	RELIABILITY OF THE MOUSE FI INSTRUMENT	151
4.3	THE RELATIONSHIP BETWEEN FRAILTY AND AGE-DEPENDENT CARDIAC CONTRACTILE DYSFUNCTION	155
4.4	THE IMPACT OF AGE AND FRAILTY ON CONTRACTILE FUNCTION FOLLOWING IR INJURY	159
4.5	LIMITATIONS AND FUTURE DIRECTIONS	168
4.6	IMPLICATIONS.....	170
	REFERENCES	171
	APPENDIX A: PUBLICATIONS.....	191
	APPENDIX B: COPYRIGHT PERMISSION LETTERS	193
	APPENDIX C: SUPPLEMENTARY TABLES	197

LIST OF TABLES

Table 1: Impact of age on the function of Langendorff-perfused hearts isolated from male rodents under normoxic conditions	8
Table 2: Impact of age on cardiomyocyte contractile function	16
Table 3: Age-dependent changes in cardiomyocyte calcium transients.....	20
Table 4: Recovery of cardiac contractile function following IR is reduced with advanced age in male rodents in vivo	26
Table 5: Effect of age on contractile function following IR in Langendorff-perfused hearts from male rodents.....	28
Table 6: Influence of age on clinical markers of injury following IR.....	33
Table 7: Effects of age on markers of injury following IR in male rodents	35
Table 8: Complete list of the descriptors and criteria for the scoring system of each deficit measured with the frailty index tool (Whitehead et al., 2014)	49
Table 9: Average body surface temperature (\pm SD) and average body weight (\pm SD) from a large cohort of more than 233 male mice at different ages.....	58
Table 10: Age and body weights of adult and aged mice used for Langendorff-perfused heart experiments.....	77
Table 11: Characteristics of male C57BL/6J mice used to assess the inter-rater reliability of the mouse clinical FI.....	92
Table 12: Refined criteria for the clinical assessment of health deficits in the mouse clinical FI tool	100
Supplementary Table 1: The scoring system used to determine a deficit in average body surface temperature and body weight when calculating the frailty index score.....	197
Supplementary Table 2: Hypertrophy and fibrosis increased with advanced age	198
Supplementary Table 3: Baseline parameters recorded from Langendorff-perfused hearts	199

Supplementary Table 4: Summary of contraction and Ca ²⁺ transient data from individual cardiomyocytes isolated from aged and adult hearts.....	200
Supplementary Table 5: Summary of Ca ²⁺ current responses and Cav1.2 protein expressions in cardiomyocytes isolated from aged and adult hearts.....	201
Supplementary Table 6: Summary of functional responses following 30 min global ischemia and 40 min reperfusion in hearts from adult and aged mice.....	202
Supplementary Table 7: Summary of functional responses expressed as a percentage of pre-ischemic values after 40 min reperfusion	203
Supplementary Table 8: Summary of IR injury in intact hearts from aged and adult mice	204

LIST OF FIGURES

Figure 1. EC-coupling pathway in a ventricular myocyte.	12
Figure 2. The FI Scoring system.	47
Figure 3. Calculation used to measure the FI score.	60
Figure 4. A Radnoti Langendorff apparatus used to assess LV pressure in hearts isolated from aged and adult mice.	63
Figure 5. Time course for LV recordings before and after exposure to IR.	65
Figure 6. Representative image of a heart slice following IR.	71
Figure 7. Cardiac hypertrophy increased with age.....	78
Figure 8. Cardiac fibrosis increased with age.	80
Figure 9. Left ventricular contractile function declined with advanced age.	82
Figure 10. Aged hearts did less work in comparison to adult hearts.....	83
Figure 11. Coronary flow rates were not affected by age.....	84
Figure 12. Ca ²⁺ transients and peak contractions declined with advanced age.....	86
Figure 13. Peak Ca ²⁺ currents and gain of SR Ca ²⁺ release declined with age.....	87
Figure 14. There was an age-dependent decline in CaV1.2 protein expression.	89
Figure 15. A representative example of the novel non-invasive FI tool developed by our lab.	91
Figure 16. The mean (\pm SEM) frailty scores for mice in Group 1 did not differ between raters.....	93
Figure 17. Various differences in assessing certain deficits were identified between raters.....	95
Figure 18. Refinement of the FI tool improved the variability in assessment between raters.....	97
Figure 19. Differences between raters declined after refinement of the FI index tool...	98

Figure 20. Response to sound declined with repeated exposure within a short time period.....	100
Figure 21. Reliability measured by the standard correlation coefficient (r), improved between raters with subsequent measurements.	105
Figure 22. The frailty index tool was highly reliable between raters.	106
Figure 23. Frailty scores increased with age.....	108
Figure 24. There was marked heterogeneity in the overall health status in mice of the same age.	110
Figure 25. Age-dependent cardiac hypertrophy increased as a function of frailty.....	111
Figure 26. Cardiac contractile dysfunction was graded by frailty scores	113
Figure 27. Average flow rates during baseline conditions were not affected by frailty scores.	114
Figure 28. Peak contractions and Ca ²⁺ transients were graded by frailty score.	116
Figure 29. The age-related decline in Ca ²⁺ current and the gain of SR Ca ²⁺ release was graded by frailty.	118
Figure 30. The age-dependent decline in CaV1.2 expression was graded by frailty.....	119
Figure 31. Contractile function declined in IR	121
Figure 32. Time course for the recovery of LV contractile function during 40 min reperfusion.....	122
Figure 33. Recovery of contractile function was better in the aged hearts during 40 min reperfusion.....	124
Figure 34. Recovery of cardiac function following IR was not correlated with frailty ..	126
Figure 35. Recovery of contractile function following IR was poor in all hearts, regardless of the overall health status of the animal.....	127
Figure 36. Age did not affect coronary flow rate following 40 min IR.	129
Figure 37. Recovery of coronary flow rate was high regardless of the frailty score.....	130
Figure 38. Coronary reflow during the initial minute of reperfusion was not due to vascular compression in both age groups.	131

Figure 39. Representative example of pressure recorded from an intact heart before and after exposure to IR.....	133
Figure 40. Aged hearts took longer to develop similar levels of contracture during ischemia compared to adult hearts.	134
Figure 41. Contracture in ischemia was not correlated with the FI score.	135
Figure 42. Aged and adult hearts exhibited similar levels of contracture during reperfusion.....	137
Figure 43. Frailty scores did not grade peak contracture in reperfusion.	138
Figure 44. Infarct sizes were smaller in the aged hearts.	139
Figure 45. cTnI release during reperfusion declined with age, not frailty.	141

ABSTRACT

Frailty is defined as the increased susceptibility to adverse health outcomes in individuals of the same age. Frail people with cardiovascular disease experience worse outcomes and higher mortality than non-frail patients, but the links between frailty and myocardial function are unclear. Assessing frailty in mice is now possible with the recent development of a mouse clinical frailty index (FI) tool. The present study investigated the links between age, frailty, and cardiac contractile function before and after exposure to ischemia and reperfusion (IR). Frailty was quantified as deficit accumulation in adult (≈ 8 mos) and aged (≈ 27 mos) C57BL/6 male mice using the mouse clinical FI tool. Contractile function was evaluated in Langendorff-perfused hearts before and after exposure to IR. Contraction and underlying Ca^{2+} homeostasis was measured in individual ventricular myocytes in voltage clamp experiments. Mean cardiac hypertrophy increased with age. Furthermore, under basal conditions, left ventricular developed pressure plus rates of pressure development and decay declined with age. Interestingly, ventricular myocytes from aged mice had smaller and slower contractions. These smaller contractions were due to smaller Ca^{2+} transients and Ca^{2+} currents. Smaller Ca^{2+} currents were attributable to a decrease in CaV1.2 expression in aged hearts in comparison to adult hearts. Interestingly this age-dependent remodelling in the intact hearts and individual myocytes was graded by frailty. By contrast, hearts from aged mice had better recovery of function and less cell death in comparison to adult hearts following exposure to IR. However, functional recovery and myocardial injury were not correlated with FI scores. These results show that age-dependent cardiac remodelling at the level of the intact heart and at the cellular and subcellular levels are graded by the overall health of the mouse and that there may be underlying mechanisms that protect against IR in ageing.

LIST OF ABBREVIATIONS AND SYMBOLS USED

TTC	2,3,5-Triphenyltetrazolium chloride
AP	Action potential
AMI	Acute myocardial infarction
ATP	Adenosine triphosphate
Bpm	Beats per minute
BW	Body weight
I _{Ca-L}	Ca ²⁺ current
cTnI	Cardiac specific troponin I
CVD	Cardiovascular disease
CI	Confidence interval
ECG	Electrocardiogram
EC	Excitation-contraction
EDTA	Ethylenediaminetetraacetic acid
FI	Frailty index
HR	Heart rate
HW	Heart weight
IL	Interleukin
ICC	Intraclass correlation
IR	Ischemia and reperfusion
IHD	Ischemic heart disease
LDH	Lactate dehydrogenase
LV	Left ventricle
LVDP	Left ventricular developed pressure
LVEDP	Left ventricular end diastolic pressure
MVO ₂	Myocardial oxygen consumption
NCX	Na ⁺ /Ca ²⁺ exchanger
pA/pF	Picoamperes per picofarad
+dP/dt	Rate of contraction
-dP/dt	Rate of relaxation
RPP	Rate pressure product
RM ANOVA	Repeated measures analysis of variance
Rpm	Revolutions per minute
RyR	Ryanodine receptors
SERCA	Sarco/endoplasmic reticulum Ca ²⁺ -ATPase
SR	Sarcoplasmic reticulum
SD	Standard deviation
SDS-PAGE	Sodium dodecyl sulfate polyacrylamide gel electrophoresis
TMB	Tetramethylbenzidine
TL	Tibia length
TNF	Tumor necrosis factor
U	Units of activity
CaV	Voltage-gated Ca ²⁺ channel

ACKNOWLEDGMENTS

First and foremost, I would like to thank Dr. Susan Howlett for taking a chance on me and allowing me to join your lab as a teenager. Thank you for creating a free and positive environment for me to try, fail, and succeed in research. You have equipped me with invaluable skills and knowledge that will help me in my future endeavors.

Second, I thank Peter Nicholl and Dr. Jie-quan Zhu for all of your help and expertise. To Dr. Randi Parks and Jeanne Egar, thank you for always giving me sound advice - even to this day. Also, I want to thank all of the past and present members of The Howlett lab. Your friendship made my time in Pharmacology an unforgettable experience.

Thank you to the Department of Pharmacology, specifically, Dr. Chris McMaster, Luisa, Sandi, and Cheryl. I would also like to express gratitude for my advisory committee members, Dr. Ryan Pelis, Dr. Jason McDougall, Dr. Robert Rose, and Dr. Morgan Langille for their expertise throughout my PhD program.

Finally, I would like to thank my family, Nahid, Amir, and Tiam for being exemplary role models to me. I learned the meaning of hard work early in life from you. To my friends and the GC – you guys are family and I would not have been able to finish my PhD without your love, support, and your infectious energy to live life to the fullest. Teamwork makes the dream work, and I have had the best team.

1 CHAPTER INTRODUCTION

1.1 OVERVIEW

Cardiovascular disease (CVD) is the leading cause of death worldwide, accounting for roughly 30 percent, or 17 million, deaths per year (Mozaffarian et al., 2016; WHO, 2013). In the U.S. alone, it is estimated that 1 in 3 people have CVD and over 2000 people die every day as a consequence of these diseases (Mozaffarian et al., 2016). Incidentally, more than 2 million Canadians have been diagnosed with CVD and in 2015, over 50 thousand Canadians died of CVD (Public Health Agency of Canada, 2017; Statistics Canada, 2018).

There are many risk factors for CVD such as smoking, lack of exercise, poor diet, high blood pressure, obesity, and diabetes. However, the primary risk factor for CVD is advanced age. Over 90 thousand Canadians over the age of 40 have been diagnosed with at least one CVD (Public Health Agency of Canada, 2017). Canada has an ageing population, where over 16 percent of the population is over the age of 65 (Statistics Canada, 2017). As the population ages, the occurrence of CVD and associated deaths is expected to rise as well. Similarly, out of the 85.6 million Americans estimated to live with CVD, 43.7 million are more than 60 years of age (Mozaffarian et al., 2016). The high incidence of CVD and ensuing mortality creates economic, societal, and clinical challenges. Therefore, it is important to study the age-associated mechanisms that cause maladaptive changes in the heart that may lead to CVD.

There is growing evidence that, while advanced age promotes CVD, it can also cause a decline in heart function even in the absence of overt CVD (Lakatta & Levy, 2003, Feridooni, Dibb & Howlett, 2015A, Keller & Howlett, 2016). This age-dependent decline in heart function only reflects an average response, inasmuch as this decline can vary

between individuals of the same age (Howlett & Rockwood, 2013). For example, while on average age promotes a decline in maximal heart rate and ejection fraction during exercise, some older individuals perform at a level that is similar to young adults (Lakatta, 2002; Lakatta & Levy, 2003). This is because people age at different rates (Clegg, Young, Iliffe, Rikkert & Rockwood, 2013). The concept of frailty is used to account for this unmeasured heterogeneity in ageing for people of the same age (Mitnitski, Howlett & Rockwood, 2017).

Frailty can be defined as a state of increased vulnerability to adverse health outcomes in individuals of the same age (Rockwood, Fox, Stolee, Robertson, & Beattie, 1994; Bergman et al., 2007). Many older adults have multiple medical problems and are said to be frail (Clegg et al., 2013; Adabag et al., 2018). Clinical studies show that frail individuals are more susceptible to stressors such as CVD (Singh, Stewart & White, 2014; Afilalo et al., 2014; Chen, 2015; Adabag et al., 2018; Kusunose et al., 2018). Indeed, frail patients who do develop CVD experience higher morbidity and mortality than non-frail individuals (Afilalo et al., 2014; Singh et al., 2014; Chen, 2015; Goldwater & Pinney, 2015; Adabag et al., 2018; Kusunose et al., 2018). Furthermore, frail patients who undergo treatment for CVD have higher morbidity and postoperative mortality than non-frail patients (Afilalo et al., 2014; Singh et al., 2014; Chen, 2015). In addition to poor postoperative outcomes, frail individuals are also more likely to be institutionalized and for longer periods of time, compared to non-frail individuals of the same age (Hubbard et al., 2017; Singh et al., 2014; Goldwater & Pinney, 2015; Rockwood et al., 2004; Clegg et al., 2013; Chen, 2015). Hence, frailty is recognized to be a major burden on the health care system.

Although it is clear that there are links between frailty and CVD, we know very little about the mechanisms that increase the susceptibility of the frail heart to CVD. This is true in part because, until recently, there had been no preclinical models of frailty. Our group has recently developed a mouse frailty index (FI) tool based on the concept of deficit accumulation, similar to the FI tool used clinically (Clegg et al., 2013; Whitehead et al., 2014; Feridooni et al., 2015B). This novel FI tool allows us to measure frailty in animals and allows us to investigate the biology of frailty and its impact on the heart.

Although it is recognized that age adversely affects heart function, elderly patients and aged animal models are underrepresented in most studies, so little is known about the impact of age on CVD (Nanayakkara, Marwick & Kaye, 2018; Feridooni et al., 2015A). Therefore, the overall goal of this thesis was to use aged mice to investigate age-dependent remodelling of cardiac contractile function in intact hearts and at the level of individual ventricular myocytes, under health and disease conditions. Furthermore, we aimed to validate our FI tool and use it to measure heterogeneity of ageing, by considering the frailty of these old mice, and relating frailty to cardiac contractile function and underlying mechanisms.

There are sex-differences in cardiac contractile function with age in both people and in animals, although evidence from females is limited, and whether a decline in contractile function with age occurs in females is controversial (Feridooni et al., 2015A; Keller & Howlett, 2016). This research project only used male mice where an age-dependent decrease in contraction has been observed (Claessens et al., 2007; Walker et al., 2006), however, parallel studies in ageing female mice are in progress in the lab. Because of this, only studies that used ageing male animals have been described in the introduction.

Parts of this introductory chapter has been used with permission from Elsevier in the Journal of Molecular and Cellular Cardiology (Feridooni et al., 2015A).

1.2 AGE-DEPENDENT CHANGES IN THE FUNCTION AND STRUCTURE OF THE MALE HEART

1.2.1 Clinical studies of the impact of age on cardiac structure and function

Clinical studies in healthy individuals have established that ageing is associated with marked changes in cardiac structure. For example, calcification can occur on the aortic valve leaflets hindering the opening and closing of the aortic valve (Collins, Munoz & Patel, Loukas & Tubbs 2014; Walker et al., 2006). In addition, hearts from healthy older adults have enlarged atria and exhibit left ventricular (LV) hypertrophy (Keller & Howlett, 2016; Lakatta & Levy, 2003). There are also age-dependent structural modifications that occur at the cellular level. In humans, there is evidence that the average number of atrial and ventricular myocytes declines with age (Olivetti, Melissari & Capasso & Anversa 1991). By contrast, hearts from older people have more cardiac fibroblasts, and concurrently higher collagen content (Horn & Trafford, 2016). The higher collagen content in aged hearts results in fibrosis in the atria and ventricles (Horn & Trafford, 2016). This age-associated fibrosis can have adverse effects on the heart's ability to contract and relax (Horn & Trafford, 2016).

Advanced age is also characterized by modifications in cardiac function in people (Lakatta & Levy, 2003). There is growing evidence that myocardial remodelling can modify the aged heart's ability to contract and relax, even in the absence of overt systemic CVD. Traditionally, studies of myocardial function in healthy individuals at rest have

shown that cardiac output and myocardial contractility are not affected by age (Bernhard & Laufer, 2008; Fleg, et al., 1995; Ruan & Nagueh, 2005; Stratton, Levy, Cerqueira, Schwartz & Abrass, 1994; Wei, 1992). Furthermore, resting heart rates (HR) are similar in young and old adults (Keller & Howlett, 2016). However, more recent evidence suggests there is a decline in both systolic function (LV ejection fraction, LV fractional shortening and systolic stiffness) and diastolic function (E/A, E/E' ratio, and diastolic stiffness) at rest in adults over the age of 65 (Liu et al., 2012; Redfield, Jacobsen & Borlaug, Rodeheffer & Kass 2005). Redfield *et al.* (2005) showed that mean left atrial pressures and diastolic elastance, a measure of stiffness, increase with age. Furthermore, this study showed that end-systolic elastance and fractional shortening are attenuated by age (Redfield et al., 2005). Aged individuals have slower contractions and less complete relaxation when compared to younger people, which suggests that diastolic function also declines with age (Lakatta & Levy, 2003; Lakatta & Sollott, 2002; Wei, 1992). Moreover, there is growing evidence that the heart's ability to augment contractile function when demand is high, such as during activities like exercise, is compromised in older adults when compared to younger individuals (Lakatta & Levy, 2003; Stratton et al., 1994; Wei, 1992). For example, the ability to increase HR during times of high demand, such as during exercise, decreases with age (Fleg & Strait, 2012; Strait & Lakatta, 2012).

The changes that occur in cardiac contractile function as a result of ageing arise, in part, from the structural remodelling such as hypertrophy and ventricular stiffness, that accompany the ageing process. These age-associated changes in cardiac contractile function also reflect underlying modifications that occur at the level of the individual ventricular myocyte. To better understand these age-dependent changes in the heart,

animal models are used to mirror the ageing process in people.

1.2.2 Impact of age on cardiac contractile function in ageing animal models

Various animal studies have been used to investigate the age-dependent changes in contractile function seen clinically. Rats and mice exhibit a 50% mortality rate at approximately 24 months of age (Turturro et al. 1999), which is comparable to the 50% mortality rate seen in 85-year-old humans (Grundy, 2003). Therefore, this introduction will focus on the studies that use male mice or rats that are approximately 18-24 months of age as models of human ageing. Structural changes similar to those seen in older humans have been demonstrated in aged mice. For example, aged animals undergo aortic valve calcification, and develop atrial and LV hypertrophy (Keller & Howlett, 2016; Lindsey et al., 2005; Walker et al., 2006; Manne, Kakarla & Arvapalli, Rice, & Blough, 2014). As in older humans, the loss of ventricular myocytes due to apoptosis increases with age (Keller & Howlett, 2016; Kajstura et al., 1996). Furthermore, there is extracellular matrix remodelling such that there is collagen accumulation and interstitial fibrosis in aged rodents (Keller & Howlett, 2016; Lindsey et al., 2005; 136. Willems, Zatta, Homgren, Ashton & Headrick, 2005; Boucher et al., 1998; Walker et al., 2006). These age-associated structural changes in the ageing heart can have adverse effects on cardiac function.

While the impact of age on cardiac contractile function at rest and during exercise has not yet been investigated in conscious rodents, *in vivo* echocardiography studies in anesthetized male animals show that age reduces fractional shortening and ejection fraction (Ceylan-Isik, et al., 2013; Hacker, McKiernan, Douglas, Wanagat & Aiken, 2006; Tang, et al., 2011; Koch et al., 2013; *c.f.* Wang et al., 2018). These studies also demonstrate a

slowing of myocardial relaxation in aged rodents, which indicates that diastolic function deteriorates with age (Hacker et al., 2006; Qin, et al., 2013; Koch et al., 2013; Walker et al., 2006). These echocardiography studies are supported by the results of an *in vivo* study by Liu *et al.* (2012), which assessed systolic and diastolic function by placing a probe in the LV of aged rats. They found that systolic function, as defined by peak LV systolic pressure and the rate of pressure development during contraction (+dP/dt), declines with age (Liu et al., 2012). In addition, the group saw a decline in diastolic function, defined by an increase in LV-end-diastolic pressure (LVEDP) and a decrease in the rate of relaxation (-dP/dt) in aged rats (Liu et al., 2012). Taken together, these studies suggest that advanced age promotes contractile dysfunction *in vivo*.

Age-dependent LV dysfunction has been further assessed in *ex vivo* Langendorff-perfused hearts. The Langendorff-perfused heart model provides data on LV pressure and therefore can evaluate both systolic and diastolic function. Systolic function is assessed by measuring the LV-developed pressure (LVDP) and +dP/dt, while diastolic function is assessed by measuring LVEDP, or the minimum pressure, and -dP/dt. Furthermore, intrinsic HR can be measured. The Langendorff model also makes it easy to assess coronary artery function by measuring coronary flow. Results of studies that have examined the influence of age on cardiac contractile function in Langendorff-perfused hearts are summarized in Table 1. Older studies using aged male mice show that there are no changes in LVDP, +dP/dt, -dP/dt, and LV diastolic pressure with age (Willems et al., 2005; Headrick et al., 2003; Ashton, Nilsson & Willems, Holmgren & Headrick, 2003). However, there is recent evidence that LVDP declines and LV diastolic pressure increases

Table 1: Impact of age on the function of Langendorff-perfused hearts isolated from male rodents under normoxic conditions

Component	Functional Change*	Species	Reference
LVDP/peak LV pressure	↓	Mice	Qin, et al., 2013
		Rats	Sample et al., 2006; Boucher et al., 1998
	↔	Mice	Willems et al., 2005; Headrick et al., 2003; Ashton et al., 2003
		Rats	Watanabe et al., 2004; Korzick et al., 2001; Escobales et al., 2014; Headrick, 1998; Lesnefsky et al., 1994
+dP/dt	↔	Mice	Willems et al., 2005; Headrick et al., 2003; Ashton et al., 2003
		Rats	Watanabe, Ichinose & Sunamori, 2004; Escobales et al., 2014; Lesnefsky et al., 1994
	↓	Rats	Korzick et al., 2001
-dP/dt	↔	Mice	Headrick et al., 2003; Ashton et al., 2003
		Rats	Watanabe et al., 2004; Korzick et al., 2001; Escobales et al., 2014
	↓	Rats	Lesnefsky et al., 1994
Heart rate	↔	Mice	Porter et al., 2014; Stein et al., 2008
		Rats	Watanabe et al., 2004; Escobales et al., 2014
	↓	Mice	Headrick et al., 2003;
		Rats	Sample et al., 2006; Headrick, 1998
Coronary flow	↔	Mice	Ashton et al., 2003; Wang et al., 2018
		Rats	Watanabe et al., 2004; Escobales et al., 2014; Headrick, 1998; Lesnefsky et al., 1994; Boucher et al., 1998
	↓	Mice	Willems et al., 2005; Headrick et al., 2003
LV diastolic pressure	↑	Mice	Qin, et al., 2013, Wang et al., 2018
	↔	Mice	Willems et al., 2005
		Rats	Watanabe et al., 2004; Korzick et al., 2001; Escobales et al., 2014; Lesnefsky et al., 1994

*↑ Arrow denotes an increase in function relative to young adults
 ↓ Arrow denotes a decrease in function relative to young adults
 ↔ Arrows denotes no difference in function between young adults and aged
 Comparisons are made between young adult (2-10 mos) and aged (18-28 mos) animals.

with age in mice (Qin et al., 2013; Wang et al., 2018). Differences between the results of earlier studies (Willems et al., 2005; Headrick et al., 2003; Ashton et al., 2003) and more recent work (Qin et al., 2013), may be attributable to differences in experimental conditions and protocols. The earlier studies used C57BL/6 mice, while Qin *et al.* (2013) used FVB/N wild type mice. Furthermore, these studies have different concentrations of ions in the perfusate. For example, Qin *et al.* (2013) used lower $[Ca^{2+}]$ compared to the earlier studies. In addition, earlier studies (Willems et al., 2005; Headrick et al., 2003; Ashton et al., 2003) are all from the Headrick group. Unlike Qin *et al.* (2013), the studies by Headrick and colleagues used exclusion criteria that excluded any heart with a systolic pressure below 100 mm Hg. This likely introduced bias in the study such that any hearts exhibiting an age-dependent decline in contractile function would be excluded from analysis. Moreover, the studies from the Headrick group paced hearts at 400 bpm, while Qin *et al.* (2013) paced hearts at ~450 bpm. The higher pacing frequency used in the Qin *et al.* (2013) study may unmask any age associated differences between the aged and young mice. This is consistent with clinical studies, in which the heart's ability to augment contractile function is compromised at higher HRs in older individuals (Fleg & Strait, 2012; Strait & Lakatta, 2012).

The effects of cardiac ageing on contractile function are similarly observed in Langendorff-perfused hearts from ageing male rats, and this is summarized in Table 1. There is evidence that hearts from aged rats have lower LVDP, and slower $+dP/dt$ and $-dP/dt$, compared to young adult rats (Sample, Cleland, & Seymour, 2006; Korzick, Holiman, Boluyt, Laughlin & Lakatta, 2001; Lesnefsky, Gallo, Ye, Whittingham & Lust, 1994; Boucher et al., 1998; *c.f.* Watanabe, Ichinose & Sunamori, 2004; Escobales et al.,

2014; Korzick et al., 2001; Headrick, 1998). Furthermore, the rate pressure product (RPP), which is a measure of cardiac effort and myocardial oxygen consumption, is reduced in aged rats (Sample et al., 2006; *c.f.* Headrick, 1998). It is unclear why there are differences in the results of these studies. However, one study used exclusion criteria that excluded any heart with an LVDP lower than 80 mm Hg (Lesnefsky et al., 1994). Thus, the use of exclusion criteria, different strains of rats (*e.g.* Wistar, F344/BN, and Sprague-Dawley rats), dissimilar experimental conditions (*e.g.* hearts perfused with constant flow vs constant pressure, pacing rates, $[Ca^{2+}]$), and different age ranges may be implicated (Sample et al., 2006; Watanabe et al., 2004; Escobales et al., 2014; Korzick et al., 2001; Headrick, 1998; Lesnefsky et al., 1994). As in people, studies in Langendorff-perfused rodent hearts show that there is no change in intrinsic HR with age (Porter, Urciuoli, Brookes & Nadtochiy, 2014; Stein et al., 2008; Watanabe et al., 2004; Escobales et al., 2014 but *c.f.* Headrick et al., 2003; Sample et al., 2006; Headrick, 1998).

In addition to measuring cardiac contractile function, coronary artery function can be assessed by measuring coronary flow in Langendorff-perfused rodent hearts (summarized in Table 1). For example, if coronary flow is compromised, the heart will not be properly perfused, which may predispose the heart to develop ischemia-reperfusion (IR) injury (discussed in detail section 1.3). There is general agreement that coronary flow is not affected by age across a wide range of perfusion pressures and flow rates (Boucher et al., 1998; Ashton et al., 2003; Watanabe et al., 2004; Escobales et al., 2014; Wang et al., 2018 *c.f.* Willems et al., 2005; Headrick et al., 2003).

Information about the effect of age on cardiac contractile function has also been obtained using isolated cardiac muscle preparations. Interestingly, some studies report that

there is no age-related decline in peak tension in isolated papillary muscles or trabeculae (Capasso, Remily & Sonnenblick, 1983; Wei, Spurgeon & Lakatta, 1984), while others report a reduction (Cappelli, Tortelli, Zani, Poggesi & Reggiani, 1988). For example, peak tension development declines with age (Jiang, Moffat & Narayanan, 1993), especially at higher HR's (Lim, Liao, Varma & Apstein, 1999). Other studies showed that the maximum rate of tension development and maximum rate of relaxation are slowed with age (Jiang et al., 1992; Lim et al. 1999). There is general agreement that contraction duration is prolonged with age, with an increase in both time-to-peak tension and half-relaxation time (Capasso et al., 1983; Cappelli et al., 1988; Lakatta, Gerstenblith, Angell, Shock & Weisfeldt, 1975a; Lakatta, Gerstenblith, Angell, Shock & Weisfeldt, 1975b; Wei et al., 1984). Thus, there is evidence from studies *in vivo*, in intact hearts, and in isolated cardiac muscles to demonstrate that contractions are smaller and slower in the ageing heart. Together, these observations indicate that cardiac contractile function declines with age, at least in male animals. The observed age-dependent contractile dysfunction may be a result of changes at the level of the cardiomyocyte, an idea that is examined in the next section.

1.2.3 Excitation-contraction coupling pathway

The excitation-contraction (EC) coupling pathway (summarized in Figure 1), converts an electrical signal, known as an action potential (AP) into intracellular Ca^{2+} release, causing Ca^{2+} -mediated contraction (Bers, 2002). APs are initiated by pacemaker cells (*i.e.* sinoatrial node) and propagate through the heart (Norbert, 2009). There are four

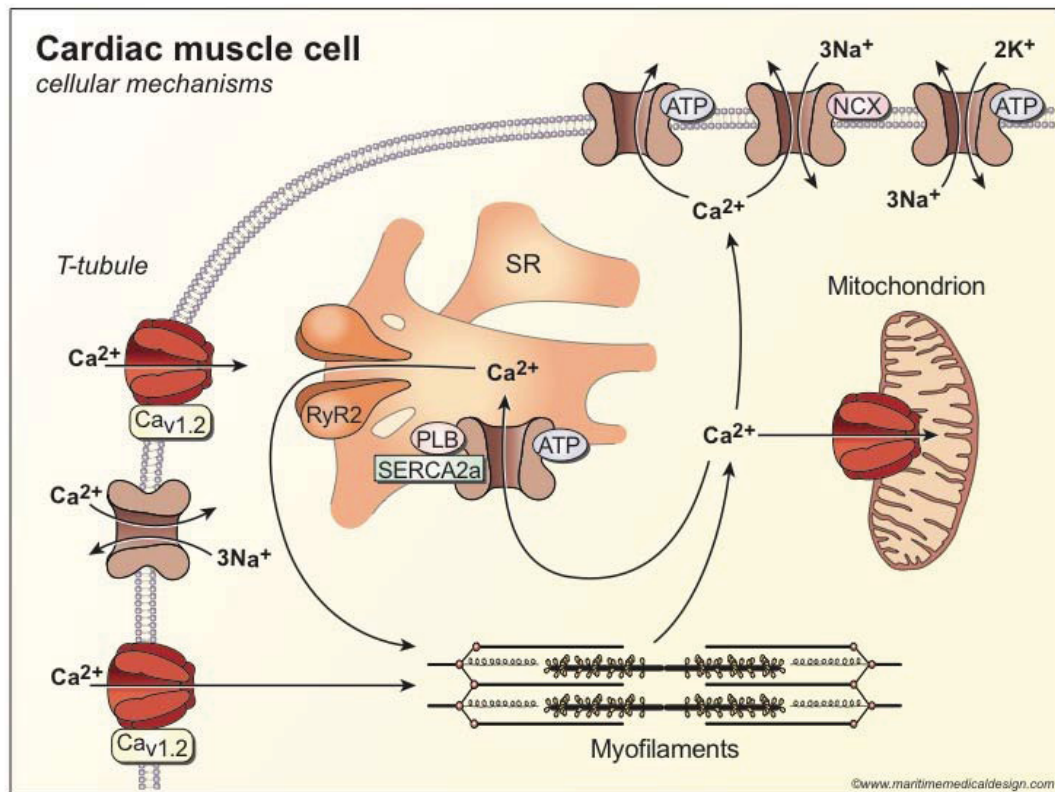


Figure 1. EC-coupling pathway in a ventricular myocyte. An action potential will propagate along the membrane and depolarize the membrane. Depolarization of the membrane opens the voltage-gated L-type Ca^{2+} channel ($\text{Ca}_v1.2$) to allow Ca^{2+} to enter the cell, giving rise to the calcium current ($\text{I}_{\text{Ca-L}}$). The Ca^{2+} that enters the cell will bind to and open the ryanodine receptors (RyR2) on the sarcoplasmic reticulum (SR). Opening of the RyR2 will release intracellular Ca^{2+} that is stored in the SR into the cytosol, giving rise to the Ca^{2+} transient. The increase in cytosolic Ca^{2+} will increase the probability of Ca^{2+} binding to the myofilament and causing a contraction. The majority of the cytosolic Ca^{2+} will be taken back up into the SR by the sarco/endoplasmic reticulum Ca^{2+} -ATPase (SERCA2a). Cytosolic Ca^{2+} will also be extruded from the cell by the $\text{Na}^{+}/\text{Ca}^{2+}$ exchanger (NCX) and to a lesser degree by the plasma membrane Ca^{2+} -ATPase. Reprinted from Feridooni et al. (2015A) with permission.

phases to an AP. The initial Phase 0 occurs after the membrane is depolarized from -80 mV (the resting potential) to a positive voltage, causing a rapid influx of Na^+ through voltage-gated Na^+ channels (Norbert, 2009). Phase 1, known as early repolarization, starts when small amounts of K^+ leave the cell through transient outward K^+ channels, which starts the repolarization process (Norbert, 2009). Phase 2, the “plateau” phase of the AP, is caused by the influx of Ca^{2+} through voltage-gated Ca^{2+} (CaV) channels (Norbert, 2009). Finally, in Phases 3 and 4 of the AP, the efflux of K^+ through outward K^+ channels repolarizes the cell and maintains resting membrane potential (Norbert, 2009).

CaV channels are subdivided into L-type and T-type channels (Norbert, 2009). Unlike the L-type CaV channels, T-type CaV channels are believed to play a negligible role in the excitation-contraction coupling process (Bers 2002; Norbert, 2009). L-type CaV channels are ubiquitous, and present in tissues such as skeletal and heart muscle (Hoppe, Brandt, Michels & Linder, 2005). All L-type CaV channels consist of five subunits: α_1 , α_2 , δ , β , and γ (Hoppe et al., 2005; Norbert, 2009). However, there are different types of L-type CaV channels, which are subdivided into four different classes according to their different α_1 -subunits (CaV1.1, CaV1.2, CaV1.3, CaV1.4) (Hoppe et al., 2005; Norbert, 2009). These different L-type CaV channels are found in different tissues. For instance, CaV1.3 can be found in the pancreas, kidney, endocrine cells and in neurons (Hoppe et al., 2005). CaV1.4, CaV1.1, and CaV1.2 are found in the retina, skeletal muscles, and the heart respectively (Hoppe et al., 2005). Moreover, L-type CaV1.2 channels are highly expressed within transverse tubules, which are in close proximity to the ventricular myocyte's intracellular Ca^{2+} release and Ca^{2+} sequestration mechanisms (Norbert, 2009).

The small influx of Ca^{2+} that enters the cell through L-type CaV1.2 channels is

referred to as the Ca^{2+} current ($I_{\text{Ca-L}}$). The Ca^{2+} that enters the cell then binds to ryanodine receptors (RyR) that are on the surface of the sarcoplasmic reticulum (SR). Binding of Ca^{2+} triggers the RyR to open and release large amounts of stored Ca^{2+} from the SR, giving rise to the Ca^{2+} transient (Bers, 2002). The increased concentration of intracellular Ca^{2+} caused by the Ca^{2+} transient will bind to the myofilaments to initiate contraction (Bers, 2002). Ca^{2+} is a major determinant of cardiac contractility. Under normal conditions, the size of the contraction is proportional to the size of the $I_{\text{Ca-L}}$ (Bers, 2002). An increase in free Ca^{2+} concentration increases force and contraction size in myocytes (Rüegg, 1998; Bers, 2002). Relaxation occurs predominantly when Ca^{2+} is sequestered by the sarco/endoplasmic reticulum Ca^{2+} -ATPase (SERCA), whose activity is modulated by its endogenous inhibitor, phospholamban. In addition, the mitochondria, the $\text{Na}^+/\text{Ca}^{2+}$ exchanger (operating in its forward-mode), and the Ca^{2+} -ATPase also remove Ca^{2+} from the cytosol (Bers, 2002). This process is summarized in Figure 1.

Contractile dysfunction in ageing hearts may arise, in part, because the ability of individual myocytes to contract is adversely affected by the ageing process. To help understand age-dependent contractile dysfunction, a number of studies have investigated how age influences components of the EC-coupling pathway at the cellular level. These findings are discussed in the subsequent sections.

1.2.4 Effects of age on cardiomyocyte contractile function in male animals

A number of studies have investigated the impact of age on cardiac contraction by comparing the amplitudes and time courses of contractions, measured as cell shortening, in ventricular myocytes isolated from young adult (2-7 mos of age) and aged (20-33 mos

of age) male rats and mice (Table 2). Because age has been shown to promote ventricular myocyte hypertrophy (Feridooni et al., 2015A; Keller & Howlett, 2016; Walker et al., 2006), contractions are typically normalized to cell length in functional studies. With this approach, there is now convincing evidence that peak cell shortening declines with age in male mice (Ceylan-Isik et al., 2013; Domeier et al., 2014; Grandy & Howlett, 2006; Li et al., 2005; Lim, Apstein, Colucci & Liao, 2000; Qin et al., 2013; Turdi et al., 2010; but *c.f.* Rueckschloss, Villmow & Klöckner, 2010; Mellor et al., 2014) and guinea pigs (Ferrara et al., 1995). Many studies also have shown similar effects in male rats (Capasso, Fitzpatrick & Anversa, 1992; Howlett, 2010; Lieber et al., 2004; Weisser-Thomas et al., 2007; Zhu, Altschaf, Hajjar, Valdivia & Schmidt, 2005), although others report that peak contraction is unaltered during ageing (Farrell & Howlett, 2007; Farrell & Howlett, 2008; Fraticelli, Josephson, Danziger, Lakatta & Spurgeon, 1989; Guo & Ren, 2006; Li et al., 2007; Ren, Li, Wu, Li & Babcock, 2007; Sakai, Danziger, Xiao, Spurgeon & Lakatta, 1992; Xiao, Spurgeon, O'Connor & Lakatta, 1994). Interestingly, all studies in rats and mice that showed a decline in peak contraction with age used rapid pacing frequencies (*e.g.* between 1 and 9 Hz), while those reporting no effect typically paced cells at slow rates (*e.g.* ≤ 0.5 Hz), well below physiological heart rates for rodents (Milani-Nejad & Janssen, 2014). This suggests that it is important to use cells that are challenged with physiological or near-physiological pacing frequencies when investigating the impact of age on cell shortening. These observations support the conclusion that a decline in the ability of individual cardiomyocytes to contract contributes to the age-dependent reduction in myocardial contractility seen in intact hearts, at least in male animals when cells are paced at physiological rates.

Table 2: Impact of age on cardiomyocyte contractile function

Component	Functional Change*	Species	References
Peak contraction	↓	Rat	Weisser-Thomas et al., 2007; Zhu et al., 2005; Lieber et al., 2004; Howlett, 2010; Capasso et al., 1992
		Mouse	Grandy & Howlett, 2006; Lim et al., 2000; Domeier et al., 2014; Ceylan-Isik et al., 2013; Li et al., 2005; Qin et al., 2013; Turdi et al., 2010
		Guinea pig	Ferrara et al., 1995
	↔	Rat	Fratricelli et al., 1989; Sakai et al., 1992; Xiao et al., 1994; Guo & Ren, 2006; Li et al., 2007; Ren et al., 2007; Farrell & Howlett 2007; 2008
		Mouse	Rueckschloss et al., 2010; Mellor et al., 2014
Time-to-peak contraction	↑	Rat	Fratricelli et al., 1989; Sakai et al., 1992; Capasso et al., 1992
		Mouse	Rueckschloss et al., 2010; Grandy & Howlett, 2006; Qin et al., 2013; Turdi et al., 2010
		Guinea pig	Ferrara et al., 1995
	↔	Rat	Xiao et al., 1994; Guo & Ren, 2006; Li et al., 2007; Ren et al., 2007; Howlett, 2010
		Mouse	Ceylan-Isik et al., 2013
	↓	Mouse	Mellor et al., 2014
Relaxation rate	slowed	Rat	Weisser-Thomas et al., 2007; Guo & Ren, 2006; Li et al., 2007; Ren et al., 2007; Lieber et al., 2004; Capasso et al., 1992
		Mouse	Rueckschloss et al., 2010; Lim et al., 2000; Ceylan-Isik et al., 2013; Li et al., 2005; Qin et al., 2013; Turdi et al., 2010
		Guinea pig	Ferrara et al., 1995
	↔	Rat	Fratricelli et al., 1989; Sakai et al., 1992; Xiao et al., 1994; Howlett, 2010
		Mouse	Grandy & Howlett, 2006; Domeier et al., 2014; Mellor et al., 2014

*↑ Arrow denotes an increase in function relative to young adults
 ↓ Arrow denotes a decrease in function relative to young adults
 ↔ Arrows denotes no difference in function between young adults and aged
 Comparisons are made between young adult (1-7 mos) and aged (13-33 mos) animals.

To determine whether the age-dependent slowing of contraction seen in multicellular preparations arises from slower contractions at the level of the cardiomyocyte, time-to-peak contraction and relaxation rates have been quantified, as summarized in Table 2. Time-to-peak contraction is prolonged with age in many studies in male animals (Capasso et al., 1992; Ferrara et al., 1995; Fraticelli, Josephson, Danziger, Lakatta & Spurgeon, 1989; Grandy & Howlett, 2006; Qin et al., 2013; Rueckschloss et al., 2010; Sakai et al., 1992; Turdi et al., 2010), although some have found no age-dependent change (Ceylan-Isik et al., 2013; Guo & Ren, 2006; Howlett, 2010; Li et al., 2007; Ren et al., 2007; Xiao et al., 1994) or even a decrease (Mellor et al., 2014). Interestingly, most of these latter studies (Ceylan-Isik et al., 2013; Guo & Ren, 2006; Li et al., 2007; Ren et al., 2007; Xiao et al., 1994) used sub-physiological pacing rates (*e.g.* 0.1-0.5 Hz), which may mask age-dependent slowing of contraction that is seen at faster rates. There also is considerable evidence that relaxation rates are slowed with age in cells from male rats, mice and guinea pigs, regardless of pacing frequency (Capasso et al., 1992; Ceylan-Isik et al., 2013; Ferrara et al., 1995; Guo & Ren, 2006; Li et al., 2005; Li et al., 2007; Lieber et al., 2004; Lim et al., 2000; Qin et al., 2013; Ren et al., 2007; Rueckschloss et al., 2010; Turdi et al., 2010; Weisser-Thomas et al., 2007), though some do report no age-dependent slowing (Domeier et al., 2014; Fraticelli et al., 1989; Grandy & Howlett, 2006; Howlett, 2010; Sakai et al., 1992; Xiao et al., 1994; Mellor et al., 2014). Taken together, these observations suggest that cardiomyocyte contractions are smaller and slower in cells from aged males when compared to younger adults. Thus, contractile dysfunction may arise as a consequence of a disruption in one or more components of the EC-coupling pathway, as discussed in the next section.

1.2.5 Age modifies Ca²⁺ homeostasis in cardiomyocytes from male animals

To determine whether age-related disruptions in cardiac contractions are accompanied by parallel changes in underlying Ca²⁺ transients, the impact of age on Ca²⁺ homeostasis in ventricular myocytes has been investigated. The results of these studies are summarized in Table 3. There is a growing consensus that peak Ca²⁺ transients decline with age in male rodents (Ceylan-Isik et al., 2013; Grandy & Howlett, 2006; Howlett, 2010; Li et al., 2005; Lim et al., 2000; Qin et al., 2013; Zhu et al., 2005), although some report no age-dependent change (Domeier et al., 2014; Farrell & Howlett 2007; 2008; Ren et al., 2007; Turdi et al., 2010) and one study even found an increase with age (Rueckschloss et al., 2010). As with contractions, smaller Ca²⁺ transients in aged myocytes are typically observed in studies that challenge cells with rapid pacing rates (Ceylan-Isik et al., 2013; Grandy & Howlett, 2006; Howlett, 2010; Li et al., 2005; Lim et al., 2000; Qin et al., 2013; Zhu et al., 2005), while those that report no effect tend to use lower stimulation rates (Domeier et al., 2014; Farrell & Howlett 2007; 2008; Ren et al., 2007). Thus, like the inability of the aged human heart to augment contractile function during exercise (as discussed in section 1.2), aged cardiomyocytes appear less able to respond to higher rates of stimulation and thus the aged phenotype may be unmasked at an increased rate.

Although age affects contractions and Ca²⁺ transients primarily at rapid pacing rates in male rodents, whether similar frequency-response results would be obtained in larger mammals is not clear. Few ageing studies have examined larger mammals (*e.g.* sheep, rabbits) and those that have used female animals, where age-dependent changes are minimal (Feridooni et al., 2015A). There may be important differences in frequency

responses between rodents and larger mammals, as rodents have much less contractile reserve than larger species (Endoh, 2004).

There is also good evidence that the time course of Ca^{2+} release is prolonged with age in males, with many studies reporting an increase in time-to-peak transient (Grandy & Howlett, 2006; Isenberg, Borschke & Rueckschloss, 2003; Ren et al., 2007; Zhu et al., 2005; but *c.f.* Howlett, 2010; Rueckschloss et al., 2010; Turdi et al., 2010; Xiao et al., 1994; Mellor et al., 2014) and virtually all reporting a marked prolongation of Ca^{2+} transient decay with age (Ceylan-Isik et al., 2013; Domeier et al., 2014; Howlett, 2010; Isenberg et al., 2003; Lim et al., 2000; Qin et al., 2013; Ren et al., 2007; Rueckschloss et al., 2010; Turdi et al., 2010; Zhu et al., 2005; but *c.f.* Xiao et al., 1994; Mellor et al., 2014). One might predict that slowed decay would lead to an increase in diastolic Ca^{2+} levels with age in cells from male animals. Still, there is no clear consensus on whether diastolic Ca^{2+} levels are affected by age, as there is evidence for unchanged, increased and reduced levels in cells from aged males (Table 3). Disparate results could be due to differences in experimental conditions between studies. Interestingly, under some circumstances, slower Ca^{2+} transients can actually augment contraction, as myofilaments are exposed to Ca^{2+} for a longer period of time (Daniels, Naya, Rundell & de Tombe, 2007). Taken together, these findings suggest that smaller and slower contractions that relax more slowly are attributable, at least in part, to smaller Ca^{2+} transients that decay more slowly in myocytes from male animals.

These changes in Ca^{2+} homeostasis with age are important. Careful control of Ca^{2+} in the cardiomyocyte is crucial, as intracellular Ca^{2+} is required to initiate contraction. Disruption of Ca^{2+} handling can contribute to CVD (Bers, 2014) and may predispose the

Table 3: Age-dependent changes in cardiomyocyte calcium transients

Component	Functional Change*	Species	References
Peak Ca²⁺ transient	↓	Rat	Howlett, 2010; Zhu et al., 2005
		Mouse	Grandy & Howlett, 2006; Lim et al., 2000; Ceylan-Isik et al., 2013; Li et al., 2005; Qin et al., 2013
	↔	Rat	Ren et al., 2007; Farrell & Howlett 2007; 2008
		Mouse	Domeier et al., 2014; Turdi et al., 2010
↑	Mouse	Rueckschloss et al., 2010	
Time-to-peak Ca²⁺ transient	prolonged	Rat	Ren et al., 2007; Zhu et al., 2005
		Mouse	Grandy & Howlett, 2006; Isenberg et al., 2003
	↔	Rat	Xiao et al., 1994; Howlett, 2010
		Mouse	Rueckschloss et al., 2010; Turdi et al., 2010; Mellor et al., 2014
Ca²⁺ transient decay rate	slower	Rat	Ren et al., 2007; Howlett, 2010; Zhu et al., 2005
		Mouse	Rueckschloss et al., 2010; Lim et al., 2000; Domeier et al., 2014; Ceylan-Isik et al., 2013; Qin et al., 2013; Isenberg et al., 2003; Turdi et al., 2010
	↔	Rat	Xiao et al., 1994
		Mouse	Mellor et al., 2014
Diastolic Ca²⁺	↑	Rat	Ren et al., 2007; Xiao et al., 1994
		Mouse	Qin et al., 2013; Isenberg et al., 2003
	↔	Rat	Howlett, 2010
		Mouse	Ceylan-Isik et al., 2013; Howlett et al., 2006; Mellor et al., 2014
	↓	Mouse	Grandy & Howlett, 2006

*↑ Arrow denotes an increase in function relative to young adults
 ↓ Arrow denotes a decrease in function relative to young adults
 ↔ Arrows denotes no difference in function between young adults and aged
 Comparisons are made between young adult (2-7 mos) and aged (20-33 mos) animals.

ageing heart towards the development of these diseases (Janczewski & Lakatta, 2010). Furthermore, disruption in the EC-coupling pathway with age may reduce the heart's ability to recover following CVD, such as ischemic heart disease (IHD).

1.3 AGE-DEPENDENT CHANGES IN CARDIAC FUNCTION AND STRUCTURE FOLLOWING IR

1.3.1 Age is a predictor of mortality in patients with IHD

The most common form of CVD in Canada and the United States is IHD (Public Health Agency of Canada, 2017; Odden et al., 2011). There are over 17 million people in Canada and the United States that have been diagnosed with IHD (Public Health Agency of Canada, 2017; Mozaffarian et al., 2016). Furthermore, the incidence of IHD in Canada and the United States has been rising and is projected to increase with the ageing population (Public Health Agency of Canada, 2017; Mozaffarian et al., 2016; Odden et al., 2011). IHD occurs when there is reduced blood flow to the heart; this is referred to as ischemia. During ischemia, the lack of oxygen and nutrients can cause extensive injury within the heart, which can lead to dysfunction and death. Pharmacological treatments such as fibrinolytic therapy, and surgical treatments such as stents and coronary artery bypass grafts, can be used to restore blood flow in patients with IHD. This restored blood flow to the ischemic heart is referred to as reperfusion. Although reperfusion is essential to salvage the ischemic myocardium, the heart can also be extensively damaged during the reperfusion process (Kloner, 1993).

A prominent example of IHD is the occurrence of acute myocardial infarction (AMI). The incidence of AMI in people increases with advanced age (van Oeffelen, Agyemang, Stronks, Bots, & Vaartjes, 2014). Furthermore, older people have higher

mortality rates following AMI when compared to younger adults (Rahimi, Duncan, Pitcher, Emdin & Goldacre, 2015; Mehta et al., 2001). In addition, surviving AMI patients live with lifelong disabling symptoms such as ischemic heart failure and angina. Moreover, patients who have experienced one AMI are at greater risk of AMI recurrence and have higher mortality rates than healthy individuals (Law, Watt & Wald, 2002; Johansson, Rosengren, Young & Jennings, 2017). The risk of AMI recurrence following a first episode is increased with advanced age (Johansson et al., 2017).

Treatment of AMI generally requires one of, or a combination of, pharmacologic or surgical reperfusion therapy. Not surprisingly, advanced age is the most powerful predictor of mortality following reperfusion therapy (Califf, Lee, Granger & Ohman, 1997). The unadjusted mortality rate following reperfusion therapies is ~30 percent in people who are 80+ years of age, in contrast to the ~5-10 percent mortality rate in patients who are between the ages of 50-65 years (Califf et al., 1997; Mehta et al., 2001). Thus, it is expected that the burden of disease will increase. More healthcare providers, treatment options and institutions will be necessary to cope with the large ageing population that is at risk for developing IHD. The projected increase in IHD also means more people undergoing reperfusion therapy. Since advanced age has a major influence on IHD and reperfusion therapy outcomes, it is essential to explore the impact of age on the underlying mechanisms that affect the heart's ability to recover following IR. In the following sections, the impact of age on cardiac contractile function following IR events in clinical and pre-clinical studies will be reviewed, with a primary focus on studies that have used the Langendorff-perfused heart model.

1.3.2 Impact of age on cardiac function following IR in humans

Section 1.2 presented evidence for age-dependent decline in contractile function in hearts from individuals without overt CVD. These age-dependent changes at the subcellular, cellular and organ levels may hinder the heart's ability to recover following IR. In fact, there is clinical evidence that ageing further exacerbates the decline in contractile function observed when the heart is exposed to IR. For example, as previously stated, the heart's ability to augment contractile function during exercise is compromised with advanced age (Lakatta & Levy, 2003; Stratton et al., 1994; Wei, 1992). This inability to increase the workload of the heart is further hindered by IHD. Older patients with IHD have higher resting HRs and lower maximal HRs during exercise than age-matched healthy individuals (Kasser & Bruce, 1969). Furthermore, older patients with IHD have lower HR reserve when compared to age-matched healthy individuals (Kasser & Bruce, 1969). Age is also a major factor in LV function at rest in IHD patients as discussed below.

Diastolic and systolic function of the LV have been assessed in hearts from older (>75 years of age) and middle-aged (~55 years of age) AMI patients at rest using echocardiography. There is evidence that the E/A ratio, a measure of diastolic function, declines in hearts from older AMI patients compared to middle-aged AMI patients (Liu et al., 2012). Furthermore, LV ejection fraction, a measure of LV systolic function, is markedly lower in older patients with AMI compared to middle-aged patients with AMI (Liu et al., 2012; Kwok et al., 2017). In addition, LV fractional shortening is also attenuated with age in AMI patients (Liu et al., 2012). Interestingly, LV function, specifically poor LV ejection fraction (ejection fraction <30%), has been associated with increased mortality rates in IHD patients (Kwok et al., 2017). Older AMI patients have

worse diastolic and systolic function compared to middle-aged AMI patients which may increase their susceptibility to heart failure and death. Indeed, the prevalence of poor LV ejection fraction, and thus the mortality rate of IHD patients, increases with advanced age (Kwok et al., 2017).

Age can also reduce IR tolerance in isolated muscle preparations from humans. For example, one study investigated the impact of age on contractile function in isolated human atrial pectinate muscle preparations under ischemic and hypoxic conditions (Mariani et al., 2000). Developed force in trabecula declines following exposure to hypoxia and ischemia (Mariani et al., 2000). This decline in developed force during reperfusion is much greater in trabecula isolated from individuals aged 60-89 years old, compared to individuals aged 34-59 years old (Mariani et al., 2000). This suggests that age may impair the ability of the heart muscle to contract following exposure to ischemic conditions, although whether this also occurs in the ventricle has not been investigated in humans.

Taken together, there is evidence that advanced age reduces IR tolerance in humans. Therefore, it is essential to explore the impact of age on cardiac contractile function following IR in pre-clinical studies to better understand the underlying mechanisms.

1.3.3 Age affects the ability of the male rodent heart to recover from IR

The effects of age on cardiac contractile function following IR has been studied in various animals under different experimental conditions. The findings from these studies are summarized in Table 4 and Table 5. There are a variety of methods that can be used to induce IR in rodents. For example, temporary occlusion of the left anterior descending artery and left coronary artery will induce ischemia, and removal of the occlusion will

induce reperfusion (Liu, Xu, Cavalieri & Hock, 2002; Liu et al., 2012). Ischemia can also be induced by reducing the perfusion pressure in Langendorff-perfused hearts, while increasing the perfusion pressure will induce reperfusion (Abete et al., 1999). The most widely used method of inducing IR is by global, no-flow ischemia, where hearts are not perfused for a period of time. Reperfusion is initiated when the heart is perfused with buffer (Wang et al., 2018; Headrick et al., 2003; Willems et al., 2005; Ashton et al., 2003). The method and duration of IR affects cardiac contractile recovery. For example, recovery of cardiac contractile function is less complete when murine hearts are exposed to 30 min of ischemia than when hearts are exposed to 20 min ischemia (Reichelt, Willems, Hack, Peart & Headrick, 2009). Because many studies use different experimental protocols, there is variability in the results of IR studies. The following discussion will group the results of IR studies based on similar experimental protocols.

It is widely accepted that cardiac contractile function is impaired following exposure to IR, regardless of age (Headrick, 1998; Escobales et al., 2014; Reichelt et al., 2009; Wang et al., 2018; Headrick et al., 2003; Willems et al., 2005; Abete et al., 1999; Liu et al., 2012). Moreover, advanced age reduces the tolerance to IR injury and further impairs cardiac contractile function following IR *in vivo* (summarized in Table 4). For example, echocardiography shows that LV ejection fraction and fractional shortening decline in murine hearts following the occlusion of the left anterior descending artery (Wang et al., 2018). The recovery of systolic function in these hearts following 24 h of reperfusion is worse in aged mice (24-26 mos) compared to young adults (4-6 mos) (Wang et al., 2018). Other *in vivo* studies in rats measured cardiac contractile function using a catheter probe inside the LV of hearts that were exposed to 30 min of left coronary artery

Table 4: Recovery of cardiac contractile function following IR is reduced with advanced age in male rodents in vivo

Species	IR conditions	Component	Functional Change*	Reference
Rats	Catheter probe in left carotid artery 30 min LCA occlusion 3hr,4hr, 24 hr reperfusion	LVSP	↓	Liu et al., 2012
		LVEDP	↑	Liu et al., 2012
		+dP/dt	↓	Liu et al., 2012
		-dP/dt	↓	Liu et al., 2012
		Cardiac index	↓	Liu et al., 2002
		Stroke volume index	↓	Liu et al., 2002
Mice	Echocardiography 45 min LAD occlusion 24 hr reperfusion	Ejection fraction	↓	Wang et al. 2018
		Fractional shortening	↓	
		HR	↔	

*↑ Arrow denotes an increase in function relative to young adults
 ↓ Arrow denotes a decrease in function relative to young adults
 ↔ Arrows denotes no difference in function between young adults and aged
 Comparisons are made between young adult (2-6 mos) and aged (19-26 mos) animals.

occlusion (Liu et al., 2002; Liu et al., 2012). Cardiac output and stroke volume is significantly lower in hearts from aged male rats compared to young rats following IR (Liu et al., 2002). Furthermore, recovery of LV systolic pressure, +dP/dt, and -dP/dt is significantly lower in aged hearts that are exposed to ischemia (Liu et al., 2012). In addition, LVEDP increased more in aged rat hearts compared to younger animals (Liu et al., 2012). By contrast, age does not affect myocardial oxygen consumption following IR (Abete et al., 1999; Headrick, 1998).

In vitro studies using Langendorff-perfused rodent hearts exposed to IR reinforce the results of *in vivo* studies. The results from studies that exposed Langendorff-perfused aged rat hearts to IR are summarized in Table 5. Middle aged (16 mos) rat hearts have less tolerance to IR injury than hearts from young rats (4 mos) (Boucher et al., 1998). Paradoxically, there is evidence that aged rats (24 mos) have higher tolerance to IR than middle aged rats (Boucher et al., 1998). Boucher *et al.* (1998) showed that LVDP recovery following IR was similar in hearts from aged and young rats. However, the recovery of LVDP was significantly smaller following IR in middle aged rats when compared to young rats (Boucher et al., 1998). Another study showed that recovery of LVDP was similar between aged and young rat hearts following IR (Abete et al., 1999). Interestingly, these studies did not discuss potential mechanisms of action for the cardioprotection following IR in aged hearts *in vitro*. Furthermore, these findings contradict human clinical data where mortality rates were higher in the older AMI patients (Kwok et al., 2017). This suggests that there may be other systems which contribute to the increased mortality *in vivo* that are omitted during *in vitro* studies. On the contrary, other studies show that recovery of LVDP, +dP/dt, -dP/dt, and RPP is less in aged rats compared to young rats following IR (Escobales

Table 5: Effect of age on contractile function following IR in Langendorff-perfused hearts from male rodents

Species	IR conditions	Component	Functional Change*	Reference	
Mice	Global Ischemia: 20-25 min Reperfusion: 30, 45, 60 min	LVDP	↓	Headrick et al., 2003; Willems et al., 2005; Ashton et al., 2003	
		+dP/dt	↓		Headrick et al., 2003; Willems et al., 2005
		RPP	↓		Wang et al. 2018; Porter et al., 2014
		Diastolic pressure	↑		Wang et al. 2018; Headrick et al., 2003; Willems et al., 2005; Ashton et al., 2003
		Coronary flow	↔		Headrick et al., 2003; Willems et al., 2005
			↓		Ashton et al., 2003
		Cardiac output	↓		Wang et al. 2018
Rats	Global Ischemia: 20-25 min Reperfusion: 30, 45, 60 min	LVDP	↓	Escobales et al., 2014; Headrick, 1998; Lesnefsky et al., 1994	
			↔		Boucher et al., 1998
		+dP/dt	↓		Escobales et al., 2014; Lesnefsky et al., 1994
		-dP/dt	↓		Escobales et al., 2014; Lesnefsky et al., 1994
		RPP	↓		Escobales et al., 2014; Headrick, 1998
		Diastolic pressure	↑		Headrick, 1998
			↔		Escobales et al., 2014; Boucher et al., 1998
			↓		Lesnefsky et al., 1994
		Coronary flow	↔		Headrick, 1998; Boucher et al., 1998
		HR	↓		Headrick, 1998
	↔	Escobales et al., 2014			
	MVO ₂	↔	Headrick, 1998		
Rats	Decreased perfusion pressure (66, 59, 51, 44, 36, 29 mmHg): Each step lasted 10 min. 20 min reperfusion after each step	LVDP	↔	Abete et al., 1999	
		+dP/dt	↓		
		LVEDP	↑		
		Coronary flow	↔		
		MVO ₂	↔		
		Fractional shortening	↓		
		HR	↔		

*↑ Arrow denotes an increase in function relative to young adults
 ↓ Arrow denotes a decrease in function relative to young adults
 ↔ Arrows denotes no difference in function between young adults and aged
 Comparisons are made between young (2-6 mos) and aged (16-29 mos) animals.

et al., 2014; Headrick, 1998). Additionally, some studies report that diastolic pressure is further increased in aged hearts following IR (Headrick, 1998; Abete et al., 1999) while others do not (Escobales et al., 2014; Boucher et al., 1998).

Interestingly, mice also exhibit age-dependent decline in cardiac contractile recovery following global no-flow ischemia (Table 5). Hearts from aged mice (16-25 mos) show less recovery of LVDP, +dP/dt, RPP, and cardiac output, compared to young mice (4-8 mos) following IR (Wang et al., 2018; Willems et al., 2005; Headrick et al., 2003; Ashton et al., 2003). Furthermore, these aged hearts have higher diastolic pressures following IR than their young counterparts (Wang et al., 2018; Willems et al., 2005; Headrick et al., 2003; Ashton et al., 2003). Interestingly, functional recovery is similar in hearts from middle aged (12-18 mos) and hearts from aged animals (24-28 mos) following IR (Willems et al., 2005). Willems *et al.* (2005) showed that IR intolerance, measured as the percent change in recovery of LVDP, improved in aged mice (24-28 mos) when compared to middle aged mice (12 mos). Together, these results indicate that recovery of cardiac contractile function following IR is reduced with advanced age in people and in male rodents. Interestingly, there is evidence that recovery of function can be similar when comparing aged and middle age hearts.

Other studies have investigated the impact of age on coronary flow following IR in male rodent hearts. There is general agreement that coronary flow does not decline with age following IR in the rat model (Headrick et al., 2003; Headrick, 1998; Abete et al., 1999; Boucher et al., 1998). The study by Willems *et al.* (2005) shows that coronary flow is reduced in aged hearts (24-28 mos) in comparison to young hearts (2-4 mos). However, there were no significant difference in flow rates between middle-aged hearts (8-12 mos)

and aged hearts (24-28 mos) following IR (Willems et al., 2005). In addition, the studies that reported an age-dependent decline in coronary flow following IR, used young (2-4 mos) and old (18 mos) animals (Ashton et al., 2003).

Taken together, evidence suggests that ageing attenuates the tolerance to IR and the heart's ability to recover following IR declines. However, there is some evidence that tolerance to IR improves in aged animals compared to middle aged and young animals, although more research in this area is warranted. Age can also impact survival and injury following exposure to IR. The impact of age on IR injury markers are explored in the next section.

1.3.4 Influence of age on myocardial injury and survival following IR

Early diagnosis and treatment of AMI is crucial in reducing IR injury and improving mortality clinically. To diagnose AMI, clinicians rely on the patient's symptoms (*i.e.* chest pain), electrocardiogram features, and biomarkers for cardiac cell death as described below. However, early diagnosis of AMI in older adults can be challenging. For instance, only 40 percent of individuals over the age of 85 display chest pain as a symptom of AMI (Saunderson et al., 2014). By contrast, 80 percent of individuals under 65 years of age display chest pain as a symptom of AMI (Saunderson et al., 2014). Furthermore, not all patients display changes in their electrocardiogram that are attributed to AMI (Saunderson et al., 2014). Therefore, clinicians also use different biomarkers of IR injury, in conjunction with the patient's symptoms and electrocardiogram tests, to quickly and effectively diagnose AMI.

Biomarkers of IR injury are assessed from an AMI patient's blood sample taken

upon admission to the hospital and several times thereafter during their stay in the hospital. The different biomarkers for IR injury used clinically are: creatine kinase isoenzyme, aspartate aminotransferase, heart fatty acid binding protein, ischemia modified albumin, myoglobin, lactate dehydrogenase (LDH), cardiac specific troponin T, and cardiac specific troponin I (cTnI) (Tiwari et al., 2012). The plasma concentrations of these markers increase with time following AMI (Tiwari et al., 2012; Bavia et al., 2018). However, these various biomarkers present themselves at different times during an AMI incident. For example, creatine kinase isoenzyme is released into the blood 3-12 hours post AMI, while LDH is present in the blood 12-24 hours after an AMI (Tiwari et al., 2012; Bavia et al., 2018). Other biomarkers such as myoglobin and cTnI are released 2-3 hours and 3-12 hours respectively, following an AMI (Tiwari et al., 2012; Bavia et al., 2018).

The most common biomarker used to diagnose AMI in people is creatine kinase (Tiwari et al., 2012). However, creatine kinase has poor specificity for AMI because it is present in other tissues throughout the body, notably the skeletal muscle (Romić, Unić, Derek & Pehar, 2009; Tiwari et al., 2012). For instance, creatine kinase concentrations can be elevated during exercise if there is skeletal muscle damage (Romić et al., 2009). Thus, plasma creatine kinase levels can be elevated by factors unrelated to the heart, which may interfere with the diagnosis of AMI. By contrast, the recent development of assays for cTnI has revolutionized the field (Bavia et al., 2018; Tiwari et al., 2012). This is because cTnI is the most specific and sensitive biomarker of AMI followed by heart fatty acid binding protein, myoglobin, and creatine kinase (Pyati et al., 2016; Tiwari et al., 2012). A recent study shows that cTnI release is substantially elevated in AMI patients compared to patients without AMI (Tecson et al., 2017). Indeed, cTnI has become the new gold

standard in the diagnosis of AMI.

Although biomarkers are useful in the diagnosis of AMI, there is emerging evidence that they are affected by a patient's age. Older AMI patients have a higher release of plasma cTnI than young adults with AMI (Liu et al., 2012; Croce et al., 2017). By contrast, a recent study shows that older AMI patients have lower plasma creatine kinase, LDH, and troponin T concentrations than younger AMI patients (Sulzgruber et al., 2018). Interestingly, extensive myocardial damage as indicated by these biomarkers in the younger AMI group was not associated with higher mortality or worse LV function when compared to the older AMI patients (Sulzgruber et al., 2018). In addition to the release of biomarkers as a sign of IR injury, there is also evidence that cardiomyocytes undergo apoptosis following AMI (Saraste et al., 1997). The apoptotic factors released following an AMI can also be measured to assess the IR injury. Older patients with AMI have higher levels of plasma apoptotic factors such as TNF- α , IL-6, and sFAS, when compared to younger AMI adults (Liu et al., 2012). There is evidence that age impacts IR-induced cardiac muscle cell death (Liu et al., 2012; Croce et al., 2017), although this has not been seen in all studies (Sulzgruber et al., 2018). The results of studies examining the influence of age on biomarkers and apoptosis following exposure to IR in humans is highlighted in Table 6. Overall, these data suggest that there is greater myocardial injury, as indicated by higher plasma cTnI concentrations, and higher cardiomyocyte death in hearts from older AMI patients. A recent study shows a decline in the biomarkers creatine kinase, LDH, and troponin T with age, which may suggest there is heterogeneity in cardiac ageing and tolerance to IR.

The influence of age on markers of IR injury has also been investigated in rodent

Table 6: Influence of age on clinical markers of injury following IR

Species	Component	Functional Change*	Reference
Humans	Plasma cTnI	↑	Liu et al., 2012; Croce et al., 2017
	Plasma apoptotic factors <i>(sFAS, TNF-α, IL-6)</i>	↑	Liu et al., 2012
	Plasma creatine kinase	↓	Sulzgruber et al., 2018
	Plasma LDH	↓	Sulzgruber et al., 2018
	Plasma troponin T	↓	Sulzgruber et al., 2018

*↑ Arrow denotes an increase in function relative to young adult

↓ Arrow denotes a decrease in function relative to young adult

Comparisons are made between young adult (<45-64 years) and aged (65-84 years) patients.

models as summarized in Table 7. As seen in the older patients, old rats have higher levels of plasma apoptotic factors (IL-6, TNF- α , sFAS) and more apoptosis after IR when compared to young rats (Liu et al., 2012; Liu et al. 2002; Escobales et al., 2014). Furthermore, there is an age-dependent increase in plasma biomarkers including cTnI, LDH, and creatine kinase following exposure to IR (Liu et al., 2012; Headrick, 1998; Lesnefsky et al., 1994 *c.f.* Abete et al., 1999). The higher levels of apoptosis and IR injury biomarkers suggest that aged rat hearts should have larger infarcts when compared to young rat hearts (Liu et al., 2012), although this has not been seen in all studies (Escobales et al., 2014). Similar to rats, mice also experience greater IR injury and myocardial cell death with increasing age (Table 7). Hearts from aged mice that are exposed to IR have increased necrosis and apoptosis (Azhar, Gao, Liu & Wei, 1999). Furthermore, IR results in increased release of LDH and cTnI (Willems et al., 2005; Headrick et al, 2003; Ashton et al., 2003; Wang et al., 2018). Interestingly, Willems *et al.* (2005) showed an increase in LDH efflux following IR with age when comparing mice ages 2-4 mos and 12 mos. However, LDH efflux following IR was similar in mice ages 2-4 mos and 18-28 mos (Willems et al., 2005). All of these factors contribute to larger infarct sizes in the aging heart (Wang et al., 2018; Azhar et al., 1999). These data suggest that age impacts the heart's ability to tolerate IR injury and help explain why there is poor LV function following IR in the aging heart. However, the heart's ability to tolerate IR injury declines as the mouse matures from young to middle aged but improves as the middle-aged mouse ages.

Table 7: Effects of age on markers of injury following IR in male rodents

Species	Component	Functional Change*	Reference
Rats	Plasma cTnI	↑	Liu et al., 2012
	Plasma apoptotic factors (<i>sFAS, TNF-α, IL-6</i>)	↑	Liu et al., 2012
	Infarct size	↑	Liu et al., 2012
		↔	Escobales et al., 2014
	Apoptosis	↑	Liu et al., 2002; Liu et al., 2012; Escobales et al., 2014
	Creatine kinase	↔	Abete et al., 1999
		↑	Headrick, 1998; Lesnefsky et al., 1994
LDH release	↑	Lesnefsky et al., 1994	
Mice	cTnI release	↑	Wang et al., 2018
	Infarct size	↑	Wang et al., 2018; Azhar et al., 1999
	LDH efflux	↑	Willems et al., 2005; Headrick et al., 2003; Ashton et al., 2003
	Apoptosis	↑	Azhar et al., 1999
	Necrosis	↑	Azhar et al., 1999

*↑ Arrow denotes an increase in function relative to young adults
 ↔ Arrows denotes no difference in function relative to young adults
 Comparisons are made between young adults (2-6 mos) and aged (16-29 mos) animals

1.3.5 Summary

Overall, there is evidence that heart function declines with age even in the absence of overt CVD. These age-dependent changes occur in the intact heart, and at the cellular and subcellular levels and are summarized in Tables 1, 2 & 3. Furthermore, age impacts the heart's ability to tolerate IR injury (Tables 4, 5, 6 & 7). However, there is evidence that the heart's ability to tolerate IR injury may improve as the adult mouse ages, although this was not observed in the clinic. Importantly, these age-dependent changes in heart function before and after exposure to IR, are reflective of average responses. Indeed, these studies do not consider the heterogeneity in ageing individuals, which may affect myocardial function. In addition, many pre-clinical studies use exclusion criteria, which may mask age-dependent heterogeneity in cardiovascular responses. The concept of frailty has been widely used to account for heterogeneity in ageing in the clinical literature and is introduced in the next section.

1.4 FRAILITY

1.4.1 Introduction to frailty

It has been observed that people age at different rates so that their chronological age may not always reflect their biological age (Clegg et al., 2013; Rockwood, Hogan & MacKnight, 2000; Mitnitski, Howlett & Rockwood, 2017). The concept of frailty has been widely used to account for this unmeasured heterogeneity in biological ageing for people of the same chronological age (Mitnitski et al., 2017). Frailty can be defined as a state of increased vulnerability to adverse health outcomes in individuals of the same age (Rockwood et al., 1994; Bergman et al., 2007; Singh et al., 2014). One common view of

frailty is that it occurs through the accumulation of deficits in health (Howlett & Rockwood, 2013; Rockwood et al., 1994). Specifically, it is believed that every individual has a physiological reserve (Rockwood et al., 1994). This physiological reserve declines over time as deficits accumulate at the subcellular and cellular levels (Howlett & Rockwood, 2013). As these deficits accumulate, the body loses the ability to remove or repair these deficits, allowing them to scale up to impair the organs and eventually the entire system (Rockwood et al., 1994; Howlett & Rockwood, 2013; Blodgett, Theou, Howlett & Rockwood, 2017). Therefore, frailty can be used to quantify an individual's overall health status and vulnerability to stressors (Hubbard et al., 2017).

Frailty is not considered to be “all-or-nothing” (Rockwood et al., 1994). In fact, it is a dynamic model where it can change over time for better or for worse (de Vries et al., 2011; Rockwood et al., 1994). Factors that affect a person's frailty are categorized into three domains: physical, psychological, and social domains (de Vries et al., 2011). Changes in factors within these domains, such as impaired mobility, can cause a person to become more frail (Theou, Blodgett & Godin, 2017). By contrast, interventions such as exercise have been seen to improve frailty (Hubbard, Fallah & Searle, 2009; de Vries et al., 2011; Theou et al., 2017). Therefore, individuals exist on a continuum between frail and not frail (de Vries et al., 2011).

There are a number of different frailty instruments that are used to quantify frailty in clinical studies (de Vries et al., 2011). However, measuring frailty in humans can be challenging. This is because some frailty instruments have components that are too specific or are too difficult to complete for certain elderly sub-populations (Hubbard et al., 2017; de Vries et al., 2011). For example, some frailty instruments may have a

performance test which would be impossible for a bedridden patient. This can impair the accuracy of the frailty tool. Furthermore, many frailty tools have poor predictive properties and limited sensitivity towards adverse outcomes (Hubbard et al., 2017; de Vries et al., 2011). In addition, many frailty tools have not been assessed for their reliability, agreement, responsiveness, floor and ceiling effects, and interpretability (de Vries et al., 2011). While there are many different ways to assess frailty in clinical populations, there is no clear consensus on which tool to use (Howlett & Rockwood, 2013). However, the Frailty Phenotype and the FI tool are the two most commonly used frailty instruments in clinical studies (de Vries et al., 2011; Howlett & Rockwood, 2013).

1.4.2 Frailty assessment tools used clinically

The Frailty Phenotype instrument considers that frailty is a syndrome (Fried et al., 2001). It defines frailty based on five specific items (Fried et al., 2001). These five items are age-associated declines in strength, walking speed, self-reported exhaustion, unintentional weight loss and low physical activity (Fried et al., 2001). Individuals are said to be frail if they have three of the five items listed above (Fried et al., 2001). If a person has one or two items, they are labelled as pre-frail (Fried et al., 2001). Finally, a robust person has none of these items (Fried et al., 2001). The Frailty Phenotype instrument has been validated through its ability to predict mortality in the elderly population. Mortality is highest in the frail group, followed by the pre-frail and the robust group (Fried et al., 2001). Furthermore, the Frailty Phenotype correlates well with the FI, which allows for some clinical comparisons across different frailty instruments (Rockwood, Andrew & Mitnitski, 2007; de Vries et al., 2011; Cigolle, Ofstedal & Tian, 2009). However, there are

certain disadvantages of using the Frailty Phenotype. First, the Frailty Phenotype is focused on a physical frailty and does not contain any frailty factors that pertain to other bodily systems or to the psychological, cognitive, and social domains (de Vries et al., 2011). Second, this instrument has performance tests that may not be readily operationalized in clinical settings and may not be feasible for all patients (Rockwood et al., 2007). Finally, the Frail Phenotype only uses five items to determine frailty, which can result in floor and ceiling effects (de Vries et al., 2011).

The other widely used frailty instrument is the FI. The FI considers frailty as a multidimensional and dynamic state, and uses the concept of deficit accumulation (Howlett & Rockwood, 2013; Rockwood & Mitnitski 2007; Mitnitski et al., 2017). This is a sensitive instrument that measures the overall health of older individuals (Mitnitski & Rockwood, 2015). The FI tool works by counting clinically recognized health deficits across many systems that fall within physical, psychological, and social domains (Mitnitski et al., 2017; Howlett & Rockwood, 2013; Rockwood et al., 2007). Interestingly, the items used as deficits in the FI are not specific and can be any sign, symptom, disability, disease, or laboratory abnormality observed clinically (Rockwood & Mitnitski, 2007; Rockwood & Mitnitski, 2011). There are only a few criteria that are required to select a health deficit for the FI tool. For example, a deficit should be prevalent in at least 1% of the population, but not be saturated (*e.g.* present) in more than 80% of people less than 90 years of age (Searle, Mitnitski & Gahbauer, 2008). In addition, these deficits should accumulate with age (Searle et al., 2008). Deficits used to construct an FI should include items that pertain to different organ systems (Searle et al., 2008). Finally, if at least 30 health deficits are included in an FI, the resulting FI score is independent of the individual deficits (Searle et

al., 2008). Frailty is measured by adding up all of the health deficits present in an individual, and dividing by the total number of deficits measured to yield an FI score that is between 0 and 1 (Mitnitski et al., 2017). For example, if the total number of deficits measured is 40, and someone has 10 health deficits, the FI score would be $10/40 = 0.25$. This method gives a frailty score between 0 (not frail) and 1 (frail) (Rockwood et al., 2017). The FI has been validated in many studies. For example, high FI scores have been shown to predict mortality, where the higher the FI score, the greater the mortality rate in people of the same age (Rockwood & Mitnitski, 2011; Rockwood, Rockwood & Mitnitski, 2010).

There are many advantages to the FI tool. The FI is the only frailty instrument that fully measures health deficits pertaining to physical, psychological, and social domains (de Vries et al., 2011). Furthermore, the concept of FI is that “the whole is greater than the sum of its parts”. This is because individual health deficits within the FI are all weighted equally (Mitnitski & Rockwood, 2015). This makes it easy to add and remove any health deficit as long as it follows the criteria explained above (Searle et al., 2008). In addition, the FI is a continuous score, which makes it more responsive to changes in health status when compared to the Frailty Phenotype (de Vries et al., 2011; Mitnitski & Rockwood, 2015). Moreover, many studies have shown that there are no floor or ceiling effects with the FI (de Vries et al., 2011). Finally, the items that make up an FI are not fixed so it is easy to modify for use in many different sub-populations of older adults (Hubbard et al., 2017).

The dynamic nature of frailty makes it an exciting research target, with the aim of preventing, maintaining, or reducing frailty. However, there are many challenges in performing clinical studies in frail, ageing individuals. For example, the frail ageing

population is diverse with different morbidities and polypharmacy. It is difficult to create ideal experimental conditions in such a vulnerable population. Therefore, it is essential to develop animal models to study the mechanisms involved in frailty and test any possible interventions.

1.4.3 Frailty assessment tools used in animal models

There are several animal models of frailty that can be used to study the biology of frailty. The two most common animal models of frailty are based on tools used clinically. These are the phenotype and the FI (Kane et al., 2017B). The phenotype method of assessing frailty in mice was developed by Liu and colleagues, and is based on Fried's clinical Frailty Phenotype model (Liu, Graber, Ferguson-Stegall & Thompson, 2014). This mouse frailty instrument assesses frailty based on the grip strength, physical activity, walking speed, and endurance (Liu et al., 2014). More specifically, grip strength is determined by using the inverted-cling grip test, physical activity is determined by voluntary wheel running, walking speed is evaluated using the rotarod test, and endurance is a composite score determined from the animal's walking speed and grip strength (Liu et al., 2014). There are several notable advantages to using the phenotype frailty method. First, studies show that the frailty phenotype can detect changes in frailty when an intervention is used (Graber, Ferguson-Stegall, Liu & Thompson, 2015). Second, this is a non-invasive method of assessing frailty, which allows its use throughout longitudinal studies (Liu et al., 2014). However, this tool only uses four items, which creates floor and ceiling effects. In fact, the phenotype frailty method failed to identify mice as frail whereas, the same mice were identified as frail by the FI tool (Kane et al., 2017B).

The FI tool used to assess frailty in mice is based on the concept of deficit accumulation used clinically (Parks et al., 2012). This approach to measuring frailty in naturally ageing C57BL/6 mice was first developed by Parks *et al.* (2012). This FI is similar to the clinical FI instrument, where 31 age-dependent health deficits were selected for the FI (Parks et al., 2012). These health deficits were derived from activity levels, hemodynamic measures, body composition, and measures of basic metabolic status of the mouse (Parks et al., 2012). Similar to clinical FI studies, FI scores are higher in aged mice compared to adult mice (Parks et al., 2012). However, there are limitations to the use of this FI tool. Some of the measures are invasive, so it would be too difficult to use this FI tool for longitudinal studies. Furthermore, this original FI requires specialized equipment that may not be available in all labs. Therefore, a more simple and non-invasive set of health deficits was selected to develop a non-invasive approach to quantify frailty in mice (Whitehead et al., 2014). Whitehead *et al.* (2014) developed this non-invasive FI tool based on the concept of deficit accumulation as in the original study (Parks et al., 2012). This FI tool measures the overall health status of a mouse by assessing changes in the integument, physical/musculoskeletal system, vestibulocochlear/auditory system, ocular/nasal system, digestive/urogenital, respiratory system, signs of discomfort, as well as the body weight and temperature (Whitehead et al., 2014). Details of all of the health deficits, and the scoring of each deficit, are presented in the original study (Whitehead et al., 2014) and in detail in the Methods section of this thesis.

This non-invasive FI tool allows researchers to follow a cohort of mice throughout their natural lifespan (Rockwood et al., 2017). The result of this work shows that the progression of frailty in these naturally ageing mice is similar to that in humans (Rockwood

et al., 2017). Interestingly, deficit accumulation in naturally ageing C57BL/6 mice also progresses in a fashion similar to deficit accumulation in humans (Rockwood et al., 2017). Furthermore, frailty increases at the same rate with age in both mice and humans (Whitehead et al., 2014; Rockwood et al., 2017). Both humans and C57BL/6 mice have a submaximal limit to their frailty score (<0.7 in humans, <0.6 in mice) (Mitnitski et al., 2017; Rockwood & Mitnitski, 2006). Thus, the non-invasive FI used in mice provides a successful animal model of frailty that resembles the FI used clinically. The mouse FI is a powerful instrument that can help in understanding underlying mechanisms at the cellular level that may lead to frailty in pre-clinical models. Furthermore, this tool can be used to investigate the links between ageing, frailty, and disease in an animal model.

1.4.4 Influence of frailty on heart function in humans and mice

Many clinical studies show that frailty increases with age (Howlett & Rockwood, 2013; Singh et al., 2014; Rockwood & Mitnitski, 2007; Rockwood et al., 2017). Likewise, elderly people are much more likely to suffer from multiple medical problems, and are thus, much more likely to be frail (Clegg et al., 2013; Adabag et al., 2018). These frail individuals are susceptible to higher morbidity and all-cause mortality when compared to non-frail individuals (Afilalo et al., 2014; Singh et al., 2014). Moreover, frail individuals are more likely to develop various diseases, including CVD, than their non-frail counterparts (Singh et al., 2014; Afilalo et al., 2014; Chen, 2015; Adabag et al., 2018; Kusunose et al., 2018). What is more, frail individuals who do develop CVD have higher mortality and morbidity than non-frail patients (Afilalo et al., 2014; Singh et al., 2014; Chen, 2015; Goldwater & Pinney, 2015; Adabag et al., 2018; Kusunose et al., 2018). There

is also evidence that individuals who undergo surgical treatment for CVD have higher mortality than non-frail patients (Afilalo et al., 2014; Singh et al., 2014; Chen, 2015). Furthermore, frail individuals are more likely to be institutionalized and for longer periods of time following treatment for CVD compared to non-frail individuals of the same age (Hubbard et al., 2017; Singh et al., 2014; Goldwater & Pinney, 2015; Rockwood et al., 2004; Clegg et al., 2013; Chen, 2015). Despite the clear links between frailty and CVD, little is known about the relationship between frailty and the heart. The relatively recent development of animal models of frailty provides an excellent opportunity to improve our understanding of the links between ageing, frailty, and heart function in a controlled setting.

Although information is limited, there is some preliminary evidence for links between frailty and heart function from preclinical studies. For example, age-dependent cardiomyocyte hypertrophy has been shown to increase with frailty in aging mice (Parks et al., 2012). Furthermore, ventricular myocyte contraction is also smaller in hearts isolated from frail mice when compared to younger animals (Parks et al., 2012). Several studies observed the impact of frailty on sinoatrial node function in mice (Moghtadaei et al., 2016; Jansen et al., 2017). These studies showed more interstitial fibrosis and collagen production in the sinoatrial node of mice with high FI scores compared to those with lower scores (Moghtadaei et al., 2016; Jansen et al., 2017). Furthermore, frailty is correlated with a decline in HR and sinoatrial function (Moghtadaei et al., 2016; Jansen et al., 2017). Conduction velocity is also slower in the sinoatrial nodes from older, more frail mice than from non-frail mice (Moghtadaei et al., 2016; Jansen et al., 2017). Together these studies

suggest that age-dependent changes in cardiac function are influenced by the overall health of the animal, which can be quantified in an FI.

1.5 Hypothesis and objectives

Based on the existing clinical and basic science literature, there is an average decline in cardiac contractile function with age, in the presence and absence of disease. However, there is heterogeneity in this age-dependent decline in heart function that may reflect the frailty status of the individual. The overall hypothesis to be tested in this thesis is that cardiac contractile function, in the absence and presence of IR, declines with age and is related to the FI score. The specific objectives are:

- 1) To determine the effect of age on cardiac contractile function and structure in adult and aged mice.
- 2) To optimize the mouse clinical FI and determine if it is reliable between raters.
- 3) To investigate the relationship between frailty and age-dependent remodelling in the ventricles from adult and aged mice using the optimized FI tool.
 - a. Quantify frailty in adult and aged C57BL/6J mice using our novel FI tool.
 - b. Determine the impact of frailty on cardiac structure and contractile function in intact hearts from adult and aged C57BL/6J mice.
 - c. Explore the relationship between frailty and underlying contractile mechanisms in isolated ventricular myocytes.
- 4) Determine the impact of age and frailty on cardiovascular dysfunction following IR injury in intact hearts.

2 CHAPTER

MATERIALS AND METHODS

2.1 ANIMALS

All experiments were approved by the Dalhousie University Committee on Laboratory Animals and followed the Animal Research: Reporting of In Vivo Experiments (ARRIVE) guidelines (Kilkenny, Browne, Cuthill, Emerson & Altman, 2010). This study used adult (6-9 mos) and variably aged (12-29 mos) male C57BL/6J mice obtained from Charles River Laboratories (St. Constant, QC). Mice were housed in micro-isolator cages as groups of five in the Carleton Animal Care Facility at Dalhousie University. The mice were subjected to a 12-h light/dark cycle and had access to food (Prolab RMH3000, LabDiet, MO) and water *ad libitum*.

2.2 FRAILTY INDEX

Our lab has developed a novel FI tool to quantify the overall health status of naturally aging mice (Whitehead, et al., 2014; Feridooni et al., 2015B). This tool is based on the concept that frailty can be measured as deficit accumulation, an idea that is widely used clinically (Rockwood & Mitnitski, 2007). This novel FI tool is non-invasive and does not require specialized laboratory equipment. Furthermore, the frailty assessment procedure can be done very rapidly, in contrast to the original, more invasive approach (Parks, et al., 2012). The clinical FI was developed based on 31 parameters that reflect deterioration in health in naturally aging mice. The individual deficits measured in the FI tool were previously published and are illustrated in Figure 2 (Feridooni et al., 2015B; Whitehead, et al., 2014).

Table 2. Mouse Frailty Assessment Form[®]

Date: _____

Mouse #: _____ Date of Birth: _____ Sex: F M
 Body weight (g): _____ Body surface temperature (°C): _____

Rating: 0 = absent 0.5 = mild 1 = severe

				NOTES:
> Integument:				
❖ Alopecia	0	0.5	1	_____
❖ Loss of fur colour	0	0.5	1	_____
❖ Dermatitis	0	0.5	1	_____
❖ Loss of whiskers	0	0.5	1	_____
❖ Coat condition	0	0.5	1	_____
> Physical/Musculoskeletal:				
❖ Tumours	0	0.5	1	_____
❖ Distended abdomen	0	0.5	1	_____
❖ Kyphosis	0	0.5	1	_____
❖ Tail stiffening	0	0.5	1	_____
❖ Gait disorders	0	0.5	1	_____
❖ Tremor	0	0.5	1	_____
❖ Forelimb grip strength	0	0.5	1	_____
❖ Body condition score	0	0.5	1	_____
> Vestibulocochlear/Auditory:				
❖ Vestibular disturbance	0	0.5	1	_____
❖ Hearing loss	0	0.5	1	_____
> Ocular/Nasal:				
❖ Cataracts	0	0.5	1	_____
❖ Corneal opacity	0	0.5	1	_____
❖ Eye discharge/swelling	0	0.5	1	_____
❖ Microphthalmia	0	0.5	1	_____
❖ Vision loss	0	0.5	1	_____
❖ Menace reflex	0	0.5	1	_____
❖ Nasal discharge	0	0.5	1	_____
> Digestive/Urogenital:				
❖ Malocclusions	0	0.5	1	_____
❖ Rectal prolapse	0	0.5	1	_____
❖ Vaginal/uterine/penile prolapse	0	0.5	1	_____
❖ Diarrhoea	0	0.5	1	_____
> Respiratory system:				
❖ Breathing rate/depth	0	0.5	1	_____
> Discomfort:				
❖ Mouse Grimace Scale	0	0.5	1	_____
❖ Piloerection	0	0.5	1	_____
❖ Temperature score: _____				
❖ Body weight score: _____				
<hr/> Total Score/ Max Score: _____ <hr/>				

© Susan E. Howlett, 2013

Figure 2. The FI Scoring system. All deficits except temperature and weight were scored on a 3-point scale where deficits were given a score of 0 if absent, 0.5 if present but mild, and 1.0 if present and severe. Temperature and weight were scored based on deviations from mean reference values from age-matched mice. Values that differed from the reference by >1 SD were scored as 0.25, >2 SD were 0.5, >3 SD were 0.75 and >4 SD received a score of 1. This FI assessment form was originally published in Whitehead *et al.* 2014 .

2.3 SCORING OF INDIVIDUAL HEALTH DEFICITS

The parameters, or health deficits used in the FI tool were measured from the integument, musculoskeletal system, vestibulocochlear/auditory systems, ocular/nasal systems, digestive/urogenital systems, as well as signs of discomfort, body surface temperature (°C), and body weight (g). All of the parameters measured, except body weight and body surface temperature, were scored on a 3-point scale. A score of 0 was given when there were no signs of the health deficit. If there were mild signs of the health deficit, a score of 0.5 was given. Finally, a score of 1 was given if a deficit was severe. Body weight (g) and body surface temperature (°C) were scored on a 5-point scale, where a score of either 0, 0.25, 0.5, 0.75, or 1 was given in comparison to mean reference values created from an age-matched cohort. The complete list of the descriptors for each deficit measured in the frailty index tool (Figure 2) is discussed in detail below and can be found summarized in Table 8 (Whitehead, et al., 2014). The references for these health deficits in ageing C57BL/6 mice are summarized in Whitehead *et al.* (2014).

2.3.1 Integument

The integument was assessed by examining the mouse inside the cage, before it was handled, looking for any evidence of alopecia, loss of fur colour, dermatitis, loss of whiskers, and the coat condition of the mouse. Alopecia was assessed by observing if the mouse had normal fur density, less than 25% fur loss, or greater than 25% fur loss. Fur color was assessed when there was a change from the normal black colour to grey or brown. If fur color changes were focal a score of 0.5 was given, but if the changes were severe and widespread, it was assigned a score of 1. Dermatitis was assessed when lesions on the skin

Table 8: Complete list of the descriptors and criteria for the scoring system of each deficit measured with the frailty index tool (Whitehead et al., 2014)

System/Parameter	Clinical assessment of deficit	Scoring
Integument		
Alopecia	Gently restrain the animal and inspect it for signs of fur loss.	0 = normal fur density 0.5 = < 25% fur loss 1 = >25% fur loss
Loss of fur colour	Note any change in fur colour from black to grey or brown.	0 = normal colour 0.5 = focal grey/brown changes 1 = grey/brown fur throughout body
Dermatitis	Document skin lesions.	0 = absent 0.5 = focal lesions (<i>e.g.</i> neck, flanks, under chin) 1 = widespread or multifocal lesions
Loss of whiskers	Inspect the animal for signs of a reduction in the number of whiskers.	0 = no loss 0.5 = reduced number of whiskers 1 = absence of whiskers
Coat condition	Inspect the animal for signs of poor grooming.	0 = smooth, sleek, shiny coat 0.5 = coat is slightly ruffled 1 = unkempt and un-groomed, matted appearance
Physical/ Musculoskeletal		
Tumours	Observe the mice to look for symmetry. Hold the base of the tail and manually examine mice for visible or palpable tumours.	0 = absent 0.5 = <1.0 cm 1 = >1.0 cm or multiple smaller tumours
Distended abdomen	Hold the mouse vertically by the base of their tail and tip backwards over your hand. Excess fluid visible as a bulge below the rib cage.	0 = absent 0.5 = slight bulge 1 = abdomen clearly distended
Kyphosis	Inspect the mouse for curvature of the spine or hunched posture. Run your fingers down both sides of the spine to detect abnormalities.	0 = absent 0.5 = mild curvature 1 = clear evidence of hunched posture
Tail stiffening	Grasp the base of the tail with one hand, and stroke the tail with a finger of the other hand. The tail should wrap freely around the finger when mouse is relaxed.	0 = no stiffening 0.5 = tail responsive but does not curl 1 = tail completely unresponsive

System/ Parameter	Clinical assessment of deficit	Scoring
Gait disorders	Observe the freely moving animal to detect abnormalities such as hopping, wobbling, circling, wide stance and weakness.	0 = no abnormality 0.5 = abnormal gait but animal can still walk 1 = marked abnormality, impairs ability to move
Tremor	Observe the freely moving animal to detect tremor, both at rest and when the animal is trying to climb up an incline.	0 = no tremor 0.5 = slight tremor 1 = marked tremor; animal cannot climb
Forelimb grip Strength	Hold the mouse. Allow it to grip the bars on the cage lid. Lift animal by the base of the tail to assess grip strength.	0 = sustained grip 0.5 = reduction in grip strength 1 = no grip strength, no resistance
Body condition score	Place mouse on flat surface, hold tail base and manually assess the flesh/fat that covers the sacroiliac region (back and pubic bones).	0 = bones palpable, not prominent 0.5 = bones prominent or barely felt 1 = bones very prominent or not felt due to obesity
Vestibulocochlear/ Auditory		
Vestibular disturbance	Hold the base of the tail and lower mouse towards a flat surface. Inspect for head tilt, spinning, circling, head tuck or trunk curling.	0 = absent 0.5 = mild head tilt and/or slight spin when lowered 1 = severe disequilibrium
Hearing loss	Test startle reflex. Hold a clicker ~10 cm from mouse, sound it 3 times and record responses.	0 = always reacts (3/3 times) 0.5 = reacts 1/3 or 2/3 times 1 = unresponsive (0/3 times)
Cataracts	Visual inspection of the mouse to detect opacity in the centre of the eye.	0 = no cataract 0.5 = small opaque spot 1 = clear evidence of opaque lens
Eye discharge/swelling	Visual inspection of the mouse to detect ocular discharge and swelling of the eyes.	0 = normal 0.5 = slight swelling and/or secretions 1 = obvious bulging and/or secretions
Microphthalmia	Inspect eyes.	0 = normal size 0.5 = one or both eyes slightly small or sunken 1 = one or both eyes very small or sunken
Corneal opacity	Visual inspection of the mouse to superficial white spots and/or clouding of the cornea.	0 = normal 0.5 = minimal changes in cornea 1 = marked clouding and/or spotting of cornea

System/Parameter	Clinical assessment of deficit	Scoring
Vision loss	Lower mouse towards a flat surface. Evaluate the height at which the mouse reaches towards the surface.	0 = reaches >8 cm above surface 0.5 = reaches 2-8 cm above surface 1 = reaches <2 cm above surface
Menace reflex	Move an object towards the mouse's face 3 times. Record whether the mouse blinks in response	0 = always responds 0.5 = no response to 1 or 2 approaches 1 = no response to 3 approaches
Nasal discharge	Visual inspection of the mouse to detect nasal discharge.	0 = no discharge 0.5 = small amount of discharge 1 = obvious discharge, both nares
Digestive/ Urogenital		
Malocclusions	Grasp the mouse by the neck scruff, invert and expose teeth. Look for uneven, overgrown teeth.	0 = mandibular longer than maxillary incisors 0.5 = teeth slightly uneven 1 = teeth very uneven and overgrown
Rectal prolapse	Grasp the mouse by the base of the tail to detect signs of rectal prolapse.	0 = no prolapse 0.5 = small amount of rectum visible below tail 1 = rectum clearly visible below tail.
Vaginal/uterine/ penile prolapse	Grasp the mouse by the base of the tail to detect signs of vaginal/uterine or penile prolapse.	0 = no prolapsed 0.5 = small amount of prolapsed tissue visible 1 = prolapsed tissue clearly visible
Diarrhoea	Grasp the mouse and invert it to check for signs of diarrhoea. Also look for fecal smearing in home cage.	0 = none 0.5 = some feces or bedding near rectum 1 = feces plus blood and bedding near rectum, home cage smearing
Respiratory		
Breathing rate/depth	Observe the animal. Note the rate and depth of breathing as well as any gasping behaviour.	0 = normal 0.5 = modest change in breathing rate and/or depth 1 = marked changes in rate/depth, gasping
Discomfort		
Mouse Grimace Scale	Note facial signs of discomfort: 1) orbital tightening, 2) nose bulge, 3) cheek bulge, 4) ear position (drawn back) or 5) whisker change (either backward or forward).	0 = no signs present 0.5 = 1 or 2 signs present 1 = 3 or more signs present

<i>System/Parameter</i>	<i>Clinical assessment of deficit</i>	<i>Scoring</i>
Piloerection	Observe the animal and look for signs of piloerection, in particular on the back of the neck.	0 = no piloerection 0.5 = involves fur at base of neck only 1 = widespread piloerection
Other		
Temperature	Measure surface body temperature with an infrared thermometer directed at the abdomen (average of 3 measures). Compare with reference values from sex-matched adult animals.	0 = differs by <1 SD from reference value 0.25 = differs by 1 SD 0.5 = differs by 2 SD 0.75 = differs by 3 SD 1 = differs by >3 SD
Weight	Weigh the mouse. Compare with reference values from sex-matched adult animals.	0 = differs by <1 SD from reference value 0.25 = differs by 1 SD 0.5 = differs by 2 SD 0.75 = differs by 3 SD 1 = differs by >3 SD

were present. A score of 0.5, and 1 was assigned when the lesions were focal, and widespread and multifocal lesions were present, respectively. Loss of whiskers was scored 1 and 0.5, when there were no whiskers or there was a thinning of the whiskers, respectively. Coat condition was assessed by inspecting the animal for signs of poor grooming. If the coat looked smooth, sleek and shiny, a score of 0 was given. A score of 0.5 was given when the coat looked ruffled. In cases of very poor coat conditions, the coat looked unkempt, un-groomed, with a matted appearance and was given a score of 1.

2.3.2 Musculoskeletal system

The musculoskeletal system was assessed by observing signs of tumours, distended abdomen, kyphosis, tail stiffening, gait disorders, tremor, weak forelimb grip strength, and the body condition. The mouse was observed for signs of asymmetry and checked for any palpable tumours. A tumor that was smaller than 1.0 cm was given a score of 0.5, whereas a tumour that was greater than 1.0 cm, or the presence of multiple tumours, was given a score of 1. Next, the abdomen was assessed by holding the mouse vertically from the base of the tail. If the abdomen wasn't distended, a score of 0 was given. If the abdomen resembled a small bulge a score of 0.5 was given, and if the abdomen was enlarged a score of 1 was given. Body condition was assessed by gently palpating the sacroiliac region of the mouse to assess how much flesh covered that area. If the bones felt palpable but there was flesh covering them, a score of 0 was given. If the back and pubic bones were barely felt or very "boney" a score of 0.5 was given and finally if the bones were protruding or were not felt because of the fat overlay, a score of 1 was given.

Kyphosis which is the curvature of the spine was assessed by running a finger down

the spine of the mouse. Scores of 0.5 and 1 were given when there was a slight curve in the spine or if there was prominent curvature in the spine, respectively. Tail stiffening was assessed by lifting the mouse by the base of their tail with one hand and stroking the tail with a pen. A score of 1 was given for a stiff tail that did not wrap around the pen. A stiff tail that partially wrapped around the pen was given a score of 0.5, whereas a mouse with a tail that was not stiff could wrap and loop its tail around the pen.

Gait was assessed based on the ease with which the mouse moved freely inside the cage. If the mouse had abnormalities such as circling, wide stance, and weakness, but it could still move, it received a score of 0.5. A score of 1 was given if there were marked abnormalities in the gait and movement was impossible or severely impaired. Tremor was assessed while the mouse was at rest inside the cage and while the mouse was trying to ascend an incline. Mice with a slight tremor received scores of 0.5, and those with extreme tremor that prevented them from climbing the incline received a score of 1. To assess the forelimb grip strength, the mouse was held by the base of the tail and allowed to grip the bars on the cage lid. Once the animal had a grip on the cage bars, it was gently lifted by the base of the tail. Scores of 0.5 or 1 were given to mice that had a weak grip, or demonstrated no resistance at all when pulled up, respectively.

2.3.3 Vestibulocochlear/Auditory systems

The vestibulocochlear and auditory systems were assessed in individual mice by observing signs of vestibular disturbance and assessing hearing loss. Vestibular disturbance was assessed by lifting the mouse by the base of the tail and gently lowering it towards a surface. We looked for signs of severe disequilibrium such as spinning or

circling for a score of 1. If there was a slight trunk curling or head tilt, a score of 0.5 was given. Hearing loss was assessed by testing the startle reflex using a standard canine Top Paw® training clicker (Pet Smart, Halifax, NS, CND). If the individual mouse responded to the clicker all three times a score of 0 was given. If the mouse responded one or two times a score of 0.5 was given. Lastly, a score of 1 was given if the mouse did not respond to the sound at all.

2.3.4 Ocular/Nasal systems

The ocular system was assessed by evaluating signs of deterioration in the eye such as cataracts, eye discharge/swelling, microphthalmia, corneal opacity, vision loss, and a declined menace reflex. Cataracts, eye discharge/swelling, microphthalmia, and corneal opacity were assessed simultaneously by observing the eyes of the mouse where a score of 0.5 was given when there was a small opaque spot in the center of the eye, the eye was slightly swollen/discharging, one or both eyes sunken or small, and white spots or clouding of the cornea were present respectively. A score of 1 was given if the deficits were severe. Vision loss was assessed by lifting the mouse by the base of the tail and gently lowering it towards a surface. If the mouse reached out towards the surface at a distance greater than 8 cm while being lowered, a score of 0 was given. If the distance was between 2-8 cm, a score of 0.5 was assigned. Finally, a mouse that reached for the surface at a distance <2cm was given a score of 1 for vision loss. Menace reflex was assessed in a mouse by moving a pen in a “flicking” motion towards the face three times. A score of 0 was given if the mouse blinked all three times, 0.5 if the mouse only responded once or twice, and a score of 1 if the mouse did not respond at all. Finally, the nasal system was assessed by looking

at nasal discharge. If the mouse had small amounts of discharge from the nose, a score of 0.5 was given, while discharge from both nares resulted in a score of 1.

2.3.5 Digestive/Urogenital systems

The digestive/urogenital systems were assessed by looking at signs of malocclusions, rectal prolapse, vaginal/uterine/penile prolapse, and diarrhoea. Rectal prolapse, vaginal/uterine/penile prolapse, and diarrhoea were assessed by grasping the base of the tail and lifting the back of the mouse slightly. A score of 0.5 was given for rectal prolapse, vaginal/uterine/penile prolapse, and diarrhoea if there were small amounts of rectum, prolapsed tissue, and signs of diarrhoea visible, respectively. If these deficits were clearly visible, a score of 1 was assigned.

To assess malocclusions, the mouse was grasped by the neck scruff and inverted to expose the teeth. If the teeth were slightly uneven a score of 0.5 was given, and if the teeth were overgrown and considerably uneven a score of 1 was assigned.

2.3.6 Respiratory system

The respiratory system was assessed by observing the breathing rate and the depth of breathing of the animal. Slight changes in the breathing rate and depth were assigned a score of 0.5. If the mouse was gasping and or had difficulty breathing, a score of 1 was given.

2.3.7 Discomfort

Discomfort was assessed using the mouse grimace scale. This scale looked at facial signs of discomfort including orbital tightening, nose bulge, cheek bulge, ears drawn back, and whiskers flattened or standing on end. If one or two of these signs were present, a score of 0.5 was given. A score of 1 was given if three or more of these signs were present. Discomfort was also assessed by observing signs of piloerection. If piloerection was observed at the base of the neck, a score of 0.5 was given. A mouse with widespread piloerection that extended further from the back of the neck was given a score of 1.

2.3.8 Body surface temperature and body weight

To measure the body surface temperature an Infrascan infrared temperature probe (La Crosse Technology; La Crosse, WI) was used to measure the surface temperature at the abdomen. Three temperature recordings were measured and averaged for each mouse. The body weight was measured using a portable balance and a mechanical scale. The average reference values for weight and body surface temperature at 6 mos, 12 mos, and 18 mos and over are illustrated in Table 9. The average BW for 6, 12, and 18 mos was 38.1 ± 4.5 g, 48.7 ± 4.8 g, and 48.0 ± 8.6 g, respectively. Mean body surface temperature at 6, 12, and 18 mos was 30.7 ± 0.9 g, 30.2 ± 0.8 g, and 30.0 ± 1.4 g, respectively. The measured body weight and average body surface temperature for an individual mouse were considered a deficit based on the number of standard deviations (SDs) they differed from mean reference values (Supplementary Table 1). Measured values that differed from the average reference value by less than 1 SD were given a score of 0. A score of 0.25 was given when values differed from the reference values by more than 1 SD. Values that

Table 9: Average body surface temperature (\pm SD) and average body weight (\pm SD) from a large cohort of more than 233 male mice at different ages

	6-month	12-month	18+ month
Body weight (g)	38.1 \pm 4.5	48.7 \pm 4.8	48.0 \pm 8.6
Body Surface Temperature ($^{\circ}$C)	30.7 \pm 0.9	30.2 \pm 0.8	30.0 \pm 1.4

differed from reference values by more than 2 SD were given a score of 0.5. A score of 0.75 was given when measured values differed from the reference values by more than 3 SD. Finally, a score of 1 was given when values were greater than 4 SD from the reference value.

2.4 CALCULATING A FRAILTY INDEX SCORE

After assigning a score for each deficit, the frailty index score for each mouse was calculated by tallying all of these scores and dividing by total number of deficits measured, which is 31 (Figure 3). Thus, a frailty score between 0 and 1 was attained for each individual mouse. The higher the score, the more frail the mouse. It is important to note that the frailty index tool was assessed for its reliability between two different raters as described below. This resulted in several modifications to the assessment procedure described in section 2.1 which optimized the tool. These optimizations are detailed later in the results section and are highlighted in Table 12 of this thesis. All subsequent frailty assessments were done using the optimized frailty index. This included all frailty assessment for all animal experiments.

2.5 RELIABILITY OF FRAILTY ASSESSMENT TOOL

To assess the reliability of the frailty index tool, two different raters calculated frailty index scores on the same cohort of mice. One of the raters was Michael Sun, a former Master's student in Dr. Howlett's lab, and the other rater was me. All frailty assessments were performed inside an animal procedure room in the Carleton Animal Care Facility at Dalhousie University. Frailty was assessed by the two raters at the same time

$$\text{Frailty Index Score} = \frac{\text{Number of deficits present}}{\text{Total number of deficits in Frailty Index (31)}}$$

Figure 3. Calculation used to measure the FI score. A frailty index score for each mouse was calculated by adding all deficit scores measured and dividing by 31, the total number of items evaluated.

between the hours of 10 am and 2 pm over a three-month period (ie. August - October 2013). Each rater had one cage housing mice and one empty cage to use for frailty assessments. Frailty was assessed as described in section 2.1 in a cohort of 233 mice. The large cohort was divided into three groups: Group 1 had 45 mice; Group 2 consisted of 50 mice; and Group 3 was made up of 138 mice. Each rater evaluated the frailty of each mouse independently. Both raters assessed the frailty of all of the mice in Group 1. The frailty index scores evaluated from this group of mice were compared between the raters. Any differences and discrepancies in the frailty assessment found were discussed by the two raters. This procedure was then repeated for groups 2 and 3. This led to refinement of the criteria for the health deficits measured in the frailty index as described in the results section.

2.6 FIBROSIS ASSAY

Fibrosis was assessed by measuring the collagen content in hearts from aged and adult animals. The concentration of hydroxyproline, a major component of collagen (de Jong, van Veen, de Bakker & van Rijen, 2011), was measured using a hydroxyproline assay kit (Sigma-Aldrich, Okaville, ON; Catalog number: MAK008). Heart samples (10-35 mg of apex tissue) were first homogenized in water (100 μ L) then hydrolyzed in \sim 12 M HCl (120°C) for 3 hours. After 3 hours, samples were centrifuged at 10 000 x g for 3 minutes. The supernatants (20 μ L) were transferred to a 96 well plate and placed in an oven to dry (60°C; 3 hours). Following 3 hours, the 96 well plate was removed from the oven and chloramine T (6 μ L) and oxidation buffer (94 μ L), perchloric acid/isopropanol solution (50 μ L), and 4-(dimethylamino)benzaldehyde (50 μ L) were added to each well. The 96 well

plate was incubated (60°C) for 90 minutes. After incubation, the absorbance was measured at 560 nm. The concentration of hydroxyproline in each sample was calculated using the measured absorbance and a standard curve created from a set of standards provided in the kit. The concentration of hydroxyproline (μg) in each well was normalized to the sample size (mg) used in the assay.

2.7 LANGENDORFF-PERFUSED ISOLATED HEARTS

2.7.1 Baseline

Frailty index scores were assessed as described in detail above immediately prior to euthanizing the animal. Mice were anesthetized with an intraperitoneal injection of sodium pentobarbital (200 mg/kg); heparin (3,000 U/kg) was also injected to inhibit blood coagulation. The depth of anesthesia was evaluated with a toe pinch test. If no pedal withdrawal reflex was observed following the toe pinch test, a thoracotomy was performed, and hearts were quickly excised and placed in a petri-dish containing ice-cold Tyrode's buffer (described below). The aorta was cannulated with a 25 5/8-gauge needle on a Radnoti Langendorff apparatus (Radnoti LLC, Monrovia, Ca, USA) (Figure 4). The heart was perfused at a constant pressure of 80 mmHg with Tyrode's solution (37°C) containing (in mM): 126 NaCl, 0.9 NaH₂PO₄, 4 KCl, 20 NaHCO₃, 0.5 MgSO₄, 5.5 glucose, and 1.8 CaCl₂. The perfusate was aerated with carbogen, a mixture of 95% O₂, 5% CO₂ gas to achieve a pH of 7.4. The perfusate was filtered with in-line 1 μm glass fiber filters (Radnoti Glass Technology Inc., Monrovia, Ca, USA) that were replaced for each experiment.

A fluid filled balloon was constructed from GLAD® Cling Wrap (The Clorox Company of Canada LTD., Brampton, ON, Canada) and was inserted into the left ventricle

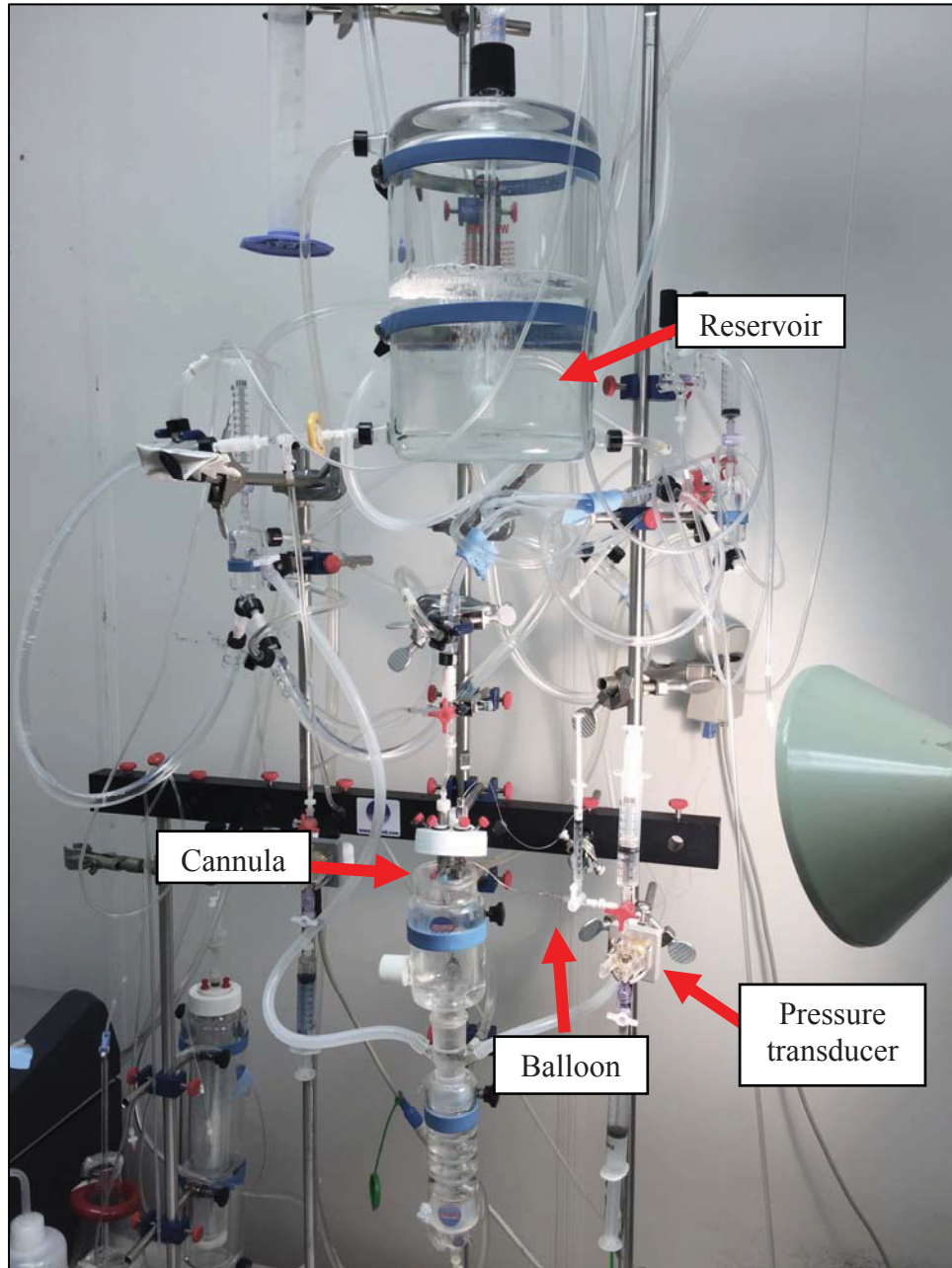


Figure 4. A Radnoti Langendorff apparatus used to assess LV pressure in hearts isolated from aged and adult mice.

through an incision made in the left atria. The balloon was inflated to a minimum pressure of 5-10 mmHg. The balloon was attached to a pressure transducer (ADInstruments, Colorado Springs, CO, USA) and a PowerLab 8/35 data acquisition system (ADInstruments, Colorado Springs, CO, USA) converted the changes in balloon pressure into a digital signal. LabChart 7 software (ADInstruments, Colorado Springs, CO, USA) was used to analyze data. Recordings of LV pressure were used to measure LVDP, HR, $+dP/dt$, $-dP/dt$, and RPP. Hearts were allowed to spontaneously beat for 30 minutes. The first 20 minutes were considered to be the equilibration period to allow the heart to stabilize. Baseline recordings were made during the final 10 minutes to assess LV function. During the recordings, effluent was collected from the hearts, then it was flash frozen in liquid nitrogen and stored in a -80°C freezer. The coronary flow rate was measured as the amount of effluent (mL) collected per minute.

Immediately after the Langendorff experiment was underway, the right tibia was isolated from the mouse. The length of the tibia (mm) was measured using calipers (Lee Valley, Halifax, NS).

2.7.2 Ischemia and Reperfusion

The protocol used for the Langendorff-perfused heart experiments is shown in Figure 5. Following 30 minutes of baseline recordings, hearts were exposed to 30 minutes of global ischemia. Global ischemia was induced by stopping the flow of perfusate to the heart. The heart was submerged in a modified Tyrode's solution that lacked glucose and calcium. This modified Tyrode's solution was warmed to 37°C but was not aerated with carbogen. The balloon was untouched and left filled within the ventricle during this period.

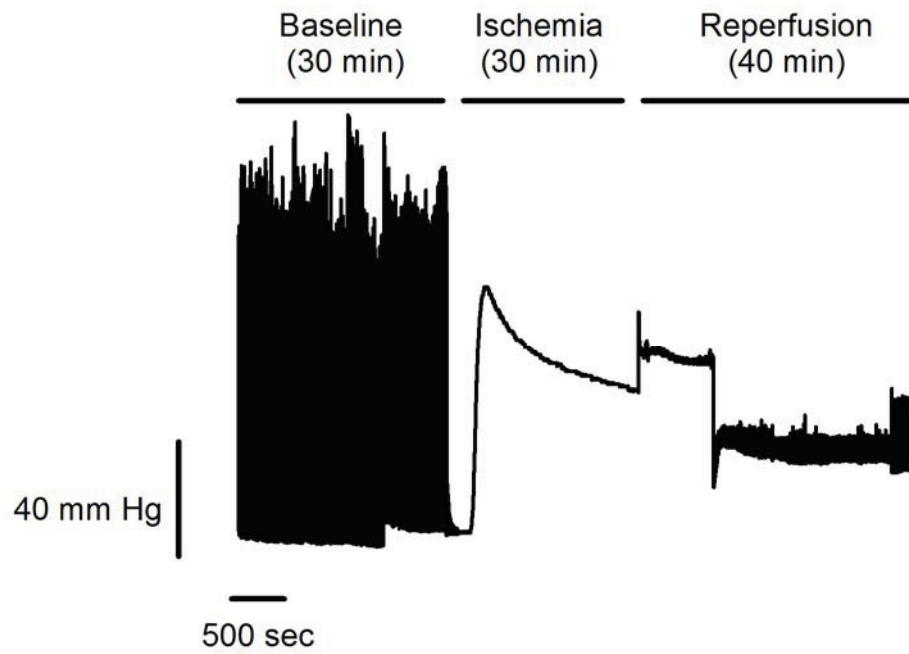


Figure 5. Time course for LV recordings before and after exposure to IR. The recording shows hearts were exposed to 30 min baseline, followed by 30 min global ischemia, and 40 min of reperfusion.

Reperfusion was induced by restarting the flow of the Tyrode's solution (37°C) to the heart. The aortic pressure was re-adjusted in order to perfuse the heart at a constant pressure of 80 mmHg. The reperfusion period lasted for 40 minutes. During this period, effluent (mL) was also collected and flash frozen in liquid nitrogen for assessment of ischemia-reperfusion injury as discussed later. At the end of reperfusion some hearts were weighed and quickly flash frozen in liquid nitrogen for future experiments. Some hearts were stained to measure the size of infarct caused by ischemia-reperfusion as described later.

2.8 CARDIAC TROPONIN-I ASSAY

Cardiac specific troponin-I was measured using a high sensitivity mouse cardiac troponin-I ELISA (Life Diagnostics, Inc., West Chester, Pa; Catalog number: CTNI-1-HS). In brief, this assay works on the premise that troponin I is subdivided into three different isoforms. One of these isoforms is specific to the heart and is different from the other isoforms that are found in skeletal muscle (Katrukha, 2013). The cTnI ELISA worked by targeting the center region of the cTnI protein which is the epitope that is resistant to proteolysis (Harris, Nageh, Marsden, Thomas & Sherwood, 2000).

2.8.1 Standard cTnI sample preparation

A standard curve was created using known concentrations of lyophilized cTnI stock. The lyophilized cTnI was reconstituted over a 5-minute period with 400 µL of de-ionized water to establish the cTnI stock (64.3 ng/mL) solution. A known maximal cTnI standard with a concentration of 10 ng/mL was initially created by pipetting an indicated volume of cTnI stock into a certain amount of cTnI diluent. The volumes of cTnI stock

and cTnI diluent required to make the 10 ng/mL standard concentration were different for each kit used. Using this 10 ng/mL standard, known standards of cTnI with concentrations of 5, 2.5, 1.25, 0.625, 0.312, and 0.156 ng/mL were created by serial dilution.

Effluent samples collected from each heart at the 40-minute time point during the ischemia-reperfusion experiments were thawed. Both effluent samples and standard cTnI samples were dispensed into anti-cTnI coated 96-well plates. This is the solid immobilization phase, where cTnI binds to the antibodies on the well plates. A second antibody, which was conjugated to horseradish peroxidase, was mixed (by gently shaking the 96 well plate) into each well. The samples were further mixed with the antibodies on an orbital shaker at 150 rpm while incubating for 60 minutes at room temperature (22°C). Any unbound horseradish peroxidase-conjugate antibody was rapidly washed away with a wash solution (50 mM Tris-Buffered Saline provided). This wash procedure was repeated five times.

At this point, each 96 well plate contained a complex of HRP-conjugate antibody bound to cTnI, which was bound to anti-cTnI antibody. The HRP substrate 3,3',5,5'-tetramethylbenzidine (TMB) was added to the wells and was incubated for 20 minutes at room temperature on an orbital shaker (150 rpm). A blue color formed as a result of the oxidization of TMB. This color development was halted with 1N HCl which changed the color inside the well plates to yellow. The absorbance of each 96 well plate was read at 450 nm using a multi-mode microplate reader (FLUOstar Omega, BMG Labtech, Guelph, ON, CA). A standard curve was created using the standard samples fitted with a 4-parameter logistic curve. The concentration of cTnI within each well was calculated using this standard curve.

2.9 INFARCT MEASUREMENT

2.9.1 Staining with Tetrazolium red

Following 40 minutes of reperfusion, hearts were stained with tetrazolium red (Sigma-Aldrich, Okaville, ON; product no. T8877) to measure the extent of the infarct caused by ischemia-reperfusion injury. This method did not measure the area at risk. Tetrazolium red or 2,3,5-Triphenyltetrazolium chloride (TTC) is reduced by the mitochondria to a give red color in living cells (Rich, Mischis, Purton & Wiskich, 2001). The infarct area, therefore, appeared white. A solution of 3.3 mM TTC was made by dissolving 0.1 g TTC with 10 mL of working buffer (Tyrode's solution). At the end of reperfusion, the balloon was removed from the left ventricle and the cannula was removed with the heart still attached. The cannula was then attached to a 10 mL syringe filled with the TTC-Tyrode's solution. The heart was then perfused, by hand, with the TTC solution slowly at a constant rate (~5 mL/min). The TTC solution that was perfused through the heart was collected in a small beaker. At the end of perfusion with 10 mL of TTC, the heart was removed from the cannula and placed in the small beaker with the TTC solution. The heart was then incubated in TTC solution at 37°C for 45 minutes using a C24 benchtop incubator shaker (New Brunswick Scientific CO., Classic Series, Enfield, CT, USA). After incubation, the hearts were removed from the TTC solution, fixed in 10% formalin solution (Sigma-Aldrich, Okaville, ON; product no. HT5012) and stored for at least 48 hours in the dark.

2.9.2 Measuring infarct area

Hearts were sliced using regular razor blades and a rodent heart slicer matrix (Zivic Instruments, Pittsburgh, PA, model #HSMA001-1). Briefly, fixed hearts were placed in the heart slicer matrix. Using multiple razor blades, hearts were sliced into 1-2 mm thick coronal (latitudinal) slices. Using a light brightfield microscope (Zeiss Axiovert 200M, Toronto, ON, CA), images from both sides of each slice were taken for infarct analysis. The heart slices were placed back in formalin and stored in the dark.

2.9.3 Infarct image analysis

Images of all of the slices were uploaded to Adobe Photoshop® CS6. If the images of the slices were too light, all images taken from that day would be filtered using the 'levels' feature of Photoshop. The viable cells appeared red, whereas infarct area appeared white (Figure 6). The image was then converted to an inverted grayscale image, where the infarct appeared dark and the healthy tissue a light gray.

The extent of infarct present in these grayscale images was analyzed using ImageJ, a program developed by the National Institutes of Health. Images were uploaded to ImageJ and, using the 'Threshold' feature, the total area of the heart slice and the total area of infarct within the slice were measured. This was repeated for all heart slices on both sides of the slice. The total amount of infarct in each heart was expressed as a percentage of the total volume of the heart.

2.10 VENTRICULAR MYOCYTE EXPERIMENTS

2.10.1 Cardiomyocyte isolation

Male C57BL/6 mice were restrained and intraperitoneally injected with 200 mg/kg sodium pentobarbital and 3000 U/kg heparin to reduce blood clotting (California, 2009). A toe pinch test was performed to assess the ability of the mouse to feel pain. If no pedal withdrawal reflex was observed, a sternal incision was made to reveal the ribs. The aorta was cannulated and perfused (10 min; flow rate of 2.2 mL/min) with 37°C Ca²⁺-free isolation solution containing in mM: 105 NaCl, 1 MgCl₂, 20 glucose, 5 KCl, 3 Na-pyruvate, 0.33 NaH₂PO₄, 25 HEPES, and 1 lactic acid, pH 7.4 with NaOH, and oxygenated with 100% O₂ (Praxair, Halifax, NS). After 10 minutes of perfusion with the Ca²⁺-free isolation solution, the heart was perfused (8-10 min) with 30 mL of enzyme solution (37°C, pH 7.4). The enzyme solution was made up of the isolation solution, supplemented with 0.5 mg trypsin (Sigma Aldrich, Oakville, ON), 3.4 mg dispase II (Roche Diagnostics, Laval QC), 8.0 mg collagenase type I (Worthington, Lakewood, NJ), 50 µM CaCl₂ and oxygenated with 100% O₂. Following 8-10 min of perfusion with the enzyme solution, the ventricles were cut into very small pieces and rinsed multiple times in a high K⁺ solution in mM: 45 KCl, 3 MgSO₄, 30 KH₂PO₄, 50 L-glutamic acid, 20 taurine, 0.5 EGTA, 10 HEPES, 10 glucose, pH 7.4 with KOH. The suspended cells were filtered through a 225 µm polyethylene mesh and stored at room temperature. Cells were used within 1-5 hours after isolation.

2.10.2 Voltage-clamp experiments

Cells were incubated with fura-2 AM (5 µM) for 20 minutes on the stage of an

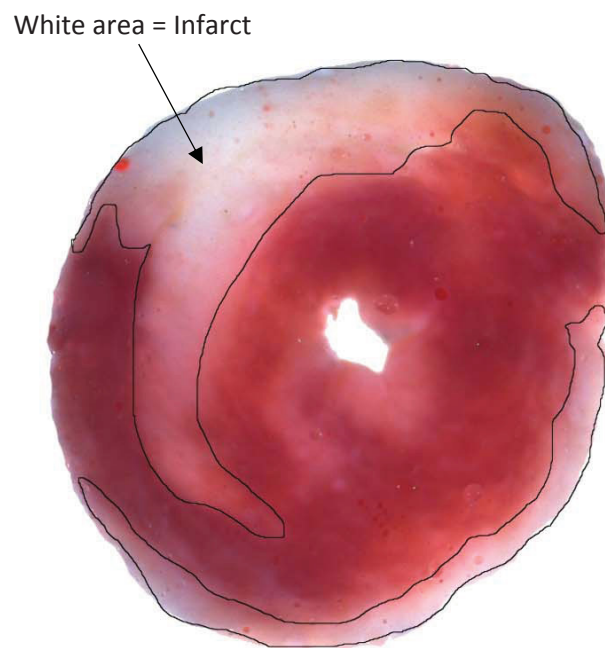


Figure 6. Representative image of a heart slice following IR. Red areas were viable cells. White areas (arrow and outline) were the infarct.

inverted microscope (Nikon Eclipse TE200; Nikon Canada, Mississauga, ON). The HEPES buffer used to superfuse (3 ml/min; pH 7.4; 37°C) the cells during the experiment contained (in mM): 10 HEPES, 145 NaCl, 10 glucose, 4 KCl, 1 CaCl₂, 1 MgCl₂, 4 4-aminopyridine, and 0.3 lidocaine. Voltage clamp experiments were done using discontinuous single electrode voltage clamp (5-6 kHz) techniques (Axoclamp 2B amplifier; Molecular Devices, Sunnyvale, CA, USA) with high resistance microelectrodes (18-25 MΩ; 2.7 M KCl). Myocytes were held at -80 mV then stimulated with 50 ms conditioning pulses (-80 to 0 mV; 2 Hz) followed by 450 ms repolarization to -40 mV and test steps (250 ms) to between -40 and +80 mV. These voltage clamp protocols were created with ClampEx v8.2 software (Molecular Devices). Simultaneous recordings of cell contractions, Ca²⁺ transients, and Ca²⁺ currents were during 250 ms test pulses to varying potentials (-40 mV to +80 mV).

A charge-coupled device camera (120 Hz; model TM-640, Pulnix America, Sunnyvale, CA, USA) coupled to a video edge detector (Crescent Electronics, Sandy, UT, USA) was used to measure unloaded cell shortening and lengthening. Myocyte contraction was calculated by subtracting peak cell shortening from diastolic cell length. Contractions were normalized to the length of the cell at rest. Contractions were analyzed with Clampfit 8.2 (Molecular Devices).

A PTI (Photon Technology International, Birmingham, NJ, USA) fluorescence system was used to measure intracellular Ca²⁺ concentrations. Intracellular Ca²⁺ was determined by exciting Fura-2 at 340 (Fura-2-Ca²⁺ complex) and 380 nm (Fura-2 Ca²⁺ free form) and recording the resulting fluorescence emission at 510 nm using a DeltaRam (Photon Technologies International, Birmingham, NJ, USA) and Felix v1.4 software

(Photon Technologies International). Fluorescence measurements were converted to Ca^{2+} concentrations using previously established techniques (O'Brien, Ferguson & Howlett, 2008). Peak Ca^{2+} transient amplitudes were calculated as the difference between peak systolic Ca^{2+} and diastolic Ca^{2+} concentrations. Felix (Photon Technologies International) and Clampfit 8.2 software (Molecular Devices) were used to analyze all fluorescence data.

Ca^{2+} current was measured as the difference between the peak inward current and the end of the test step, and normalized to the cell capacitance. Cell capacitance was measured by taking the integral of the capacitive transients (Clampfit 8.2, Molecular Devices). The gain of SR Ca^{2+} release was calculated as the ratio of the rate of rise of the Ca^{2+} transient (nM/s) to normalized Ca^{2+} current (pA/pF).

2.11 WESTERN BLOTS

CaV1.2 protein expression was assessed in LV apical tissue. The LV of the heart was placed in lysis buffer containing radioimmunoprecipitation assay buffer supplemented with EDTA, protease inhibitor cocktail (ThermoFisher #78430), and phosphatase inhibitor cocktail (ThermoFisher #78420) and homogenized with a Dounce homogenizer. Next the homogenate was centrifuged at 8000 r.p.m for 15 min at 4°C and the supernatant was collected. CaV1.2 protein levels were measured using RC DC™ protein assay kit (Bio-Rad, (#500-0122)). SDS-PAGE was used to separate protein (30 µg) under reducing conditions. The separated protein was transferred to polyvinylidene fluoride (0.45 µm) membranes. Membranes were stained with the housekeeping protein Ponceau S (0.2% in 5% acetic acid). Next, the membranes were blocked in skim milk (5%; 1 h; room temperature) and incubated with CaV1.2 primary antibody (Alomone labs #ACC-033,

1:2000; Jerusalem, Israel) overnight (4°C). A secondary antibody solution containing 5% skim milk, goat secondary antibody (1:10000, Abcam, Cambridge, MA, USA) was used to incubate (1 h; room temperature) the membranes. Clarity Western ECL substrate (Bio-Rad, Hercules, CA, USA) was used to expose proteins bands. Exposed bands were detected with a Biorad Chemidoc XRS system that detected chemiluminescence. ImageJ (v1.41) was used for densitometry analysis. The loading control for all Western blot experiments was Ponceau S because there is evidence suggesting other housekeeping genes such as GAPDH and β -actin are affected by age (Li & Shen, 2013; Low, Degens, Chen & Alway, 2000; Mennes, Dungan, Frendo-Cumbo, Williamson & Wright, 2014). Protein bands were normalized to the Ponceau staining at 250 kDa and results were presented as arbitrary densitometric values.

2.12 STATISTICS

All statistical analyses were performed using Sigmaplot software (v11.0, Systat Software Inc., Chicago, IL, USA). Differences between means (\pm SEM) were assessed with a Student's *t* test (for normally distributed) or a Mann-Whitney rank sum test (for data that were not normally distributed). Two-way repeated-measures analysis of variance (2-way RM ANOVA) was used to evaluate differences between means in the IR experiments. Linear regression analysis was used to determine linear relationships between functional response and frailty and reliability between raters. Reliability between raters was also assessed using Cohen's kappa statistic. A one-way ANOVA was used to determine the difference in mean kappa statistics between the three groups. Finally, inter-rater reliability was also assessed by using a two-way random model and consistency analysis of the

intraclass correlation (ICC) \pm 95% confidence intervals (CI). An ANOVA test was used to determine significant difference between ICC \pm 95% CI. In all statistical tests, a $P \leq 0.05$ was determined to be significant.

2.13 CHEMICALS

Chemicals used in the Langendorff-perfused experiments and cell experiments were purchased from Sigma-Aldrich (Oakville, ON, Canada) or BDH Inc. (Toronto, ON, Canada).

3 CHAPTER RESULTS

3.1 THE EFFECTS OF ADVANCED AGE ON CARDIAC CONTRACTILE FUNCTION AND STRUCTURE

3.1.1 Phenotypic characteristics of male mice change with advanced age

The phenotypic characteristics of mice used in the perfused heart experiments were investigated. The aged group (832 ± 11 days; $n = 16$) was significantly older than the adult group (281 ± 15 days; $n = 32$). In addition, body weight was significantly lower in the aged group in comparison to the adult group (34.9 ± 0.8 g vs. 39.1 ± 1.2 for aged and adult mice, respectively). These results are summarized in Table 10.

The relationship between advanced age and cardiac hypertrophy was assessed by measuring tibia length (TL), heart weight (HW), HW to body weight (HW:BW) ratio, and HW:TL ratio. Mean values (\pm SEM) for these parameters are summarized in Supplementary Table 2. In addition, scatterplots and box and whisker plots for these data are shown in Figure 7. The line within the scatterplots represents the mean value for each group. Each box and whisker plots the median, 10th, 25th, 75th and 90th percentiles. Results show that there was no difference in tibia length between the aged and adult groups (18.7 ± 0.1 mm, $n = 16$; 18.8 ± 0.1 , $n = 32$; for aged and adult groups, respectively) (Figure 7A). By contrast, on average, HW was significantly higher in the aged group (283 ± 9 mg, $n = 31$) in comparison to the adult group (234 ± 7 mg, $n = 13$) (Figure 7B). Furthermore, average HW:BW and HW:TL ratios were significantly greater in the aged group (8.2 ± 0.3 mg/g, $n = 31$; 15.2 ± 0.5 mg/mm, $n = 31$; for HW:BW and HW:TL, respectively) in comparison to the adult group (6.1 ± 0.2 mg/g, $n = 13$; 12.6 ± 0.4 mg/mm, $n = 12$; for

Table 10: Age and body weights of adult and aged mice used for Langendorff-perfused heart experiments.

	Adult (N = 16)	Aged (N = 32)	P-value
Age (days)	281 ± 15	832 ± 11*	≤0.001
Body weight (BW, g)	39.1 ± 1.2	34.9 ± 0.8*	0.006

* represents significant difference from adult group. Numbers represent mean ± SEM. N represents the sample size of each group. P-values were determined with a Student's *t* test.

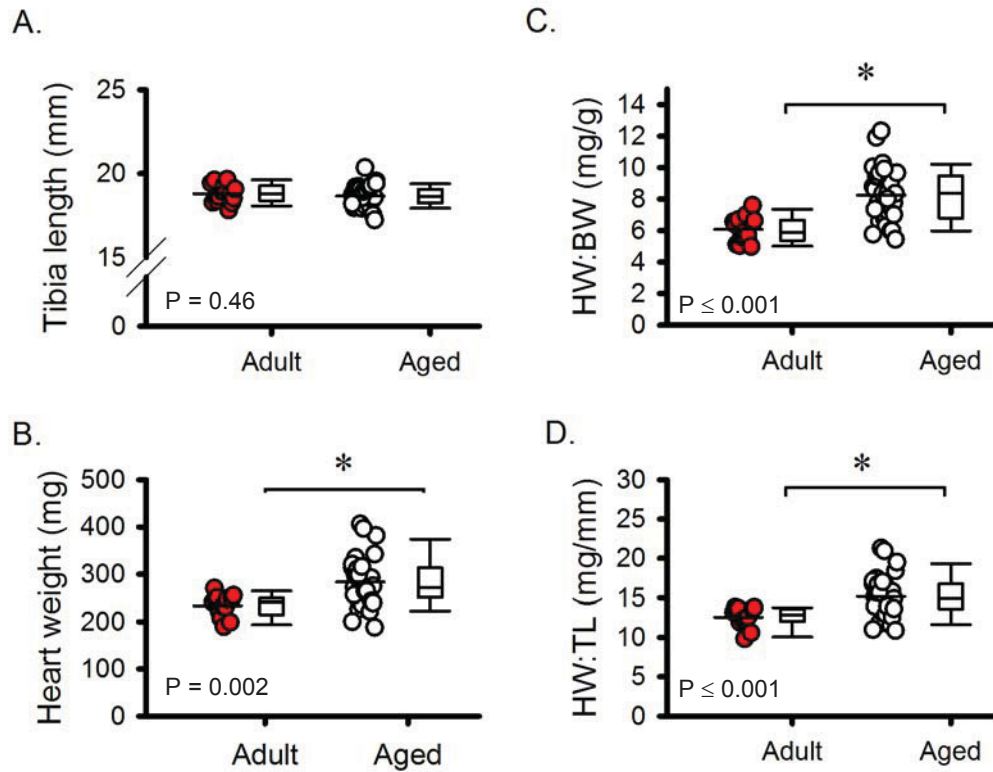


Figure 7. Cardiac hypertrophy increased with age. **A)** Tibia length (TL) was similar ($P = 0.46$) in aged animals ($n = 32$) and adult animals ($n = 16$). **B-D)** Mean HW ($N = 13$ adult and 31 aged), HW:BW ratios ($N = 13$ adult and 31 aged), and HW:TL ratios ($N = 12$ adult and 31 aged) were higher in the aged animals ($P \leq 0.002$ for all). *denotes significant difference between adult group. Differences between groups were assessed with a Student's t test or a Mann-Whitney Rank Sum test for data that were non-parametric. HW = Heart weight, HW:BW = Heart weight to body weight ratio, HW:TL = Heart weight to tibia length. Adapted with permission from Feridooni *et al.*, 2017.

HW:BW and HW:TL, respectively) (Figure 7C, D). These results indicate that aged hearts exhibit hypertrophy in comparison to younger adult hearts. Hypertrophy is closely associated with fibrosis (Creemers & Pinto, 2011). Therefore, collagen content was quantified by measuring the concentration of hydroxyproline in hearts isolated from aged and adult animals (Supplementary Table 2). On average, hearts isolated from aged animals had more hydroxyproline in comparison to hearts isolated from adult animals (0.24 ± 0.03 $\mu\text{g}/\text{mg}$, $n = 8$; 0.15 ± 0.01 $\mu\text{g}/\text{mg}$, $n = 8$; for aged and adult groups, respectively) (Figure 8).

Together these findings indicate the aged group was significantly older, and weighed less than the adult group. Furthermore, cardiac hypertrophy was significantly greater in the aged group compared to the adult group, consistent with age-dependent cardiac hypertrophy. Moreover, hearts from aged mice had higher levels of fibrosis in comparison to hearts from adult mice. Interestingly, there was marked heterogeneity in the aged group, where many individual animals had age-dependent hypertrophy and fibrosis, but others had values that overlapped with results seen in the adult group (Figure 7B-D, Figure 8).

3.1.2 Influence of advanced age on contractile function in intact hearts

The next set of experiments was designed to investigate the effects of advanced age on cardiac contractile function in intact hearts. Changes in pressure were recorded from Langendorff-perfused hearts at baseline, and results are summarized in Supplementary Table 3 as mean \pm SEM. The parameters HR, diastolic pressure, LVDP, $+dP/dt$, and $-dP/dt$ were plotted as a function of age (Figure 9). Figure 9A shows representative pressure recordings from adult and aged mice. These recordings indicate that hearts isolated from

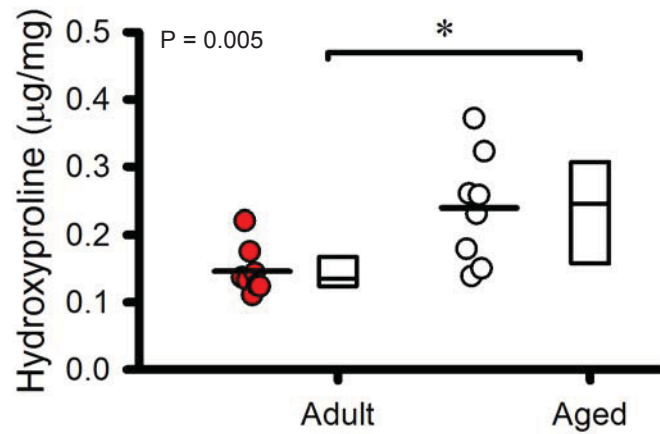


Figure 8. Cardiac fibrosis increased with age. Total collagen content was assessed by measuring hydroxyproline. Hearts isolated from aged animals had higher hydroxyproline concentration than hearts isolated from adult animals ($P = 0.005$). Sample size was $N = 8$ for aged and 8 for adult groups. *denotes significant difference from adult group. Differences between groups were assessed with a Mann-Whitney Rank Sum test.

adult mice had higher LVDP and faster +dP/dt and -dP/dt than hearts isolated from aged mice (Figure 9A). Indeed, LVDP (Figure 9D) was significantly lower in the aged hearts (65.6 ± 3.3 mm Hg) in comparison to adult hearts (88.6 ± 3.5 mm Hg) ($P \leq 0.001$). Similarly, mean +dP/dt (1535 ± 84 mm Hg/s for aged mice and 2090 ± 79 mm Hg/s for adult animals; $P \leq 0.001$) and -dP/dt (-1416 ± 73 mm Hg/s for aged mice and -2011 ± 80 mm Hg/s for adult animals; $P \leq 0.001$) declined with advanced age (Figure 9E & F). By contrast, results showed that intrinsic HR (Figure 9C), measured as the number of beats per minute (bpm), was similar in aged and adult mice (317 ± 11 bpm; 288 ± 11 bpm; for aged and adult mice, respectively. $P = 0.11$). Also, mean diastolic pressure was similar between both age groups (6.7 ± 0.5 mm Hg vs. 6.2 ± 0.5 mm Hg for adult and aged, respectively; $P = 0.18$). Interestingly, RPP (Figure 10A), a measure of work done by the heart, was similar between the two groups (25248 ± 1009 mm Hg*bpm in the adult group vs 21312 ± 1492 mm Hg*bpm; $P = 0.12$). However, when RPP was normalized to the HW, RPP index (Figure 10B), the aged group (76.4 ± 5.8 mm Hg*bpm/mg) had lower RPP index in comparison to the adult group (110.3 ± 5.7 mm Hg*bpm/mg) ($P = 0.002$). Coronary flow rate (Figure 11A) was similar between in the two groups (6.6 ± 1.0 ml/min in adult hearts and 4.9 ± 0.5 ml/min in aged hearts; $P = 0.10$) regardless of the size of the heart (Figure 11B) (0.021 ± 0.002 ml/min in adult hearts and 0.018 ± 0.003 ml/min in aged hearts; $P = 0.06$). These data demonstrate that, on average, hearts from aged animals had smaller and slower contractions. However, there was high variability within each group (Figure 9, 10 & 11), such that many aged hearts had similar contractile function as hearts isolated from young adult mice.

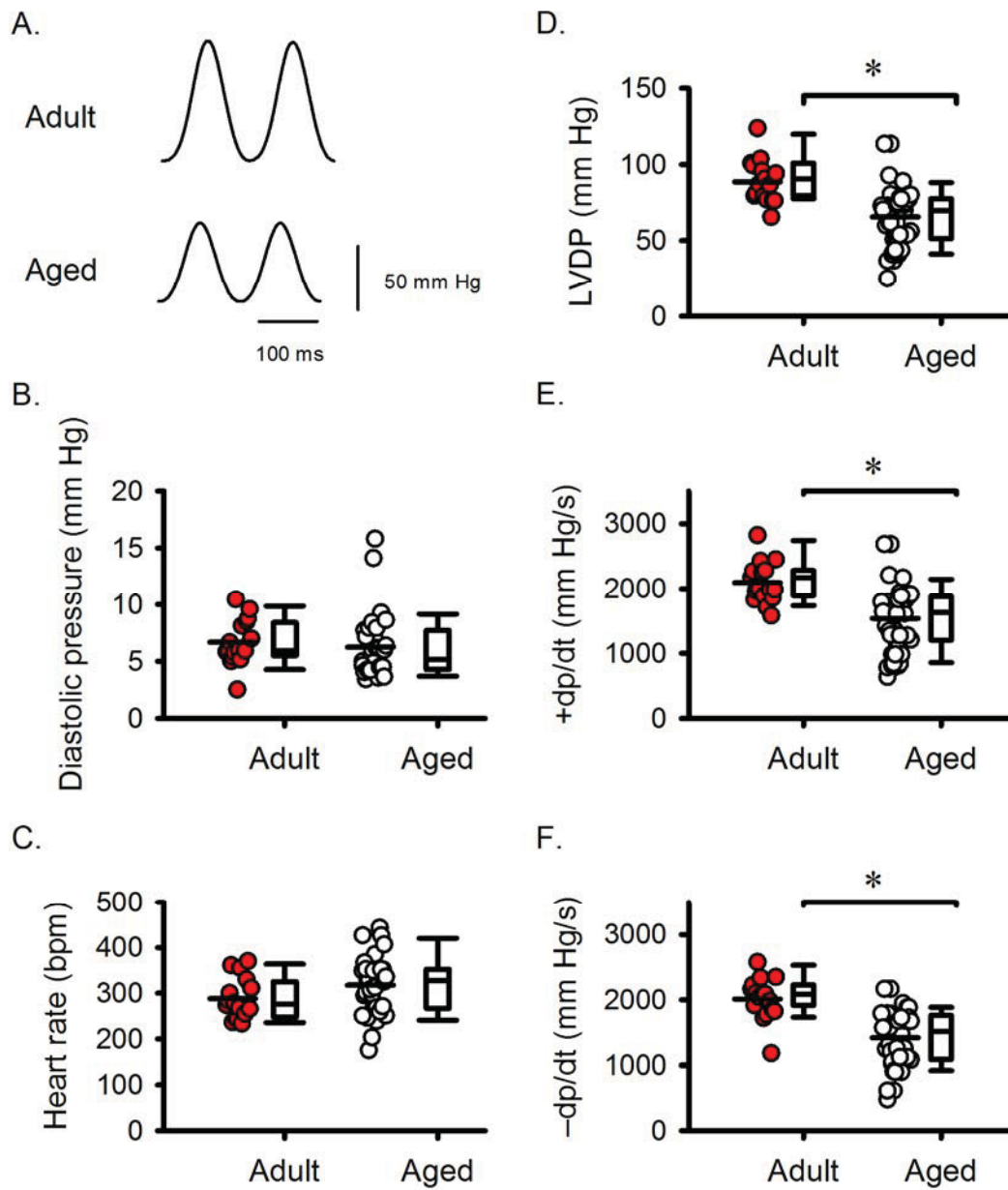


Figure 9. Left ventricular contractile function declined with advanced age. A) Representative pressure recordings from mice in the adult and aged groups. B) Diastolic pressure was similar between both age groups ($P = 0.18$). C) Intrinsic HR was similar in both groups ($P = 0.11$). D-F) Mean LVDP, +dP/dt, and -dP/dt were higher in the aged animals compared to young adults ($P \leq 0.001$ for all). Sample size was $N = 16$ adult and 32 aged for all parameters. *represents significant difference from adult group. P-values were determined with a Student's t test or a Mann-Whitney Rank Sum test for data that were non-parametric. LVDP = Left ventricular developed pressure; +dP/dt = rate of contraction; -dP/dt = rate of relaxation. Adapted with permission from Feridooni *et al.*, 2017.

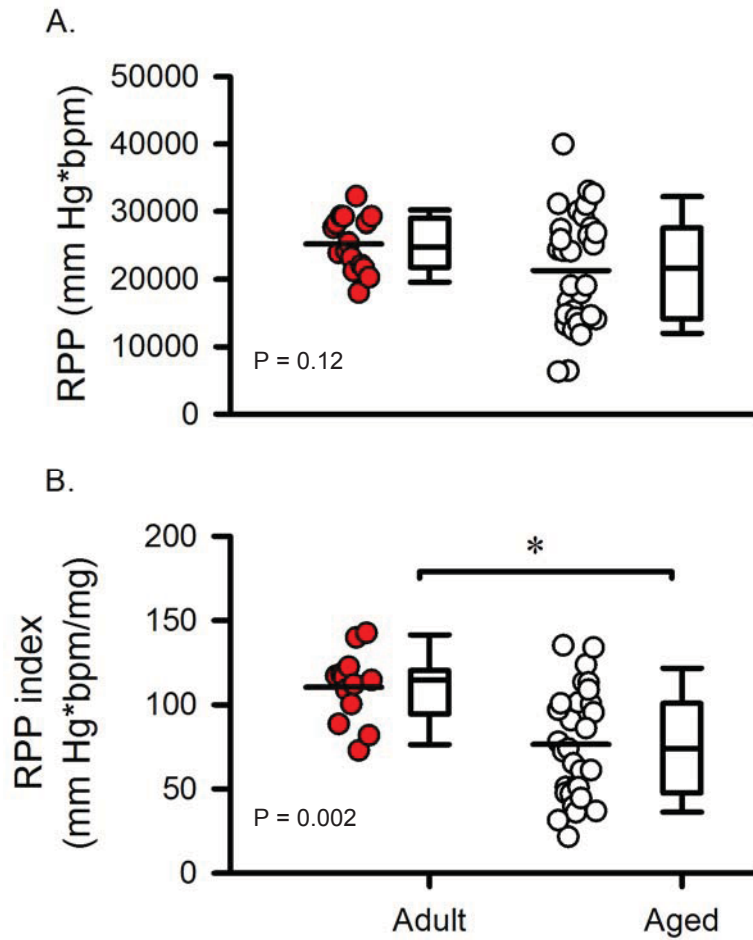


Figure 10. Aged hearts did less work in comparison to adult hearts. **A)** RPP was similar in aged (N = 32) and adult (N = 16) hearts (P = 0.12). **B)** Mean values for RPP were normalized to heart weight, aged hearts (N = 31) had a smaller RPP index when compared to adult (N = 13) hearts (P = 0.002). *denotes significant difference from adult group. P-values were determined with a Mann-Whitney Rank Sum test. RPP = rate pressure product.

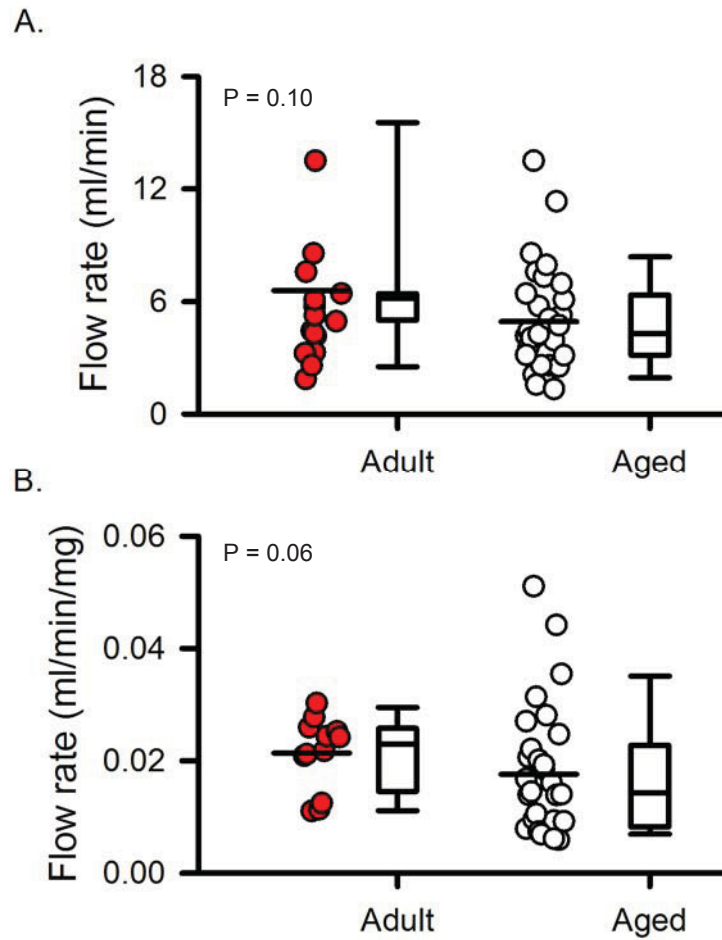


Figure 11. Coronary flow rates were not affected by age. **A)** Mean coronary flow rates were similar in adult and aged hearts ($P = 0.10$). **B)** Coronary flow rate normalized to heart weight was also similar in the two groups ($P = 0.06$). Sample size was $N = 16$ for the adult group and 32 for the aged group. P-values were determined with a Mann-Whitney Rank Sum test.

3.1.3 Effects of advanced age on cell shortening, Ca²⁺ transients, L-type Ca²⁺ current density, and CaV1.2 expression

To determine whether the contractile dysfunction observed in aging intact hearts was also present at the cellular level, myocytes from adult (223 ± 28 days old) and aged (836 ± 15 days old) mice were isolated and examined using voltage clamp experiments. The results of these experiments are summarized in Supplementary Table 3 as mean ± SEM. Figure 12A & B show that, on average, peak contractions normalized to cell size were smaller in myocytes isolated from aged hearts when compared to myocytes from adult hearts (8.0 ± 0.8 %, n = 10 myocytes; 4.1 ± 0.4 %, n = 24 myocytes; for adult and aged mice, respectively) (P < 0.0001). Similarly, the velocities of shortening (Figure 12C) and lengthening (Figure 12D) declined in myocytes from aged mice (5.9 ± 0.6 μm/s velocity of shortening; 3.1 ± 0.3 μm/s velocity of lengthening) when compared to cells from adult mice (10.8 ± 1.5 μm/s velocity of shortening; 5.4 ± 0.7 μm/s velocity of lengthening) (P = 0.007 and 0.001, respectively).

Contraction is initiated when there is an increase in intracellular Ca²⁺ as discussed previously (Bers, 2002). Therefore, peak Ca²⁺ transients were measured simultaneously with the contractions. Figure 12E shows mean peak Ca²⁺ transient responses were smaller in cells from aged animals (33.8 ± 1.9 nM; n = 32 myocytes) when compared to cells from adult animals (43.3 ± 3.3 nM, n = 9 myocytes) (P = 0.02). Ca²⁺ transients are triggered when Ca²⁺ enters the cell through L-type Ca²⁺ channels. Thus, Ca²⁺ currents were measured to see if the smaller Ca²⁺ transients were due to smaller Ca²⁺ currents (results summarized in Supplementary Table 5). Mean Ca²⁺ currents (Figure 13 A & B) were smaller (P = 0.008) in the aged group (-4.7 ± 0.3 pA/pF, n = 32 myocytes) compared to the

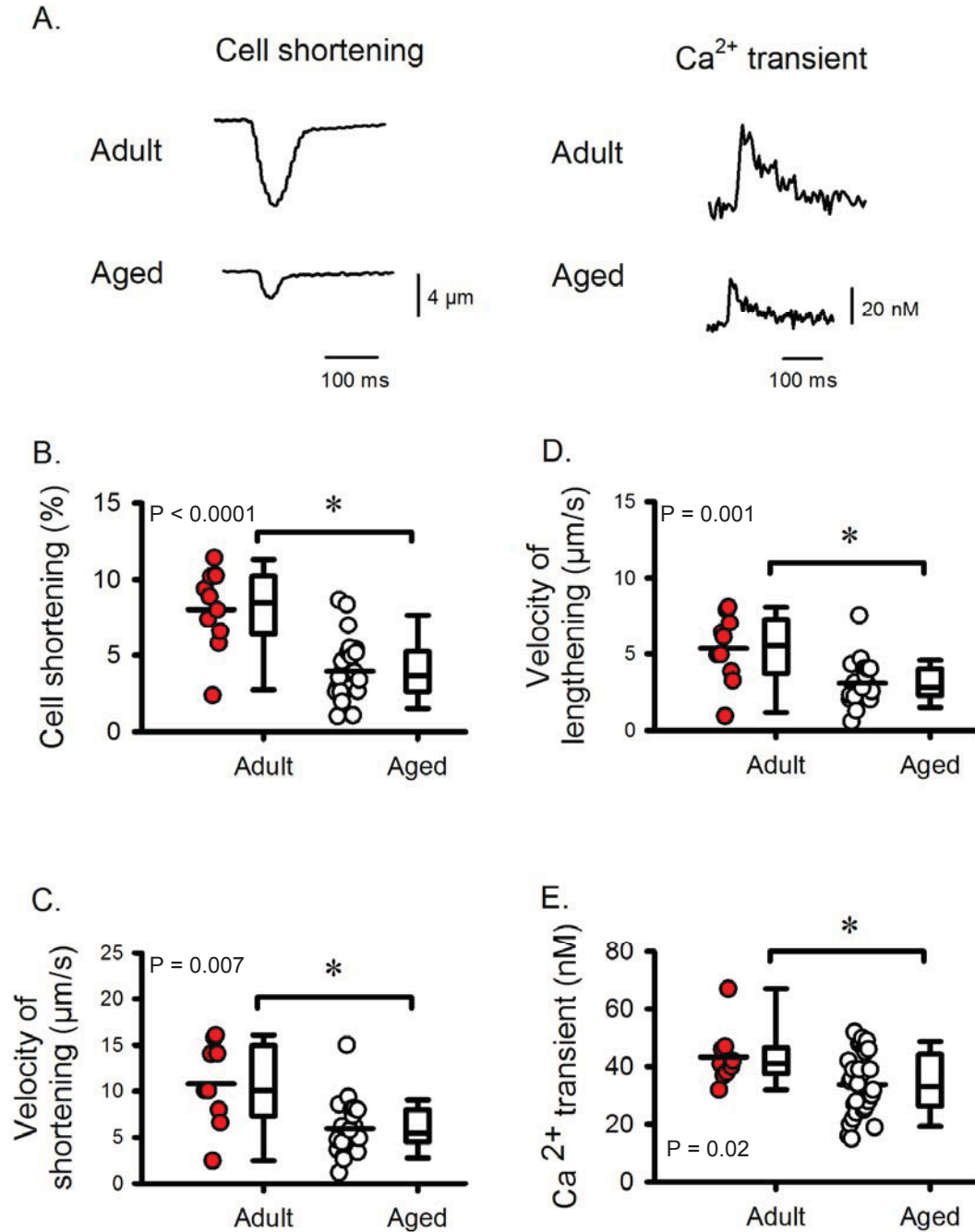


Figure 12. Ca^{2+} transients and peak contractions declined with advanced age. **A)** Representative recordings of peak cell shortening and Ca^{2+} transient recorded in myocytes isolated from adult and aged mice. **B)** peak contractions normalized to cell size declined with advanced age ($P < 0.0001$) **C, D)** The velocity of shortening ($P = 0.007$) and velocity of lengthening ($P = 0.001$) were slower in aged animals when compared to adult animals. **E)** Mean Ca^{2+} transient declined with age ($P = 0.02$). *denotes significant difference from adult group. P-values were determined with a Student's *t* test or a Mann-Whitney Rank Sum test for data that were non-parametric. $n = 10$ adult or 24 aged myocytes. Adapted with permission from Feridooni *et al.*, 2017.

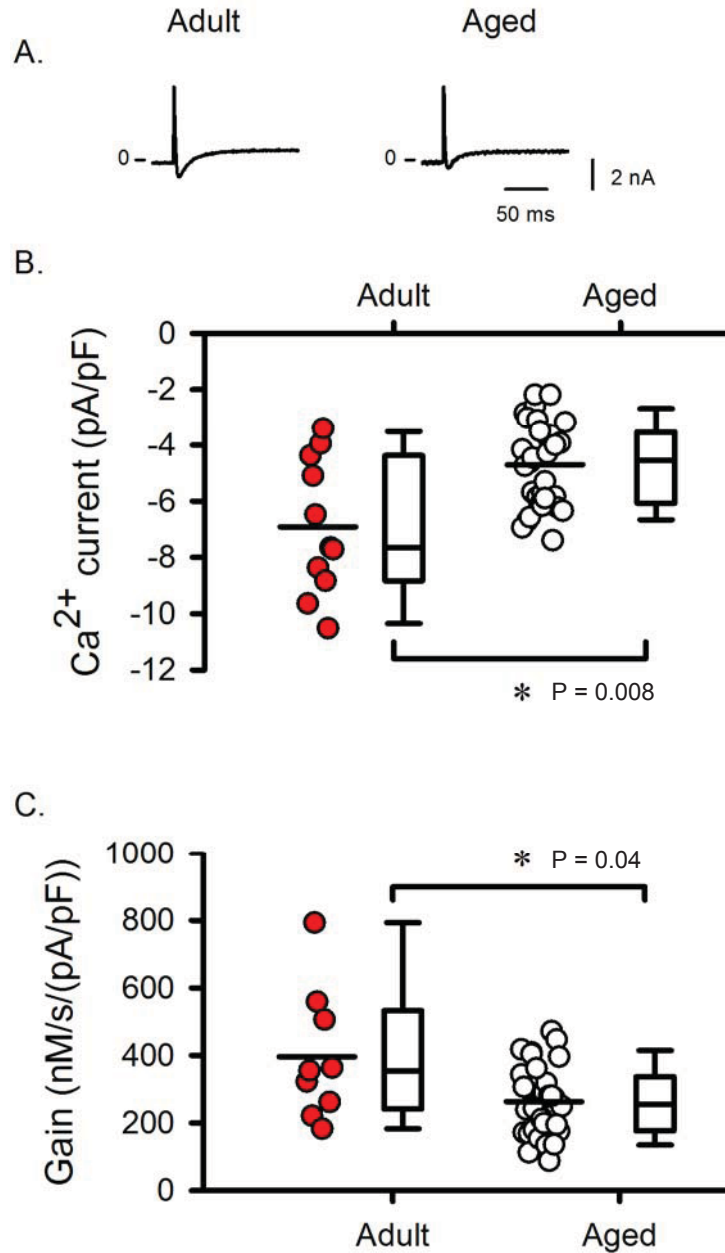


Figure 13. Peak Ca^{2+} currents and gain of SR Ca^{2+} release declined with age. A) Representative Ca^{2+} currents recorded from an adult and aged cell. **B)** Mean peak Ca^{2+} current was smaller in the aged group ($P = 0.008$; $n = 11$ adult and 32 aged myocytes). **C)** The gain of SR Ca^{2+} release declined with age ($P = 0.04$; $n = 9$ adult and 32 aged myocytes). *represents significant difference from adult group. P-values were determined with a Mann-Whitney Rank Sum test. Adapted with permission from Feridooni *et al.*, 2017.

adult group (-6.9 ± 0.7 pA/pF, $n = 11$ myocytes). Furthermore, the amount of Ca^{2+} released from the SR per unit of Ca^{2+} current, known as the gain of SR Ca^{2+} release, was also measured in cells from both groups. Figure 13C shows that the gain declined ($P = 0.04$) with age (396 ± 64 nM/s/(pA/pF), $n = 9$; 263 ± 18 nM/s/(pA/pF), $n = 32$). The major pore forming unit of the L-type Ca^{2+} channel is the CaV1.2 protein. Therefore, to determine if the decrease in Ca^{2+} current was a result of fewer of Ca^{2+} channels, the expression of CaV1.2 was investigated with Western blot analysis in aged and adult mice. Figure 14A shows representative Western blots for Cav1.2 expression in adult and aged hearts. Each band was normalized to the Ponceau S loading control, at 250 kDa (Figure 14A). Mean CaV1.2 expression (Figure 14B, Supplementary Table 5) was significantly lower in cells from aged hearts (0.60 ± 0.06) when compared to cells from adult hearts (0.93 ± 0.09 ; $P = 0.03$). These results imply that the age-dependent decline in cardiac contractile function observed in intact hearts was a result of a decrease in peak contraction size and slower velocities of shortening and lengthening of individual cardiomyocytes. Furthermore, the smaller contractions in aged hearts may be due to smaller peak Ca^{2+} transients which may be due to smaller Ca^{2+} currents. Fewer L-type Ca^{2+} channels may contribute to the smaller Ca^{2+} currents in the aged hearts. Interestingly, there was marked heterogeneity in cardiac function within each age group, regardless of what parameter was being measured. To account for this heterogeneity in cardiac contractile function, the FI tool was utilized to quantify the overall health of each animal, as described in the next section.

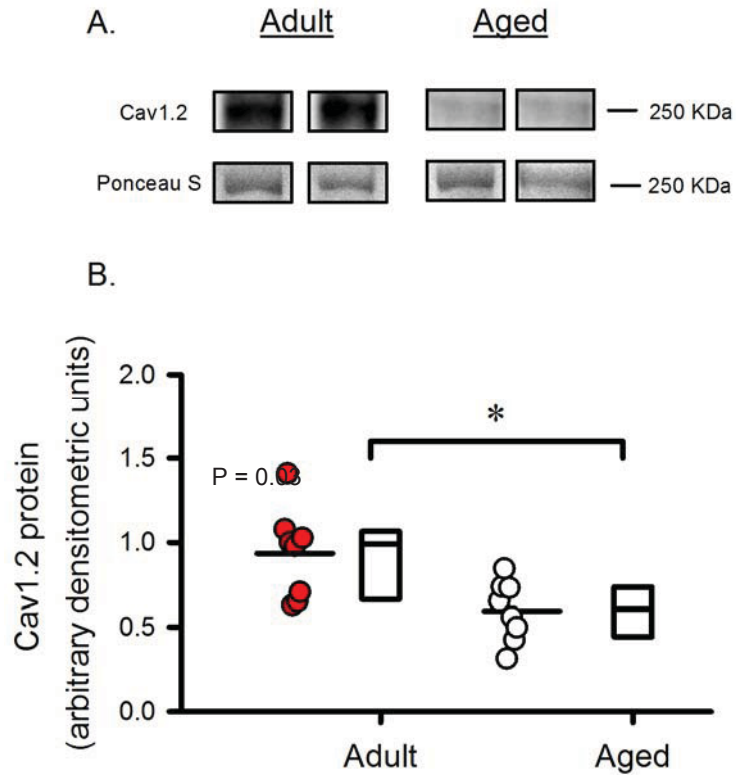


Figure 14. There was an age-dependent decline in CaV1.2 protein expression. A) Representative Western blots of CaV1.2 expression from adult and aged mice. **B)** Mean CaV1.2 protein expression was lower in the aged hearts when comparing to adult hearts ($P = 0.03$). *denotes significant difference from adult group. Significance was assessed using a Mann-Whitney Rank Sum test. ($N = 8$ adult and 8 aged hearts). Adapted with permission from Feridooni *et al.*, 2017.

3.2 INTER-RATER RELIABILITY OF THE MOUSE CLINICAL FI TOOL

3.2.1 Refining the clinical FI tool by quantifying frailty in a large cohort of mice

The mouse clinical FI tool was originally developed by Whitehead *et al.* (2014) to account for heterogeneity in ageing by quantifying the overall health status of the mouse as an FI score. To assess the reliability of this tool, the FI scores for a large cohort (n = 233) of ageing mice were evaluated using two raters. Figure 15 depicts a representative FI assessment form that was used to measure the health status of each mouse. As illustrated in this form, an FI was calculated by tallying all of the scores assigned to each deficit and dividing by 31 (Figure 15). Two independent raters (rater 1 = Hirad; rater 2 = Mike) used this form to calculate a unique FI score for each mouse.

The physical characteristics of the large cohort of mice that were used to assess frailty in this study are summarized as mean \pm SD in Table 11. Both raters independently assessed the same mouse each day. Therefore, the mice were the same age for raters 1 and 2 in all three groups (Table 11). However, mice in group 3 were significantly older than mice in groups 1 and 2, and mice in group 2 were older than mice in group 1 (Table 11). By contrast, average body weight was similar in all three groups for both raters (Table 11). Rater 1 measured higher mean body surface temperatures in all groups compared to rater 2 (Table 11). Body surface temperature also varied between groups in some cases (Table 11). However, even though there was a significant difference in the body surface temperature measured by the two raters, the variation between them was small.

Figure 16 shows that the mean (\pm SEM) FI scores measured by rater 1 (0.182 ± 0.005) and rater 2 (0.183 ± 0.004) were similar in group 1 ($P = 0.83$, $n = 45$). By contrast,

Date: Aug 27/13, ~11 am

Mouse #: 6 Date of Birth: Sept 18/12 Sex: F (M)

Body weight (g) 46 Surface body temperature (°C) 30.2, 30.2, 30.5

Mouse Frailty Assessment Form Avg: 30.3 °C

Rating: 0 = absent 0.5 = mild 1 = severe

System	Parameter	0	0.5	1	Notes
Integument:	❖ Alopecia (hair loss)	0	0.5	1	
	❖ Loss of fur colour	0	0.5	1	
	❖ Dermatitis	0	0.5	1	
	❖ Loss of whiskers	0	0.5	1	
	❖ Coat condition	0	0.5	1	
Muscoskeletal system:	❖ Tumours	0	0.5	1	
	❖ Distended abdomen	0	0.5	1	
	❖ Kyphosis/hunched posture	0	0.5	1	
	❖ Tail stiffening	0	0.5	1	
	❖ Gait	0	0.5	1	
	❖ Tremor	0	0.5	1	
	❖ Forelimb grip strength	0	0.5	1	
	❖ Body condition score	0	0.5	1	
Vestibulocochlear/Auditory:	❖ Head tilt	0	0.5	1	
	❖ Hearing loss	0	0.5	1	
Ocular/Nasal:	❖ Cataracts	0	0.5	1	
	❖ Discharge/swollen/ squinting	0	0.5	1	
	❖ Microphthalmia	0	0.5	1	
	❖ Corneal opacity	0	0.5	1	
	❖ Vision loss	0	0.5	1	
	❖ Menace reflex	0	0.5	1	
	❖ Nasal discharge	0	0.5	1	
Digestive/Urogenital system:	❖ Malocclusions	0	0.5	1	
	❖ Rectal prolapse	0	0.5	1	
	❖ Penile/Uterine prolapse	0	0.5	1	
	❖ Diarrhoea	0	0.5	1	
Respiratory:	❖ Breathing rate/depth	0	0.5	1	
Discomfort:	❖ Mouse Grimace Scale	0	0.5	1	
	❖ Piloerection	0	0.5	1	

Total Score/ Max Score:

5.5 + 0 + 0 = 5.5

$\frac{5.5}{31} = 0.1774$

Figure 15. A representative example of the novel non-invasive FI tool developed by our lab. A representative example of a completed frailty index form to assess the frailty of mouse #6 in our large cohort of ageing mice. The potential age-dependent health deficits are scored as 0, 0.5, or 1, summed and divided by 31 to get a score of 0.177.

Table 11: Characteristics of male C57BL/6J mice used to assess the inter-rater reliability of the mouse clinical FI

Characteristic*	Rater 1	Rater 2
Group 1		
Age (days)	349.6 ± 6.3	349.6 ± 6.3
Weight (g)	47.6 ± 5.6	47.5 ± 5.8
Body surface temperature (°C)	31.3 ± 0.8	30.9 ± 0.6 ^a
Number of mice	45	45
Group 2		
Age (days)	374.8 ± 3.8 ^b	374.8 ± 3.8 ^b
Weight (g)	48.9 ± 4.0	49.0 ± 3.9
Body surface temperature (°C)	30.7 ± 0.9 ^b	30.1 ± 0.8 ^{a,b}
Number of mice	50	50
Group 3		
Age (days)	405.2 ± 11.8 ^{b,c}	405.2 ± 11.8 ^{b,c}
Weight (g)	48.9 ± 4.8	49.0 ± 4.7
Body surface temperature (°C)	30.4 ± 0.9 ^{b,c}	30.0 ± 0.8 ^{a,b}
Number of mice	138	138

*Values represent the mean ± SD. Weight and body surface temperature data were evaluated with 2-way ANOVA with rater and group as main factors; differences between groups for age were assessed with a 1-way ANOVA on ranks. Used with permission from Feridooni *et al.*, 2015.

^a Denotes significantly different from Rater 1.

^b Denotes significantly different from Group 1.

^c Denotes significantly different from Group 2.

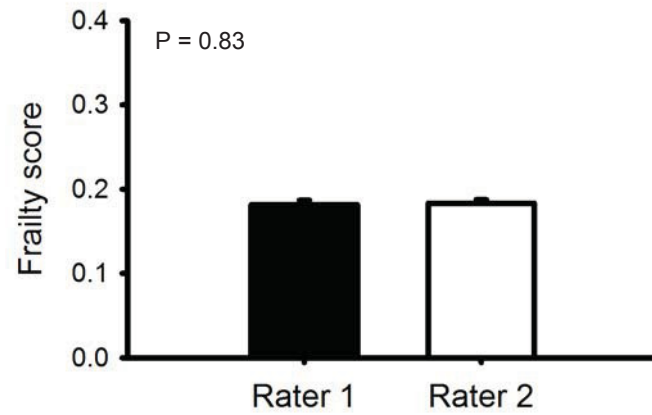
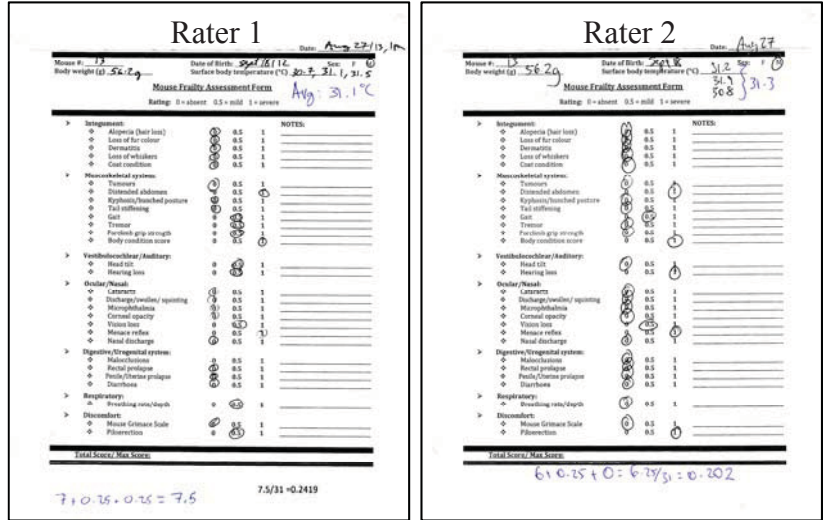


Figure 16. The mean (\pm SEM) frailty scores for mice in Group 1 did not differ between raters. $P = 0.83$, $N = 45$. P-value was determined with a Student's t test. Adapted with permission from Feridooni *et al.*, 2015.

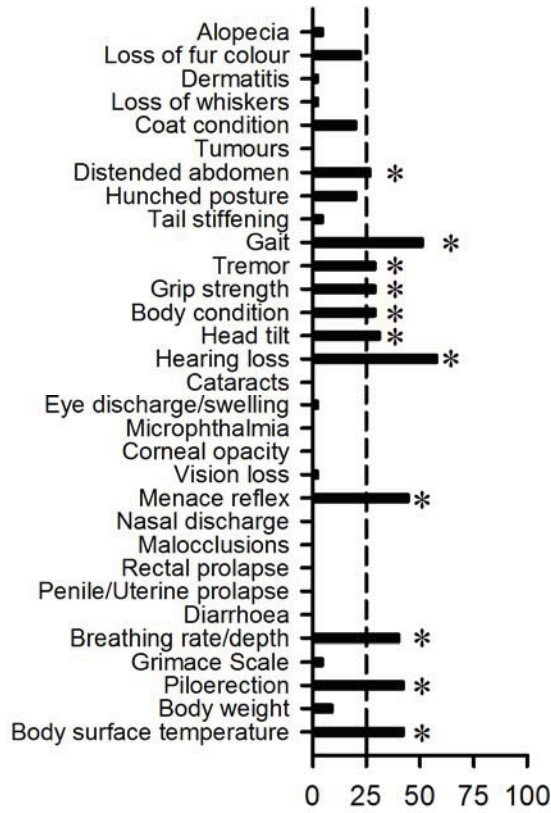
there were several differences in the assessment of individual items in the FI tool between raters. Figure 17A is a representative example of frailty assessments by rater 1 and rater 2 for mouse #13. The differences between rater 1 and rater 2 in the assessment of individual health deficits used to construct the FI tool is shown in Figure 17B. Differences between raters were calculated by taking the total number of discrepancies between raters and dividing that number by the total number of animals within each group. Results are expressed as a percentage of the total number of mice in group 1 (Figure 17B). The dashed line expresses a 25% difference between the two raters (Figure 17B). Items that differed by more than 25% in group 1 were identified by an asterisk (Figure 17B). These items were: distended abdomen, gait, tremor, grip strength, body condition, head tilt, hearing loss, menace reflex, breathing rate/depth, piloerection, and body surface temperature (Figure 17B). These observations indicate that even though there were discrepancies in assessments of frailty items between raters, mean FI scores did not differ between raters.

Based on results from group 1, the rating criteria and descriptions used to assess these items were refined and the frailty of mice in group 2 was evaluated. Results show that mean (\pm SEM) FI scores measured by rater 1 (0.225 ± 0.005) and rater 2 (0.215 ± 0.005) for group 2 ($P = 0.17$, $n = 50$) were similar (Figure 18A). The number of discrepancies between raters did decline in group 2. However, kyphosis, tremor, hearing loss, menace reflex, piloerection, and body surface temperature still differed by more than 25% between raters (Figure 18B). Therefore, the assessment criteria and descriptions of the items that differed between raters was further refined and FI scores were evaluated in group 3. Figure 19A shows that FI scores for both raters were similar (rater 1 = 0.217 ± 0.003 ; rater 2 = 0.221 ± 0.003 ; $P = 0.33$, $n = 138$). The number of discrepancies between

A.



B.



Difference between raters (%)

Figure 17. Various differences in assessing certain deficits were identified between raters. A) Representative FI assessments of the same mouse by rater 1 and rater 2. **B)** The number of differences between raters for each individual item in the FI expressed as a percentage of the total number of mice (N = 45). Dashed line indicates a difference of 25%. * represent

items that varied by more than 25% between raters ($P < 0.05$). Adapted with permission from Feridooni *et al.*, 2015.

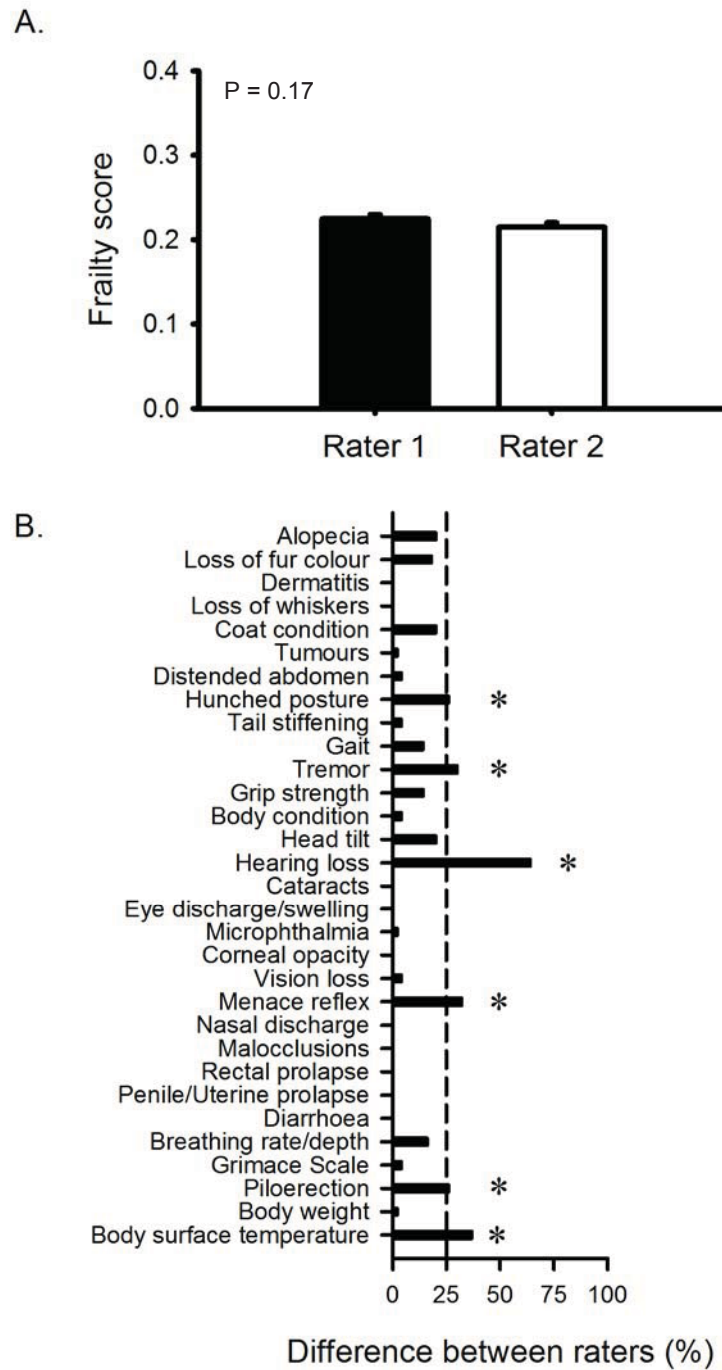


Figure 18. Refinement of the FI tool improved the variability in assessment between raters. A) Mean FI scores were similar for rater 1 and rater 2 ($P = 0.17$, $N = 50$). P-value was determined with a Student's t test. B) The number of differences between raters for each individual item in the FI expressed as a percentage of the total number of mice ($N = 50$). Dashed line indicates a difference of 25%. * represent items that varied by more than 25% between raters ($P < 0.05$). Adapted with permission from Feridooni *et al.*, 2015.

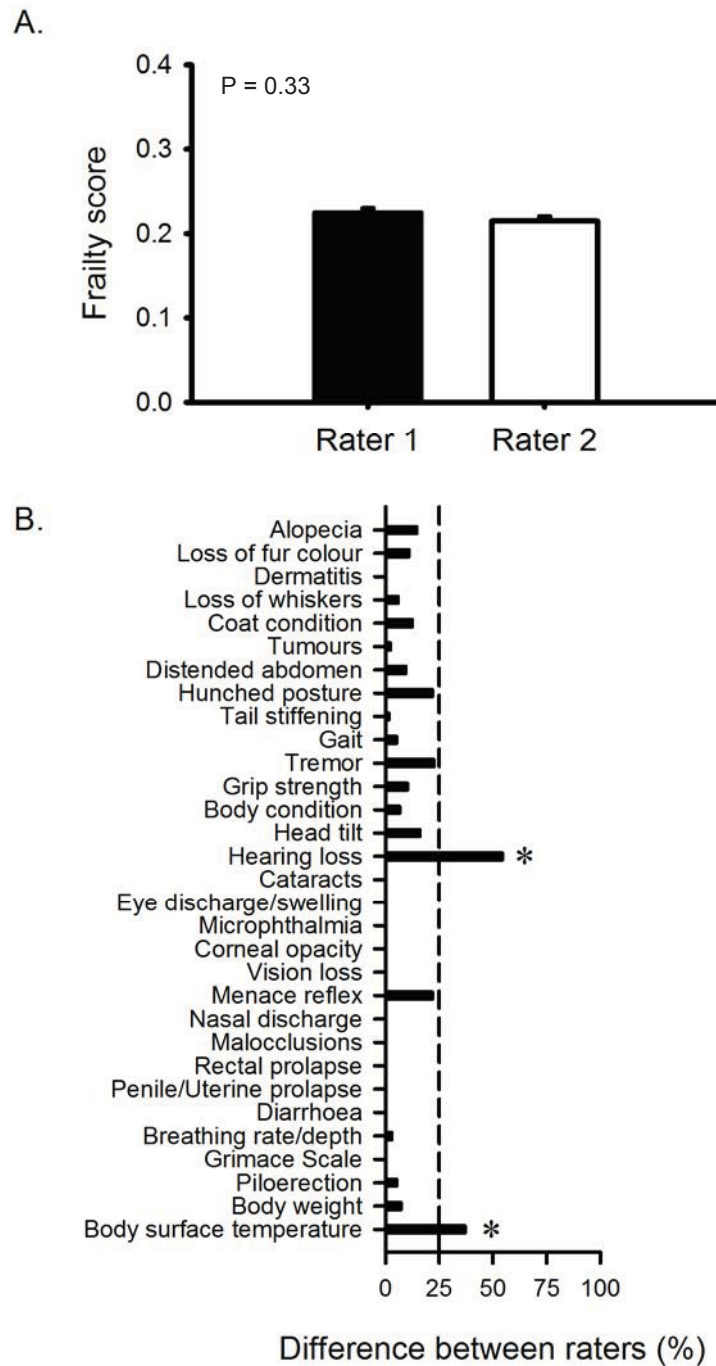


Figure 19. Differences between raters declined after refinement of the FI index tool. **A)** Frailty scores were similar between raters ($P = 0.33$, $N = 138$). P-value was determined with a Student's t test. **B)** Differences between raters for each individual item in the FI is expressed as a percentage of the total number of mice ($N = 138$). Dashed line indicates a difference of 25%. * represent items that varied by more than 25% between raters ($P < 0.05$). Adapted with permission from Feridooni *et al.*, 2015.

raters declined, so that only two items, the hearing test and body surface temperature, differed by more than 25% between raters (Figure 19B).

Interestingly, body surface temperature and the hearing test were the two items where there was consistent disagreement between raters (Figures 17B, 18B, & 19B). Body surface temperature was found to vary depending on the position of the temperature probe. It was determined that reliable and consistent measurement of the body surface temperature could be made when the temperature probe was aimed 2 cm directly above the center of the abdomen. Interestingly, it was determined that when mice were repeatedly exposed to the sound of the clicker, they habituated to the sound (Figure 20). A group of young adult mice ($n = 11$) that had no hearing loss were exposed to repeated clicking sound (Figure 20). The percentage of mice that responded to the clicker sound declined with increasing number of clicks (Figure 20). Therefore, discrepancies in the hearing test between the two raters was due to the mice, who were tested in the same room, habituating to the clicker sound. This was resolved by limiting the number of mice taken into the procedure room at any given time when frailty was being assessed. Furthermore, the mouse cage was covered using a large rat cage to limit the exposure to the clicker sound.

A refined table of the list of descriptors and criteria for the scoring system for each deficit measured in the FI are shown in italics in Table 12. These data indicate that the mouse clinical FI tool can be used to assess frailty in a large cohort of mice. Furthermore, even though there were differences in scoring certain deficits, the mean FI scores were similar between two raters. Finally, the description and criteria of the items with the most discrepancies in the FI were refined.

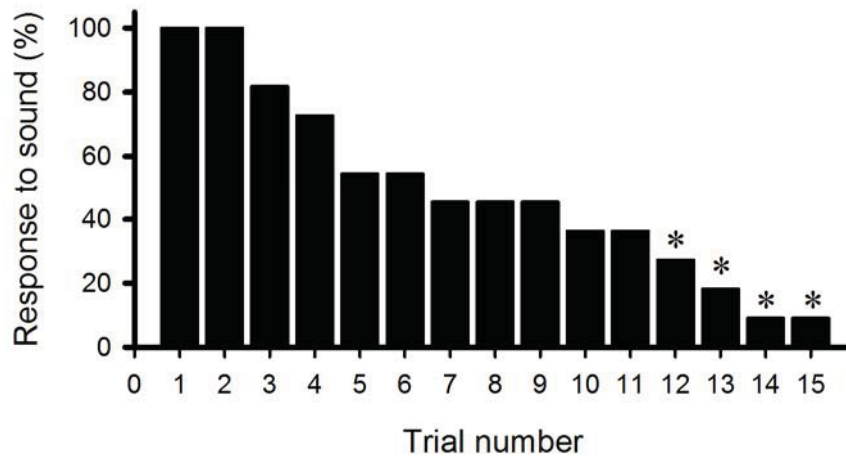


Figure 20. Response to sound declined with repeated exposure within a short time period. The percentage of mice that responded to the clicking sound was plotted as a function of the trial number (number of clicks). Data represents the ratio between the number of mice that responded to the clicker and the total number of mice tested (N = 11). * denotes significantly different from trial 1. Statistical difference was determined using ANOVA on ranks ($p < 0.05$). Adapted with permission from Feridooni *et al.*, 2015.

Table 12: Refined criteria for the clinical assessment of health deficits in the mouse clinical FI tool

System/ Parameter	Clinical assessment of deficit	Scoring
Integument		
<i>Alopecia</i>	<i>Gently restrain the animal and inspect it for signs of fur loss including signs of barbering.</i>	0 = normal fur density 0.5 = < 25% fur loss 1 = >25% fur loss
<i>Loss of fur colour</i>	<i>Note any change in fur colour from black to grey or brown.</i>	0 = normal colour 0.5 = patchy, focal grey, brown or white changes 1 = grey, brown or white fur on >25% of body
Dermatitis	Document skin lesions.	0 = absent 0.5 = focal lesions (e.g. neck, flanks, under chin) 1 = widespread or multifocal lesions
Loss of whiskers	Inspect the animal for signs of a reduction in the number of whiskers.	0 = no loss 0.5 = reduced number of whiskers 1 = absence of whiskers
<i>Coat condition</i>	<i>Inspect the animal for signs of poor grooming. Alopecia and loss of fur colour can contribute to poor coat condition.</i>	0 = smooth, sleek, shiny coat 0.5 = coat is slightly ruffled 1 = unkempt and un-groomed, matted appearance
Physical/ Musculoskeletal		
Tumours	Observe the mice to look for symmetry. Hold the base of the tail and manually examine mice for visible or palpable tumours.	0 = absent 0.5 = <1.0 cm 1 = >1.0 cm or multiple smaller tumours
<i>Distended abdomen</i>	<i>Hold the mouse vertically at the base of the tail and tip backwards over your hand. Excess fluid visible as a “W-shaped” bulge below the rib cage.</i>	0 = absent 0.5 = slight bulge 1 = abdomen distended, distinct “W-shaped” bulge
<i>Kyphosis</i>	<i>Inspect the mouse for curvature of the spine or hunched posture, typically seen in the upper back. Run your fingers down both sides of the spine to detect prominent processes or abnormalities.</i>	0 = absent 0.5 = mild curvature 1 = clear evidence of hunched posture
Tail stiffening	Grasp the base of the tail with one hand, and stroke the tail with a finger of the other hand. The tail should wrap freely around the finger when mouse is relaxed.	0 = no stiffening 0.5 = tail responsive but does not curl 1 = tail completely unresponsive

Table 12 continued

System/ Parameter	Clinical assessment of deficit	Scoring
<i>Tremor</i>	<i>Observe the freely moving animal to detect tremor, both at rest and when the animal is trying to climb up an incline (~60°). Paws shake during climb.</i>	<i>0 = no tremor 0.5 = paw shake and/or tremor during climb 1 = marked tremor; animal cannot climb</i>
<i>Forelimb grip Strength</i>	<i>Hold the mouse. Allow it to grip the bars on the cage lid. Lift animal by the base of the tail to assess grip strength. Practice this on young mice with normal grip strength.</i>	<i>0 = sustained grip 0.5 = reduction in grip strength 1 = no grip strength, no resistance</i>
<i>Body condition score</i>	<i>Place mouse on flat surface, hold tail base and manually assess the amount of flesh/fat that covers the sacroiliac region (back & pubic bones) looking for excess or insufficient flesh/fat.</i>	<i>0 = bones palpable, not prominent 0.5 = bones prominent or barely felt 1 = bones very prominent or not felt due to obesity</i>
Vestibulocochlear/ Auditory		
<i>Vestibular disturbance</i>	<i>Hold the base of the tail and lower mouse towards a flat surface. Inspect for head tilt, spinning, circling, head tuck or trunk curling. Ensure that animal is tilting, not simply trying to reach your finger.</i>	<i>0 = absent 0.5 = mild head tilt and/or slight spin when lowered 1 = severe disequilibrium</i>
<i>Hearing loss</i>	<i>Test startle reflex. Hold a clicker ~10 cm from mouse, sound it 3 times and record responses. Note that mice will habituate to this sound, so test mice individually, in a quiet room.</i>	<i>0 = always reacts (3/3 times) 0.5 = reacts 1/3 or 2/3 times 1 = unresponsive (0/3 times)</i>
<i>Cataracts</i>	<i>Visual inspection of the mouse to detect opacity in the centre of the eye.</i>	<i>0 = no cataract 0.5 = small opaque spot 1 = clear evidence of opaque lens</i>
<i>Eye discharge/swelling</i>	<i>Visual inspection of the mouse to detect ocular discharge and swelling of the eyes.</i>	<i>0 = normal 0.5 = slight swelling and/or secretions 1 = obvious bulging and/or secretions</i>
<i>Microphthalmia</i>	<i>Inspect eyes.</i>	<i>0 = normal size 0.5 = one or both eyes slightly small or sunken 1 = one or both eyes very small or sunken</i>

Table 12 continued.

System/ Parameter	Clinical assessment of deficit	Scoring
Vestibulocochlear/ Auditory		
<i>Vision loss</i>	<i>Lower mouse towards a flat surface. Evaluate the height at which the mouse reaches towards the surface.</i>	<p>0 = reaches >5 cm above surface</p> <p>0.5 = reaches 2-5 cm above surface</p> <p>1 = reaches <2 cm above surface</p>
<i>Menace reflex</i>	<i>Move an object rapidly towards the mouse's face 3 times. Record whether the mouse blinks, flinches or squints in response. Response should be immediate.</i>	<p>0 = always responds</p> <p>0.5 = no response to 1 or 2 approaches</p> <p>1 = no response to 3 approaches</p>
Nasal discharge	Visual inspection of the mouse to detect nasal discharge.	<p>0 = no discharge</p> <p>0.5 = small amount of discharge</p> <p>1 = obvious discharge, both nares</p>
Digestive/ Urogenital		
Malocclusions	Grasp the mouse by the neck scruff, invert and expose teeth. Look for uneven, overgrown teeth.	<p>0 = mandibular longer than maxillary incisors</p> <p>0.5 = teeth slightly uneven</p> <p>1 = teeth very uneven and overgrown</p>
Rectal prolapse	Grasp the mouse by the base of the tail to detect signs of rectal prolapse.	<p>0 = no prolapse</p> <p>0.5 = small amount of rectum visible below tail</p> <p>1 = rectum clearly visible below tail.</p>
Vaginal/uterine/penile prolapse	Grasp the mouse by the base of the tail to detect signs of vaginal/uterine or penile prolapse.	<p>0 = no prolapsed</p> <p>0.5 = small amount of prolapsed tissue visible</p> <p>1 = prolapsed tissue clearly visible</p>
Diarrhoea	Grasp the mouse and invert it to check for signs of diarrhoea. Also look for fecal smearing in home cage.	<p>0 = none</p> <p>0.5 = some feces or bedding near rectum</p> <p>1 = feces, blood and bedding near rectum, home cage smearing</p>
Respiratory		
<i>Breathing rate/depth</i>	<i>Observe the animal. Note the rate and depth of breathing as well as any gasping behaviour. This can be difficult to evaluate when mice are sniffing & exploring new environments. Allow acclimation.</i>	<p>0 = normal</p> <p>0.5 = modest change in breathing rate and/or depth</p> <p>1 = marked changes in rate/depth, gasping</p>

Table 12 continued.

<i>System/ Parameter</i>	<i>Clinical assessment of deficit</i>	<i>Scoring</i>
Discomfort		
Mouse Grimace Scale	Note facial signs of discomfort: 1) orbital tightening, 2) nose bulge, 3) cheek bulge, 4) ear position (drawn back) or 5) whisker change (either backward or forward).	0 = no signs present 0.5 = 1 or 2 signs present 1 = 3 or more signs present
<i>Piloerection</i>	<i>Observe the animal and look for signs of piloerection on fur throughout the body, but particularly at the base of the neck.</i>	<i>0 = no piloerection 0.5 = involves fur at base of neck only 1 = widespread piloerection</i>
Other		
<i>Temperature</i>	<i>Measure surface body temperature with an infrared thermometer directed ≈ 2 cm above the centre of the abdomen. Position of device should be consistent. Compare the average of 3 measurements with reference values from sex-matched adult animals.</i>	<i>0 = differs by <1 SD from reference value 0.25 = differs by 1 SD 0.5 = differs by 2 SD 0.75 = differs by 3 SD 1 = differs by >3 SD</i>
Weight	Weigh the mouse. Compare with reference values from sex-matched adult animals.	0 = differs by <1 SD from reference value 0.25 = differs by 1 SD 0.5 = differs by 2 SD 0.75 = differs by 3 SD 1 = differs by >3 SD

Items that are in italics have been refined from the original table published by Whitehead *et al.* 2014. Used with permission from Feridooni *et al.*, 2015.

3.2.2 Assessing the inter-rater reliability of the mouse clinical FI tool

There is very little test-to-test variability when the clinical FI is used by a single rater (Whitehead et al., 2014). However, the reliability of this instrument had not been assessed when used by different raters. To determine the reliability of the clinical FI instrument between two separate raters, the inter-rater reliability was measured in groups 1-3 with three measures: the standard correlation coefficients, the Cohen's kappa statistic, and the ICC. Figure 21 shows simple linear regression graphs where the FI scores assessed by rater 1 were plotted as a function of FI scores from rater 2 for each individual mouse. The correlation coefficient (r) for the linear regression for group 1 was 0.35 ($P = 0.02$) (Figure 21A). The values of r increased to 0.59 ($P < 0.0001$) and 0.62 ($P < 0.0001$) for group 2 and group 3, respectively (Figure 21B & C). Next, the inter-rater reliability was calculated using the Cohen's kappa statistics, which accounts for agreement between raters that would otherwise occur by chance. Results show that the mean (\pm) kappa values for group 1 were 0.61 ± 0.13 (Figure 22A). The mean kappa values improved to 0.75 ± 0.11 and 0.82 ± 0.10 in group 2 and group 3, respectively ($P < 0.05$) (Figure 22A). Lastly, inter-rater reliability was assessed with the ICC and a two-way random model and consistency analysis. The 95% CI was calculated for the ICC of each group. Similar to the kappa statistic and the linear correlation analysis, the mean ICC values also improved over the course of the study (Figure 22B). Results showed that the ICC values increased ($P < 0.05$) from 0.51 (CI = 0.11-0.73) in group 1, to 0.74 (CI = 0.54-0.85) in group 2, and 0.77 (CI = 0.67-0.83) in group 3 (Figure 22B). These results indicate that the mouse clinical FI tool had high initial inter-rater reliability as quantified by the correlation coefficient, Cohen's

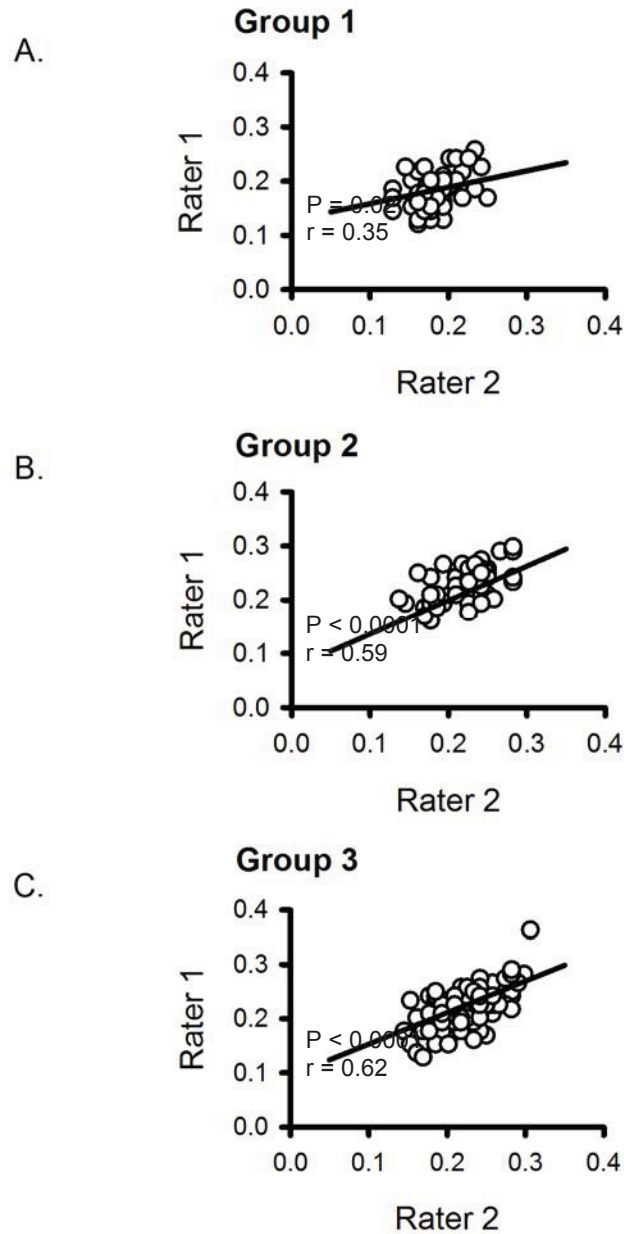


Figure 21. Reliability measured by the standard correlation coefficient (r), improved between raters with subsequent measurements. FI scores for rater 1 were plotted as a function of FI scores for rater 2. The plots were fit with a simple linear regression. **A,B,C** The r values for groups 1, 2, and 3 were 0.35 ($P = 0.02$, $N = 45$), 0.59 ($P < 0.0001$, $N = 50$), and 0.62 ($P < 0.0001$, $N = 138$), respectively. Used with permission from Feridooni *et al.*, 2015.

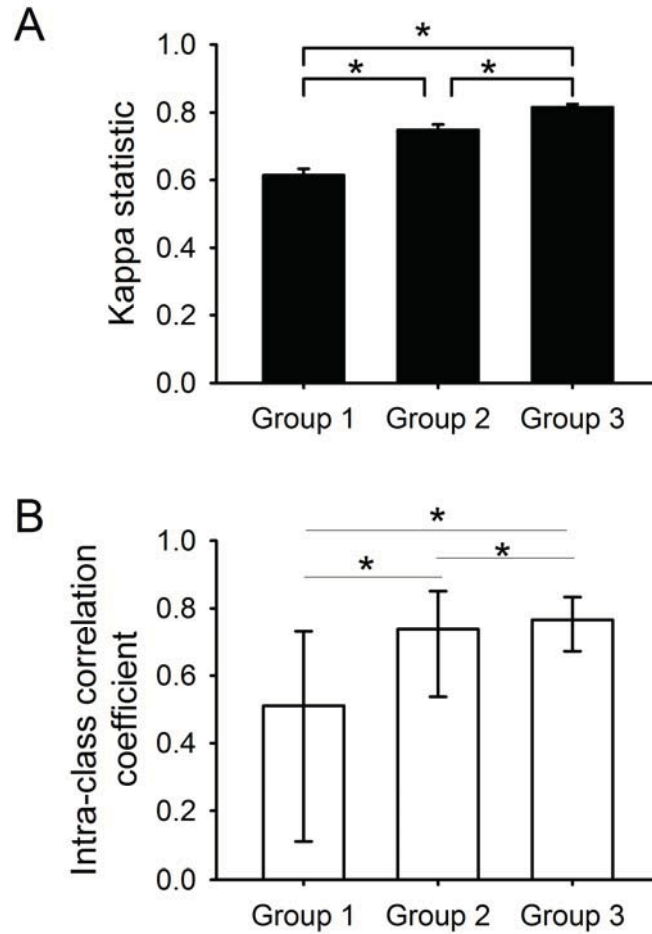


Figure 22. The frailty index tool was highly reliable between raters. Inter-rater reliability as assessed by the kappa statistic and ICC improved with each group. **A)** Mean (\pm SEM) kappa values increased progressively from group 1 to groups 2 and 3 (one-way ANOVA, $P < 0.05$). **B)** ICC values represent correlation coefficients \pm 95% CI. ICC significantly improved between raters throughout the study (ANOVA, $P < 0.5$). (N = 45, 50, and 138 for groups 1, 2, and 3, respectively). *denotes significant difference from comparison group. Used with permission from Feridooni *et al.*, 2015.

kappa statistic, and ICC (Figures 21 & 22). The inter-rater reliability was further improved through the refinement of the instrument, as highlighted above (section 3.2.1). This study improved this index making it a more reliable tool to assess frailty in ageing mice.

3.2.3 Frailty increases with age

The relationship between frailty and age was investigated by comparing the frailty scores of the large cohort of individual mice to their respective age ($n = 233$). The scatterplot of this relationship is shown in Figure 23A. The FI scores are plotted as a function of age for all mice examined by both raters (Figure 23A). Results show that FI scores increased with age for both rater 1 ($r = 0.31$, $P < 0.0001$) and rater 2 ($r = 0.36$, $P < 0.0001$). Interestingly, there is marked variability in individual FI scores at each age. However, as described above, mean (\pm SEM) FI scores were similar for both raters in each group, although the mean frailty scores increased with age ($P < 0.05$) (Figure 23B). These findings indicate that on average, frailty increased with age, although there was marked differences in the overall health status for individual mice of the same chronological age.

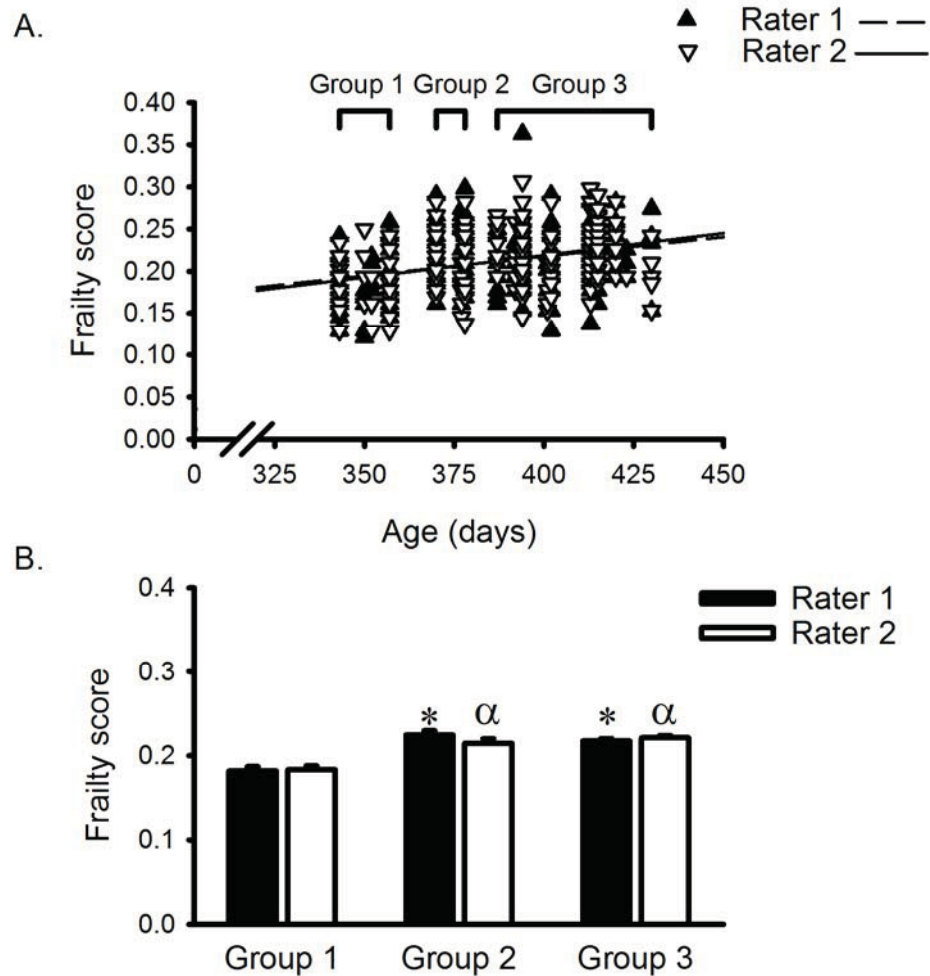


Figure 23. Frailty scores increased with age. Frailty scores were similar between raters at all time points within each group. **A)** Scatterplot of the relationship between age and frailty scores of all mice ($n = 233$) assessed by rater 1 ($r = 0.31$, $P < 0.0001$) and rater 2 ($r = 0.36$, $P < 0.0001$). **B)** Mean (\pm SEM) frailty scores were not significantly different between raters in any group ($P = 0.83$, 0.17 , 0.33 for groups 1, 2, and 3, respectively). FI scores were significantly lower in group 1 than FI scores from groups 2, and 3. *denotes significant difference ($P < 0.05$) from group 1 for rater 1. α denotes significant difference ($P < 0.05$) from group 1 for rater 2. Data were analyzed using a two-way ANOVA. In all cases, $n = 45$, 50 , 133 in groups 1, 2, and 3, respectively. Adapted with permission from Feridooni *et al.*, 2015.

3.3 THE RELATIONSHIP BETWEEN FRAILTY AND AGE-DEPENDENT CARDIAC CONTRACTILE DYSFUNCTION

3.3.1 FI scores in adult and aging mice

Using the refined clinical FI tool discussed above, individual FI scores were obtained for each mouse prior to experiments. Figure 24 shows the FI scores for all animals used to assess cardiac contractile function separated into two age groups. Results show that the two groups were significantly different in age (808 ± 11 vs. 219 ± 19 days of age; $P \leq 0.001$). Furthermore, Figure 24 shows that the mean (\pm SEM) FI scores were significantly higher in the aged group in comparison to the adult group (0.374 ± 0.01 for aged vs. 0.118 ± 0.01 for adult; $P \leq 0.001$). The scatterplot in Figure 24 demonstrates that mice of similar ages have FI scores across a wide range of values. This marked heterogeneity was especially prominent in the aged group, where frailty scores in this group overlapped with values for the adult mice (Figure 24). These results showed that mice with similar age exhibited different overall health status and this measured health status may overlap between the aged and adult groups despite the substantial age difference.

3.3.2 The relationship between frailty and age-dependent cardiac hypertrophy

As previously stated, cardiac hypertrophy increased with age (Supplementary Table 2 in section 3.1), although there was noticeable heterogeneity within the adult and aged groups (Figure 7 in section 3.1). To determine whether this age-dependent cardiac hypertrophy was associated with the overall health status of the animal, FI scores were plotted as a function of HW, HW:BW, TL, and HW:TL (Figure 25). Results show that TL

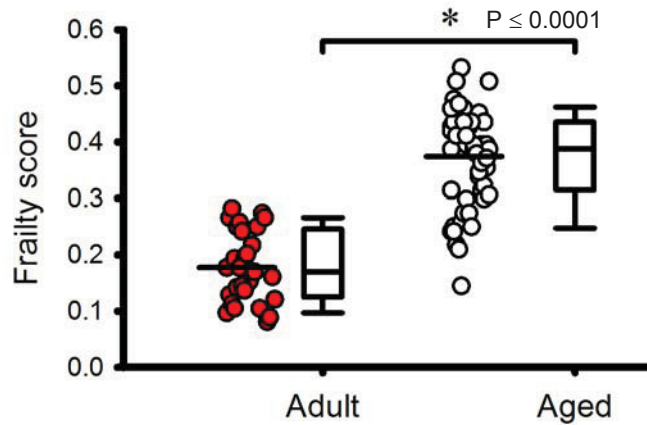


Figure 24. There was marked heterogeneity in the overall health status in mice of the same age. The overall health of adult and aged mice were separated into two age groups (808 ± 11 vs. 219 ± 19 days of age; $P \leq 0.001$). Frailty scores were higher in the aged group compared to the adult group ($P \leq 0.001$). Differences between age groups were assessed using a Mann-Whitney Rank Sum test. $N= 29$ adult and 56 aged mice. Used with permission from Feridooni *et al.*, 2017.

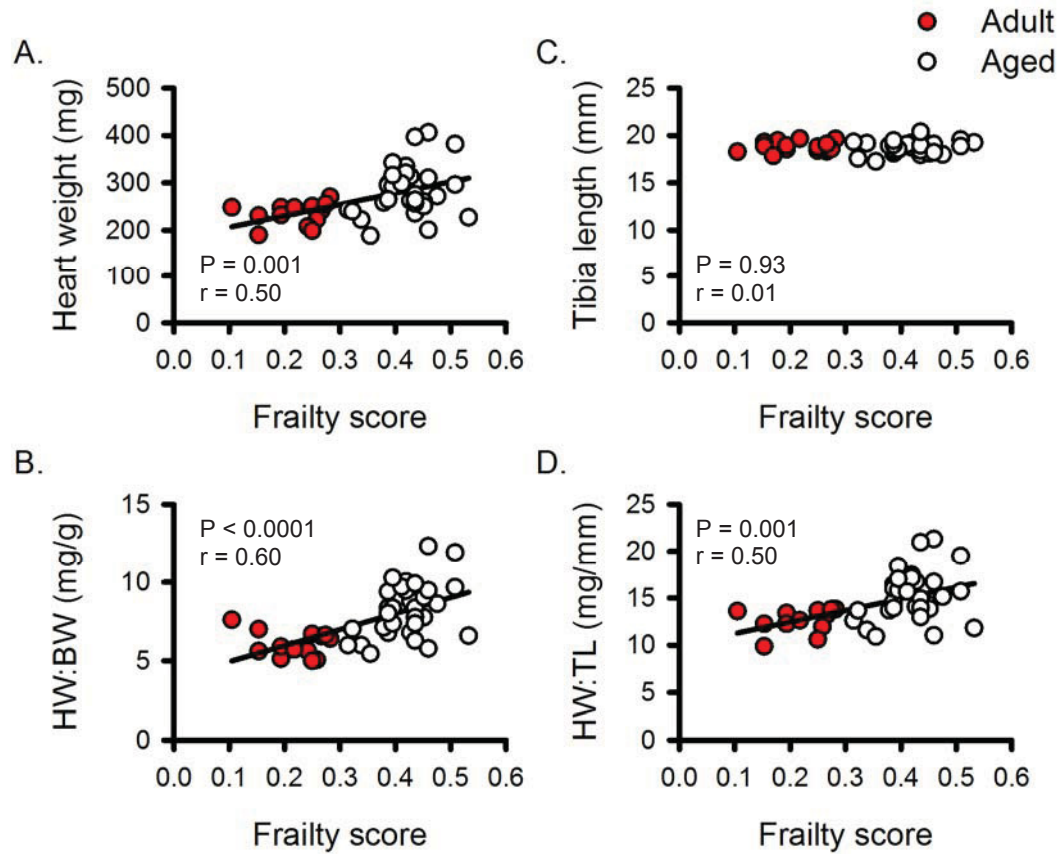


Figure 25. Age-dependent cardiac hypertrophy increased as a function of frailty. **A)** HW increased as frailty increased ($r = 0.50$, $N = 13$; $P = 0.001$). **B)** HW:BW had a positive correlation with frailty ($r = 0.60$, $N = 13$; $P < 0.0001$). **C)** TL was not associated with frailty ($r = 0.01$, $N = 16$; $P = 0.93$). **D)** The increase in HW:TL was graded by frailty scores ($r = 0.50$, $N = 12$; $P = 0.001$). Correlations were evaluated using linear regression analysis. HW = heart weight; HW:BW = heart weight to body weight ratio; TL = tibia length; HW:TL = heart weight to tibia length ratio. Adapted with permission from Feridooni *et al.*, 2017.

($r = 0.01$, $P = 0.93$) was not associated with FI score (Figure 25C). By contrast, HW ($r = 0.50$, $P = 0.001$), HW:BW ($r = 0.60$, $P < 0.0001$), and HW:TL ($r = 0.50$, $P = 0.001$) was associated with a linear increase in frailty scores (Figure 25A, B & D). This increase in heart size, which was graded by frailty, demonstrated that age-dependent hypertrophy was associated with the overall health status of the mouse.

3.3.3 Left ventricular contractile dysfunction is graded by frailty

On average, cardiac contractile function (LVDP, +dP/dt, -dP/dt, and RPP) declined with age in intact hearts (Supplementary Table 3, Figure 9 in section 3.1). However, there was a wide range of responses in these Langendorff-perfused hearts within each age group (Figure 9 in section 3.1). To investigate the relationship between frailty and age-dependent cardiac dysfunction, individual parameters of LV function were plotted as a function of the frailty score for each animal. Figure 26A shows representative pressure recordings from mice with varying FI scores. There were no relationships between age (Figure 9B in section 3.1), frailty ($r = 0.07$, $P = 0.62$), and diastolic pressure (Figure 26B). Furthermore, there were no changes in intrinsic HR ($r = 0.17$, $P = 0.24$) associated with changes in frailty scores (Figure 26C). By contrast, Figure 26D shows that the overall health of the animal was associated with a decline in LVDP ($r = -0.49$, $P = 0.0004$). Similarly, +dP/dt ($r = -0.48$, $P = 0.001$) and -dP/dt ($r = -0.55$, $P < 0.0001$) declined as frailty increased (Figure 26E & F). Furthermore, lower RPP index values ($r = -0.53$, $P = 0.0003$) were seen in hearts isolated from animals with high FI scores (Figure 26G). An increase in frailty score was not associated with changes in coronary flow rate ($r = 0.19$, $P = 0.20$) (Figure 27A) even

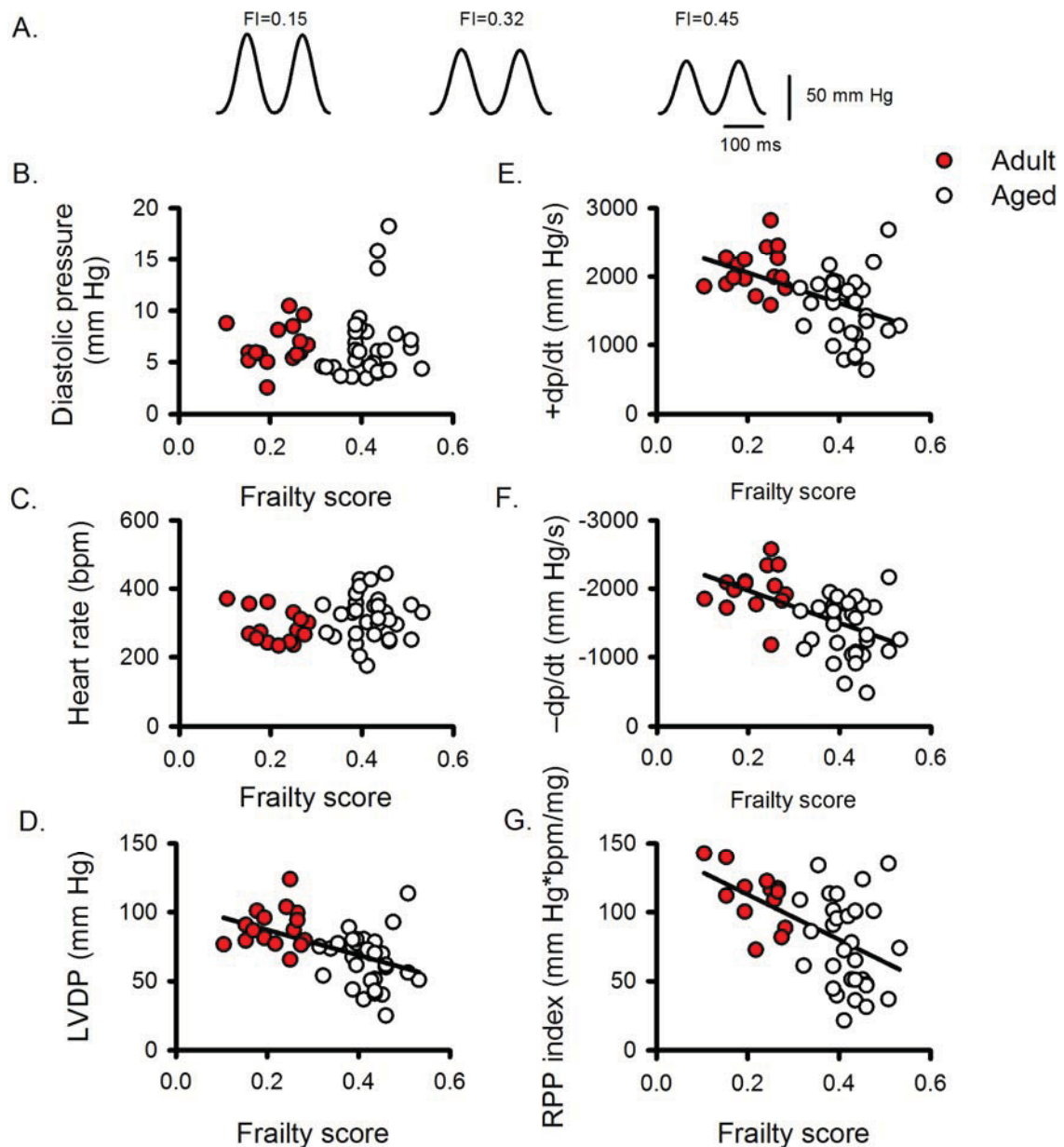


Figure 26. Cardiac contractile dysfunction was graded by frailty scores. A) Representative examples of pressure recorded from perfused hearts from mice with different FI scores. B,C) Diastolic pressure ($r = 0.07$, $P = 0.62$) and HR ($r = 0.17$, $P = 0.24$) were not associated with frailty. D-G) Regression lines show that LVDP ($r = -0.49$, $P = 0.0004$), +dP/dt ($r = -0.48$, $P = 0.001$), -dP/dt ($r = -0.55$, $P < 0.0001$), and RPP index ($r = -0.53$, $P = 0.0003$) were graded by FI score and declined as frailty increased. N=16 adult and 32 aged mice. HR = heart rate; LVDP = Left ventricular developed pressure; +dP/dt = rate of contraction; -dP/dt = rate of relaxation; RPP = Rate pressure product. Adapted with permission from Feridooni *et al.*, 2017.

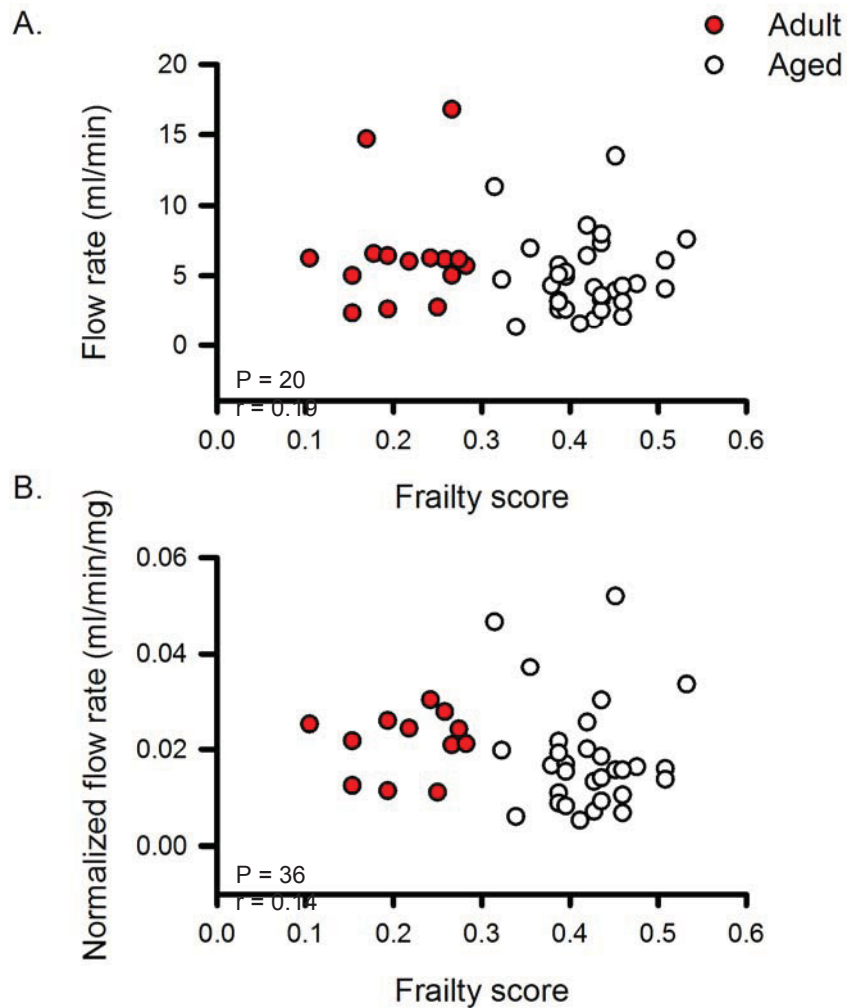


Figure 27. Average flow rates during baseline conditions were not affected by frailty scores. **A)** Average coronary flow rate was not associated with FI scores ($r = 0.19$, $P = 0.20$) ($N=16$ adult and 32 aged mice). **B)** Average coronary flow rate was normalized to the size of the heart. Frailty was not associated with normalized coronary flow rate ($r = 0.14$, $P = 0.36$). ($N = 12$ and 31 for adult and aged mice, respectively).

when data were normalized to the size of the heart ($r = 0.14$, $P = 0.36$) (Figure 27B). These observations indicated that there was an association between the overall health of the animal, quantified by frailty, and age-dependent cardiac contractile dysfunction. Thus, hearts isolated from animals with higher frailty scores did less work (RPP index), had smaller contractions (LVDP), and slower rates of contraction and relaxation ($+dP/dt$ and $-dP/dt$, respectively). This decline in heart function occurred without any observable changes in intrinsic HR or the coronary flow rate.

3.3.4 Age-dependent decline in cell shortening and key Ca^{2+} handling mechanisms are graded by frailty

Previous results in section 3.1 of this thesis showed that the age-dependent decline in cardiac function observed in intact hearts was a result of an age-dependent decline in function at the cellular and subcellular levels. Cardiomyocytes isolated from aged mice had smaller peak contractions and slower velocities of shortening and lengthening compared to cardiomyocytes isolated from adult mice (Figure 12 A-D in section 3.1). There was marked heterogeneity in contractile responses within the adult and aged groups. To account for this heterogeneity, the age-dependent contractile dysfunction was compared to the overall health status of the animal. Representative examples of cell shortening recorded in voltage-clamped myocytes isolated from animals with varying FI scores are shown on the top panel of Figure 28A. These traces show that the size and velocities of contraction were smaller in myocytes isolated from animals that had higher FI scores. Indeed, Figure 28B shows that there was a negative correlation between the frailty score

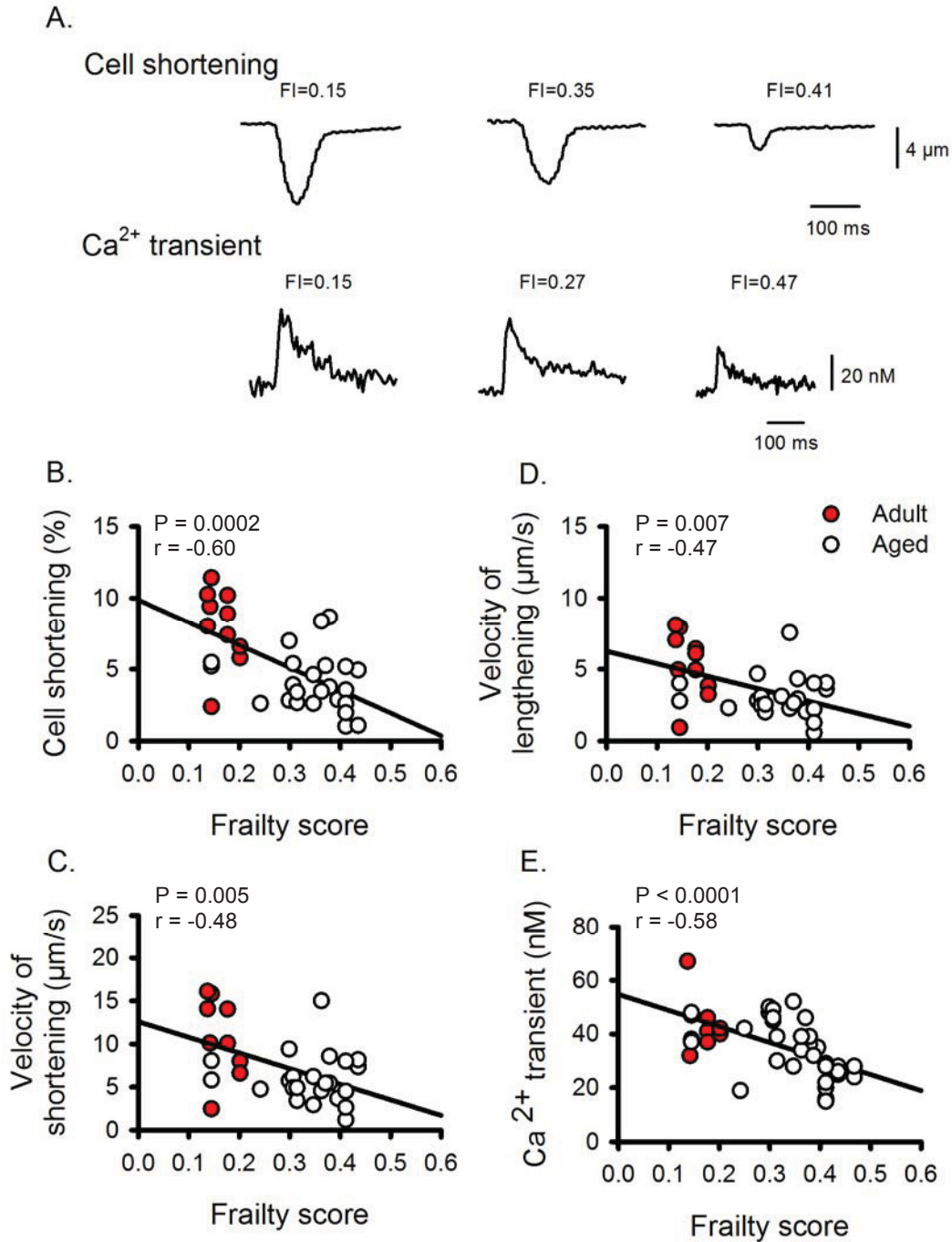


Figure 28. Peak contractions and Ca²⁺ transients were graded by frailty score. A) Representative recordings of cell shortening and Ca²⁺ transients in mice with different FI scores. **B-D)** Cell shortening ($r = -0.60$, $P = 0.0002$) and the velocities of shortening ($r = -0.48$, $P = 0.005$) and lengthening ($r = -0.47$, $P = 0.007$) were negatively associated with frailty. **E)** Ca²⁺ transient amplitude declined with increasing FI scores ($r = -0.58$, $P < 0.0001$). Correlations were made using linear regression analysis. $n = 14-15$ adult and $19-23$ aged myocytes. Adapted with permission from Feridooni *et al.*, 2017.

of the animal and the peak cell shortening ($r = -0.60$, $P = 0.0002$). Similarly, the speed of contraction and relaxation ($r = -0.48$, $P = 0.005$; $r = -0.47$, $P = 0.007$; for velocities of shortening and lengthening, respectively) was inversely related to the FI value (Figure 28C & D).

Cells isolated from aged hearts also had smaller peak Ca^{2+} transients caused by smaller Ca^{2+} currents as a result of fewer L-type Ca^{2+} channels. These Ca^{2+} handling responses were also highly variable (Figure 12E, 13, & 14 in section 3.1). To determine whether there was a relationship between the observed changes in Ca^{2+} handling and frailty, these Ca^{2+} parameters were plotted as a function of frailty scores. Representative traces of Ca^{2+} transients recorded from cardiomyocytes isolated from mice with varying FI scores are shown on the bottom panel of Figure 28A. These traces show that peak Ca^{2+} transients were smaller in cells isolated from mice that had higher FI scores (Figure 28A). Indeed, this age-dependent decline in the Ca^{2+} transient was graded by frailty ($r = -0.58$, $P < 0.0001$) (Figure 28E). Representative Ca^{2+} current recordings show that myocytes isolated from mice with higher FI scores had smaller Ca^{2+} currents (Figure 29A). Indeed, peak Ca^{2+} current declined ($r = 0.40$, $P = 0.008$) as FI scores increased (Figure 29B). The gain of SR Ca^{2+} release, which is the amount of Ca^{2+} released from the SR per unit Ca^{2+} current, was also measured. The overall health of the animal was also associated with decrease in gain of SR Ca^{2+} release ($r = -0.37$, $P = 0.02$) (Figure 29C). The next set of experiments investigated whether the smaller Ca^{2+} current and reduced gain of SR Ca^{2+} release in the aged animals compared to the adult animals were due to a decrease in L-type Ca^{2+} channels. Figure 30A shows representative Western blots for CaV1.2 expression from mice with different frailty values. There was a clear inverse relationship between frailty and CaV1.2

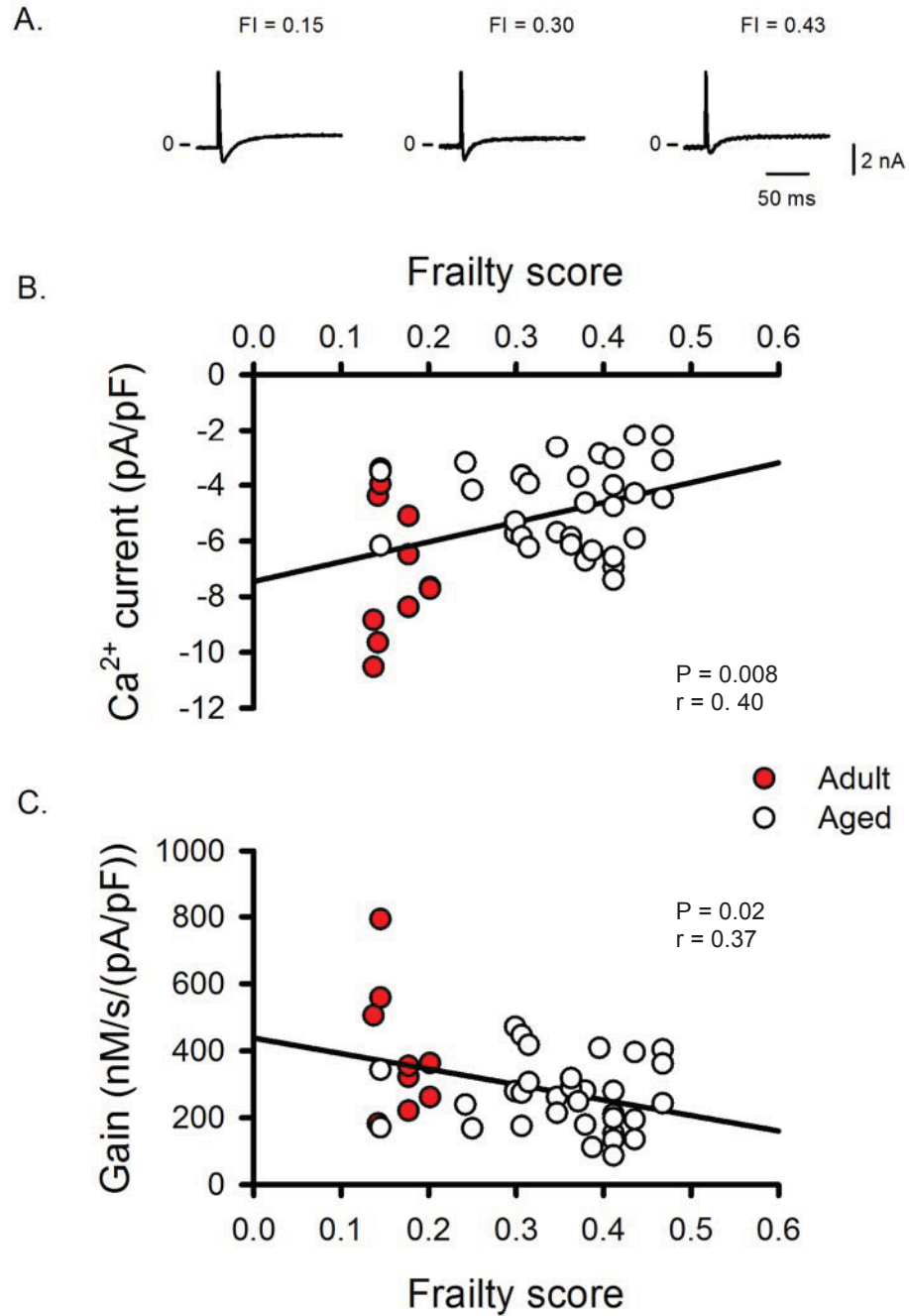


Figure 29. The age-related decline in Ca^{2+} current and the gain of SR Ca^{2+} release was graded by frailty. A) Representative Ca^{2+} currents recorded from cardiomyocytes isolated from mice with varying frailty scores. **B)** Peak Ca^{2+} current was inversely associated with FI scores ($r = 0.40$, $P = 0.008$). **C)** The gain of SR Ca^{2+} release was graded by frailty ($r = -0.37$, $P = 0.02$). Linear regression analysis was used to evaluate correlations. $n = 11$ adult and 32 aged myocytes. Adapted with permission from Feridooni *et al.*, 2017.

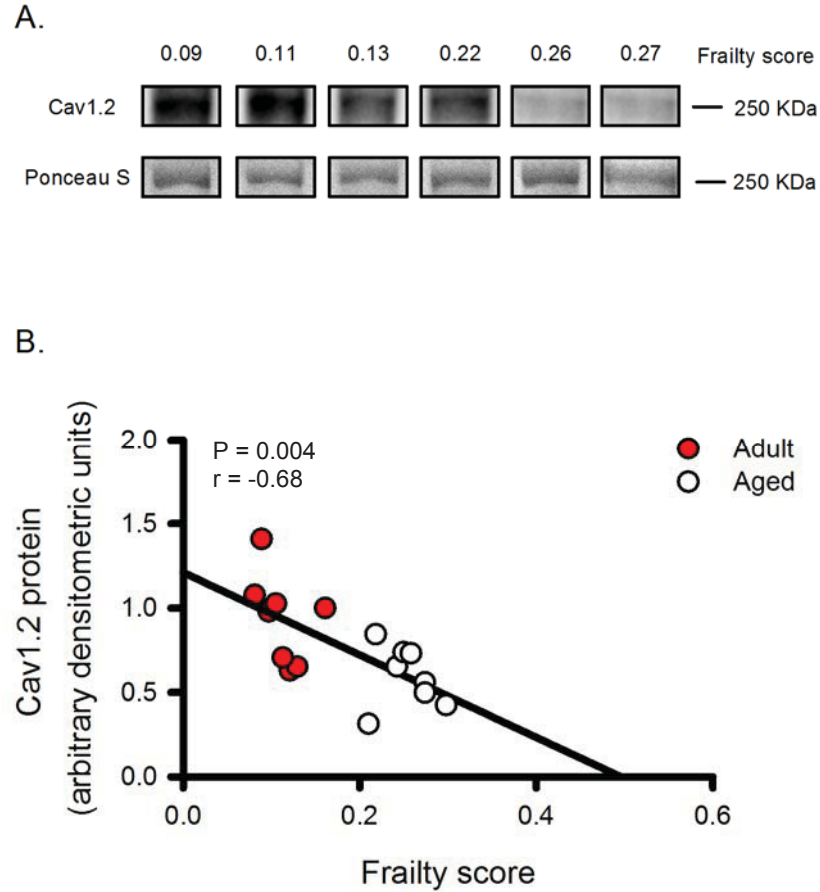


Figure 30. The age-dependent decline in CaV1.2 expression was graded by frailty. **A)** Examples of Western blots for CaV1.2 expression. **B)** CaV1.2 expression was graded by the overall health of the animal, as quantified by a frailty score ($r = -0.68$, $P = 0.004$). Linear regression analysis was used to evaluate correlation. $N = 8$ adult and 8 aged hearts. Adapted with permission from Feridooni *et al.*, 2017.

expression (Figure 30B). These associations between frailty and myocyte contraction were similar to the inverse relationship between frailty and cardiac contractile dysfunction seen in intact hearts. This decrease in contraction with high levels of frailty is due to smaller Ca^{2+} transients triggered by reduced Ca^{2+} currents. Smaller Ca^{2+} current may be due to a decline in the expression of CaV1.2, which was also graded by the FI score of the animal. These results demonstrated that the overall health of the animal, as quantified with a frailty score, was associated with cardiac contractile dysfunction.

3.4 THE IMPACT OF AGE AND FRAILITY ON CONTRACTILE FUNCTION FOLLOWING IR INJURY IN INTACT HEARTS

3.4.1 The relationship between age, frailty, and functional recovery from IR in isolated perfused hearts

The relationship between age, frailty, and recovery of contractile function following IR was investigated in Langendorff-perfused hearts. Hearts were exposed to global ischemia and reperfusion. Figure 31 shows the changes in LVDP, $+\text{dP}/\text{dt}$, and $-\text{dP}/\text{dt}$ before and after exposure to 30 min ischemia, and 40 min reperfusion. Age-related changes in cardiac function under normoxic conditions were previously discussed in section 3.1 of this thesis. Contractions were completely abolished by ischemia (Figure 31). In addition, hearts from both age groups had a significantly smaller LVDP, $+\text{dP}/\text{dt}$, $-\text{dP}/\text{dt}$ throughout reperfusion compared to baseline values ($P < 0.001$) (Figure 31).

The time course for the recovery of contractile function throughout reperfusion is shown in Figures 32. Raw diastolic pressure ($P > 0.05$) and intrinsic heart rate ($P > 0.11$) were not different in the aged and adult groups (Figure 32A & B). By contrast, the aged

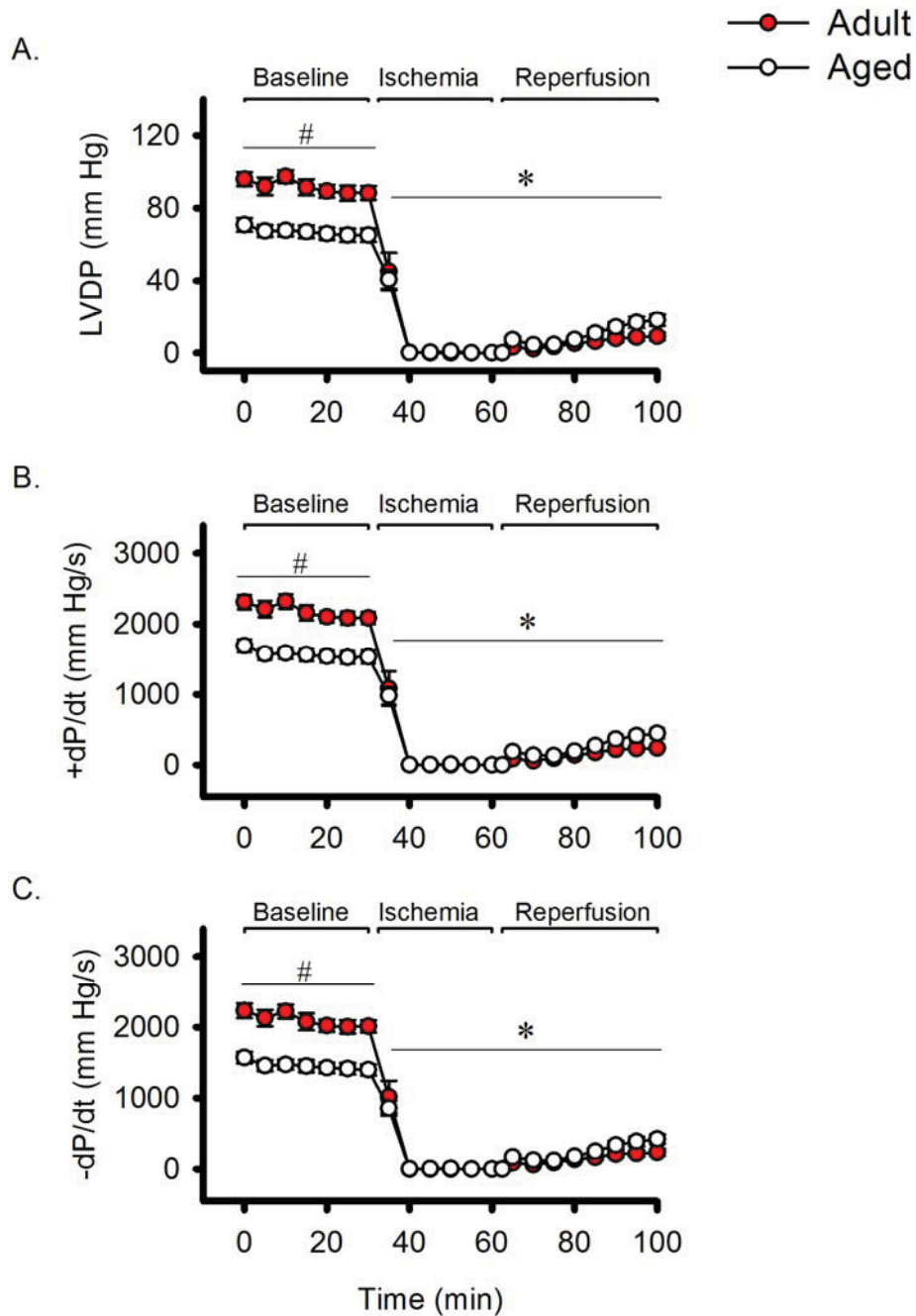


Figure 31. Contractile function declined in IR. A-C) LVDP, +dP/dt, and -dP/dt were diminished following IR in both age groups ($P < 0.001$). Baseline LVDP, +dP/dt, and -dP/dt were significantly lower in the aged hearts compared to the adult hearts ($P < 0.001$). There were no significant differences between LVDP, +dP/dt, and -dP/dt during ischemia and reperfusion between the adult and aged animals. # denotes differences between adult and aged animals. * indicates a significant difference in IR compared to baseline values within each group. Significance was determined by a two-way RM ANOVA. $N = 16$ adult and 32 aged hearts.

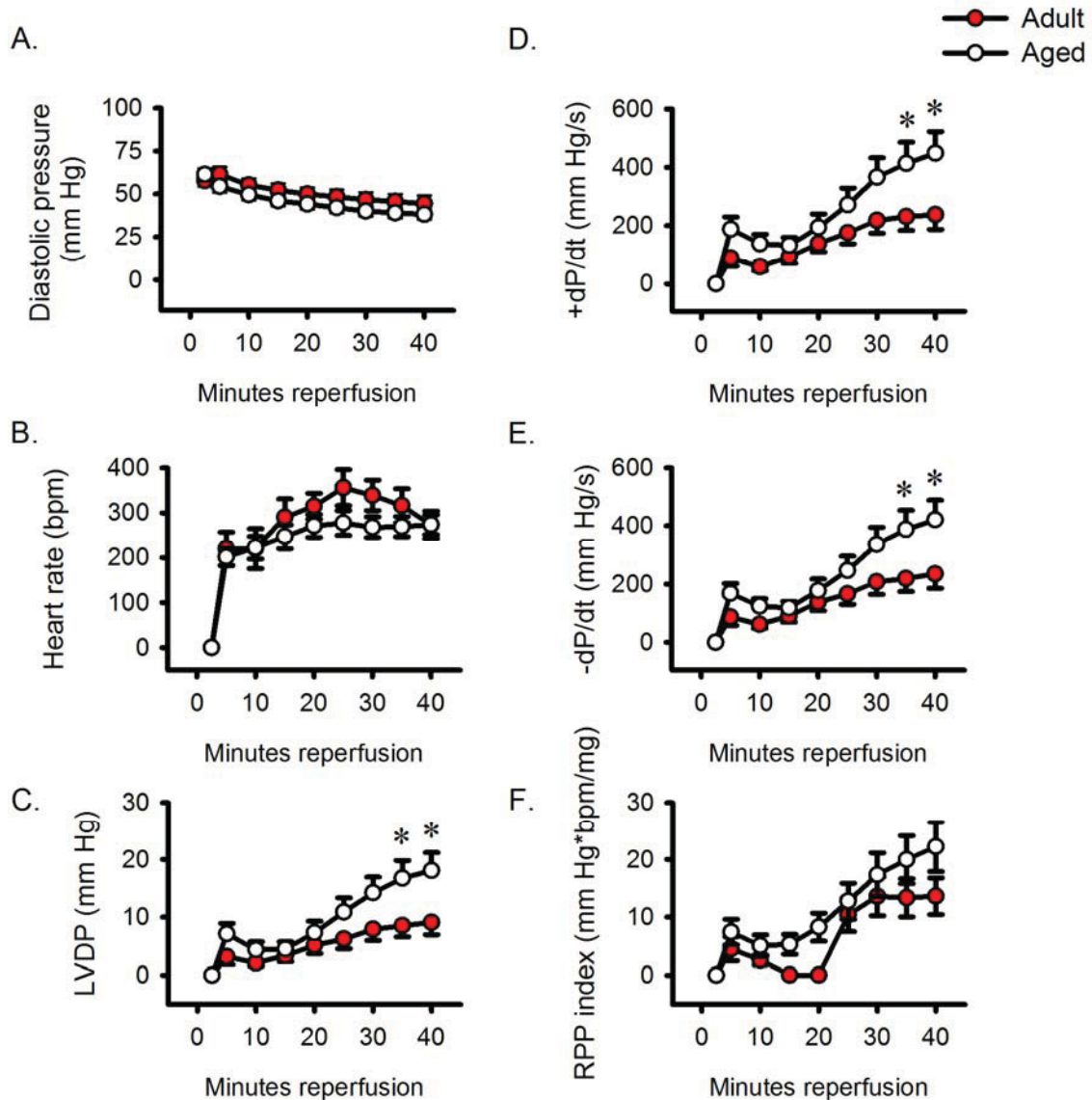


Figure 32. Time course for the recovery of LV contractile function during 40 min reperfusion. A) Diastolic pressure was not significantly different between groups ($P > 0.05$). B) Intrinsic heart rate recovered to the same extent in both age groups ($P > 0.11$). C-E) LVDP ($P < 0.02$), +dP/dt ($P < 0.02$), and -dP/dt ($P < 0.02$) recovered more in aged hearts than adult hearts at the end of reperfusion. F) RPP index ($P > 0.07$) did not change with age at any point throughout reperfusion. Sample size was $n = 13-15$ adult and $30-31$ aged. *denotes $P < 0.05$ for aged vs. adult hearts. Significant difference was determined using a 2-way RM ANOVA test. LVDP = Left ventricular developed pressure; +dP/dt = rate of contraction; -dP/dt = rate of relaxation; RPP = rate pressure product.

group had a larger recovery of LVDP ($P < 0.02$), $+dP/dt$ ($P < 0.02$), and $-dP/dt$ ($P < 0.02$) after 35 min of reperfusion (Figure 32 C-E). The amount of work done by aged and adult hearts was similar throughout reperfusion (Figure 32F). The mean values for the recovery of contractile function at 40 min of reperfusion are summarized in Supplementary Table 6. Following 40 min of reperfusion mean (\pm SEM) diastolic pressure was similar in the adult and aged group (44 ± 4 mm Hg for adult; 38 ± 3 mm Hg for aged; $P = 0.06$) (Supplementary Table 6). Furthermore, there were no significant differences in mean (\pm SEM) HR (278 ± 29 for adult vs. 273 ± 22 bpm for aged; $P = 0.94$) (Supplementary Table 6). By contrast LVDP (8.9 ± 2 for adult vs. 18 ± 3 mm Hg for aged; $P < 0.01$), $+dP/dt$ (235 ± 48 for adult vs. 448 ± 74 mm Hg/s for aged; $P < 0.01$), and $-dP/dt$ (-230 ± 46 for adult vs. -421 ± 67 mm Hg/s for aged; $P < 0.01$) were significantly higher in the aged heart in comparison to adult hearts (Supplementary Table 6). The RPP index (13.6 ± 3.2 for adult vs. 20.3 ± 4.0 mm Hg x bpm/s for aged; $P = 0.09$) at 40 min reperfusion was the same in both age groups (Supplementary Table 6).

Figure 33 shows the recovery of function throughout reperfusion normalized to the heart's function prior to exposure to IR. Recovery of diastolic pressure ($P > 0.90$) as a percentage of pre-ischemic values was the same in both age groups throughout reperfusion (Figure 33A). Intrinsic HR was significantly higher at 25 min reperfusion ($P = 0.03$) in the aged group compared to the adult group (Figure 33B). However, both age groups had the same recovery of HR ($P > 0.1$) after 25 min of reperfusion (Figure 33B). In addition, hearts from the aged animals had a larger recovery of LVDP ($P < 0.04$) and $+dP/dt$ ($P < 0.05$) after 30 minutes of reperfusion than hearts from adult animals (Figure 33C & D).

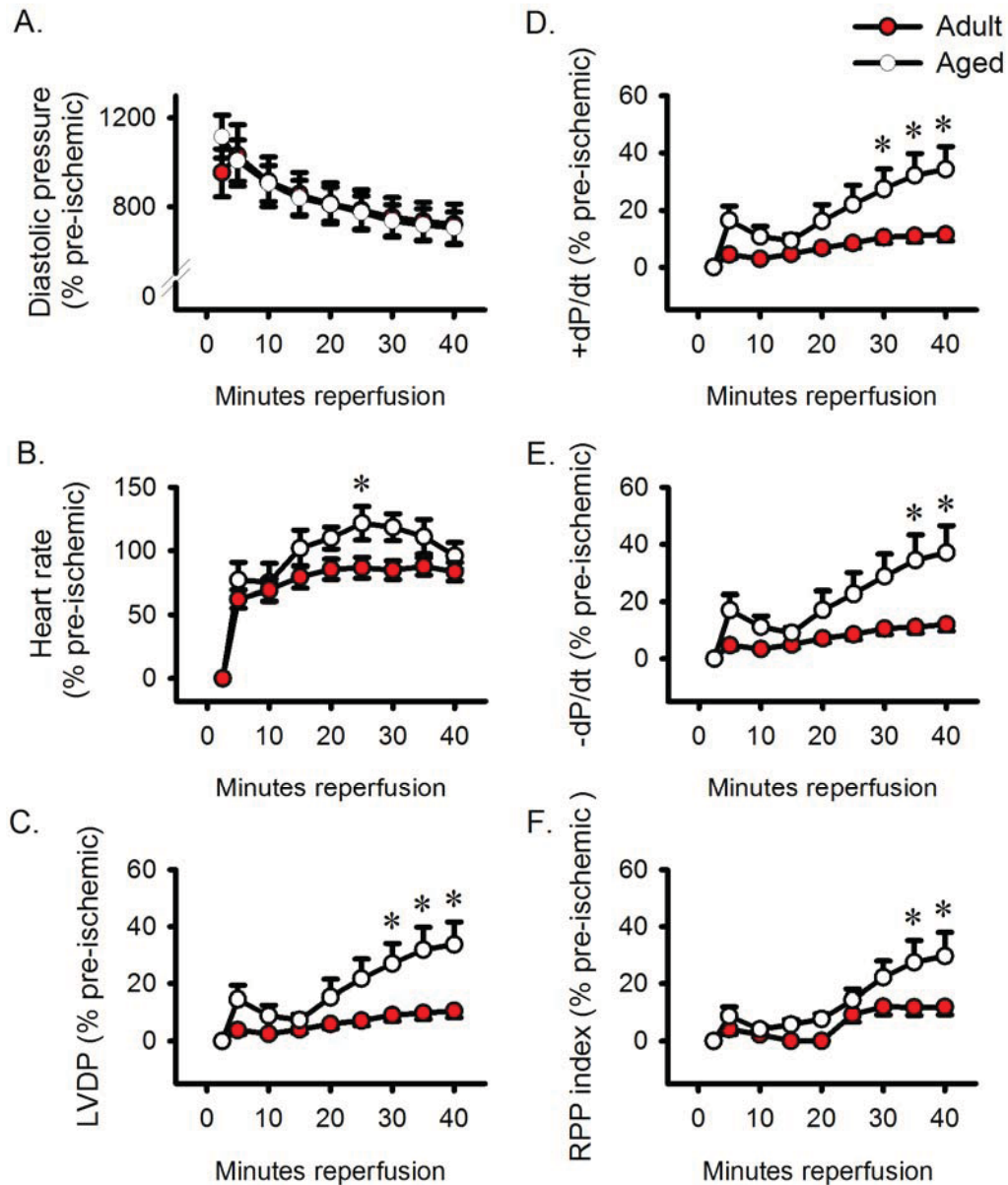


Figure 33. Recovery of contractile function was better in the aged hearts during 40 min reperfusion. Data were normalized to baseline values prior to ischemia. **A)** Diastolic pressure ($P > 0.90$) was the same in both age groups. **B)** Intrinsic heart rate ($P = 0.03$) was significantly higher in the aged group at 25 min reperfusion time. **C-F)** LVDP ($P < 0.04$), +dP/dt ($P < 0.05$), -dP/dt ($P < 0.02$), and RPP index ($P < 0.04$) recovered better in aged hearts in comparison to adult hearts at the end of reperfusion. Sample size was $n = 13-15$ adult and 30-31 aged. *denotes $P < 0.05$ for aged vs. adult hearts. Significant difference was determined using a 2-way RM ANOVA test. LVDP = Left ventricular developed pressure; +dP/dt = rate of contraction; -dP/dt = rate of relaxation; RPP = rate pressure product.

Similarly, aged hearts also had better recovery of $-dP/dt$ ($P < 0.02$) and RPP index ($P < 0.04$) after 35 min reperfusion in comparison to adult hearts (Figure 33E & F). Supplementary Table 7 summarizes the mean values for the recovery of contractile function normalized to pre-ischemic values at 40 min of reperfusion. These results show that there was a similar increase in diastolic pressure ($P = 0.92$) by $721 \pm 92\%$ in adult and $704 \pm 72\%$ in aged at the end of reperfusion, relative to pre-ischemic values (Supplementary Table 7). Similarly, after 40 min of reperfusion, HR's recovered to $96.0 \pm 10.4\%$ and $83.5 \pm 7.3\%$ of pre-ischemic values in adult and aged hearts, respectively ($P = 0.44$) (Supplementary Table 7). By contrast, LVDP recovered to $10.6 \pm 2.3\%$ in adult and $33.7 \pm 8\%$ aged hearts relative to pre-ischemic values (adult vs. aged: $P < 0.01$) (Supplementary Table 7). Similarly, recovery of $+dP/dt$ (11.5 ± 2.4 for adult vs. $34.2 \pm 9.5\%$ pre-ischemic for aged; $P < 0.01$), $-dP/dt$ (12.1 ± 2.4 for adult vs. $37.1 \pm 9.5\%$ pre-ischemic for aged; $P = 0.01$), and RPP index (13.6 ± 3.2 for adult vs. $20.3 \pm 4.0\%$ pre-ischemic; $P = 0.02$) was higher in the aged group in comparison to the adult (Supplementary Table 7).

It is possible that mice with high levels of frailty could be more susceptible to IR injury. Therefore, the relationship between the overall health of the animal, as quantified by the FI score, and recovery of function in hearts exposed to IR was investigated by plotting diastolic pressure, HR, LVDP, $+dP/dt$, $-dP/dt$, and RPP as a function of frailty scores (Figure 34 and 35). Frailty was not correlated with diastolic pressure ($r = 0.15$; $P = 0.30$), HR ($r = 0.22$; $P = 0.15$), LVDP ($r = 0.19$, $P = 0.21$), $+dP/dt$ ($r = 0.17$, $P = 0.25$), $-dP/dt$ ($r = 0.19$, $P = 0.21$) or RPP index ($r = 0.07$, $P = 0.67$) (Figure 34A-F). Figure 35

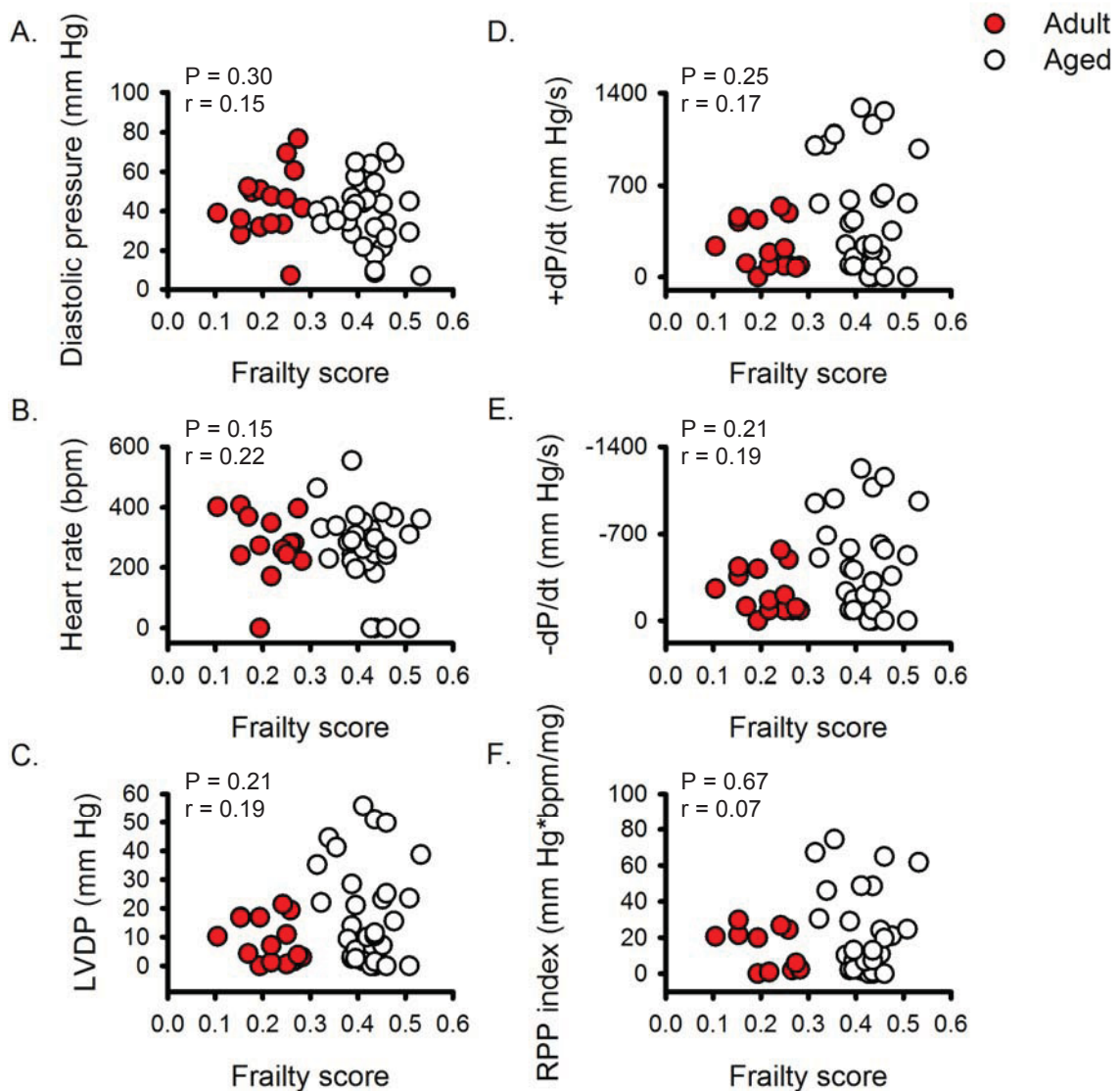


Figure 34. Recovery of cardiac function following IR was not correlated with frailty. A-F) Frailty scores were not associated with recovery of diastolic pressure ($r = 0.15$; $P = 0.30$), heart rate ($r = 0.22$; $P = 0.15$), LVDP ($r = 0.19$, $P = 0.21$), +dP/dt ($r = 0.17$, $P = 0.25$), -dP/dt ($r = 0.19$, $P = 0.21$) and RPP index ($r = 0.07$, $P = 0.67$). $N = 13-15$ adult and 30-31 aged hearts. Linear regression analysis was used to evaluate correlations. LVDP = Left ventricular developed pressure; +dP/dt = rate of contraction; -dP/dt = rate of relaxation; RPP = rate pressure product.

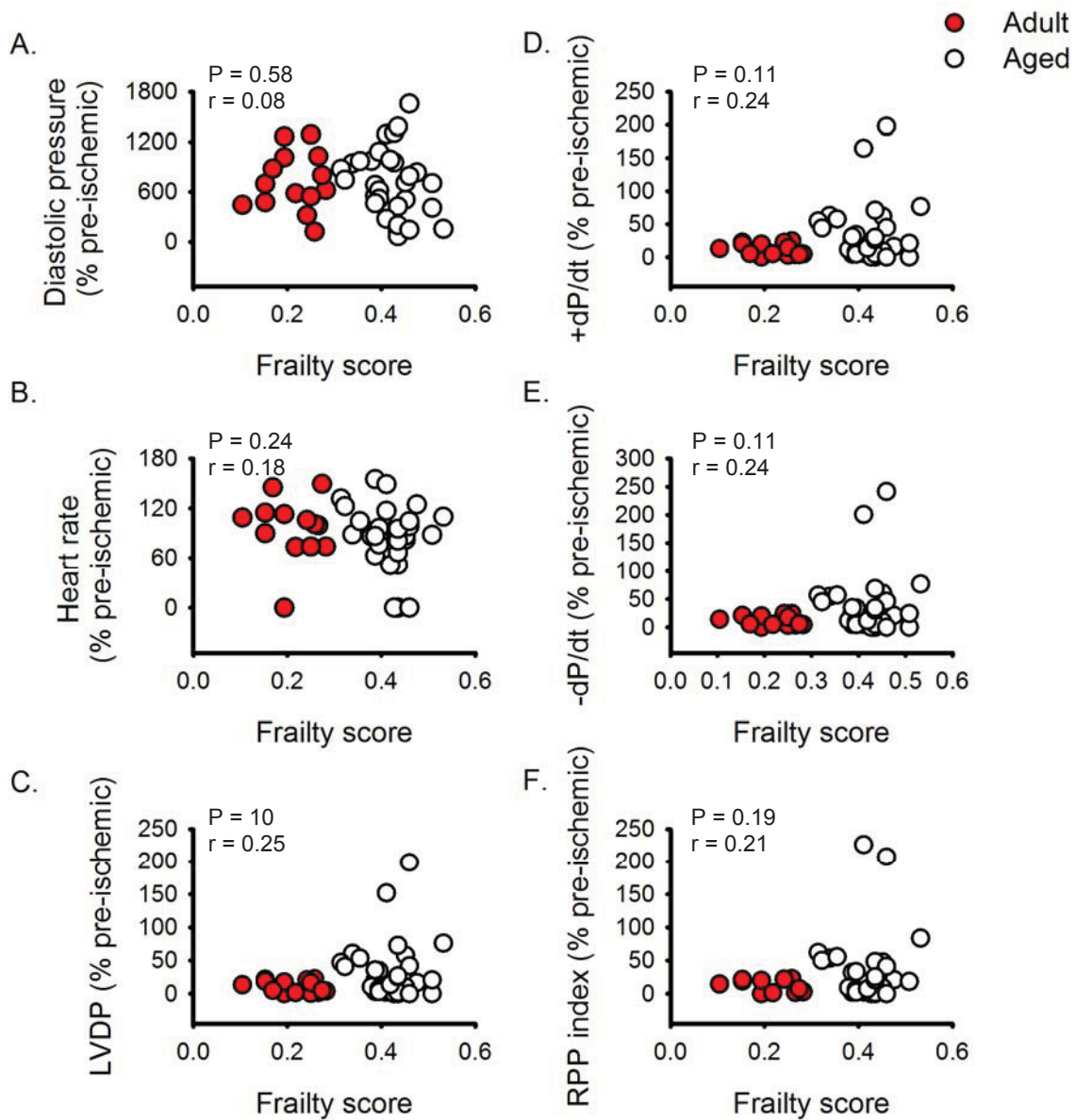


Figure 35. Recovery of contractile function following IR was poor in all hearts, regardless of the overall health status of the animal. Contractile function was analyzed as a percentage of baseline function prior to IR. **A-F)** Frailty scores were not associated with diastolic pressure ($r = 0.08$, $P = 0.58$), heart rate ($r = 0.18$, $P = 0.24$), LVDP ($r = 0.25$, $P = 0.10$), +dP/dt ($r = 0.24$, $P = 0.11$), -dP/dt ($r = 0.24$, $P = 0.11$), and RPP index ($r = 0.21$, $P = 0.19$). $N = 13-15$ adult and $31-32$ aged hearts. Linear regression analysis was used to evaluate correlations. LVDP = Left ventricular developed pressure; +dP/dt = rate of contraction; -dP/dt = rate of relaxation; RPP = rate pressure product.

shows the relationship of frailty to these parameters expressed as a percentage of baseline function. These results show that there was no correlation between the overall health of the animal and recovery of diastolic pressure ($r = 0.08$, $P = 0.58$), HR ($r = 0.18$, $P = 0.24$), LVDP ($r = 0.25$, $P = 0.10$), $+dP/dt$ ($r = 0.24$, $P = 0.11$), $-dP/dt$ ($r = 0.24$, $P = 0.11$), and RPP index ($r = 0.21$, $P = 0.19$).

To determine whether age or frailty affected coronary flows, the coronary flow rates were assessed at 40 min reperfusion by measuring flow rate and flow rate normalized to heart weight (Figure 36A & B). Figure 36A shows mean absolute flow rate in adult hearts (6.3 ± 1.3 ml/min) was similar to flow rate in aged hearts (4.7 ± 0.5 ml/min; $P = 0.35$) (Table 18). Likewise, flow rate normalized to heart weight was unaffected by age (0.019 ± 0.002 for adult vs. 0.018 ± 0.002 ml/min/mg for aged; $P = 0.34$) (Figure 36B; Supplementary Table 6). Furthermore, mean absolute flow rate (90 ± 6 for adult vs. 101 ± 8 % pre-ischemic for aged; $P = 0.49$) and flow rate normalized to heart size (87 ± 7 vs. 102 ± 8 % pre-ischemic for aged; $P = 0.32$) values expressed as a percentage of pre-ischemic values were the same in both age groups (Figure 36C & D; Supplementary Table 7). In addition, FI scores were not correlated with a change in flow rate regardless of how it was measured (Figure 37). To determine if coronary flow was impeded due to vascular compression, the coronary reflow was measured by plotting the normalized flow rate as a function of the diastolic pressure measured during the initial minute of reperfusion (Figure 38). There were no linear correlations between the coronary flow and the diastolic pressure in the adult hearts ($r = 0.26$, $P = 0.44$) and the aged hearts ($r = 0.05$, $P = 0.81$) (Figure 38).

These results indicated that the aged hearts had better functional recovery in

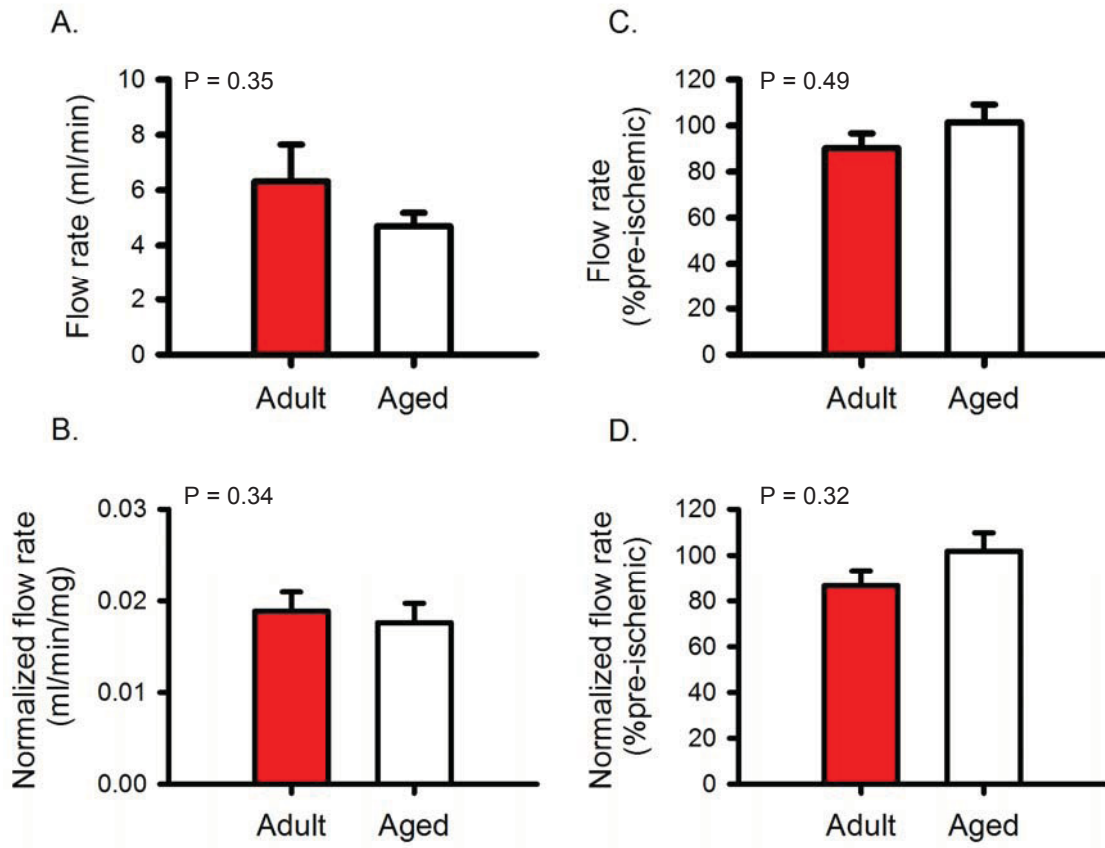


Figure 36. Age did not affect coronary flow rate following 40 min IR. **A)** Average coronary flow rates in reperfusion were similar in adult and aged hearts ($P = 0.35$) **B)** Average flow rates were normalized to the size of the heart. Normalized flow rates were the same in both age groups ($P = 0.34$). **C)** Average flow rate, presented as a percent of baseline flow rate, was similar in both age groups ($P = 0.49$). **D)** The recovery of the average flow rate normalized to heart weight, and presented as a percent of pre-ischemic flow rate, was similar in the aged and adult hearts ($P = 0.32$). $N = 12-15$ adult and 31 aged hearts for absolute flow rate. P-values were determined with a Student's t test or a Mann-Whitney Rank Sum test for data that were non-parametric.

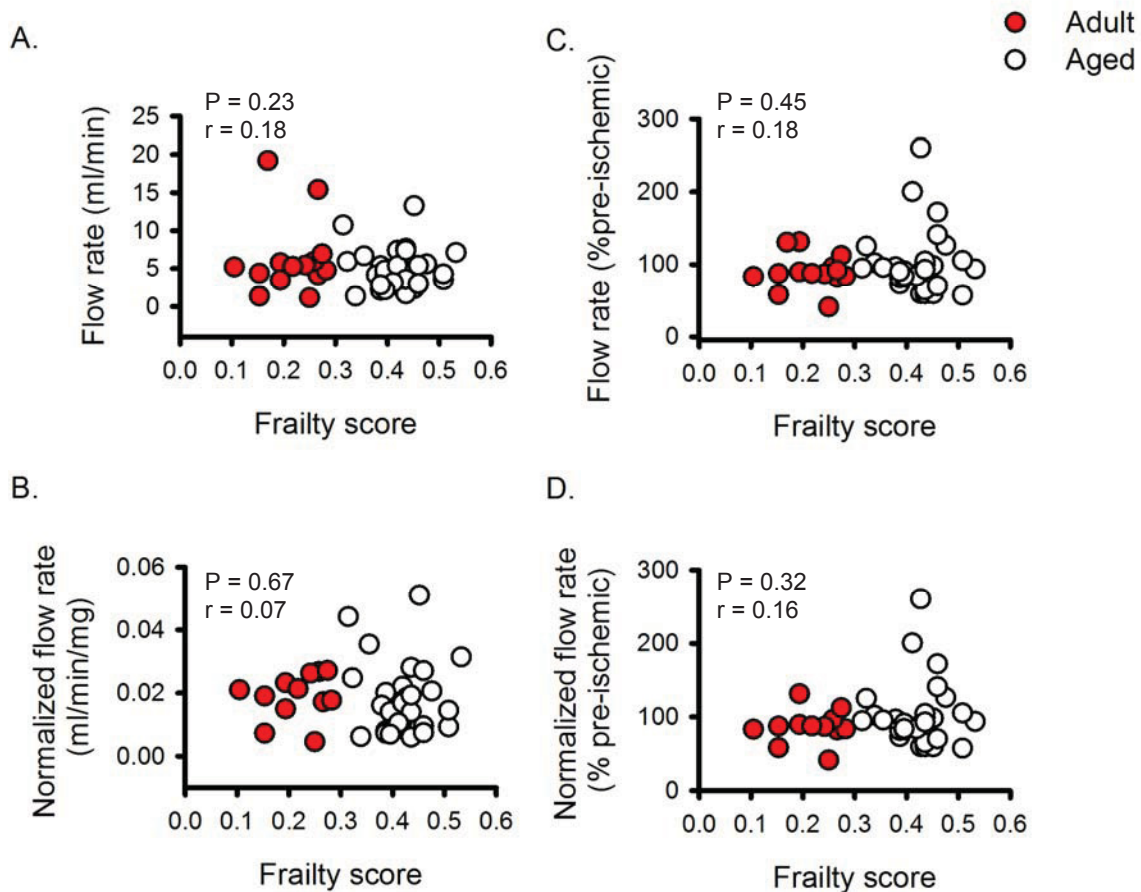


Figure 37. Recovery of coronary flow rate was high regardless of the frailty score. **A,B)** There was no significant correlation between frailty and either absolute absolute flow rate ($r = 0.18$, $P = 0.23$) or flow rate normalized to heart weight ($r = 0.07$, $P = 0.67$). **C,D)** Coronary flow rates were presented as a percent of pre-ischemic baseline flow values. Absolute flow rate ($r = 0.12$, $P = 0.45$) and flow rate normalized to heart weight ($r = 0.16$, $P = 0.32$) were not correlated with FI scores. Correlations were evaluated using linear regression analysis. $N = 12-15$ adult and 31 aged hearts.

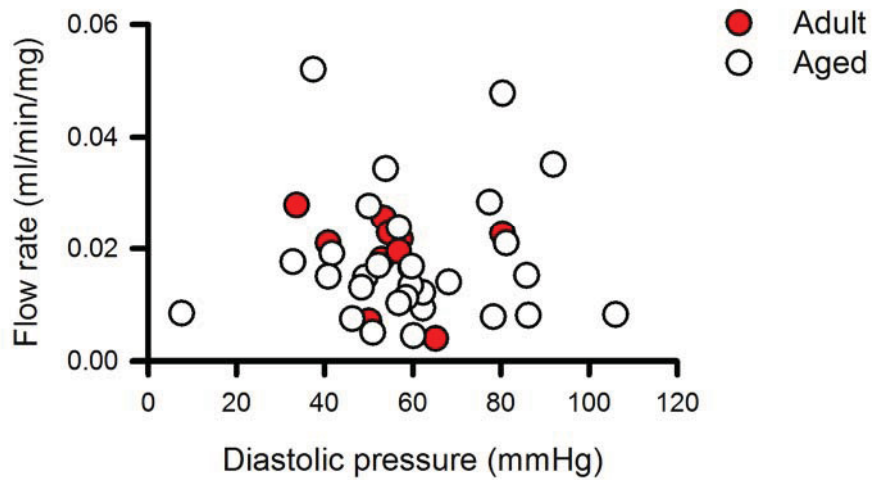


Figure 38. Coronary reflow during the initial minute of reperfusion was not due to vascular compression in both age groups. There was no significant correlation between initial diastolic pressures and coronary flow rate in the adult hearts ($r = 0.26$, $P = 0.44$) and aged hearts ($r = 0.05$, $P = 0.81$). Correlation was evaluated using linear regression analysis. $N = 11$ adult and 29 aged hearts).

comparison to adult hearts following IR. By contrast, the overall health status of the mouse was not a predictor of the heart's ability to recover following exposure to IR. These findings are summarized in Supplementary Tables 6 and 7.

3.4.2 Assessment of myocardial injury following IR in aged and adult hearts isolated from mice with varying FI scores

Myocardial injury was assessed in hearts that were exposed to global ischemia and reperfusion. One marker of IR injury is stone heart, also known as contracture, where the heart cannot relax and is said to be 'frozen in a state of systole' (Cooper, 1975). Figure 39 shows an example recording of pressure in intact hearts under basal conditions and during IR. Peak contracture was measured from the highest diastolic pressure in both the ischemic and reperfusion periods, as indicated by arrows in Figure 39. Figure 40A shows that mean (\pm SEM) peak contracture during ischemia was not significantly different in adult hearts (55.7 ± 4.7 mm Hg) compared to aged hearts (48.8 ± 3.3 mm Hg) ($P = 0.23$). Peak contracture was similar in both age groups ($P = 0.73$). It was 901 ± 118 % higher than baseline diastolic pressure in adult hearts and 852 ± 80 % higher than baseline diastolic pressure in aged hearts (Figure 40B). Interestingly, the time to reach peak contracture was longer in the aged hearts compared to adult hearts (aged: 1163 ± 75 sec; adult: 926 ± 80 sec; $P = 0.05$) (Figure 40C). The relationship between frailty and the development of contracture was further investigated by plotting these parameters of contracture as a function of frailty scores (Figure 41). Figure 41 shows that frailty was not a predictor of the development of contracture during ischemia ($r = 0.23$, $P = 0.14$ for peak contracture; $r = 0.02$, $P = 0.88$ for peak contracture normalized to baseline diastolic pressure; $r = 0.20$, P

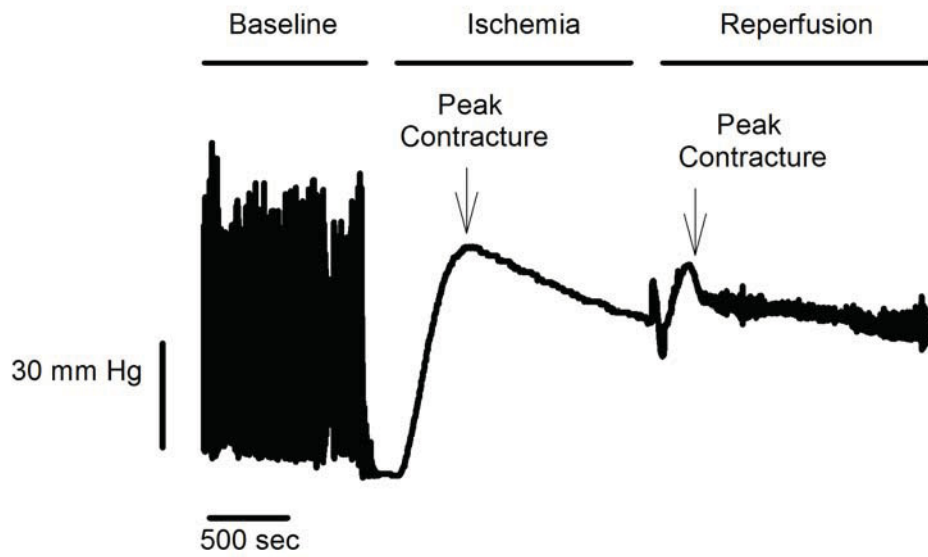


Figure 39. Representative example of pressure recorded from an intact heart before and after exposure to IR. The recording shows pressure at baseline, during ischemia and in reperfusion. Peak contracture was measured from the highest pressures in ischemia and reperfusion as indicated by the arrows.

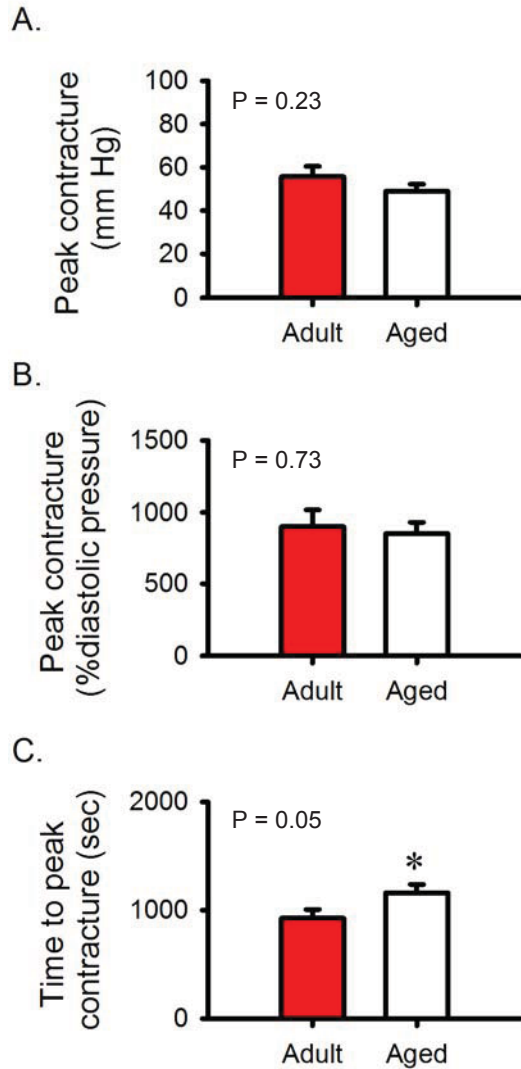


Figure 40. Aged hearts took longer to develop similar levels of contracture during ischemia compared to adult hearts. A,B) Peak contracture in ischemia was similar in adult and aged mice ($P = 0.23$ for peak contracture; $P = 0.73$ for peak contracture normalized to baseline diastolic pressures). **C)** Time to peak contracture in ischemia was longer in aged animals than in adult animals ($P = 0.05$). * indicates a significant difference from adult hearts. P- values were obtained using a Student's t test. $N = 15$ for adult and 31 aged hearts.

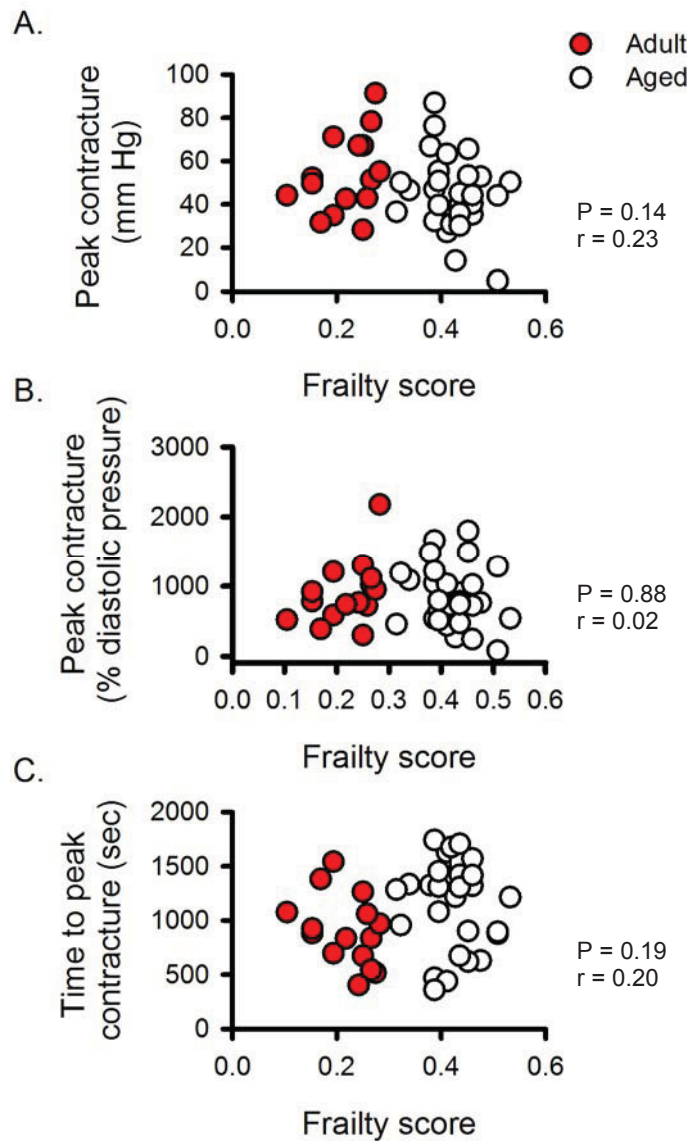


Figure 41. Contracture in ischemia was not correlated with the FI score. A-C) There were no significant correlations with peak contracture ($r = 0.23$, $P = 0.14$), peak contracture normalized to baseline diastolic pressures ($r = 0.02$, $P = 0.88$), and time to peak contracture ($r = 0.20$, $P = 0.19$). Linear regression analysis was used to assess correlations. $N = 15$ adult and 31 aged animals.

= 0.19 for time to peak contracture). These results suggest that, although both age groups had similar levels of contracture, the aged hearts were slower to develop contracture during ischemia.

The peak contracture during reperfusion was also measured in these hearts. The mean peak contracture in adult (68.1 ± 4.1 mm Hg) and aged hearts (68.2 ± 3.9) was high, although there were no differences between groups ($P = 0.98$) (Figure 42A). Similarly, peak contracture as a percentage of baseline diastolic pressure (adult: 1120 ± 128 % pre-ischemic; aged: 1248 ± 108 % pre-ischemic; $P = 0.48$) and time to peak contracture (adult: 179 ± 27 sec; aged: 110 ± 26 sec; $P = 0.07$) were similar in the both age groups (Figure 42B & C). Furthermore, Figure 43 shows that there were no correlations between frailty scores and peak contracture ($r = 0.01$, $P = 0.93$), peak contracture normalized to baseline diastolic pressure ($r = 0.001$, $P = 0.995$), and time to peak contracture ($r = 0.21$, $P = 0.15$). These results indicated that all hearts experienced similar levels of contracture regardless of age or frailty. Supplementary table 8 summarizes the contracture measured in these hearts during IR.

Exposure to ischemia and reperfusion is known to lead cell death (Wu et al., 2018). To investigate measures of myocardial cell death, infarct size was measured in hearts that were exposed to IR. Each heart was cut into 3-4 slices. Representative slices that were used to analyze infarct size are shown in Figure 44A. The representative heart slices show viable tissue stained in red and infarct shown in white (Figure 44A). The slice from the adult heart had a larger area of infarct than the slice from aged hearts (Figure 44A). Indeed, mean values show that the infarcts in adult hearts (62.2 ± 8.6 %) were significantly larger

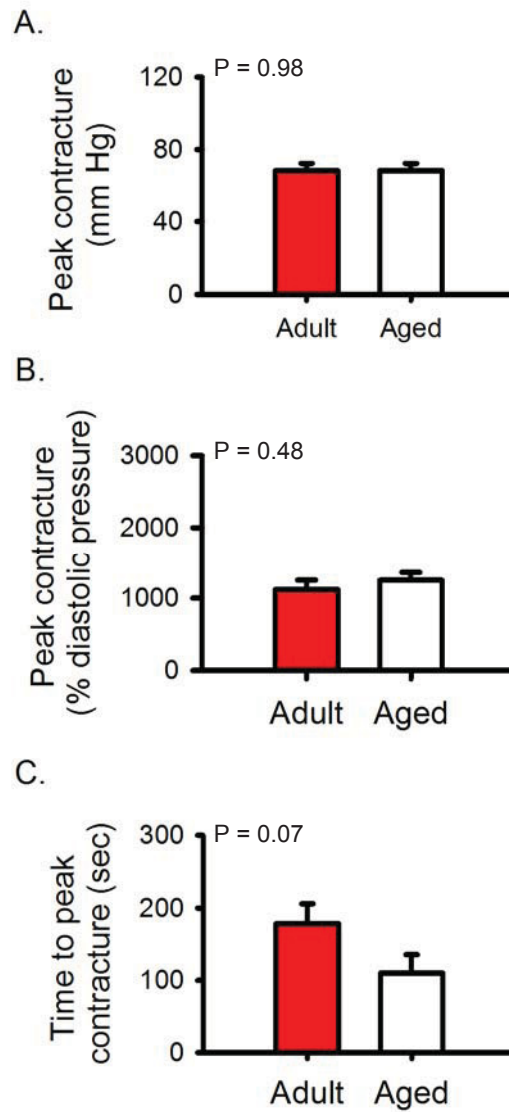


Figure 42. Aged and adult hearts exhibited similar levels of contracture during reperfusion. **A)** Peak contracture was similar between both age groups ($P = 0.98$). **B)** Age did not affect peak contracture normalized to baseline diastolic pressure ($P = 0.48$). **C)** The time to peak contracture during reperfusion was not significantly different in adult and aged hearts ($P = 0.07$). Student's *t* test was used to obtain P-values. $N = 15$ adult and 31 aged hearts.

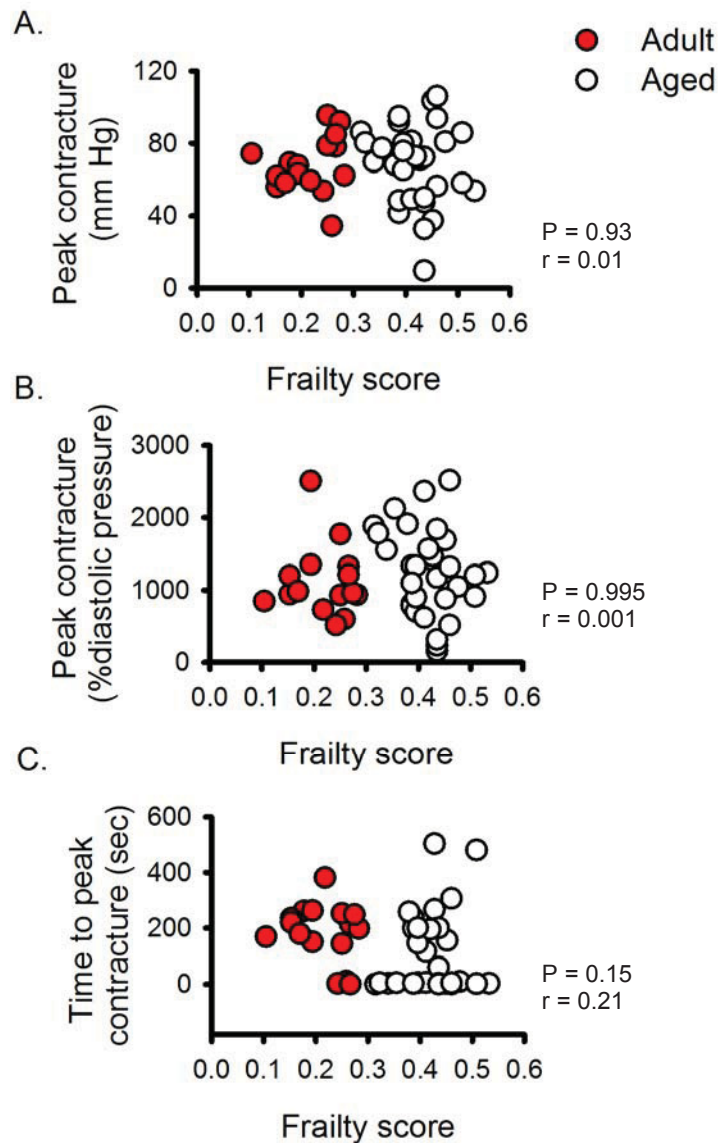


Figure 43. Frailty scores did not grade peak contracture in reperfusion. **A)** FI scores were not correlated with peak contracture ($r = 0.01$, $P = 0.93$). **B)** Peak contracture reported as a percentage of baseline diastolic pressure was not associated with frailty ($r = 0.001$, $P = 0.995$). **C)** There was no significant correlation between time to peak contracture during reperfusion and frailty ($r = 0.21$, $P = 0.15$). Correlations were evaluated using linear regression analysis. $N = 15$ adult and 31 aged animals.

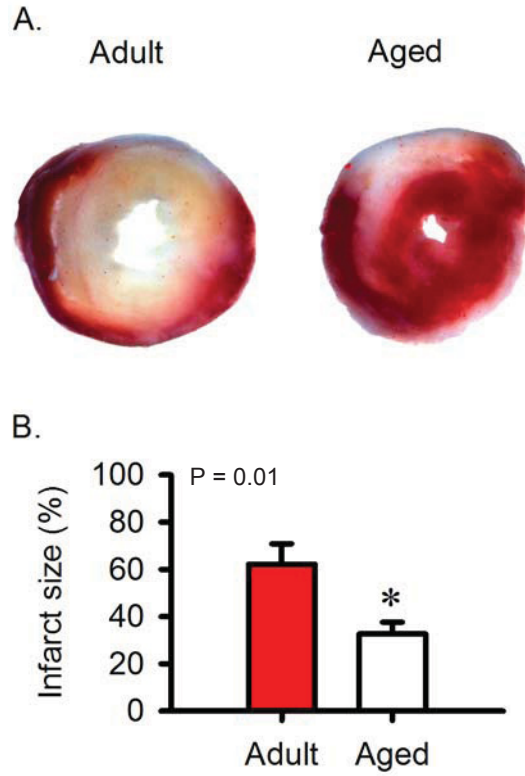


Figure 44. Infarct sizes were smaller in the aged hearts. **A)** Representative heart slices from an aged (876 days old) and an adult (252 days old) mouse following IR. **B)** Infarct size was expressed as the total infarcted area as a percentage of the total area of the slice. Mean infarct size was smaller in aged hearts compared to adult hearts ($P = 0.01$). *denotes significant difference from adult group. Significance was assessed using a Student's *t* test. ($N = 4$ adult and 6 aged hearts).

than the infarcts in aged hearts (32.6 ± 5.0 %) following exposure to IR ($P = 0.01$) (Figure 44B). Cell death is also indicated by higher cTnI levels in the effluent released from the heart during reperfusion. Figure 45A shows cTnI release measured from samples collected at the 30 min time point during baseline and throughout reperfusion (60-100 min) from one adult and one aged heart. Based on these data, cTnI levels were assessed from effluent collected at the end of reperfusion. Mean (\pm SEM) cTnI release at the end of reperfusion was significantly lower ($P = 0.01$) in aged hearts (2.09 ± 0.47 ng/ml) compared to adult hearts (3.97 ± 0.59 ng/ml) (Figure 45B). However, frailty did not grade this age-related decline in cTnI release ($r = 0.26$, $P = 12$) (Figure 45C). These results are summarized in Supplementary Table 8.

Taken together, these results show that all hearts experienced similar levels of contracture during IR. Interestingly, aged hearts took longer to develop peak contracture compared to the hearts isolated from adult animals. Furthermore, aged hearts had smaller infarct sizes and less cTnI release. This may explain why hearts from aged animals had better functional recovery than adult hearts. Interestingly, although the overall health status of the mouse, quantified by the frailty score, was associated with age-dependent heart function under baseline conditions, it did not correlate with functional recovery and myocardial injury after hearts were exposed to IR.

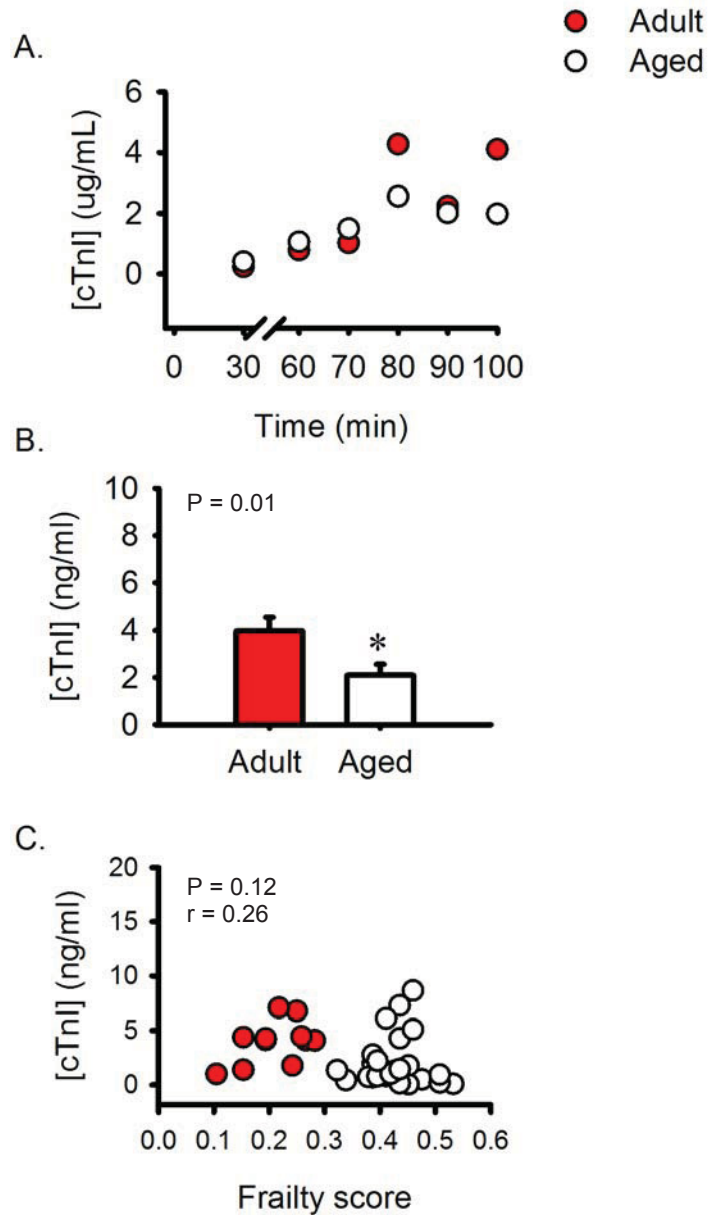


Figure 45. cTnI release during reperfusion declined with age, not frailty. **A)** cTnI was initially measured in effluent samples collected during baseline (30 min) and throughout reperfusion (60-100 min) from one adult and one aged heart. Further analysis of cTnI was from effluent collected from hearts at the 100 min time point. **B)** Mean cTnI level was lower in aged hearts compared to adult hearts following IR ($P = 0.01$). **C)** cTnI release was not associated with frailty scores ($r = 0.26$, $P = 0.12$). *denotes significant difference between adult group. P-values were determined from a Student's *t* test. Correlations were evaluated using linear regression analysis. (N = 11 adult and 25 aged hearts).

4 CHAPTER DISCUSSION

The overall objective of this study was to validate and optimize the mouse clinical FI tool and use it to investigate the impact of frailty on age-dependent cardiac remodelling under basal conditions and in the setting of ischemia reperfusion in naturally ageing mice. The use of aged animals is underrepresented in most studies (Nanayakkara et al., 2018; Jackson et al., 2017). Many researchers consider 5-12 weeks of age to be an adult mouse (Jackson et al., 2017). Furthermore, many studies use ~10 weeks old mice to study age-related CVDs such as myocardial infarction. A 5-12 The incidence of myocardial infarction is increased in people over the age of 60 years (van Oeffelen et al., 2014). Therefore, using aged animals (20+ months of age) would produce a more translational model. Thus, the first goal of this study was to investigate age-dependent remodelling in intact hearts and at the level of the individual ventricular myocyte. Results showed LV contractile function declined with age in intact hearts. Furthermore, peak contractions were smaller in cells from aged animals compared to young adults, consistent with observations in the intact heart. These changes in contraction in the older animals were a result of disruption in Ca^{2+} homeostasis. These results indicated that, on average, age attenuated contractile function. However, there was marked heterogeneity in cardiac function in individual hearts. To measure this heterogeneity in cardiac ageing, the mouse clinical FI was used to quantify the overall health status of the mouse as a frailty score.

The second objective was to validate and optimize the mouse clinical FI and determine if it was reliable between raters. The mouse clinical FI was used to quantify the overall health status frailty scores for a large cohort of mice by two different raters. Results

showed that the mouse clinical FI tool exhibited high overall inter-rater reliability as quantified by the correlation coefficient, Cohen's kappa statistic, and ICC. The inter-rater reliability was increased as the techniques used to assess individual deficits were refined. This improved FI was used to quantify the overall health status as a frailty score.

The third objective was to investigate the relationship between frailty and age-dependent remodelling in the ventricles from adult and aged mice using the optimized FI tool. Results showed that age-dependent cardiac contractile dysfunction in the intact heart was inversely proportional to the FI score. Consistent with results observed in the intact heart, age-related decreases in peak contraction and Ca^{2+} homeostasis were also graded by frailty. These results showed that the overall health of the mouse was correlated with its heart function.

The final objective was to determine the impact of age and frailty on cardiovascular dysfunction following IR injury in intact hearts. The results showed that hearts from aged animals had better recovery of contractile function following IR in comparison to hearts from adult animals. Interestingly, the hearts from aged animals also exhibited more tolerance to IR injury. Aged hearts had smaller infarct size and cTnI release following IR compared to hearts from adult animals. By contrast, frailty was not associated with the susceptibility to IR injury and functional recovery following IR. This increase in tolerance to IR with age is an interesting observation that requires further research.

4.1 THE EFFECTS OF ADVANCED AGEING ON CARDIAC CONTRACTILE FUNCTION IN THE HEART

4.1.1 Summary of results

Two distinct age groups were used in this study where the “aged” group was significantly older than the “adult” group. Also, the aged mice weighed significantly less than the adult mice. By contrast, results showed that ageing correlated with cardiac hypertrophy in the aged animals. Similarly, aged hearts had more fibrosis compared to the aged animals. Moreover, aged hearts had poor cardiac function compared to hearts isolated from adult mice. Specifically, LVDP, +dP/dt and -dP/dt were smaller in the aged hearts in comparison to the adult hearts. Furthermore, the adult hearts could perform more work than the aged hearts, as RPP index was higher in the adult group in comparison to the aged group. By contrast, HR was similar in both age groups. The age-dependent decline in contractile function in intact hearts was mirrored by a decline in peak contraction in isolated ventricular myocytes in the aged group in comparison to cells in the adult group. In addition, peak Ca^{2+} transient amplitude was significantly smaller in the aged mice when compared to the adult mice. Further investigation showed that this decline in Ca^{2+} transient amplitude in the aged heart was due to smaller Ca^{2+} current entering the cell. Interestingly, Ca^{2+} currents are smaller in the aged cardiomyocytes because aged hearts had less expression of CaV1.2 protein compared to adult hearts. This study found that these age-related changes in cardiac contractile function in intact hearts and in individual cardiomyocytes only represented average responses. There was considerable heterogeneity in responses within each group such that many aged hearts had similar contractile function as hearts isolated from young adult mice.

4.1.2 Age related remodelling in cardiac structure in intact hearts

This study showed that aged hearts were hypertrophied in comparison to adult hearts. This is consistent with previous studies where hypertrophy increases with age in mice, rats, and humans (Lindsey et al., 2005; Burgess, McCrea & Hedrick, 2001; Slama, Ahn, Varagic, Susic & Frohlich, 2004; Lakatta & Levy, 2003; Walker et al., 2006). Hypertrophy in aged hearts occurs if there is an increase in the size of individual myocytes. Indeed, there is overwhelming evidence that there is a marked increase in the length, width, and area of ventricular myocytes with age in male mice (Grandy & Howlett, 2006; Domeier et al., 2014; Turdi et al., 2010; Lim et al., 2000; Li et al., 2005; Ceylan-Isik et al. 2013). Male rats also exhibit an increase in cell length, width, and area with age (Lieber et al., 2004; Mace et al., 2003; Liu et al., 2000; Howlett, 2010; Farrell & Howlett, 2007). This increase in cell size may be as a consequence of a loss of ventricular myocytes which occurs during the ageing process in humans and in rodents (Olivetti et al., 1991; Kajstura et al., 1996; Walker et al., 2006). This loss in cardiomyocytes occurs as a result of an age-associated increase in the apoptotic and necrotic processes, which may lead to compensatory hypertrophy (Keller & Howlett, 2016; Olivetti et al., 1991; Olivetti et al., 1995; Kajstura et al., 1996; Walker et al., 2006). Hypertrophy of the heart can lead to contractile dysfunction and cardiac failure (Manne et al., 2014).

Furthermore, age-related loss of cardiomyocytes leads to extracellular matrix remodelling where there is collagen accumulation and interstitial fibrosis in aged mice (Keller & Howlett, 2016; Lindsey et al., 2005; Willems et al., 2005; Boucher et al., 1998; Walker et al., 2006). Consistent with previous work, results from this study showed that fibrosis levels were higher in the aged hearts in comparison to adult hearts. These age-

associated structural remodelling changes may compromise cardiac function in the ageing heart.

4.1.3 Myocardial contractile function in aged hearts

This thesis explored the influence of age on cardiac contractile function in Langendorff-perfused hearts isolated from male mice. We found that hearts from aged mice had worse contractile function compared to hearts from adult hearts. Our study showed that aged hearts had lower LVDP, RPP index and slower $+dP/dt$ and $-dP/dt$ in comparison to hearts from adult animals. Similar to our findings, previous studies show a decline in peak LV pressure, $+dP/dt$, $-dP/dt$, and RPP with age in rodent hearts (Qin, et al., 2013; Sample et al., 2006; Boucher et al., 1998; Korzick et al., 2001; Lesnefsky et al., 1994). Our results also showed that diastolic pressure was similar in aged and adult hearts. Previous studies also support the observation that diastolic pressure does not change with age (Watanabe et al., 2004; Korzick et al., 2001; Escobales et al., 2014; Lesnefsky et al., 1994; Willems et al., 2005). Furthermore, we showed that intrinsic HR was similar in both aged groups. Several other studies, support our results that HR remains unchanged with age in Langendorff-perfused hearts (Porter et al., 2014; Stein et al., 2008; Watanabe et al., 2004; Escobales et al., 2014). However, this is controversial as other studies have reported a decline in HR with age in intact hearts (Headrick et al., 2003; Sample et al., 2006; Headrick, 1998). Furthermore, a previous study investigated the impact of age on HR and sinoatrial node function. This detailed study found that HR declines with age as a result of remodelling in structure and function in the sinoatrial node (Moghtadaei et al., 2016; Jansen

et al., 2017). Careful measurement of the HR with ECG rather than from the pressure recordings may provide a more precise measurement of HR and may have revealed a decline in HR with age. Our results also showed that coronary flow was similar in adult hearts and aged hearts similar to previous studies (Watanabe et al., 2004; Escobales et al., 2014; Headrick, 1998; Lesnefsky et al., 1994; Boucher et al., 1998; Ashton et al., 2003; Wang et al., 2018). Therefore, our findings are in agreement with the results of many other studies of the ageing heart.

In contrast to studies that support our results, there are some studies that do not show an age-dependent decrease in cardiac function in intact hearts isolated from rodents (Willems et al., 2005; Headrick et al., 2003; Ashton et al., 2003; Watanabe et al., 2004; Korzick et al., 2001; Escobales et al., 2014; Headrick, 1998; Lesnefsky et al., 1994). The difference between our results and the results of these studies may be attributable to differences in experimental conditions (*i.e.* different concentrations of ions in the perfusate), protocols (*i.e.* different perfusion pressure, different pacing frequency) and different animal strains (*i.e.* FVB/N vs. C57BL/6). More importantly, many of the studies that did not report a decline in contractile function with age used exclusion criteria where hearts are excluded from the study if: 1) the systolic pressure is below 100 mm Hg, 2) If the HR < 320 bpm and 3) If the coronary flow rate was >5ml/min (Willems et al., 2005; Headrick et al., 2003; Ashton et al., 2003; Headrick, 1998; Lesnefsky et al., 1994). The use of exclusion criteria can introduce bias, which may mask any age-dependent decline in cardiac function **that** is present.

The decline in contractility in the intact hearts may be a result of increased fibrosis in these aged hearts. As previously stated, our results showed that aged hearts had

increased levels of fibrosis in comparison to adult hearts. Studies show that fibrosis in aged hearts is associated with increased LV stiffness (Horn & Trafford, 2016; Lau et al., 2013). This increased stiffness can impair the relaxation of the heart and cause diastolic dysfunction (Horn & Trafford, 2016). Thus, increased fibrosis may contribute to the slowing of the relaxation we observed in the aged hearts. Although ventricular stiffness is predominately associated with diastolic dysfunction, it is hypothesized that fibrosis may also disrupt systolic function by disrupting the transmission of force generated by myocytes (Janicki & Brower; 2002). Therefore, fibrosis may help explain the age-associated decline in myocardial contractility observed here.

Interestingly, contractile dysfunction in intact hearts was mirrored by a decline in contractile function in individual cardiomyocytes. We showed that peak contraction was smaller and velocities of shortening and lengthening were slower in cells from aged hearts in comparison to adult hearts. Previous studies have also shown that peak contraction declines with age in ventricular myocytes from male mice (Grandy & Howlett, 2006; Lim et al., 2000; Domeier et al., 2014; Ceylan-Isik et al., 2013; Li et al., 2005; Qin et al., 2013), rats (Weisser-Thomas et al., 2007; Zhu et al., 2005; Lieber et al., 2004; Howlett, 2010) and guinea pigs (Ferrara et al., 1995). Similarly, current literature also agrees that the velocities of shortening and lengthening slow with age in ventricular myocytes from aged male mice (Grandy & Howlett, 2006; Qin et al., 2013; Rueckschloss et al., 2010; Lim et al., 2000; Ceylan-Isik et al., 2013; Li et al., 2005; Qin et al., 2013), rats (Fraticeilli et al., 1989; Sakai et al., 1992; Weisser-Thomas et al., 2007; Guo & Ren, 2006; Li et al., 2007) and guinea pigs (Ferrara et al., 1995). Our findings suggest that age-dependent contractile dysfunction

observed in individual cells contributes to the age-dependent decline in cardiac function observed in the intact heart.

Changes in contractile proteins may contribute to the age-associated decline in contraction observed in ventricular myocytes. Studies show that there are age-dependent modifications in myofilament proteins. For example, the fast α myosin heavy chain isoform shifts to the slower β myosin heavy chain isoform, which slows relaxation in aged myocytes (Lompré, Lambert, Lakatta & Schwartz, 1991; Buttrick et al., 1991; Fitzsimons, Patel & Moss, 1999). Furthermore, cTnI phosphorylation is associated with cardiac muscle relaxation (Zhang, Zhao, Mandveno & Potter, 1995). The phosphorylation of cTnI declines with age which slows relaxation of the myocyte (Sakai et al., 1989). Similarly, the velocity of contraction is slowed by a reduction in myofilament Ca^{2+} ATPase activity (Bhatnagar, Walford, Beard, Humphreys & Lakatta, 1984; Buttrick et al., 1991; Cappelli et al., 1988; Rueckschloss et al. 2010). Therefore, our observations of the slowing of the rates of relaxation and contraction may be attributable, in part, to age-dependent modifications in myofilament proteins.

4.1.4 Components involved in the EC-coupling pathway are modified with age

Cardiac contraction is mediated by the EC-coupling pathway described in section 1.2.3 of this thesis. The present study investigated components of the EC-coupling pathway to determine if the contractile dysfunction observed in ventricular myocytes was due to age-related modifications in Ca^{2+} handling. Studies show that peak Ca^{2+} transient declines with age in cardiomyocytes from rats (Howlett, 2010; Zhu et al., 2005) and mice

(Grandy & Howlett, 2006; Lim et al., 2000; Ceylan-Isik et al., 2013; Li et al., 2005; Qin et al., 2013). The results of the present study showed that peak Ca^{2+} transient amplitude was smaller in aged hearts in comparison to adult hearts. Thus, the smaller contractions seen in the aged hearts appear to be attributable to smaller Ca^{2+} transient amplitudes.

This study showed that Ca^{2+} current density was smaller in cells isolated from aged hearts in comparison to the adult group. This is consistent with previous studies where peak Ca^{2+} current is smaller in aged rats (Howlett, 2010; Liu et al., 2000), mice (Grandy & Howlett, 2006), and rabbits (Salameh et al., 2010) hearts. The present study also reports the novel and key finding that CaV1.2 protein expression is lower in aged hearts in comparison to adult hearts. This age-associated decrease in the expression of L-type Ca^{2+} channels may be responsible for the decrease in Ca^{2+} current. Furthermore, the smaller Ca^{2+} currents may be responsible for smaller peak Ca^{2+} transient amplitudes. This was supported by our observation that there was a decline in the amount of Ca^{2+} released from the SR per unit of Ca^{2+} current in cells from the aged group. This decline in Ca^{2+} transient amplitude is, in part, responsible for the smaller contractions.

The functional responses observed in the intact hearts and the individual ventricular myocytes represented only average responses. The present study found considerable heterogeneity in age-dependent cardiac structure and function in both age groups. Furthermore, there were aged hearts that had functional responses and measures of cardiac structure that were similar to or even greater than hearts isolated from young adult mice. Based on these observations, we concluded that chronological age did not necessarily reflect biological age. Biological age, quantified as frailty, is also considered as the overall health status of the mouse (Mitnitski, Mogilner & Rockwood, 2001; Rockwood et al.,

2017). The mouse clinical FI was used to measure the biological age of the animals to determine if this accounts for heterogeneity in cardiac ageing.

4.2 RELIABILITY OF THE MOUSE FI INSTRUMENT

4.2.1 Summary of results

The biological age or overall health of male C57BL/6 mice was quantified as a FI score in a large cohort of 343-430-day-old mice. Results showed that frailty increased with age. Furthermore, there were considerable differences in the overall health status for mice of the same chronological age. To investigate the inter-rater reliability of the mouse clinical FI, frailty scores were independently assessed in mice by two different raters. Results showed that mean FI scores did not differ between raters throughout the study. However, several items within the FI tool were scored differently by the two raters in each group of mice assessed. The number of these discordant measures between raters decreased as the techniques used to assess frailty in each group were refined. The inter-rater reliability of the FI was quantified using correlation coefficients, Cohen's kappa statistic, and ICC. Reliability was high in the assessment of mice in group 1 between the two raters. The correlation coefficient, average kappa values, and ICC increased throughout the study between raters following refinement of the FI tool. Thus, the inter-rater reliability of the mouse clinical FI tool was very high by the end of the study.

4.2.2 The clinical FI tool

The overall health status of a mouse can be quantified using the concept of frailty. There are different methods of identifying and quantifying frailty in aging animal models (Parks et al., 2012; Whitehead et al., 2014, Liu et al., 2014). These studies have adapted frailty scales that are commonly used clinically to quantify frailty in ageing animals. There are two common frailty instruments used clinically. One is the 5-point clinical frailty phenotype (Fried et al., 2001) and the second is the frailty index developed based on the concept of deficit accumulation (Searle et al., 2008; Mitnitski et al., 2001). Liu *et al.* (2014) developed a murine frailty scale based on the frailty phenotype. By contrast, previous studies in the Howlett lab have developed different tools to assess frailty in mice based on the concept of deficit accumulation (Parks et al., 2012; Whitehead et al., 2014). Parks *et al.* (2012) developed an FI that measured parameters such as heart rate, blood pressure, blood volume, activity levels, body composition and metabolism. Many of these measures were invasive, and thus it would be too difficult to use this FI tool for longitudinal studies. Furthermore, the original FI required specialized equipment that may not be available in all labs (Parks et al., 2012). A more simplified FI tool was developed by Whitehead *et al.* (2014), where health deficits across a wide variety of systems (described in detail in the Methods section of this thesis) were non-invasively assessed. Notably, this non-invasive frailty instrument did not include any measures of cardiac function *per se* (Whitehead et al., 2014). The present study used this non-invasive mouse clinical FI tool to quantify the overall health status of a mouse as a frailty score in a large cohort of mice. Results showed that frailty increased with age. This is consistent with previous studies that also showed that frailty increases with age in naturally ageing mice (Parks et al., 2012; Whitehead et

al., 2014; Rockwood et al., 2017). Furthermore, results showed that there was considerable variability in the overall health status in mice of the same chronological age. This observation demonstrates that, as in people, mice can age at varying rates (Rockwood et al., 2017).

The clinical FI is a useful instrument to measure the biology of ageing in humans and in C57BL/6 mice. An intriguing feature of the clinical FI is that both the human and the mouse clinical FI share features of deficit accumulation (Rockwood et al., 2017). For example, mean FI scores increase with age in humans and mice, consistent with the findings in this study (Rockwood et al., 2017; Whitehead et al., 2014). In addition, the distribution of mean frailty scores broadens with age in both humans and mice (Rockwood et al., 2017). This illustrates the variability in deficit accumulation over time in both species. Moreover, individual deficits accumulate at varying rates in both species (Rockwood et al., 2017). Interestingly, higher frailty scores correlate with higher mortality in both humans and mice (Rockwood et al. 2017; Whitehead et al., 2014). In addition, the FI approach has been adapted to be used in rats (Yorke, Kane, Hancock Friesen, Howlett, & O'Blenes, 2017). The recent development of a rat FI tool is particularly valuable as rats are frequently utilized in ageing studies (Mitchell, Scheibye-Knudsen, Longo & de Cabo, 2015). Overall, the clinical FI is a tool that allows researchers to investigate the ageing process in humans and in animal models. The non-invasive nature of the mouse clinical FI makes it a useful tool for measuring the overall health status of a mouse and correlating it to a wide spectrum of detectable changes. The FI can also be applied in investigating the effects of interventions that could help modify frailty and age-dependent deterioration.

4.2.3 Reliability of the mouse clinical FI

The mouse clinical FI tool has been shown to be highly reproducible with very little test-to-test variability when used by a single rater (Whitehead et al., 2014). A key finding in this study was that the mouse clinical FI was a reliable tool between two different raters. Results showed that mean FI scores were not different between the two raters, although there was some disagreement on the scoring of several health deficits during the frailty assessments of the first group of mice. The items in the FI that caused the most disagreement between raters were more fully described and refined. The refinement process decreased the number of discordant measures between raters throughout the study in the evaluation of frailty in the second and third groups of mice. Hearing test and body surface temperature were the two particular items on the FI that had the highest disagreement between raters even after the third group of mice were evaluated. This was because mice habituated to repeated exposure to the clicking sound used to assess hearing loss and would not react to the noise. We concluded that in order to maintain the novelty of the clicking noise, each mouse should only be exposed to the sound of the clicker once. Moreover, we determined that the position of the temperature probe should be placed 2 cm directly above the center of the abdomen for consistent measurement. Overall, the inter-rater reliability increased throughout the study.

The inter-rater reliability of the mouse clinical FI has also been assessed by another research group (Kane et al., 2015). Similar to the observations in the present study, Kane *et al.* (2015) reported a high inter-rater reliability between two scientist raters. However, scientists were not correlated well with raters that did not have a scientific background (Kane et al., 2015). Therefore, when comparing FI scores, it is important to compare scores

from raters with a scientific background. By contrast, the reliability of the FI tool is high between scientists, even between raters with different experience levels (Kane, Ayaz, Ghimire, Feridooni & Howlett, 2017). Furthermore, this study shows that the mouse clinical frailty index is reliable when used by raters of both sexes (Kane et al., 2017A).

Based on our findings and subsequent findings from others, this optimized mouse FI is an exciting tool that allowed us to investigate the impact of biological age on cardiac contractile structure and function.

4.3 THE RELATIONSHIP BETWEEN FRAILTY AND AGE-DEPENDENT CARDIAC CONTRACTILE DYSFUNCTION

4.3.1 Summary of results

Individual FI scores were obtained for each mouse prior to experiments. Results showed that the mean frailty scores were significantly greater in the aged group in comparison of the adult group. However, mice with similar ages exhibited variable overall health status. To investigate the impact of frailty on age-dependent hypertrophy, FI scores were plotted as a function of different measures of hypertrophy. Specifically, there was a linear correlation where an increase in FI scores correlated with an increase in HW, HW:BW, and HW:TL. In terms of LV-function in intact hearts, diastolic pressure, HR, LVDP, +dP/dt, -dP/dt, -dP/dt, and RPP index were plotted as a function of frailty. Diastolic pressure and HR were not associated with frailty. By contrast, there was an inverse relationship between FI scores and LVDP, +dP/dt, -dP/dt, -dP/dt, and RPP index. Frailty was not associated with the average coronary flow rate.

Frailty graded the age-dependent decline in peak contraction in individual cardiomyocytes. In addition, cells isolated from frail animals had slower velocities of shortening and lengthening. This age-associated contractile dysfunction was attributable to smaller Ca^{2+} transients. The age-dependent decrease in peak Ca^{2+} transient amplitude was associated with frailty. Furthermore, FI scores were positively correlated with Ca^{2+} current density. By contrast, the gain of SR Ca^{2+} release was inversely proportional to the FI score of the animal. Our results showed that the age-dependent decline in CaV1.2 was graded by frailty.

4.3.2 The relationship between frailty and age-dependent cardiac dysfunction

Despite clear links between frailty and CVD in humans (Singh et al., 2014; Afilalo et al., 2014; Chen, 2015; Adabag et al., 2018; Kusunose et al., 2018), very little is actually known about the relationship between frailty and heart function. This is because until recently, frailty could not be measured in animals. The recent development of the mouse clinical FI has provided us with a tool to understand the relationship between frailty and age-dependent cardiac dysfunction.

In the present study, the mouse clinical FI tool was used to quantify the overall health of a mouse as a frailty score prior to each experiment. Frailty was assessed in an adult group that had an average age of ~8 mos and an aged group of mice that were approximately 27 mos old. Results showed that, similar to previous studies, mean FI scores were higher in the aged group in comparison to the adult group (Parks et al., 2012; Whitehead et al., 2014, Moghtadaei et al., 2016; Jansen et al., 2017; Rockwood et al.,

2017). However, mice of similar chronological age had FI scores across a wide range of values. This marked heterogeneity in FI scores existed in both groups of animals such that the distribution of frailty scores in the adult and aged mice overlapped, despite the significant age difference. Furthermore, other studies also show a broad distribution of FI scores in mice of the same chronological age (Rockwood et al., 2017; Jansen et al., 2017; Moghtadaei et al., 2016). Our results in this study show that the FI tool can be used to measure the high variability in the overall health status of naturally ageing C57BL/6 mice.

This study also reported a high degree of variability in age-dependent hypertrophy within the aged and adult groups. The relationship between frailty and hypertrophy was investigated by plotting measures of hypertrophy (HW, HW:BW, and HW:TL) as a function of FI scores. Results showed that HW, HW:BW, and HW:TL increased as frailty increased. A previous study that used a different FI tool showed age-dependent hypertrophy in cardiomyocytes was higher in mice with higher frailty scores (Parks et al., 2012). Together, these results suggest that the overall health status of the animal as quantified by a FI score is correlated with age-dependent hypertrophy.

A previous study showed preliminary evidence of the links between frailty and heart function at the cellular level (Parks et al., 2012). This study showed an inverse correlation between peak contraction in ventricular myocytes and the FI score of the mouse (Parks et al., 2012). The current study builds on this finding by exploring the links between frailty and contractile function in intact hearts and in individual cells in a larger cohort of mice. Contractile responses in intact hearts were plotted as a function of the overall health status of the animal. Results showed that there was no relationship between frailty and either diastolic pressure or coronary flow rate in intact hearts. By contrast, the age-

dependent decline in LVDP, +dP/dt, -dP/dt, and RPP was graded by frailty.

The current study did not find any changes in intrinsic HR with relation to age or frailty. Some studies that used Langendorff-perfused hearts also did not report a decline in HR with age (Porter et al., 2014; Stein et al., 2008; Watanabe et al., 2004; Escobales et al., 2014) while others saw a decrease in HR with age (Headrick et al., 2003; Sample et al., 2006; Headrick, 1998). To date, our group is the first group that has investigated the links between HR in Langendorff-perfused hearts and frailty. In our study, HR could only be estimated from the pressure recordings, because an ECG was not available at the time. However, a more in-depth study assessed HR using ECG recordings and sinoatrial node function in a large cohort of mice with varying age and FI scores (Moghtadaei et al., 2016). This study shows a decrease in HR with age and frailty (Moghtadaei et al., 2016). Furthermore, they show that sinoatrial function is impaired in aged mice as a result of age-related changes in conduction velocity and action potential morphology (Moghtadaei et al., 2016; Jansen et al., 2017). The age-related sinoatrial dysfunction was inversely correlated with frailty. Therefore, future Langendorff-perfused heart experiments should use ECG recordings for a more sensitive measurement of HR.

The present study reported a decline in peak contraction and slowing of the velocities of shortening and lengthening in ventricular myocytes in the aged group in comparison to the adult group. Furthermore, we found that this decline in contraction correlated with smaller Ca^{2+} transients which may be due to a smaller Ca^{2+} current density. We stratified this age-dependent decline in contraction and Ca^{2+} handling by FI score. Results showed that the speed and amplitude of contraction in individual cells were inversely correlated with frailty. Furthermore, there was a negative correlation between FI scores and the age-

related decline in peak Ca^{2+} transient amplitude and Ca^{2+} current density. In addition, the expression of CaV1.2 protein declined as frailty scores increased.

The major finding in this study was the clear evidence that age-dependent hypertrophy and cardiac contractile dysfunction at the macroscopic and microscopic levels were correlated with frailty. Based on these results, animals with higher frailty may be predisposed to CVDs where contractile function is disrupted, such as heart failure.

4.4 THE IMPACT OF AGE AND FRAILTY ON CONTRACTILE FUNCTION FOLLOWING IR INJURY

4.4.1 Summary of results

The present study investigated the relationship between age, frailty, and functional recovery following IR in Langendorff-perfused hearts. Results showed that contractions were completely abolished during ischemia in the aged and adult groups. Recovery of contractile function during reperfusion was significantly reduced compared to baseline function in both age groups. Recovery of diastolic pressure and HR throughout reperfusion was similar in both age groups. By contrast, LVDP, +dP/dt, -dP/dt, and RPP index following IR were higher in the aged hearts compared to the adult hearts. The relationship between frailty and functional recovery was explored by plotting diastolic pressure, HR, LVDP, +dP/dt, -dP/dt, and RPP index as a function of frailty scores. Our results showed that recovery of contractile function was not associated with the overall health status of the animal as quantified by a FI score. Similarly, coronary flow rate was also not affected by age or frailty.

This study also investigated the effects of age and frailty on myocardial injury by measuring contracture, infarct size, and cTnI release in hearts exposed to IR. Peak contracture during IR was similar in both age groups and was not correlated with frailty. Interestingly, the time to peak contracture was longer during ischemia in the aged animals in comparison to the adult group. By contrast, time to peak contracture was not significantly different between the two groups during reperfusion. Myocardial injury was also assessed by measuring infarct size and cTnI levels in adult and aged hearts following exposure to IR. Results showed that aged hearts had significantly smaller infarcts compared to adult hearts. In addition, mean cTnI levels were lower in aged hearts in comparison to adult hearts. These observations suggest that aged hearts recover better than adult hearts after exposure to IR. Interestingly, these markers of ischemic damage were not correlated with FI score.

4.4.2 Influence of age on functional recovery after IR

The present study investigated the links between age and recovery of contractile function following IR in intact hearts from adult and aged mice. Results showed that following IR, HR recovered to values that were comparable to baseline HR in both age groups. The recovered HR was not significantly different between the two different age groups at the end of reperfusion. This is consistent with a study that reported similar HR's in aged and adult Langendorff-perfused rat hearts following IR (Escobales et al., 2014 *c.f.* Headrick, 1998). Moreover, our results showed that coronary flow rate recovered to levels that were comparable to pre-ischemic values following IR and was similar in both age

groups. This supports findings from previous studies where coronary flow rates following IR are not affected by age in mouse (Headrick et al., 2003; Willems et al., 2005) and rat hearts (Headrick, 1998; Boucher et al., 1998; Abete et al., 1999). Taken together, our results showed that HR and coronary flow recovered to pre-ischemic values following IR. This suggests that the contractile recovery reported in this study reflects changes in diastolic and systolic function rather than flow or HR-dependent changes.

This study also showed that diastolic pressure increased following IR relative to baseline values in both age groups. However, there was no difference in diastolic pressures at the end of reperfusion between the aged and adult groups. Similar to our findings, studies show that diastolic pressure increases during reperfusion in mouse (Wang et al. 2018; Headrick et al., 2003; Ashton et al., 2003; Willems et al., 2005) and rat (Escobales et al., 2014; Boucher et al., 1998; Headrick, 1998) hearts. Studies in mice report that there is a greater increase in diastolic pressure in aged (18-26 mos) hearts in comparison to diastolic pressures in hearts from young (2-6 mos) animals following IR (Wang et al. 2018; Headrick et al., 2003; Ashton et al., 2003). Interestingly, this age-related difference is not present when diastolic pressure is compared in aged (18-26 mos) and adult (8-12 mos) mouse hearts during reperfusion (Willems et al., 2005). In the present study, diastolic pressure during reperfusion was measured in mice with an average age of ~9 mos and aged mice with a mean age of ~27 mos. Studies in rats also showed no differences in diastolic pressure during reperfusion in aged hearts in comparison to adult hearts (Escobales et al., 2014; Boucher et al., 1998 *c.f.* Headrick, 1998). Thus, our results support previous findings that the sustained post ischemic increase in diastolic pressure is similar in aged and adult hearts.

Most studies show an age-dependent decline in the recovery of contractile function in rats (Boucher et al., 1998; Headrick, 1998; Escobales et al., 2014; Lesnefsky et al., 1994) and mice (Willems et al., 2005; Ashton et al., 2003; Headrick et al., 2003; Wang et al., 2018) following exposure to IR. However, some studies show that functional recovery following IR is similar in adult (8-12 mos), middle aged (18 mos), and aged (24-28 mos) hearts in mice (Willems et al., 2005). Willems *et al.* (2005) reported the observations that the recovery of LVDP and $+dP/dt$ at the end of reperfusion was similar in adult (8-12 mos), middle aged (18 mos), and aged (24-28 mos) mice. Similar studies using rats also reported that recovery of LVDP at the end of reperfusion was similar in aged (24 mos) and middle-aged (16 mos) hearts following IR (Boucher et al., 1998). In addition, there is also evidence that the recovery of developed pressure is similar in young (6 mos) and aged (24 mos) rats (Abete et al., 1999). Interestingly, we showed that recovery of LVDP, $+dP/dt$, $-dP/dt$, and RPP was actually better in aged hearts in comparison to adult hearts. Differences in the results of our study and studies of others may be due to differences in factors, such as cardioprotection, that could affect recovery.

It is proposed that tolerance to IR could be biphasic. Functional recovery following IR declines with age in young (2-4 mos) vs. middle aged mice (~16 mos) (Willems et al., 2005). As the mouse transitions from middle age to aged (28 mos) functional recovery (*e.g.* LVDP) following IR improves (Willems et al., 2005). This idea is supported in another study that showed an age-dependent decrease in functional recovery where young rats had better contractile recovery than middle aged and aged rat hearts (Boucher et al., 1998). However, there was no age-dependent improvement in recovery in middle aged hearts in comparison to aged hearts (Boucher et al., 1998). In fact, there was a trend for

aged hearts to recover better, but this was not significant (Boucher et al., 1998). This suggests that IR tolerance may actually improve with age. Indeed, this idea is supported by the results from the present study, where aged hearts had better recovery than adult hearts.

The reason that older hearts are resistant to IR injury is unclear. There was a significant decrease in body weight in the aged group of mice in comparison to the adult group used in this study. It is possible that aged animals consumed fewer calories than the adult mice, although food intake was not measured in this study. Interestingly, there is evidence that caloric restriction induces cardioprotection from IR injury and improves functional recovery in aged rodent hearts (Peart, See Hoe, Pepe, Johnson & Headrick, 2012; Abete et al., 2002). Peart *et al.* (2012) showed caloric restriction abolishes any age differences in IR tolerance. Specifically, diastolic pressure, LVDP, +dP/dt, and -dP/dt recovery following IR is the same in young and young adult caloric restricted mice (Peart et al., 2012). Similarly, aged rats that are calorie restricted have functional recovery similar to young rats that had an *ad libitum* diet (Abete et al., 2002; Shinmura, Tamaki & Bolli, 2005). Many studies show that caloric restriction improves tolerance to IR by increasing the expression levels of Sirt1 (Yamamoto et al., 2016; Ungvari, Parrado-Fernandez, Csiszar & de Cabo, 2008; Shinmura, Tamaki & Bolli, 2008; Shinmura et al., 2011). Sirt1 is believed to increase nitric oxide synthase expression levels and promote anti-oxidant activity to reduce IR injury (Yamamoto et al., 2016; Shinmura et al., 2015). Therefore, it is possible that the aged mice used in the present study could have had cardioprotection from IR if they consumed fewer calories.

Interestingly, there is also evidence that leptin, a hormone made in adipocytes that regulates food intake increases with age in rodents (Shinmura et al., 2005; Collins et al., 2009 *c.f.* Levy et al., 2015). Studies show that high leptin levels are associated with protection from IR in humans (Dellas et al., 2013) and rodents (Levy et al., 2015; Smith et al., 2006). Patients with pulmonary embolism who have low plasma leptin concentrations are at approximately three times more risk for 30-day-complications (eg. morbidity and mortality) than patients with high plasma leptin (Dellas et al., 2013). Levy *et al.*, (2015) showed high leptin levels improve functional recovery post IR in aged mice. The aged mice in the present study may have high endogenous leptin which could have provided cardioprotection from IR.

In addition, our results showed that hearts isolated from aged animals had fewer CaV1.2 channels, smaller Ca²⁺ currents, and smaller Ca²⁺ transients. These results suggest that there may be less Ca²⁺ loading in aged cardiomyocytes during IR. Less Ca²⁺ loading may attenuate the mitochondrial permeability transition pore opening and thus prevent cell apoptosis following IR (Garcia-Dorado, Ruiz-Meana, Insete, Rodriguez-Sinovas & Piper, 2012). The mitochondrial permeability transition pore opening can also be inhibited through the cardioprotective mechanism called ischemic preconditioning. Ischemic preconditioning is an adaptive response where a heart that is exposed to a brief period of ischemia becomes more resistant to subsequent more prolonged IR (Murry, Jennings & Reimar, 1986). The population of aged mice used in this study were quite old and thus may have experienced intermittent ischemia. This exposure to ischemia may be one mechanism for the improved recovery of function observed in the aged mice compared to

adult mice following IR. The mechanisms for the cardioprotection in the aged hearts following IR requires further research.

4.4.3 Myocardial injury following IR in mice of different age

The present study showed high levels of peak contracture during IR in both age groups. There was no significant difference between peak contracture during IR between the aged and adult group, consistent with previous studies (Boucher et al., 1998; Escobales et al., 2014; Lesnefsky et al., 1994 *c.f.* Headrick, 1998; Headrick et al., 2003). The mechanisms for ischemic contracture are not fully understood. However, ischemic contracture during global ischemia is believed to be predominantly ATP-dependent (Piper, Meuter & Schäfer, 2003; Hearse, Garlick & Humphrey, 1977). ATP-dependent contracture occurs through a rigor-type mechanism where shortened myofibrils are unable to relax after the ATP reserves are depleted in ischemia (Piper et al., 2003; Hearse et al., 1977). Indeed, ATP-dependent contracture occurs when ATP levels are below 100 μM , independent of an increase in intracellular Ca^{2+} (Nichols & Lederer, 1990). Furthermore, contracture can also occur if there is an increase in intracellular Ca^{2+} (Eisner, Nichols, O'Neill, Smith & Valdeolmillos, 1989). For example, studies in individual cardiomyocytes show an increase in intracellular Ca^{2+} (*e.g.* Ca^{2+} overload) during ischemia can cause injury during reperfusion (O'Brien et al., 2008; Ataka, Chen, Levitsky, Jimenez & Feinberg, 1992). This increase in intracellular Ca^{2+} may activate protein kinases that phosphorylate contractile proteins to induce contracture (Lee & Allen, 1991).

Interestingly, the time to onset of peak contracture during ischemia was significantly longer in aged hearts than adult hearts. This may be due to the age-dependent shift from α myosin heavy chain isoform to the β myosin heavy chain isoform which slows down contraction kinetics in aged hearts (Lompré et al. 1991; Buttrick et al., 1991; Fitzsimons et al., 1999). The aged hearts in the present study may take longer to develop contracture during ischemia because of the lower ATPase activity of β myosin heavy chain (Carnes, Geisbuhler & Reiser, 2004). Contracture also persisted throughout the reperfusion period in all hearts used in this study. This sustained post-ischemic diastolic dysfunction may be due to reduced tolerance to Ca^{2+} imbalances (such as Ca^{2+} overload and Ca^{2+} oscillations) that lead to uncontrollable myofibrillar activation (Piper et al., 2003). This study did not observe any differences in contracture development during IR between the two age groups. This may have been as a result of extensive IR injury due to the prolonged ischemic period.

The present study also measured IR injury by assessing infarct size and cTnI release. Paradoxically, we saw significantly smaller infarct sizes and less cTnI release in the aged hearts in comparison to adult hearts following IR. By contrast, previous studies show cell death, measured by cTnI, LDH, and creatine kinase efflux is higher in middle aged and aged hearts compared to young animals following IR (Willems et al., 2005; Ashton et al., 2003; Headrick et al., 2003; Headrick, 1998; Wang et al., 2018). Similarly, infarct size is also reported to be higher in aged hearts in comparison to young hearts (Wang et al., 2018). These results suggest the aged hearts used in the present study may experience cardioprotection when compared to younger hearts. The underlying mechanisms for this are unclear. Using the same arguments used above, aged mice in this study may have had

high levels of serum leptin or low-calorie intake. Hearts from aged animals with high leptin concentrations or calorie restriction have smaller infarct size in comparison to young animals (Levy et al., 2015; Smith et al., 2006). Similarly, creatine kinase and cTnI release following IR is also lower in hearts when there are high levels of leptin or caloric restriction (Levy et al., 2015; Smith et al., 2006). This cardioprotection by leptin and caloric restriction is attributed to activation of PI3K-Akt, MAPK, and AMPK pathways. The IR tolerance in the aged hearts in the present study, and the potential role of leptin in this cardioprotection are an exciting area that requires further research.

4.4.4 The relationship between frailty and recovery following IR

The relationship between frailty and recovery following IR was investigated by exposing hearts from animals with varying FI scores to IR. Contractile parameters (diastolic pressure, LVDP, +dP/dt, -dP/dt, and RPP) and myocardial injury markers following IR were plotted as a function of FI scores. Interestingly, there was no correlation between recovery of function and frailty. These findings contrast with clinical studies where there are clear links between frailty and CVD. Frail individuals who develop CVD have higher morbidity and mortality compared to non-frail patients (Afilalo et al., 2014; Singh et al., 2014; Chen, 2015; Goldwater & Pinney, 2015; Adabag et al., 2018; Kusunose et al., 2018). Furthermore, frail individuals who undergo surgical treatment for CVD have higher mortality than non-frail patients (Afilalo et al., 2014; Singh et al., 2014; Chen, 2015). By contrast, a recent study examined the bidirectional longitudinal association between CVD and frailty (Kleipool et al., 2018). This study found that there was an

increased frailty risk in individuals with CVD (Kleipool et al., 2018). When they assessed the reverse association between CVD and frailty, they found frailty is not associated with an increased risk of CVD (Kleipool et al., 2018). The data in this study appears to support the findings by Kleipool *et al.* (2018) where frailty was not correlated with recovery following IR. Our results did show an association between poor heart function and frailty under basal conditions. We determined that poor heart function contributes to frailty, but whether frailty sets the stage for heart failure is less clear. Future research can assess this bidirectional association. On the other hand, we assessed frailty with an FI tool that did not include any markers for heart function. Thus, the links we observed between frailty and heart function are due to poor overall health, independent of cardiac function *per se*.

4.5 LIMITATIONS AND FUTURE DIRECTIONS

There are some limitations in this study. First, this study only used male animals. There are many studies that report distinct age differences in cardiac function between male and female hearts (Feridooni et al., 2015A). For example, contractile function declines with age in males and not in females (Feridooni et al., 2015A). In addition, the presentation of CVDs is different in men and in women. For example, men develop heart failure with reduced ejection fraction and women develop heart failure with preserved ejection fraction (Feridooni et al., 2015A). Future studies using female mice to determine the impact of age on female hearts would be interesting to pursue.

Second, this study only assessed frailty in male C57BL/6 mice and only assessed the reliability of the FI tool in male but not female mice. A future direction for this study

would be to investigate the relationship between frailty and contractile function in female hearts. Because of the existing sex-differences, it would be interesting to see how frailty is associated with contractile function in female hearts.

Third, this study used young adult (~9 mos) and aged (~27 mos) mice. However, we did not use young (3-6 mos) or middle aged (14-18 mos) animals. Many studies compare young animals to middle aged animals or to aged animals when reporting any age differences in contractile function. As discussed above, there may be an initial age-dependent increase in IR intolerance that declines with advanced age. Furthermore, we saw high levels of contracture in both age groups. A shorter exposure to ischemia may induce less damage and unmask any potential age differences in ischemic tolerance.

This study did not investigate the relationship between frailty and age-dependent fibrosis. There was a clear correlation between age-dependent hypertrophy but we did not have the samples to measure fibrosis in mice with varying FI scores. Similarly, we did not measure the impact of frailty on infarct size following IR due to limited tissue availability. Future experiments could investigate the relationship between the overall health status of the mouse in relation to the infarct size following IR. This would be particularly interesting because our results showed an age-dependent decline in infarct size.

Lastly, we did not explore the mechanisms involved in cardioprotection in aged hearts. We could measure serum hormone levels, such as leptin, which are implicated in cardioprotection from IR. We also did not measure food intake and adipocyte levels in the mouse. It would be interesting to see if the aged animals that have smaller infarcts are associated with higher adipocyte and leptin levels.

4.6 IMPLICATIONS

Many older patients who have CVD typically have one or more co-existing diseases (Bell & Saraf, 2016). Multimorbidity is prevalent in 70% of people that are over the age of 75 (Bell & Saraf, 2016). Thus, as Fontana *et al.* (2014) stated, “the problems of old age come as a package”. However, most treatment care utilizes single disease practice guidelines, ignoring the complex interplay between the other morbidities (Bell & Saraf, 2016). Employing the frailty index, which can measure the overall health status of a person, can accommodate the complete “package” referred to by Fontana *et al.* (2014). The present study has validated a mouse clinical FI tool, similar to the clinical FI used in people, that allows researchers to quantify the overall health status of an animal. Using this tool, we established links between frailty and age-related cardiac contractile dysfunction. We showed that the overall health status of the mouse was correlated with age-dependent remodelling at the level of the intact heart and at the cellular and subcellular levels. This successful animal model of frailty can be used to study the biology of ageing, with the aims of using interventions to attenuate frailty and see if these impact cardiac function as well. The present study also reported that aged hearts had better functional recovery than adult hearts. In addition, these aged hearts had less myocardial injury. Further exploration of mechanisms involved may provide new insights on potential cardioprotection mechanisms in aged mice.

REFERENCES

- Abete, P., Cioppa, A., Calabrese, C., Pascucci, I., Cacciatore, F., & Napoli, C. et al. (1999). Ischemic threshold and myocardial stunning in the aging heart. *Experimental Gerontology*, 34(7), 875-884. doi: 10.1016/s0531-5565(99)00060-1
- Abete, P., Testa, G., Ferrara, N., De Santis, D., Capaccio, P., & Viati, L. et al. (2002). Cardioprotective effect of ischemic preconditioning is preserved in food-restricted senescent rats. *American Journal Of Physiology-Heart And Circulatory Physiology*, 282(6), H1978-H1987. doi: 10.1152/ajpheart.00929.2001
- Adabag, S., Vo, T., Langsetmo, L., Schousboe, J., Cawthon, P., & Stone, K. et al. (2018). Frailty as a Risk Factor for Cardiovascular Versus Noncardiovascular Mortality in Older Men: Results From the MrOS Sleep (Outcomes of Sleep Disorders in Older Men) Study. *Journal Of The American Heart Association*, 7(10), e008974. doi: 10.1161/jaha.118.008974
- Afilalo, J., Alexander, K., Mack, M., Maurer, M., Green, P., & Allen, L. et al. (2014). Frailty Assessment in the Cardiovascular Care of Older Adults. *Journal Of The American College Of Cardiology*, 63(8), 747-762. doi: 10.1016/j.jacc.2013.09.070
- Ahluwalia, S., Gross, C., Chaudhry, S., Leo-Summers, L., Van Ness, P., & Fried, T. (2011). Change in Comorbidity Prevalence with Advancing Age Among Persons with Heart Failure. *Journal Of General Internal Medicine*, 26(10), 1145-1151. doi: 10.1007/s11606-011-1725-6
- Ashton, K., Nilsson, U., Willems, L., Holmgren, K., & Headrick, J. (2003). Effects of aging and ischemia on adenosine receptor transcription in mouse myocardium. *Biochemical And Biophysical Research Communications*, 312(2), 367-372. doi: 10.1016/j.bbrc.2003.10.127
- Ataka, K., Chen, D., Levitsky, S., Jimenez, E., & Feinberg, H. (1992). Effect of aging on intracellular Ca²⁺, pHi, and contractility during ischemia and reperfusion. *Circulation*, 86(5 Suppl):II371-6.
- Azhar, G., Gao, W., Liu, L., & Wei, J. (1999). Ischemia-reperfusion in the adult mouse heart. *Experimental Gerontology*, 34(5), 699-714. doi: 10.1016/s0531-5565(99)00031-5
- Bavia, L., Lidani, K., Andrade, F., Sobrinho, M., Nisihara, R., & de Messias-Reason, I. (2018). Complement activation in acute myocardial infarction: An early marker of inflammation and tissue injury?. *Immunology Letters*, 200, 18-25. doi: 10.1016/j.imlet.2018.06.006

- Bell, S., & Saraf, A. (2016). Epidemiology of Multimorbidity in Older Adults with Cardiovascular Disease. *Clinics In Geriatric Medicine*, 32(2), 215-226. doi: 10.1016/j.cger.2016.01.013
- Bergman, H., Ferrucci, L., Guralnik, J., Hogan, D., Hummel, S., Karunanathan, S., & Wolfson, C. (2007). Frailty: An Emerging Research and Clinical Paradigm--Issues and Controversies. *The Journals Of Gerontology Series A: Biological Sciences And Medical Sciences*, 62(7), 731-737. doi: 10.1093/gerona/62.7.731
- Bernhard, D., & Laufer, G. (2008). The Aging Cardiomyocyte: A Mini-Review. *Gerontology*, 54(1), 24-31. doi: 10.1159/000113503
- Bers, D. (2002). Cardiac excitation-contraction coupling. *Nature*, 415(6868), 198-205. doi: 10.1038/415198a
- Bers, D. (2014). Cardiac Sarcoplasmic Reticulum Calcium Leak: Basis and Roles in Cardiac Dysfunction. *Annual Review Of Physiology*, 76(1), 107-127. doi: 10.1146/annurev-physiol-020911-153308
- Bhatnagar, G., Walford, G., Beard, E., Humphreys, S., & Lakatta, E. (1984). ATPase activity and force production in myofibrils and twitch characteristics in intact muscle from neonatal, adult, and senescent rat myocardium. *Journal Of Molecular And Cellular Cardiology*, 16(3), 203-218. doi: 10.1016/s0022-2828(84)80587-8
- Blodgett, J., Theou, O., Howlett, S., & Rockwood, K. (2017). A frailty index from common clinical and laboratory tests predicts increased risk of death across the life course. *Geroscience*, 39(4), 447-455. doi: 10.1007/s11357-017-9993-7
- Boucher, F., Tanguy, S., Besse, S., Tresallet, N., Favier, A., & de Leiris, J. (1998). Age-dependent changes in myocardial susceptibility to zero flow ischemia and reperfusion in isolated perfused rat hearts: relation to antioxidant status. *Mechanisms Of Ageing And Development*, 103(3), 301-316. doi: 10.1016/s0047-6374(98)00050-5
- Böning, A., Rohrbach, S., Kohlhepp, L., Heep, M., Hagmüller, S., Niemann, B., & Mühlfeld, C. (2015). Differences in ischemic damage between young and old hearts — Effects of blood cardioplegia. *Experimental Gerontology*, 67, 3-8. doi: 10.1016/j.exger.2015.04.012
- Burgess, M., McCrea, J., & Hedrick, H. (2001). Age-associated changes in cardiac matrix and integrins. *Mechanisms Of Ageing And Development*, 122(15), 1739-1756. doi: 10.1016/s0047-6374(01)00296-2
- Buttrick, P., Malhotra, A., Factor, S., Greenen, D., Leinwand, L., & Scheuer, J. (1991). Effect of aging and hypertension on myosin biochemistry and gene expression in the rat heart. *Circulation Research*, 68(3), 645-652. doi: 10.1161/01.res.68.3.645

- Califf, R., Lee, K., Granger, C., & Ohman, E. (1997). Predictors of outcome of reperfusion therapy. *European Heart Journal*, 18(5), 728-735. doi: 10.1093/oxfordjournals.eurheartj.a015338
- Capasso, J., Fitzpatrick, D., & Anversa, P. (1992). Cellular mechanisms of ventricular failure: myocyte kinetics and geometry with age. *American Journal Of Physiology-Heart And Circulatory Physiology*, 262(6), H1770-H1781. doi: 10.1152/ajpheart.1992.262.6.h1770
- Capasso, J., Remily, R., & Sonnenblick, E. (1983). Age-related differences in excitation-contraction coupling in rat papillary muscle. *Basic Research In Cardiology*, 78(5), 492-504. doi: 10.1007/bf01906460
- Cappelli, V., Tortelli, O., Zani, B., Poggesi, C., & Reggiani, C. (1988). Age-dependent changes of relaxation and its load sensitivity in rat cardiac muscle. *Basic Research In Cardiology*, 83(1), 65-76. doi: 10.1007/bf01907106
- Carnes, C., Geisbuhler, T., & Reiser, P. (2004). Age-dependent changes in contraction and regional myocardial myosin heavy chain isoform expression in rats. *Journal Of Applied Physiology*, 97(1), 446-453. doi: 10.1152/jappphysiol.00439.2003
- Ceylan-Isik, A., Dong, M., Zhang, Y., Dong, F., Turdi, S., & Nair, S. et al. (2013). Cardiomyocyte-specific deletion of endothelin receptor A rescues aging-associated cardiac hypertrophy and contractile dysfunction: role of autophagy. *Basic Research In Cardiology*, 108(2). doi: 10.1007/s00395-013-0335-3
- Chen, M. (2015). Frailty and cardiovascular disease: potential role of gait speed in surgical risk stratification in older adults. *Journal Of Geriatric Cardiology*, 12(1), 44-56. doi: 10.11909/j.issn.1671-5411.2015.01.006
- Cigolle, C., Ofstedal, M., Tian, Z., & Blaum, C. (2009). Comparing Models of Frailty: The Health and Retirement Study. *Journal Of The American Geriatrics Society*, 57(5), 830-839. doi: 10.1111/j.1532-5415.2009.02225.x
- Claessens, T., Rietzschel, E., De Buyzere, M., De Bacquer, D., De Backer, G., & Gillebert, T. et al. (2007). Noninvasive assessment of left ventricular and myocardial contractility in middle-aged men and women: disparate evolution above the age of 50?. *American Journal Of Physiology-Heart And Circulatory Physiology*, 292(2), H856-H865. doi: 10.1152/ajpheart.00759.2006
- Clegg, A., Young, J., Iliffe, S., Rikkert, M., & Rockwood, K. (2013). Frailty in elderly people. *The Lancet*, 381(9868), 752-762. doi: 10.1016/s0140-6736(12)62167-9

- Collins, A., Lyon, C., Xia, X., Liu, J., Tangirala, R., & Yin, F. et al. (2009). Age-Accelerated Atherosclerosis Correlates With Failure to Upregulate Antioxidant Genes. *Circulation Research*, *104*(6), e42-e54. doi: 10.1161/circresaha.108.188771
- Collins, J., Munoz, J., Patel, T., Loukas, M., & Tubbs, R. (2014). The anatomy of the aging aorta. *Clinical Anatomy*, *27*(3), 463-466. doi: 10.1002/ca.22384
- Cooper, D. (1975). Observations on ischaemic contracture of the heart ('stone heart'). *Cardiovascular Research*, *9*(2), 246-248. doi: 10.1093/cvr/9.2.246
- Creemers, E., & Pinto, Y. (2011). Molecular mechanisms that control interstitial fibrosis in the pressure-overloaded heart. *Cardiovascular Research*, *89*(2), 265-272. doi: 10.1093/cvr/cvq308
- Croce, A., Brunati, P., Colzani, C., Terramocci, R., Favero, S., Bordoni, G., & Galli, C. (2017). A Rational Adoption of the High Sensitive Assay for Cardiac Troponin I in Diagnostic Routine. *Disease Markers*, *2017*, 1-11. doi: 10.1155/2017/4523096
- Daniels, M., Naya, T., Rundell, V., & de Tombe, P. (2007). Development of contractile dysfunction in rat heart failure: hierarchy of cellular events. *American Journal Of Physiology-Regulatory, Integrative And Comparative Physiology*, *293*(1), R284-R292. doi: 10.1152/ajpregu.00880.2006
- de Jong, S., van Veen, T., de Bakker, J., & van Rijen, H. (2011). Monitoring cardiac fibrosis: a technical challenge. *Netherlands Heart Journal*, *20*(1), 44-48. doi: 10.1007/s12471-011-0226-x
- de Vries, N., Staal, J., van Ravensberg, C., Hobbelen, J., Olde Rikkert, M., & Nijhuis-van der Sanden, M. (2011). Outcome instruments to measure frailty: A systematic review. *Ageing Research Reviews*, *10*(1), 104-114. doi: 10.1016/j.arr.2010.09.001
- Dellas, C., Lankeit, M., Reiner, C., Schäfer, K., Hasenfuß, G., & Konstantinides, S. (2013). BMI-independent inverse relationship of plasma leptin levels with outcome in patients with acute pulmonary embolism. *International Journal Of Obesity*, *37*(2), 204-210. doi: 10.1038/ijo.2012.36
- Domeier, T., Roberts, C., Gibson, A., Hanft, L., McDonald, K., & Segal, S. (2014). Dantrolene suppresses spontaneous Ca²⁺ release without altering excitation-contraction coupling in cardiomyocytes of aged mice. *American Journal Of Physiology-Heart And Circulatory Physiology*, *307*(6), H818-H829. doi: 10.1152/ajpheart.00287.2014
- Eisner, D., Nichols, C., O'Neill, S., Smith, G., & Valdeolmillos, M. (1989). The effects of metabolic inhibition on intracellular calcium and pH in isolated rat ventricular cells. *The Journal Of Physiology*, *411*(1), 393-418. doi: 10.1113/jphysiol.1989.sp017580

- Endoh, M. (2004). Force–frequency relationship in intact mammalian ventricular myocardium: physiological and pathophysiological relevance. *European Journal Of Pharmacology*, 500(1-3), 73-86. doi: 10.1016/j.ejphar.2004.07.013
- Escobales, N., Nuñez, R., Jang, S., Parodi-Rullan, R., Ayala-Peña, S., & Sacher, J. et al. (2014). Mitochondria-targeted ROS scavenger improves post-ischemic recovery of cardiac function and attenuates mitochondrial abnormalities in aged rats. *Journal Of Molecular And Cellular Cardiology*, 77, 136-146. doi: 10.1016/j.yjmcc.2014.10.009
- Farrell, S., & Howlett, S. (2007). The effects of isoproterenol on abnormal electrical and contractile activity and diastolic calcium are attenuated in myocytes from aged Fischer 344 rats. *Mechanisms Of Ageing And Development*, 128(10), 566-573. doi: 10.1016/j.mad.2007.08.003
- Farrell, S., & Howlett, S. (2008). The age-related decrease in catecholamine sensitivity is mediated by β 1-adrenergic receptors linked to a decrease in adenylate cyclase activity in ventricular myocytes from male Fischer 344 rats. *Mechanisms Of Ageing And Development*, 129(12), 735-744. doi: 10.1016/j.mad.2008.09.017
- Feridooni, H., Dibb, K., & Howlett, S. (2015). How cardiomyocyte excitation, calcium release and contraction become altered with age. *Journal Of Molecular And Cellular Cardiology*, 83, 62-72. doi: 10.1016/j.yjmcc.2014.12.004
- Feridooni, H., Sun, M., Rockwood, K., & Howlett, S. (2015). Reliability of a Frailty Index Based on the Clinical Assessment of Health Deficits in Male C57BL/6J Mice. *The Journals Of Gerontology Series A: Biological Sciences And Medical Sciences*, 70(6), 686-693. doi: 10.1093/gerona/glu161
- Ferrara, N., Ogara, P., Wynne, D., Brown, L., Delmont, F., Poolewilson, P., & Harding, S. (1995). Decreased contractile responses to isoproterenol in isolated cardiac myocytes from ageing guinea-pigs. *Journal Of Molecular And Cellular Cardiology*, 27(5), 1141-1150. doi: 10.1016/0022-2828(95)90050-0
- Fitzsimons, D., Patel, J., & Moss, R. (1999). Aging-dependent depression in the kinetics of force development in rat skinned myocardium. *American Journal Of Physiology-Heart And Circulatory Physiology*, 276(5), H1511-H1519. doi: 10.1152/ajpheart.1999.276.5.h1511
- Fleg, J., O'Connor, F., Gerstenblith, G., Becker, L., Clulow, J., Schulman, S., & Lakatta, E. (1995). Impact of age on the cardiovascular response to dynamic upright exercise in healthy men and women. *Journal Of Applied Physiology*, 78(3), 890-900. doi: 10.1152/jap.1995.78.3.890

- Fleg, J., & Strait, J. (2012). Age-associated changes in cardiovascular structure and function: a fertile milieu for future disease. *Heart Failure Reviews*, *17*(4-5), 545-554. doi: 10.1007/s10741-011-9270-2
- Fontana, L., Kennedy, B., Longo, V., Seals, D., & Melov, S. (2014). Medical research: Treat ageing. *Nature*, *511*(7510), 405-407. doi: 10.1038/511405a
- Fratricelli, A., Josephson, R., Danziger, R., Lakatta, E., & Spurgeon, H. (1989). Morphological and contractile characteristics of rat cardiac myocytes from maturation to senescence. *American Journal Of Physiology-Heart And Circulatory Physiology*, *257*(1), H259-H265. doi: 10.1152/ajpheart.1989.257.1.h259
- Fried, L., Tangen, C., Walston, J., Newman, A., Hirsch, C., & Gottdiener, J. et al. (2001). Frailty in Older Adults: Evidence for a Phenotype. *The Journals Of Gerontology Series A: Biological Sciences And Medical Sciences*, *56*(3), M146-M157. doi: 10.1093/gerona/56.3.m146
- Garcia-Dorado, D., Ruiz-Meana, M., Inserte, J., Rodriguez-Sinovas, A., & Piper, H. M. (2012). Calcium-mediated cell death during myocardial reperfusion. *Cardiovascular Research*, *94*(2), 168-180. doi:10.1093/cvr/cvs116
- Graber, T., Ferguson-Stegall, L., Liu, H., & Thompson, L. (2015). Voluntary Aerobic Exercise Reverses Frailty in Old Mice. *The Journals Of Gerontology Series A: Biological Sciences And Medical Sciences*, *70*(9), 1045-1058. doi: 10.1093/gerona/glu163
- Grandy, S., & Howlett, S. (2006). Cardiac excitation-contraction coupling is altered in myocytes from aged male mice but not in cells from aged female mice. *American Journal Of Physiology-Heart And Circulatory Physiology*, *291*(5), H2362-H2370. doi: 10.1152/ajpheart.00070.2006
- Goldwater, D., & Pinney, S. (2015). Frailty in Advanced Heart Failure: A Consequence of Aging or a Separate Entity?. *Clinical Medicine Insights: Cardiology*, *9s2*, CMC.S19698. doi: 10.4137/cmc.s19698
- Grundy, E. M. D. (2003). The epidemiology of aging. Brocklehurst's Textbook of Geriatric Medicine and Gerontology, 6th ed. London. Churchill Livingstone. p. 4–20.
- Guo, K., & Ren, J. (2006). Cardiac overexpression of alcohol dehydrogenase (ADH) alleviates aging-associated cardiomyocyte contractile dysfunction: role of intracellular Ca²⁺ cycling proteins. *Aging Cell*, *5*(3), 259-265. doi: 10.1111/j.1474-9726.2006.00215.x
- Hacker, T., McKiernan, S., Douglas, P., Wanagat, J., & Aiken, J. (2006). Age-related changes in cardiac structure and function in Fischer 344 × Brown Norway hybrid rats. *American Journal Of Physiology-Heart And Circulatory Physiology*, *290*(1), H304-H311. doi: 10.1152/ajpheart.00290.2005

- Harris, B., Nageh, T., Marsden, J., Thomas, M., & Sherwood, R. (2000). Comparison of cardiac troponin T and I and CK-MB for the detection of minor myocardial damage during interventional cardiac procedures. *Annals Of Clinical Biochemistry*, 37(6), 764-769. doi: 10.1258/0004563001900075
- Headrick, J. (1998). Aging Impairs Functional, Metabolic and Ionic Recovery from Ischemia-Reperfusion and Hypoxia-Reoxygenation. *Journal Of Molecular And Cellular Cardiology*, 30(7), 1415-1430. doi: 10.1006/jmcc.1998.0710
- Headrick, J., Willems, L., Ashton, K., Holmgren, K., Peart, J., & Matherne, G. (2003). Ischaemic Tolerance in Aged Mouse Myocardium: The Role of Adenosine and Effects of A1 Adenosine Receptor Overexpression. *The Journal Of Physiology*, 549(3), 823-833. doi: 10.1113/jphysiol.2003.041541
- Hearse, D., Garlick, P., & Humphrey, S. (1977). Ischemic contracture of the myocardium: Mechanisms and prevention. *The American Journal Of Cardiology*, 39(7), 986-993. doi: 10.1016/s0002-9149(77)80212-9
- Hoppe, U., Brandt, M., Michels, G., & Linder, M. (2005). L-type calcium channel recording. In S. Dhein, F. Mohr & M. Delmar, *Practical Methods in Cardiovascular Research*. (pp. 324–354). Heidelberg: Springer Verlag.
- Horn, M., & Trafford, A. (2016). Aging and the cardiac collagen matrix: Novel mediators of fibrotic remodelling. *Journal Of Molecular And Cellular Cardiology*, 93, 175-185. doi: 10.1016/j.yjmcc.2015.11.005
- Howlett, S. (2010). Age-associated changes in excitation-contraction coupling are more prominent in ventricular myocytes from male rats than in myocytes from female rats. *American Journal Of Physiology-Heart And Circulatory Physiology*, 298(2), H659-H670. doi: 10.1152/ajpheart.00214.2009
- Howlett, S., & Rockwood, K. (2013). New horizons in frailty: ageing and the deficit-scaling problem. *Age And Ageing*, 42(4), 416-423. doi: 10.1093/ageing/aft059
- Hubbard, R., Fallah, N., Searle, S., Mitnitski, A., & Rockwood, K. (2009). Impact of Exercise in Community-Dwelling Older Adults. *Plos ONE*, 4(7), e6174. doi: 10.1371/journal.pone.0006174
- Hubbard, R., Peel, N., Samanta, M., Gray, L., Mitnitski, A., & Rockwood, K. (2017). Frailty status at admission to hospital predicts multiple adverse outcomes. *Age And Ageing*, 46(5), 801-806. doi: 10.1093/ageing/afx081
- Isenberg, G., Borschke, B., & Rueckschloss, U. (2003). Ca²⁺ transients of cardiomyocytes from senescent mice peak late and decay slowly. *Cell Calcium*, 34(3), 271-280. doi: 10.1016/s0143-4160(03)00121-0

- Jackson, S., Andrews, N., Ball, D., Bellantuono, I., Gray, J., & Hachoumi, L. et al. (2017). Does age matter? The impact of rodent age on study outcomes. *Laboratory Animals*, 51(2), 160-169. doi: 10.1177/0023677216653984
- Janczewski, A., & Lakatta, E. (2010). Modulation of sarcoplasmic reticulum Ca²⁺ cycling in systolic and diastolic heart failure associated with aging. *Heart Failure Reviews*, 15(5), 431-445. doi: 10.1007/s10741-010-9167-5
- Jansen, H., Moghtadaei, M., Mackasey, M., Rafferty, S., Bogachev, O., & Sapp, J. et al. (2017). Atrial structure, function and arrhythmogenesis in aged and frail mice. *Scientific Reports*, 7(1). doi: 10.1038/srep44336
- Janicki, J., & Brower, G. (2002). The role of myocardial fibrillar collagen in ventricular remodeling and function. *Journal Of Cardiac Failure*, 8(6), S319-S325. doi: 10.1054/jcaf.2002.129260
- Jiang, M., Moffat, M., & Narayanan, N. (1993). Age-related alterations in the phosphorylation of sarcoplasmic reticulum and myofibrillar proteins and diminished contractile response to isoproterenol in intact rat ventricle. *Circulation Research*, 72(1), 102-111. doi: 10.1161/01.res.72.1.102
- Johansson, S., Rosengren, A., Young, K., & Jennings, E. (2017). Mortality and morbidity trends after the first year in survivors of acute myocardial infarction: a systematic review. *BMC Cardiovascular Disorders*, 17(1). doi: 10.1186/s12872-017-0482-9
- Kajstura, J., Cheng, W., Sarangarajan, R., Li, P., Li, B., & Nitahara, J. et al. (1996). Necrotic and apoptotic myocyte cell death in the aging heart of Fischer 344 rats. *American Journal Of Physiology-Heart And Circulatory Physiology*, 271(3), H1215-H1228. doi: 10.1152/ajpheart.1996.271.3.h1215
- Kane, A., Ayaz, O., Ghimire, A., Feridooni, H., & Howlett, S. (2017). Implementation of the mouse frailty index. *Canadian Journal Of Physiology And Pharmacology*, 95(10), 1149-1155. doi: 10.1139/cjpp-2017-0025
- Kane, A., Hilmer, S., Huizer-Pajkos, A., Mach, J., Nines, D., & Boyer, D. et al. (2015). Factors that Impact on Interrater Reliability of the Mouse Clinical Frailty Index. *The Journals Of Gerontology Series A: Biological Sciences And Medical Sciences*, 70(6), 694-695. doi: 10.1093/gerona/glv032
- Kane, A., Huizer-Pajkos, A., Mach, J., Mitchell, S., de Cabo, R., & Le Couteur, D. et al. (2017). A Comparison of Two Mouse Frailty Assessment Tools. *The Journals Of Gerontology: Series A*, 72(7), 904-909. doi: 10.1093/gerona/glx009

- Kasser, I., & Bruce, R. (1969). Comparative Effects of Aging and Coronary Heart Disease on Submaximal and Maximal Exercise. *Circulation*, 39(6), 759-774. doi: 10.1161/01.cir.39.6.759
- Katrukha, I. (2013). Human cardiac troponin complex. Structure and functions. *Biochemistry (Moscow)*, 78(13), 1447-1465. doi: 10.1134/s0006297913130063
- Keller, K., & Howlett, S. (2016). Sex Differences in the Biology and Pathology of the Aging Heart. *Canadian Journal Of Cardiology*, 32(9), 1065-1073. doi: 10.1016/j.cjca.2016.03.017
- Kilkenny, C., Browne, W., Cuthill, I., Emerson, M., & Altman, D. (2010). Improving Bioscience Research Reporting: The ARRIVE Guidelines for Reporting Animal Research. *Plos Biology*, 8(6), e1000412. doi: 10.1371/journal.pbio.1000412
- Kleipool, E., Hoogendijk, E., Trappenburg, M., Handoko, M., Huisman, M., Peters, M., & Muller, M. (2018). Frailty in Older Adults with Cardiovascular Disease: Cause, Effect or Both?. *Aging And Disease*, 9(3), 489. doi: 10.14336/ad.2017.1125
- Kloner, R. (1993). Does reperfusion injury exist in humans?. *Journal Of The American College Of Cardiology*, 21(2), 537-545. doi: 10.1016/0735-1097(93)90700-b
- Koch, S., Haworth, K., Robbins, N., Smith, M., Lather, N., & Anjak, A. et al. (2013). Age- and Gender-Related Changes in Ventricular Performance in Wild-Type FVB/N Mice as Evaluated by Conventional and Vector Velocity Echocardiography Imaging: A Retrospective Study. *Ultrasound In Medicine & Biology*, 39(11), 2034-2043. doi: 10.1016/j.ultrasmedbio.2013.04.002
- Korzick, D., Holiman, D., Boluyt, M., Laughlin, M., & Lakatta, E. (2001). Diminished α 1-adrenergic-mediated contraction and translocation of PKC in senescent rat heart. *American Journal Of Physiology-Heart And Circulatory Physiology*, 281(2), H581-H589. doi: 10.1152/ajpheart.2001.281.2.h581
- Kusunose, K., Okushi, Y., Yamada, H., Nishio, S., Torii, Y., & Hirata, Y. et al. (2018). Prognostic Value of Frailty and Diastolic Dysfunction in Elderly Patients. *Circulation Journal*, 82(8), 2103-2110. doi: 10.1253/circj.cj-18-0017
- Kwok, C., Bachmann, M., Mamas, M., Stirling, S., Shepstone, L., Myint, P., & Zaman, M. (2017). Effect of age on the prognostic value of left ventricular function in patients with acute coronary syndrome: A prospective registry study. *European Heart Journal: Acute Cardiovascular Care*, 6(2), 191-198. doi: 10.1177/2048872615623038
- Lakatta, E., & Levy, D. (2003). Arterial and Cardiac Aging: Major Shareholders in Cardiovascular Disease Enterprises: Part II: The Aging Heart in Health: Links to Heart Disease. *Circulation*, 107(2), 346-354. doi: 10.1161/01.cir.0000048893.62841.f7

- Lakatta, E., Gerstenblith, G., Angell, C., Shock, N., & Weisfeldt, M. (1975). Diminished inotropic response of aged myocardium to catecholamines. *Circulation Research*, 36(2), 262-269. doi: 10.1161/01.res.36.2.262
- Lakatta, E., Gerstenblith, G., Angell, C., Shock, N., & Weisfeldt, M. (1975). Prolonged contraction duration in aged myocardium. *Journal Of Clinical Investigation*, 55(1), 61-68. doi: 10.1172/jci107918
- Lakatta, E., & Sollott, S. (2002). Perspectives on mammalian cardiovascular aging: humans to molecules. *Comparative Biochemistry And Physiology Part A: Molecular & Integrative Physiology*, 132(4), 699-721. doi: 10.1016/s1095-6433(02)00124-1
- Lakatta, E. (2002). *Heart Failure Reviews*, 7(1), 29-49. doi: 10.1023/a:1013797722156
- Lau, D., Shipp, N., Kelly, D., Thanigaimani, S., Neo, M., & Kuklik, P. et al. (2013). Atrial Arrhythmia in Ageing Spontaneously Hypertensive Rats: Unraveling the Substrate in Hypertension and Ageing. *Plos ONE*, 8(8), e72416. doi: 10.1371/journal.pone.0072416
- Law, M., Watt, H., & Wald, N. (2002). The Underlying Risk of Death After Myocardial Infarction in the Absence of Treatment. *Archives Of Internal Medicine*, 162(21), 2405. doi: 10.1001/archinte.162.21.2405
- Lee, J., & Allen, D. (1991). Mechanisms of acute ischemic contractile failure of the heart. Role of intracellular calcium. *Journal Of Clinical Investigation*, 88(2), 361-367. doi: 10.1172/jci115311
- Lesnefsky, E., Gallo, D., Ye, J., Whittingham, S., & Lust, D. (1994). Aging increases ischemia-reperfusion injury in the isolated, buffer-perfused heart. *The Journal Of Laboratory And Clinical Medicine*, 124(6), 843 -851.
- Levy, E., Kornowski, R., Gavrieli, R., Fratty, I., Greenberg, G., & Waldman, M. et al. (2015). Long-Lived α MUPA Mice Show Attenuation of Cardiac Aging and Leptin-Dependent Cardioprotection. *PLOS ONE*, 10(12), e0144593. doi: 10.1371/journal.pone.0144593
- Li R & Shen Y (2013). An old method facing a new challenge: re-visiting housekeeping proteins as internal reference control for neuroscience research. *Life Sci* 92, 747–751.
- Li, S., Du, M., Dolence, E., Fang, C., Mayer, G., & Ceylan-Isik, A. et al. (2005). Aging induces cardiac diastolic dysfunction, oxidative stress, accumulation of advanced glycation endproducts and protein modification. *Aging Cell*, 4(2), 57-64. doi: 10.1111/j.1474-9728.2005.00146.x

- Li, Q., Wu, S., Li, S., Lopez, F., Du, M., & Kajstura, J. et al. (2007). Cardiac-specific overexpression of insulin-like growth factor 1 attenuates aging-associated cardiac diastolic contractile dysfunction and protein damage. *American Journal Of Physiology-Heart And Circulatory Physiology*, 292(3), H1398-H1403. doi: 10.1152/ajpheart.01036.2006
- Lieber, S., Aubry, N., Pain, J., Diaz, G., Kim, S., & Vatner, S. (2004). Aging increases stiffness of cardiac myocytes measured by atomic force microscopy nanoindentation. *American Journal Of Physiology-Heart And Circulatory Physiology*, 287(2), H645-H651. doi: 10.1152/ajpheart.00564.2003
- Lim, C., Apstein, C., Colucci, W., & Liao, R. (2000). Impaired Cell Shortening and Relengthening with Increased Pacing Frequency are Intrinsic to the Senescent Mouse Cardiomyocyte. *Journal Of Molecular And Cellular Cardiology*, 32(11), 2075-2082. doi: 10.1006/jmcc.2000.1239
- Lim, C., Liao, R., Varma, N., & Apstein, C. (1999). Impaired lusitropy-frequency in the aging mouse: role of Ca²⁺-handling proteins and effects of isoproterenol. *American Journal Of Physiology-Heart And Circulatory Physiology*, 277(5), H2083-H2090. doi: 10.1152/ajpheart.1999.277.5.h2083
- Lindsey, M., Goshorn, D., Squires, C., Escobar, G., Hendrick, J., & Mingoia, J. et al. (2005). Age-dependent changes in myocardial matrix metalloproteinase/tissue inhibitor of metalloproteinase profiles and fibroblast function. *Cardiovascular Research*, 66(2), 410-419. doi: 10.1016/j.cardiores.2004.11.029
- Liu, H., Graber, T., Ferguson-Stegall, L., & Thompson, L. (2014). Clinically Relevant Frailty Index for Mice. *The Journals Of Gerontology Series A: Biological Sciences And Medical Sciences*, 69(12), 1485-1491. doi: 10.1093/gerona/glt188
- Liu, M., Zhang, P., Chen, M., Zhang, W., Yu, L., Yang, X., & Fan, Q. (2012). Aging might increase myocardial ischemia / reperfusion-induced apoptosis in humans and rats. *AGE*, 34(3), 621-632. doi: 10.1007/s11357-011-9259-8
- Liu, P., Xu, B., Cavalieri, T., & Hock, C. (2002). Age-related difference in myocardial function and inflammation in a rat model of myocardial ischemia-reperfusion. *Cardiovascular Research*, 56(3), 443-453. doi: 10.1016/s0008-6363(02)00603-x
- Lompré, A., Lambert, F., Lakatta, E., & Schwartz, K. (1991). Expression of sarcoplasmic reticulum Ca(2+)-ATPase and calsequestrin genes in rat heart during ontogenic development and aging. *Circulation Research*, 69(5), 1380-1388. doi: 10.1161/01.res.69.5.1380

- Lowe DA, Degens H, Chen KD & Alway SE (2000). Glyceraldehyde-3-phosphate dehydrogenase varies with age in glycolytic muscles of rats. *J Gerontol A Biol Sci Med Sci* **55**, B160–164
- Mace, L., Palmer, B., Brown, D., Jew, K., Lynch, J., & Glunt, J. et al. (2003). Influence of age and run training on cardiac Na⁺/Ca²⁺ exchange. *Journal Of Applied Physiology*, *95*(5), 1994-2003. doi: 10.1152/jappphysiol.00551.2003
- Manne, N., Kakarla, S., Arvapalli, R., Rice, K., & Blough, E. (2014). Molecular Mechanisms of Age-Related Cardiac Hypertrophy in the F344XBN Rat Model. *Journal Of Clinical & Experimental Cardiology*, *05*(12). doi: 10.4172/2155-9880.1000353
- Mariani, J., Ou, R., Bailey, M., Rowland, M., Nagley, P., Rosenfeldt, F., & Pepe, S. (2000). Tolerance to ischemia and hypoxia is reduced in aged human myocardium. *The Journal Of Thoracic And Cardiovascular Surgery*, *120*(4), 660-667. doi: 10.1067/mtc.2000.106528
- Mehta, R., Rathore, S., Radford, M., Wang, Y., Wang, Y., & Krumholz, H. (2001). Acute myocardial infarction in the elderly: differences by age. *Journal Of The American College Of Cardiology*, *38*(3), 736-741. doi: 10.1016/s0735-1097(01)01432-2
- Mellor, K., Curl, C., Chandramouli, C., Pedrazzini, T., Wendt, I., & Delbridge, L. (2014). Ageing-related cardiomyocyte functional decline is sex and angiotensin II dependent. *AGE*, *36*(3). doi: 10.1007/s11357-014-9630-7
- Mennes E, Dungan CM, Frendo-Cumbo S, Williamson DL & Wright DC (2014). Aging-associated reductions in lipolytic and mitochondrial proteins in mouse adipose tissue are not rescued by metformin treatment. *J Gerontol A Biol Sci Med Sci* **69**, 1060–1068.
- Milani-Nejad, N., & Janssen, P. (2014). Small and large animal models in cardiac contraction research: Advantages and disadvantages. *Pharmacology & Therapeutics*, *141*(3), 235-249. doi: 10.1016/j.pharmthera.2013.10.007
- Mitchell, S., Scheibye-Knudsen, M., Longo, D., & de Cabo, R. (2015). Animal Models of Aging Research: Implications for Human Aging and Age-Related Diseases. *Annual Review Of Animal Biosciences*, *3*(1), 283-303. doi: 10.1146/annurev-animal-022114-110829
- Mitnitski, A., & Rockwood, K. (2015). Aging as a Process of Deficit Accumulation: Its Utility and Origin. *Interdisciplinary Topics In Gerontology*, 85-98. doi: 10.1159/000364933
- Mitnitski, A., Mogilner, A., & Rockwood, K. (2001). Accumulation of Deficits as a Proxy Measure of Aging. *The Scientific World JOURNAL*, *1*, 323-336. doi: 10.1100/tsw.2001.58

- Mitnitski, A., Howlett, S., & Rockwood, K. (2017). Heterogeneity of Human Aging and Its Assessment. *The Journals Of Gerontology Series A: Biological Sciences And Medical Sciences*, 877-884. doi: 10.1093/gerona/glw089
- Moghtadaei, M., Jansen, H., Mackasey, M., Rafferty, S., Bogachev, O., & Sapp, J. et al. (2016). The impacts of age and frailty on heart rate and sinoatrial node function. *The Journal Of Physiology*, 594(23), 7105-7126. doi: 10.1113/jp272979
- Moran, A., Forouzanfar, M., Roth, G., Mensah, G., Ezzati, M., & Flaxman, A. et al. (2014). The Global Burden of Ischemic Heart Disease in 1990 and 2010: The Global Burden of Disease 2010 Study. *Circulation*, 129(14), 1493-1501. doi: 10.1161/circulationaha.113.004046
- Mozaffarian, D., Benjamin, E., Go, A., Arnett, D., Blaha, M., & Cushman, M. et al. (2016). Heart Disease and Stroke Statistics—2016 Update. *Circulation*, 133(4), e38-e360. doi: 10.1161/cir.0000000000000350
- Murry, C. E., Jennings, R. B., & Reimer, K. A. (1986). Preconditioning with ischemia: A delay of lethal cell injury in ischemic myocardium. *Circulation*, 74(5), 1124-1136. doi:10.1161/01.cir.74.5.1124
- Nanayakkara, S., Marwick, T., & Kaye, D. (2018). The ageing heart: the systemic and coronary circulation. *Heart*, 104(5), 370-376. doi: 10.1136/heartjnl-2017-312114
- Nichols, C., & Lederer, W. (1990). The role of ATP in energy-deprivation contractures in unloaded rat ventricular myocytes. *Canadian Journal Of Physiology And Pharmacology*, 68(2), 183-194. doi: 10.1139/y90-029
- Norbert, J. (2009). Transmembrane ionic currents underlying cardiac action potential in mammalian hearts. In P. Nanasi, *Advances in Cardiomyocyte Research* (pp. 1-45). Kerala, India: Transworld Research Network.
- O'Brien, J., Ferguson, J., & Howlett, S. (2008). Effects of ischemia and reperfusion on isolated ventricular myocytes from young adult and aged Fischer 344 rat hearts. *American Journal Of Physiology-Heart And Circulatory Physiology*, 294(5), H2174-H2183. doi: 10.1152/ajpheart.00058.2008
- Odden, M., Coxson, P., Moran, A., Lightwood, J., Goldman, L., & Bibbins-Domingo, K. (2011). The Impact of the Aging Population on Coronary Heart Disease in the United States. *The American Journal Of Medicine*, 124(9), 827-833.e5. doi: 10.1016/j.amjmed.2011.04.010

Olivetti, G., Giordano, G., Corradi, D., Melissari, M., Lagrasta, C., Gambert, S., & Anversa, P. (1995). Gender differences and aging: Effects on the human heart. *Journal Of The American College Of Cardiology*, 26(4), 1068-1079. doi: 10.1016/0735-1097(95)00282-8

Olivetti, G., Melissari, M., Capasso, J., & Anversa, P. (1991). Cardiomyopathy of the aging human heart. Myocyte loss and reactive cellular hypertrophy. *Circulation Research*, 68(6), 1560-1568. doi: 10.1161/01.res.68.6.1560

Parks, R., Fares, E., MacDonald, J., Ernst, M., Sinal, C., Rockwood, K., & Howlett, S. (2012). A Procedure for Creating a Frailty Index Based on Deficit Accumulation in Aging Mice. *The Journals Of Gerontology: Series A*, 67A(3), 217-227. doi: 10.1093/gerona/qlr193

Peart, J., See Hoe, L., Pepe, S., Johnson, P., & Headrick, J. (2012). Opposing Effects of Age and Calorie Restriction on Molecular Determinants of Myocardial Ischemic Tolerance. *Rejuvenation Research*, 15(1), 59-70. doi: 10.1089/rej.2011.1226

Piper, H., Meuter, K., & Schäfer, C. (2003). Cellular mechanisms of ischemia-reperfusion injury. *The Annals Of Thoracic Surgery*, 75(2), S644-S648. doi: 10.1016/s0003-4975(02)04686-6

Porter, G., Urciuoli, W., Brookes, P., & Nadtochiy, S. (2014). SIRT3 deficiency exacerbates ischemia-reperfusion injury: implication for aged hearts. *American Journal Of Physiology-Heart And Circulatory Physiology*, 306(12), H1602-H1609. doi: 10.1152/ajpheart.00027.2014

Public Health Agency of Canada. (2017). *Heart disease in Canada: Highlights from the Canadian Chronic Disease Surveillance System*. Government of Canada.

Pyati, A., Devaranavadagi, B., Sajjannar, S., Nikam, S., Shannawaz, M., & Patil, S. (2016). Heart-Type Fatty Acid-Binding Protein, in Early Detection of Acute Myocardial Infarction: Comparison with CK-MB, Troponin I and Myoglobin. *Indian Journal Of Clinical Biochemistry*, 31(4), 439-445. doi: 10.1007/s12291-015-0544-7

Qin, F., Siwik, D., Lancel, S., Zhang, J., Kuster, G., & Luptak, I. et al. (2013). Hydrogen Peroxide-Mediated SERCA Cysteine 674 Oxidation Contributes to Impaired Cardiac Myocyte Relaxation in Senescent Mouse Heart. *Journal Of The American Heart Association*, 2(4), e000184-e000184. doi: 10.1161/jaha.113.000184

Rahimi, K., Duncan, M., Pitcher, A., Emdin, C., & Goldacre, M. (2015). Mortality from heart failure, acute myocardial infarction and other ischaemic heart disease in England and Oxford: a trend study of multiple-cause-coded death certification. *Journal Of Epidemiology And Community Health*, 69(10), 1000-1005. doi: 10.1136/jech-2015-205689

- Redfield, M., Jacobsen, S., Borlaug, B., Rodeheffer, R., & Kass, D. (2005). Age- and Gender-Related Ventricular-Vascular Stiffening: A Community-Based Study. *Circulation*, *112*(15), 2254-2262. doi: 10.1161/circulationaha.105.541078
- Reichelt, M., Willems, L., Hack, B., Peart, J., & Headrick, J. (2008). Cardiac and coronary function in the Langendorff-perfused mouse heart model. *Experimental Physiology*, *94*(1), 54-70. doi: 10.1113/expphysiol.2008.043554
- Ren, J., Li, Q., Wu, S., Li, S., & Babcock, S. (2007). Cardiac overexpression of antioxidant catalase attenuates aging-induced cardiomyocyte relaxation dysfunction. *Mechanisms Of Ageing And Development*, *128*(3), 276-285. doi: 10.1016/j.mad.2006.12.007
- Rich, P., Mischis, L., Purton, S., & Wiskich, J. (2001). The sites of interaction of triphenyltetrazolium chloride with mitochondrial respiratory chains. *FEMS Microbiology Letters*, *202*(2), 181-187. doi: 10.1111/j.1574-6968.2001.tb10801.x
- Rockwood, K., & Mitnitski, A. (2006). Limits to deficit accumulation in elderly people. *Mechanisms Of Ageing And Development*, *127*(5), 494-496. doi: 10.1016/j.mad.2006.01.002
- Rockwood, K., & Mitnitski, A. (2011). Frailty Defined by Deficit Accumulation and Geriatric Medicine Defined by Frailty. *Clinics In Geriatric Medicine*, *27*(1), 17-26. doi: 10.1016/j.cger.2010.08.008
- Rockwood, K., & Mitnitski, A. (2007). Frailty in Relation to the Accumulation of Deficits. *The Journals Of Gerontology Series A: Biological Sciences And Medical Sciences*, *62*(7), 722-727. doi: 10.1093/gerona/62.7.722
- Rockwood, K., Andrew, M., & Mitnitski, A. (2007). A Comparison of Two Approaches to Measuring Frailty in Elderly People. *The Journals Of Gerontology Series A: Biological Sciences And Medical Sciences*, *62*(7), 738-743. doi: 10.1093/gerona/62.7.738
- Rockwood, K., Blodgett, J., Theou, O., Sun, M., Feridooni, H., & Mitnitski, A. et al. (2017). A Frailty Index Based On Deficit Accumulation Quantifies Mortality Risk in Humans and in Mice. *Scientific Reports*, *7*(1). doi: 10.1038/srep43068
- Rockwood, K., Fox, R., Stolee, P., Robertson, D., & Beattie, B. (1994). Frailty in elderly people: an evolving concept. *The Canadian Medical Association Journal*, *150*(4), 489-495.
- Rockwood, K., Hogan, D., & MacKnight, C. (2000). Conceptualisation and Measurement of Frailty in Elderly People. *Drugs & Aging*, *17*(4), 295-302. doi: 10.2165/00002512-200017040-00005

- Rockwood, K., Howlett, S., MacKnight, C., Beattie, B., Bergman, H., & Hébert, R. et al. (2004). Prevalence, Attributes, and Outcomes of Fitness and Frailty in Community-Dwelling Older Adults: Report From the Canadian Study of Health and Aging. *The Journals Of Gerontology: Series A*, 59(12), 1310-1317. doi: 10.1093/gerona/59.12.1310
- Rockwood, K., Rockwood, M., & Mitnitski, A. (2010). Physiological Redundancy in Older Adults in Relation to the Change with Age in the Slope of a Frailty Index. *Journal Of The American Geriatrics Society*, 58(2), 318-323. doi: 10.1111/j.1532-5415.2009.02667.x
- Romić, E., Unić, A., Derek, L., & Pehar, M. (2009). [Biochemical markers in the diagnosis of acute coronary syndrome]. *Acta Med Croatica*, 63(1), 15 -19.
- Ruan, Q., & Nagueh, S. (2005). Effect of age on left ventricular systolic function in humans: a study of systolic isovolumic acceleration rate. *Experimental Physiology*, 90(4), 527-534. doi: 10.1113/expphysiol.2005.030007
- Rueckschloss, U., Villmow, M., & Klöckner, U. (2010). NADPH oxidase-derived superoxide impairs calcium transients and contraction in aged murine ventricular myocytes. *Experimental Gerontology*, 45(10), 788-796. doi: 10.1016/j.exger.2010.05.002
- Rüegg, J. (1998). Cardiac Contractility: How Calcium Activates the Myofilaments. *Naturwissenschaften*, 85(12), 575-582. doi: 10.1007/s001140050554
- Sakai, M., Danziger, R., Xiao, R., Spurgeon, H., & Lakatta, E. (1992). Contractile response of individual cardiac myocytes to norepinephrine declines with senescence. *American Journal Of Physiology-Heart And Circulatory Physiology*, 262(1), H184-H189. doi: 10.1152/ajpheart.1992.262.1.h184
- Salameh, A., Dhein, S., Fleischmann, B., Grohe, C., Hescheler, J., Linz, K., & Meyer, R. (2010). The aging heart: changes in the pharmacodynamic electrophysiological response to verapamil in aged rabbit hearts. *JOURNAL OF PHYSIOLOGY AND PHARMACOLOGY*, 61(2), 141-151.
- Sample, J., Cleland, J., & Seymour, A. (2006). Metabolic remodeling in the aging heart. *Journal Of Molecular And Cellular Cardiology*, 40(1), 56-63. doi: 10.1016/j.yjmcc.2005.09.018
- Saraste, A., Pulkki, K., Kallajoki, M., Henriksen, K., Parvinen, M., & Voipio-Pulkki, L. (1997). Apoptosis in Human Acute Myocardial Infarction. *Circulation*, 95(2), 320-323. doi: 10.1161/01.cir.95.2.320
- Saunderson, C., Brogan, R., Simms, A., Sutton, G., Batin, P., & Gale, C. (2014). Acute coronary syndrome management in older adults: guidelines, temporal changes and challenges. *Age And Ageing*, 43(4), 450-455. doi: 10.1093/ageing/afu034

Searle, S., Mitnitski, A., Gahbauer, E., Gill, T., & Rockwood, K. (2008). A standard procedure for creating a frailty index. *BMC Geriatrics*, 8(1). doi: 10.1186/1471-2318-8-24

Shinmura, K., Tamaki, K., & Bolli, R. (2008). Impact of 6-mo caloric restriction on myocardial ischemic tolerance: possible involvement of nitric oxide-dependent increase in nuclear Sirt1. *American Journal Of Physiology-Heart And Circulatory Physiology*, 295(6), H2348-H2355. doi: 10.1152/ajpheart.00602.2008

Shinmura, K., Tamaki, K., & Bolli, R. (2005). Short-term caloric restriction improves ischemic tolerance independent of opening of ATP-sensitive K channels in both young and aged hearts. *Journal Of Molecular And Cellular Cardiology*, 39(2), 285-296. doi: 10.1016/j.yjmcc.2005.03.010

Shinmura, K., Tamaki, K., Ito, K., Yan, X., Yamamoto, T., & Katsumata, Y. et al. (2015). Indispensable role of endothelial nitric oxide synthase in caloric restriction-induced cardioprotection against ischemia-reperfusion injury. *American Journal Of Physiology-Heart And Circulatory Physiology*, 308(8), H894-H903. doi: 10.1152/ajpheart.00333.2014

Shinmura, K., Tamaki, K., Sano, M., Nakashima-Kamimura, N., Wolf, A., & Amo, T. et al. (2011). Caloric Restriction Primes Mitochondria for Ischemic Stress by Deacetylating Specific Mitochondrial Proteins of the Electron Transport Chain. *Circulation Research*, 109(4), 396-406. doi: 10.1161/circresaha.111.243097

Singh, M., Stewart, R., & White, H. (2014). Importance of frailty in patients with cardiovascular disease. *European Heart Journal*, 35(26), 1726-1731. doi: 10.1093/eurheartj/ehu197

Slama, M., Ahn, J., Varagic, J., Susic, D., & Frohlich, E. (2004). Long-term left ventricular echocardiographic follow-up of SHR and WKY rats: effects of hypertension and age. *American Journal Of Physiology-Heart And Circulatory Physiology*, 286(1), H181-H185. doi: 10.1152/ajpheart.00642.2003

Smith, C., Mocanu, M., Davidson, S., Wynne, A., Simpkin, J., & Yellon, D. (2006). Leptin, the obesity-associated hormone, exhibits direct cardioprotective effects. *British Journal Of Pharmacology*, 149(1), 5-13. doi: 10.1038/sj.bjp.0706834

Statistics Canada. (2017, November 15). *Statistics Canada*. Retrieved May 4, 2018, from 2016 Census topic: Age and sex: <https://www12.statcan.gc.ca/census-recensement/2016/rt-td/as-eng.cfm>.

Statistics Canada. (2018, February 22). *Statistics Canada*. Retrieved May 4, 2018, from Leading causes of death, total population, by sex, Canada, provinces and territories (age standardization using 2011 population): <https://www150.statcan.gc.ca/t1/tbl1/en/tv.action?pid=1310080101>.

- Stein, M., Noorman, M., van Veen, T., Herold, E., Engelen, M., & Boulaksil, M. et al. (2008). Dominant arrhythmia vulnerability of the right ventricle in senescent mice. *Heart Rhythm*, 5(3), 438-448. doi: 10.1016/j.hrthm.2007.10.033
- Strait, J., & Lakatta, E. (2012). Aging-Associated Cardiovascular Changes and Their Relationship to Heart Failure. *Heart Failure Clinics*, 8(1), 143-164. doi: 10.1016/j.hfc.2011.08.011
- Stratton, J., Levy, W., Cerqueira, M., Schwartz, R., & Abrass, I. (1994). Cardiovascular responses to exercise. Effects of aging and exercise training in healthy men. *Circulation*, 89(4), 1648-1655. doi: 10.1161/01.cir.89.4.1648
- Su, N., & Narayanan, N. (1993). Age related alteration in cholinergic but not adrenergic response of rat coronary vasculature. *Cardiovascular Research*, 27(2), 284-290. doi: 10.1093/cvr/27.2.284
- Sulzgruber, P., Schnaubelt, S., Koller, L., Goliash, G., Niederdöckl, J., & Simon, A. et al. (2018). Cardiac arrest as an age-dependent prognosticator for long-term mortality after acute myocardial infarction: the potential impact of infarction size. *European Heart Journal: Acute Cardiovascular Care*, 204887261878137. doi: 10.1177/2048872618781370
- Tang, T., Hammond, H., Firth, A., Yang, Y., Gao, M., Yuan, J., & Lai, N. (2011). Adenylyl Cyclase 6 Improves Calcium Uptake and Left Ventricular Function in Aged Hearts. *Journal Of The American College Of Cardiology*, 57(18), 1846-1855. doi: 10.1016/j.jacc.2010.11.052
- Tecson, K., Arnold, W., Barrett, T., Birkhahn, R., Daniels, L., & Defilippi, C. et al. (2017). Interpretation of Positive Troponin Results Among Patients with and Without Myocardial Infarction. *Baylor University Medical Center Proceedings*, 30(1), 11-15. doi: 10.1080/08998280.2017.11929513
- Theou, O., Blodgett, J., Godin, J., & Rockwood, K. (2017). Association between sedentary time and mortality across levels of frailty. *Canadian Medical Association Journal*, 189(33), E1056-E1064. doi: 10.1503/cmaj.161034
- Tiwari, R., Jain, A., Khan, Z., Kohli, V., Bharmal, R., Kartikeyan, S., & Bisen, P. (2012). Cardiac Troponins I and T: Molecular Markers for Early Diagnosis, Prognosis, and Accurate Triaging of Patients with Acute Myocardial Infarction. *Molecular Diagnosis & Therapy*, 16(6), 371-381. doi: 10.1007/s40291-012-0011-6
- Turturro, A., Witt, W., Lewis, S., Hass, B., Lipman, R., & Hart, R. (1999). Growth Curves and Survival Characteristics of the Animals Used in the Biomarkers of Aging Program. *The Journals Of Gerontology Series A: Biological Sciences And Medical Sciences*, 54(11), B492-B501. doi: 10.1093/gerona/54.11.b492

- Turdi, S., Fan, X., Li, J., Zhao, J., Huff, A., Du, M., & Ren, J. (2010). AMP-activated protein kinase deficiency exacerbates aging-induced myocardial contractile dysfunction. *Aging Cell*, 9(4), 592-606. doi: 10.1111/j.1474-9726.2010.00586.x
- Ungvari, Z., Parrado-Fernandez, C., Csiszar, A., & de Cabo, R. (2008). Mechanisms Underlying Caloric Restriction and Lifespan Regulation: Implications for Vascular Aging. *Circulation Research*, 102(5), 519-528. doi: 10.1161/circresaha.107.168369
- van Oeffelen, A., Agyemang, C., Stronks, K., Bots, M., & Vaartjes, I. (2014). Incidence of first acute myocardial infarction over time specific for age, sex, and country of birth. *Netherlands Journal Of Medicine*, 72(1), 20 -27.
- Walker Jr., E. M., Nillas, M. S., Mangiarua, E. I., Cansino, S., Morrison, R. G., Perdue, R. R. et al. (2006). Age-associated changes in hearts of male fischer 344/Brown norway F1 rats. *Annals of Clinical and Laboratory Science*, 36(4), 427-438.
- Wang, L., Quan, N., Sun, W., Chen, X., Cates, C., & Rousselle, T. et al. (2018). Cardiomyocyte-specific deletion of Sirt1 gene sensitizes myocardium to ischaemia and reperfusion injury. *Cardiovascular Research*, 114(6), 805-821. doi: 10.1093/cvr/cvy033
- Watanabe, M., Ichinose, S., & Sunamori, M. (2004). Age-related changes in gap junctional protein of the rat heart. *Experimental And Clinical Cardiology*, 9(2), 130-132.
- Wei, J. (1992). Age and the Cardiovascular System. *New England Journal Of Medicine*, 327(24), 1735-1739. doi: 10.1056/nejm199212103272408
- Wei, J., Spurgeon, H., & Lakatta, E. (1984). Excitation-contraction in rat myocardium: alterations with adult aging. *American Journal Of Physiology-Heart And Circulatory Physiology*, 246(6), H784-H791. doi: 10.1152/ajpheart.1984.246.6.h784
- Weisser-Thomas, J., Nguyen, Q., Schuettel, M., Thomas, D., Dreiner, U., Grohé, C., & Meyer, R. (2007). Age and hypertrophy related changes in contractile post-rest behavior and action potential properties in isolated rat myocytes. *AGE*, 29(4), 205-217. doi: 10.1007/s11357-007-9040-1
- Whitehead, J., Hildebrand, B., Sun, M., Rockwood, M., Rose, R., Rockwood, K., & Howlett, S. (2014). A Clinical Frailty Index in Aging Mice: Comparisons With Frailty Index Data in Humans. *The Journals Of Gerontology: Series A*, 69(6), 621-632. doi: 10.1093/gerona/glt136
- Willems, L., Zatta, A., Homgren, K., Ashton, K., & Headrick, J. (2005). Age-related changes in ischemic tolerance in male and female mouse hearts. *Journal Of Molecular And Cellular Cardiology*, 38(2), 245-256. doi: 10.1016/j.yjmcc.2004.09.014

World Health Organization (WHO). A global brief on hypertension: silent killer, global public health crisis. WHO/DCO/WHD/2013.2. April 3, 2013 (http://apps.who.int/iris/bitstream/10665/79059/1/WHO_DCO_WHD_2013.2_eng.pdf).

Wu, M., Yiang, G., Liao, W., Tsai, A., Cheng, Y., & Cheng, P. et al. (2018). Current Mechanistic Concepts in Ischemia and Reperfusion Injury. *Cellular Physiology And Biochemistry*, 46(4), 1650-1667. doi: 10.1159/000489241

Xiao, R., Spurgeon, H., O'Connor, F., & Lakatta, E. (1994). Age-associated changes in beta-adrenergic modulation on rat cardiac excitation-contraction coupling. *Journal Of Clinical Investigation*, 94(5), 2051-2059. doi: 10.1172/jci117559

Xu, J., Gao, F., Ma, X., Gao, E., Friedman, E., & Snyder, D. et al. (1999). Effect of Aging on the Negative Chronotropic and Anti- β -Adrenergic Actions of Adenosine in the Rat Heart. *Journal Of Cardiovascular Pharmacology*, 34(6), 904-912. doi: 10.1097/00005344-199912000-00020

Yamamoto, T., Tamaki, K., Shirakawa, K., Ito, K., Yan, X., & Katsumata, Y. et al. (2016). Cardiac Sirt1 mediates the cardioprotective effect of caloric restriction by suppressing local complement system activation after ischemia-reperfusion. *American Journal Of Physiology-Heart And Circulatory Physiology*, 310(8), H1003-H1014. doi: 10.1152/ajpheart.00676.2015

Yorke, A., Kane, A., Hancock Friesen, C., Howlett, S., & O'Blenes, S. (2017). Development of a Rat Clinical Frailty Index. *The Journals Of Gerontology: Series A*, 72(7), 897-903. doi: 10.1093/gerona/glw339

Zhang, R., Zhao, J., Mandveno, A., & Potter, J. (1995). Cardiac Troponin I Phosphorylation Increases the Rate of Cardiac Muscle Relaxation. *Circulation Research*, 76(6), 1028-1035. doi: 10.1161/01.res.76.6.1028

Zhu, X., Altschaf, B., Hajjar, R., Valdivia, H., & Schmidt, U. (2005). Altered Ca²⁺ sparks and gating properties of ryanodine receptors in aging cardiomyocytes. *Cell Calcium*, 37(6), 583-591. doi: 10.1016/j.ceca.2005.03.002

APPENDIX A: PUBLICATIONS

PUBLICATIONS:

Feridooni HA, Kane AE, Ayaz O, Boroumandi A, Polidovitch N, Tsushima RG, Rose RA, Howlett SE. The impact of age and frailty on ventricular structure and function in C57BL/6J mice. *J Physiol*. 2017 Jun 15;595(12):3721-3742. doi: 10.1113/JP274134. Epub 2017 May 14. PMID: 28502095.

Kane AE, Ayaz O, Ghimire A, **Feridooni HA**, Howlett SE. Implementation of the mouse frailty index. *Can J Physiol Pharmacol*. 2017 May 2;1-7. doi: 10.1139/cjpp-2017-0025.

Rockwood K, Blodgett JM, Theou O, Sun MH, **Feridooni HA**, Mitnitski A, Rose RA, Godin J, Gregson E, Howlett SE. A Frailty Index Based On Deficit Accumulation Quantifies Mortality Risk in Humans and in Mice. *Sci Rep*. 2017 Feb 21;7:43068. doi: 10.1038/srep43068. PMID: 28220898.

Feridooni HA, MacDonald JK, Ghimire A, Pyle WG, Howlett SE. Acute exposure to progesterone attenuates cardiac contraction by modifying myofilament calcium sensitivity in the mouse heart. *Am J Physiol Heart Circ Physiol*. 2016 Oct 28;ajpheart.00073.2016. doi: 10.1152/ajpheart.00073.2016. PMID:27793852.

Gao T, **Feridooni HA**, Howlett SE, Pelis RM. Influence of Age on Intestinal Bile Acid Transport in C57BL/6 Mice. *Pharmacol Res Perspect*, 5(2), 2017, e00287. doi: 10.1002/prp2.287.

Feridooni HA, Dibb KM, Howlett SE. How cardiomyocyte excitation, calcium release and contraction become altered with age. *J Mol Cell Cardiol*. 2015 Jun;83:62-72. doi: 10.1016/j.yjmcc.2014.12.004. Review.

Feridooni HA, Sun MH, Rockwood K, Howlett SE. Reliability of a Frailty Index Based on the Clinical Assessment of Health Deficits in Male C57BL/6J Mice. *J Gerontol A Biol Sci Med Sci*. 2015 Jun;70(6):686-93. doi: 10.1093/gerona/glu161.

ABSTRACTS:

Feridooni HA, Rose RA, Howlett SE. The impact of age and frailty on ventricular function before and after ischemia-reperfusion in C57BL/6 mice. *J Mol Cell Cardiol*. In press. Poster Presentation.

Feridooni HA, Kane AE, Ayaz O, Boroumandi A, Polidovitch N, Tsushima RG, Rose RA, Howlett SE. The impact of age and frailty on ventricular structure and function in ageing C57BL/6 mice. *J Mol Cell Cardiol*. 112(2017) 148; 042.

Feridooni HA, Boroumandi A, Polidovitch N, Rose RA, Tsushima RG, Howlett SE. Frailty, not age, predicts age-dependent cardiac contractile dysfunction under basal and ischemic conditions in Langendorff-perfused hearts from C57BL/6J mice. *J Mol Cell Cardiol.* 98(2016) S36.

Feridooni HA, Boroumandi A, Polidovitch N, Rose RA, Tsushima RG, Howlett SE. Age-dependent cardiac contractile dysfunction is graded by frailty, not age, in senescent C57BL/6J mice. *J Mol Cell Cardiol.* 85(2015) S1-61.




MacDonald JK, **Feridooni HA**, Pyle WG, Howlett SE. The impact of acute exposure of progesterone on mechanisms of cardiac excitation-contraction coupling in isolated murine ventricular myocytes. *J Mol Cell Cardiol.* 85(2015) S1-61.


Feridooni HA, Pyle WG, Howlett SE. Acute application of progesterone modifies mechanisms involved in cardiac excitation-contraction coupling in isolated murine ventricular myocytes. *J Mol Cell Cardiol.* Sep 2014;74:S29,P2-40.Poster Presentation.

APPENDIX B: COPYRIGHT PERMISSION LETTERS

5/14/2018

Rightslink® by Copyright Clearance Center

HomeCreate AccountHelp



Title: How cardiomyocyte excitation, calcium release and contraction become altered with age

Author: Hiran A. Feridooni, Katharine M. Dibb, Susan E. Howlett

Publication: Journal of Molecular and Cellular Cardiology

Publisher: Elsevier

Date: June 2015

Copyright © 2014 The Authors. Published by Elsevier Ltd.

LOGIN

If you're a **copyright.com** user, you can login to RightsLink using your copyright.com credentials.

Already a **RightsLink user** or want to [learn more?](#)

Please note that, as the author of this Elsevier article, you retain the right to include it in a thesis or dissertation, provided it is not published commercially. Permission is not required, but please ensure that you reference the journal as the original source. For more information on this and on your other retained rights, please visit: <https://www.elsevier.com/about/our-business/policies/copyright#Author-rights>

BACK

CLOSE WINDOW

Copyright © 2018 Copyright Clearance Center, Inc. All Rights Reserved. [Privacy statement](#). [Terms and Conditions](#). Comments? We would like to hear from you. E-mail us at customer-care@copyright.com

**JOHN WILEY AND SONS LICENSE
TERMS AND CONDITIONS**

Jul 11, 2018

This Agreement between Mr. Hiran Feridooni ("You") and John Wiley and Sons ("John Wiley and Sons") consists of your license details and the terms and conditions provided by John Wiley and Sons and Copyright Clearance Center.

License Number	4363240507736
License date	Jun 06, 2018
Licensed Content Publisher	John Wiley and Sons
Licensed Content Publication	Journal of Physiology
Licensed Content Title	The impact of age and frailty on ventricular structure and function in C57BL/6J mice
Licensed Content Author	H. A. Feridooni, A. E. Kane, O. Ayaz, et al
Licensed Content Date	May 14, 2017
Licensed Content Volume	595
Licensed Content Issue	12
Licensed Content Pages	22
Type of use	Dissertation/Thesis
Requestor type	Author of this Wiley article
Format	Print and electronic
Portion	Full article
Will you be translating?	No
Title of your thesis / dissertation	The impact of age and frailty on cardiac function in health and disease conditions in naturally ageing mice.
Expected completion date	Aug 2018
Expected size (number of pages)	250
Requestor Location	Mr. Hiran Feridooni 5850 College St. Tupper Medical Building Halifax, NS B3H 4R2 Canada Attn: Mr. Hiran Feridooni
Publisher Tax ID	EU826007151
Total	0.00 CAD

**OXFORD UNIVERSITY PRESS LICENSE
TERMS AND CONDITIONS**

Jul 11, 2018

This Agreement between Mr. Hiran Feridooni ("You") and Oxford University Press ("Oxford University Press") consists of your license details and the terms and conditions provided by Oxford University Press and Copyright Clearance Center.

License Number	4363240994266
License date	Jun 06, 2018
Licensed content publisher	Oxford University Press
Licensed content publication	Journals of Gerontology - Series A: Biological Sciences and Medical Sciences
Licensed content title	Reliability of a Frailty Index Based on the Clinical Assessment of Health Deficits in Male C57BL/6J Mice
Licensed content author	Feridooni, Hiran A.; Sun, Michael H.
Licensed content date	Sep 9, 2014
Type of Use	Thesis/Dissertation
Institution name	
Title of your work	The impact of age and frailty on cardiac function in health and disease conditions in naturally ageing mice.
Publisher of your work	n/a
Expected publication date	Aug 2018
Permissions cost	0.00 CAD
Value added tax	0.00 CAD
Total	0.00 CAD
Title	The impact of age and frailty on cardiac function in health and disease conditions in naturally ageing mice.
Instructor name	n/a
Institution name	n/a
Expected presentation date	Aug 2018
Portions	Introduction Methods Results Discussion
Requestor Location	Mr. Hiran Feridooni 5850 College St. Tupper Medical Building Halifax, NS B3H 4R2 Canada Attn: Mr. Hiran Feridooni
Publisher Tax ID	GB125506730
Billing Type	Invoice
Billing Address	Mr. Hiran Feridooni 5850 College St. Tupper Medical Building Halifax, NS B3H 4R2 Canada Attn: Mr. Hiran Feridooni
Total	0.00 CAD

**OXFORD UNIVERSITY PRESS LICENSE
TERMS AND CONDITIONS**

Jul 11, 2018

This Agreement between Mr. Hiran Feridooni ("You") and Oxford University Press ("Oxford University Press") consists of your license details and the terms and conditions provided by Oxford University Press and Copyright Clearance Center.

License Number	4363240895285
License date	Jun 06, 2018
Licensed content publisher	Oxford University Press
Licensed content publication	Journals of Gerontology - Series A: Biological Sciences and Medical Sciences
Licensed content title	Reliability of a Frailty Index Based on the Clinical Assessment of Health Deficits in Male C57BL/6J Mice
Licensed content author	Feridooni, Hiran A.; Sun, Michael H.
Licensed content date	Sep 9, 2014
Type of Use	Thesis/Dissertation
Institution name	
Title of your work	The impact of age and frailty on cardiac function in health and disease conditions in naturally ageing mice.
Publisher of your work	n/a
Expected publication date	Aug 2018
Permissions cost	0.00 CAD
Value added tax	0.00 CAD
Total	0.00 CAD
Title	The impact of age and frailty on cardiac function in health and disease conditions in naturally ageing mice.
Instructor name	n/a
Institution name	n/a
Expected presentation date	Aug 2018
Portions	Figures 1, 2, 3, 4 Table 1 Supplementary Table 1
Requestor Location	Mr. Hiran Feridooni 5850 College St. Tupper Medical Building Halifax, NS B3H 4R2 Canada Attn: Mr. Hiran Feridooni
Publisher Tax ID	GB125506730
Billing Type	Invoice
Billing Address	Mr. Hiran Feridooni 5850 College St. Tupper Medical Building Halifax, NS B3H 4R2 Canada Attn: Mr. Hiran Feridooni
Total	0.00 CAD

APPENDIX C: SUPPLEMENTARY TABLES

Supplementary Table 1: The scoring system used to determine a deficit in average body surface temperature and body weight when calculating the frailty index score

Deviations from reference values (SD)	Score given
< 1 SD	0
> 1 SD	0.25
>2 SD	0.50
>3 SD	0.75
>4 SD	1

Supplementary Table 2: Hypertrophy and fibrosis increased with advanced age

	Adult	Aged	P-value
<i>Hypertrophy</i>			
Tibia Length (TL,mm)	18.8 ± 0.1 (N = 16)	18.7 ± 0.1 (N = 32)	0.46
Heart weight (HW,mg)	234 ± 7 (N = 13)	283 ± 9* (N = 31)	0.002
HW:BW (mg/g)	6.1 ± 0.2 (N = 13)	8.2 ± 0.3* (N = 31)	≤0.001
HW:TL (mg/mm)	12.6 ± 0.4 (N = 12)	15.2 ± 0.5* (N = 31)	≤0.001
<i>Fibrosis</i>			
Hydroxyproline (µg/mg)	0.146 ± 0.013 (N = 8)	0.239 ± 0.029* (N = 8)	0.005

* represents significant difference from adult group. Numbers represent mean ± SEM. N represents the sample size of each group. P-values were determined with a Student's *t* test or a Mann-Whitney Rank Sum test for data that were non-parametric.

Supplementary Table 3: Baseline parameters recorded from Langendorff-perfused hearts

Parameter	Adult (N = 16)	Aged (N = 32)	P-value
Diastolic pressure (mm Hg)	6.7 ± 0.5	6.2 ± 0.5	0.18
HR (bpm)	288 ± 11	317 ± 11	0.11
LVDP (mm Hg)	88.6 ± 3.5	65.6 ± 3.3*	≤0.001
+dP/dt (mm Hg/s)	2090 ± 79	1535 ± 84*	≤0.001
-dP/dt (mm Hg/s)	-2011 ± 80	-1416 ± 73*	≤0.001
RPP (mm Hg x bpm)	25248 ± 1009	21312 ± 1492	0.12
RPP (mm Hg x bpm/mg)	110.3 ± 5.7	76.4 ± 5.8*	0.002
Flow rate (ml/min)	6.6 ± 1.0	4.9 ± 0.5	0.10
Flow rate normalized to HW (ml/min/mg)	0.021 ± 0.002 (N = 12)	0.018 ± 0.003 (N = 31)	0.06

* denotes significant difference from adult group. Numbers represent mean ± SEM. P-values were determined with a Student's *t* test or a Mann-Whitney Rank Sum test for data that were non-parametric. N represents the sample size of each group.

Supplementary Table 4: Summary of contraction and Ca²⁺ transient data from individual cardiomyocytes isolated from aged and adult hearts.

	Adult	Aged	P-value
Age (days)	223 ± 28	836 ± 15*	≤0.0001
<i>Contraction</i>			
Cell shortening (%)	8.0 ± 0.8 (n = 10)	4.1 ± 0.4* (n = 24)	<0.0001
Velocity of shortening (µm/s)	10.8 ± 1.5 (n = 10)	5.9 ± 0.6* (n = 24)	0.007
Velocity of lengthening (µm/s)	5.4 ± 0.7 (n = 10)	3.1 ± 0.3* (n = 24)	0.001
<i>Ca²⁺ concentration</i>			
Ca ²⁺ transient (nM)	43.3 ± 3.3 (n = 9)	33.8 ± 1.9 * (n = 32)	0.02

*denotes significant difference from adult group. Numbers represent mean ± SEM. P-values were determined with a Student's *t* test or a Mann-Whitney Rank Sum test for data that were non-parametric. n represents the sample size of each group.

Supplementary Table 5: Summary of Ca²⁺ current responses and Cav1.2 protein expressions in cardiomyocytes isolated from aged and adult hearts

	Adult	Aged	P-value
<i>Ca²⁺ current</i>			
Ca ²⁺ current (pA/pF)	-6.9 ± 0.7 (n = 11)	-4.7 ± 0.3* (n = 32)	0.008
Gain (nM/s/(pA/pF))	396 ± 64 (n = 9)	263 ± 18* (n = 32)	0.04
<i>CaV1.2 expression</i>			
CaV1.2 protein	0.93 ± 0.09 (n = 8)	0.60 ± 0.06* (n = 8)	0.03

*denotes significant difference from adult group. Numbers represent mean ± SEM. P-values were determined with a Mann-Whitney Rank Sum test. n represents the sample size of each group.

Supplementary Table 6: Summary of functional responses following 30 min global ischemia and 40 min reperfusion in hearts from adult and aged mice

Parameter	Adult (N = 15)	Aged (N = 31)	P-value
Diastolic pressure (mm Hg)	44 ± 4	38 ± 3	0.06
HR (bpm)	278 ± 29	273 ± 22	0.94
LVDP (mm Hg)	8.9 ± 2	18 ± 3*	<0.01
+dP/dt (mm Hg/s)	235 ± 48	448 ± 74*	<0.01
-dP/dt (mm Hg/s)	-230 ± 46	-421 ± 67*	<0.01
RPP (mm Hg x bpm/mg)	13.6 ± 3.2 (N = 13)	20.3 ± 4.0 (N = 30)	0.09
Flow rate (ml/min)	6.3 ± 1.3	4.7 ± 0.5	0.35
Flow rate normalized to HW (ml/min/mg)	0.019 ± 0.002 (N = 12)	0.018 ± 0.002 (N = 31)	0.34

Numbers represent mean ± SEM. *represents significant difference between aged and adult groups. P-values compare differences between the adult and aged group and were determined with a 2-way RM ANOVA. N represents the sample size of each group.

Supplementary Table 7: Summary of functional responses expressed as a percentage of pre-ischemic values after 40 min reperfusion

Parameter (% pre-ischemic)	Adult (N = 15)	Aged (N = 31)	P-value
Diastolic pressure (%)	721 ± 92	704 ± 72	0.92
HR (%)	96 ± 10	84 ± 7	0.44
LVDP (%)	10.6 ± 2.3	33.7 ± 8.0*	<0.01
+dP/dt (%)	11.5 ± 2.4	34.2 ± 8.0*	<0.01
-dP/dt (%)	12.1 ± 2.4	37.1 ± 9.5*	0.01
RPP (%)	11.7 ± 2.4 (N = 13)	35.7 ± 9.6* (N = 30)	0.02
Flow rate (%)	90 ± 6	101 ± 8	0.49
Flow rate normalized to HW (%)	87 ± 7 (N = 12)	102 ± 8 (N = 31)	0.32

Numbers represent mean ± SEM. *represents significant difference between aged and adult groups. P-values compare differences between the adult and aged group and were determined with a 2-way RM ANOVA. N represents the sample size of each group.

Supplementary Table 8: Summary of IR injury in intact hearts from aged and adult mice

Parameter	Adult	Aged	P-value
<i>Ischemia</i>			
Peak contracture (mm Hg)	55.7 ± 4.7	48.8 ± 3.3	0.23
Peak contracture (% diastolic pressure)	901 ± 118	852 ± 80	0.73
Time to peak contracture (sec)	926 ± 80	1163 ± 75*	0.05
	(N = 15)	(N = 31)	
<i>Reperfusion</i>			
Peak contracture (mm Hg)	68.1 ± 4.1	68.2 ± 3.9	0.98
Peak contracture (% diastolic pressure)	1120 ± 128	1248 ± 108	0.48
Time to peak contracture (sec)	179 ± 27	110 ± 26	0.07
	(N = 15)	(N = 31)	
cTnI (ng/ml)	3.97 ± 0.59	2.09 ± 0.47*	0.01
	(N = 11)	(N = 25)	
Infarct size (%)	62.2 ± 8.6	32.6 ± 5.0 *	0.01
	(N = 4)	(N = 6)	

Numbers represent mean ± SEM. *represents significant difference between aged and adult groups. P-values were determined with a Student's *t* test or a Mann-Whitney Rank Sum test for data that were non-parametric. P-values compare differences between adult and aged groups. N represents the sample size of each group.